

**Comment Response Matrix
for
Nuclear Regulatory Commission RAI-2009-02
Second Request for Additional Information (RAI) on the
Saltstone Disposal Facility Performance Assessment
(SRR-CWDA-2009-00017, Revision 0, dated October 29, 2009)**

August 2011

Prepared by: Savannah River Remediation LLC
Closure & Waste Disposal Authority
Aiken, SC 29808



TABLE OF CONTENTS

TABLE OF CONTENTS	2
LIST OF FIGURES.....	5
LIST OF TABLES	10
ACRONYMS	13
Executive Summary	15
Performance Assessment Methods (PA)	19
PA-1	19
PA-2	20
PA-3	21
PA-4	22
PA-5	31
PA-6	66
PA-7	67
PA-8	69
PA-9	105
PA-10	114
PA-11	120
PA-12	127
PA-13	130
PA-14	133
Inventory (IN)	136
IN-1	136
IN-2	137
IN-3	139
IN-4	140
IN-5	142
IN-6	144
Infiltration and Erosion Control (IEC).....	145
IEC-1	145
IEC-2	146
IEC-3	147
IEC-4	148
IEC-5	149
IEC-6	150
IEC-7	151
IEC-8	156

Saltstone Performance (SP).....	162
SP-1	162
SP-2	165
SP-3	167
SP-4	169
SP-5	170
SP-6	179
SP-7	181
SP-8	182
SP-9	190
SP-10	191
SP-11	194
SP-12	196
SP-13	198
SP-14	206
SP-15	208
SP-16	211
SP-17	212
SP-18	214
SP-19	217
 Vault Performance (VP)	 224
VP-1	224
VP-2	225
VP-3	233
VP-4	236
VP-5	237
VP-6	239
 Far-Field Transport (FFT).....	 243
FFT-1	243
FFT-2	245
FFT-3	246
FFT-4	252
 Air Pathway (AP).....	 255
AP-1	255
AP-2	256
 Inadvertent Intrusion (II)	 257
II-1	257
II-2	261
 Biosphere (B)	 263

B-1	263
B-2	266
B-3	275
B-4	279
B-5	281
ALARA Analysis (A)	284
A-1	284
Clarifying Questions (C)	287
C-4	288
C-8	290
C-22	291
C-23	292
REFERENCES FOR COMMENT RESPONSES	294

LIST OF FIGURES

Figure EX-1: Major Sources of Radiation Exposure to the Average US Citizen.....	17
Figure PA-4.1: Case C, Sector B Total Dose Comparison	26
Figure PA-4.2: Dose Contributors for PA-4 Case and Comparison of Total Dose with the Benchmark Case (Sector B)	27
Figure PA-4.3: Dose Contributors for Benchmark Case and Comparison of Total Dose with the PA-4 Case (Sector B)	27
Figure PA-4.4: Case C, Sector I Total Dose Comparison	28
Figure PA-4.5: Dose Contributors for PA-4 Case and Comparison of Total Dose with the Benchmark Case (Sector I).....	29
Figure PA-4.6: Dose Contributors for the Benchmark Case and Comparison of Total Dose with the PA-4 Case (Sector I)	30
Figure PA-5.1-1: Vault 1 Ra-226 Release from the Unsaturated Zone without Benchmarking – Base Case.....	34
Figure PA-5.1-2: Vault 1 I-129 Release from the Unsaturated Zone without Benchmarking – Base Case.....	35
Figure PA-5.1-3: Vault 1 Tc-99 Release from the Unsaturated Zone without Benchmarking – Base Case.....	35
Figure PA-5.1-4: FDC Ra-226 Release from the Unsaturated Zone without Benchmarking – Base Case.....	36
Figure PA-5.1-5: FDC I-129 Release from the Unsaturated Zone without Benchmarking – Base Case.....	36
Figure PA-5.1-6: FDC Tc-99 Release from the Unsaturated Zone without Benchmarking – Base Case.....	37
Figure PA-5.1-7: Vault 4 Ra-226 Release from the Unsaturated Zone without Benchmarking – Base Case.....	37
Figure PA-5.1-8: Vault 4 I-129 Release from the Unsaturated Zone without Benchmarking – Base Case.....	38
Figure PA-5.1-9: Vault 4 Tc-99 Release from the Unsaturated Zone without Benchmarking – Base Case.....	38
Figure PA-5.1-10: FDC Ra-226 Release from the Unsaturated Zone with Wall Floor/Soil Benchmarking Factor – Base Case.....	39
Figure PA-5.1-11: FDC I-129 Release from the Unsaturated Zone with Wall Floor/Soil Benchmarking Factor – Base Case.....	40
Figure PA-5.1-12: FDC Tc-99 Release from the Unsaturated Zone with Wall Floor/Soil Benchmarking Factor – Base Case.....	40

Figure PA-5.1-13: FDC Ra-226 Release from the Unsaturated Zone with Wall Floor/Soil and Grout Benchmarking Factors – Base Case	41
Figure PA-5.1-14: FDC I-129 Release from the Unsaturated Zone with Wall Floor/Soil and Grout Benchmarking Factors – Base Case	42
Figure PA-5.1-15: FDC Tc-99 Release from the Unsaturated Zone with Wall Floor/Soil and Grout Benchmarking Factors – Base Case	42
Figure PA-5.1-16: Vault 4 Ra-226 Release from the Unsaturated Zone with Wall Floor/Soil and Grout Benchmarking Factors – Base Case	43
Figure PA-5.1-17: Vault 4 I-129 Release from the Unsaturated Zone with Wall Floor/Soil and Grout Benchmarking Factors – Base Case	43
Figure PA-5.2-18: Vault 4 Tc-99 Release from the Unsaturated Zone with Wall Floor/Soil and Grout Benchmarking Factors – Base Case	44
Figure PA-5.1-19: Vault 1 Ra-226 Release from the Unsaturated Zone with Wall Floor/Soil, Grout and Wall Benchmarking Factors – Base Case	45
Figure PA-5.1-20: Vault 1 I-129 Release from the Unsaturated Zone with Wall Floor/Soil, Grout and Wall Benchmarking Factors – Base Case	45
Figure PA-5.1-21: Vault 1 Tc-99 Release from the Unsaturated Zone with Wall Floor/Soil, Grout and Wall Benchmarking Factors – Base Case	46
Figure PA-5.1-22: Vault 4 Ra-226 Release from the Unsaturated Zone with Wall Floor/Soil, Grout, and Wall Benchmarking Factors – Base Case	46
Figure PA-5.1-23: Vault 4 I-129 Release from the Unsaturated Zone with Wall Floor/Soil, Grout, and Wall Benchmarking Factors – Base Case	47
Figure PA-5.1-24: Vault 4 Tc-99 Release from the Unsaturated Zone with Wall Floor/Soil, Grout, and Wall Benchmarking Factors – Base Case	47
Figure PA-5.1-25: Vault 1 Ra-226 Release from the Unsaturated Zone with All Benchmarking Factors – Base Case	48
Figure PA-5.1-26: Vault 1 I-129 Release from the Unsaturated Zone with All Benchmarking Factors – Base Case	49
Figure PA-5.1-27: Vault 1 Tc-99 Release from the Unsaturated Zone with All Benchmarking Factors – Base Case	49
Figure PA-5.1-28: FDC Ra-226 Release from the Unsaturated Zone with All Benchmarking Factors – Base Case	50
Figure PA-5.1-29: FDC I-129 Release from the Unsaturated Zone with All Benchmarking Factors – Base Case	50
Figure PA-5.1-30: FDC Tc-99 Release from the Unsaturated Zone with All Benchmarking Factors – Base Case	51

Figure PA-5.1-31: Vault 4 Ra-226 Release from the Unsaturated Zone with All Benchmarking Factors – Base Case	51
Figure PA-5.1-32: Vault 4 I-129 Release from the Unsaturated Zone with All Benchmarking Factors – Base Case	52
Figure PA-5.1-33: Vault 4 Tc-99 Release from the Unsaturated Zone with All Benchmarking Factors – Base Case	52
Figure PA-5.2-1: Southern Sectors Concentration Comparisons without Benchmarking – Base Case	56
Figure PA-5.2-2: Northern Sectors Concentration Comparisons without Benchmarking – Base Case	57
Figure PA-5.2-3: Southern Sectors Concentration Comparisons with Additional Disposal Unit Contributions – Base Case	58
Figure PA-5.2-4: Northern Sectors Concentration Comparisons with Additional Disposal Unit Contributions – Base Case	59
Figure PA-5.2-5: Southern Sectors Concentration Comparisons with 0.5 Benchmarking Factor – Base Case	61
Figure PA-5.2-6: Northern Sectors Concentration Comparisons with 0.5 Benchmarking Factor – Base Case	62
Figure PA-5.2-7: Southern Sectors Concentration Comparisons with Adjustment for the Flow Divide and Vault 4 Contributions – Base Case	63
Figure PA-5.2-8: Northern Sectors Concentration Comparisons with Adjustment for the Flow Divide and Vault 4 Contributions – Base Case	64
Figure PA-8.1: Example of Hydraulic Degradation for Vault 4 Cementitious Materials in Alternative Sensitivity Case K	77
Figure PA-8.2: Example of Progressive Fracturing Through Time	80
Figure PA-8.3: Conceptual Model of a Degraded Cementitious Material Assuming Equilibrium of Dissolved Species	81
Figure PA-8.4: Single Continuum Model Representation	82
Figure PA-8.5: Effective Sorption Coefficients for Technetium in Partially Oxidized Cementitious Materials	86
Figure PA-8.6: Comparison of Saturated Hydraulic Conductivities of the Lower Lateral Drainage Layer Using Base Case and Case K Time Steps	87
Figure PA-8.7: Alternative Sensitivity Case K 100-Meter Peak Groundwater Pathways Dose by Sector	98
Figure PA-8.8: Alternative Sensitivity Case K Contributors to the Sector B 100-Meter Peak Groundwater Pathways Dose, 20,000 Years	99

Figure PA-8.9: Alternative Sensitivity Case K Contributors to the Sector I 100-Meter Peak Groundwater Pathways Dose, 20,000 Years	99
Figure PA-8.10: Alternative Sensitivity Case K Chronic Intruder Dose at the Vicinity of an SDF Disposal Unit, 20,000 Years	104
Figure PA-9.1: Synergistic Case, Sector B Total Dose Comparison	108
Figure PA-9.2: PA Synergistic Case, Sector B Radionuclide Doses	109
Figure PA-9.3: PA-9 Analysis Case, Sector B Radionuclide Doses	110
Figure PA-9.4: Synergistic Case, Sector I Total Dose Comparison	111
Figure PA-9.5: PA Synergistic Case, Sector I Radionuclide Doses	112
Figure PA-9.6: PA-9 Analysis Case, Sector I Radionuclide Doses	112
Figure PA-10.1: Infiltration Rate from Closure Cap	116
Figure PA-10.2: LLDL Hydraulic Conductivity	117
Figure PA-10.3: Infiltration Rate and Flux through the Saltstone for Vault 4	118
Figure PA-10.4: Infiltration Rate and Flux through the Saltstone for an FDC	119
Figure SP-5.1: Graphical Presentation of Data from Table SP-5.2	172
Figure SP-5.2: Graphical Presentation of Data from Table SP-5.4	174
Figure SP-5.3: Graphical Presentation of Data from Table SP-5.6	176
Figure SP-8.1: Mineralogical Controls on E_h and pH Transitions	184
Figure SP-8.2: Reaction Path Showing Difference in pH if Amorphous Silica is Substituted for Quartz and Quartz is not Allowed to Precipitate	185
Figure SP-8.3: Reaction Paths of Saltstone with Similar Formula but Differing Bulk Densities and Porosities; Saltstone Assumed to React with Groundwater	188
Figure SP-10.1: Pu(IV) and Pu(V) Sorption Edge at 25 hours and Pu(V) at 33 Days on an SRS Subsurface Sandy Sediment	192
Figure SP-19.1: Release of Technetium to the Water Table from Vault 4	219
Figure SP-19.2: Release of Technetium to the Water Table from an FDC	220
Figure SP-19.3: Sector I Dose Comparison for Alternative Sensitivity Case K and Additional K_d Sensitivity Evaluations, to 10,000 Years	221
Figure SP-19.4: Sector I Dose Comparison for Alternative Sensitivity Case K and Additional K_d Sensitivity Evaluations, to 20,000 Years	222
Figure VP-2.1: Plot of Average Carbonation Measurements for P-Reactor Interior and Exterior Specimens Relative to Carbonation Rates of Interior Concrete	227

Figure VP-6.1: Hydraulic Conductivity of Walls for Vaults 1 and 4 and Backfill Soil (PA Analysis).....	240
Figure VP-6.2: Hydraulic Conductivity of Walls for Vaults 1 and 4 and Backfill Soil (Case K).....	241
Figure VP-6.3: Vault 1 Flow Profile through Saltstone and Wall, Base Case and Case K	241
Figure VP-6.4: Vault 4 Flow Profile through Saltstone and Wall, Base Case and Case K	242
Figure FFT-3.1: Adsorption of Selenate on Two Concentrations of Amorphous Iron Oxyhydroxide in 0.1 mol/L KCl as a Function of pH.....	247
Figure II-1.1: Base Case Chronic Intruder Dose at the Vicinity of Vault 4 and an FDC, within 20,000 Years	260

LIST OF TABLES

Table PA-4.1: Radionuclide Summary for PA-4 Sensitivity Runs	24
Table PA-4.2: Case C Model Configurations for PA-4.....	25
Table PA-5-1: GoldSim Files Used in the Benchmarking Analysis.....	32
Table PA-5.1-1: Adjustment Multiplicative Factors for Flow Values	33
Table PA-7.1: PA Maintenance Activities to Address Model Support.....	68
Table PA-8.1: Summary of Alternative Sensitivity Case K Attributes	75
Table PA-8.2: Initial Hydraulic Conductivities and Assumed Degradation Times of Cementitious Materials for Alternative Sensitivity Case K.....	78
Table PA-8.3: Initial Fracture Spacing of Cementitious Materials Assumed for Alternative Sensitivity Case K	80
Table PA-8.4: Updated K_d Values for Backfill and the Vadose Zone.....	89
Table PA-8.5: Saltstone Specific K_d Values	90
Table PA-8.6: Updated K_d Values for Reducing Cementitious Materials.....	91
Table PA-8.7: Updated K_d Values for Oxidizing Cementitious Materials	94
Table PA-8.8: Occurrences of Model Changes by Case for Vault 1	96
Table PA-8.9: Occurrences of Model Changes by Case for Vault 4.....	97
Table PA-8.10: Occurrences of Model Changes by Case for FDCs.....	97
Table PA-8.11: 100-Meter MOP Peak Groundwater Pathways Dose by Sector	100
Table PA-8.12: 100-Meter MOP Peak Groundwater Pathways Dose in 10,000 Years.....	101
Table PA-8.13: 100-Meter MOP Peak Groundwater Pathways Dose in 20,000 Years.....	101
Table PA-8.14: Peak 10,000 Year Chronic Intruder Dose, Vault 4 Contributors	103
Table PA-8.15: Peak 10,000 Year Chronic Intruder Dose, FDC Contributors	103
Table PA-9.1: Radionuclide Summary for PA-9 Sensitivity Runs.....	107
Table PA-9.2: Model Configurations for PA-9	108
Table PA-11.1: Preliminary SDF PA Alternate Modeling Case Probabilities	123
Table PA-11.2: Final SDF PA Alternate Modeling Case Probabilities	124
Table PA-11.3: Remaining Stochastic Elements within the Probabilistic SDF Model	125
Table PA-13.1: Cementitious Material Parameters	132
Table PA-13.2: Time for Oxygen Diffusion through Saltstone and Vault Concrete	132

Table IN-4.1: Vault 4 and FDC Drainage System Volumes.....	141
Table IEC-7.1: SDF Closure Cap Layer Nominal Saturation with Time.....	152
Table IEC-7.2: Average Annual Head on SDF Closure Cap HDPE Geomembrane ..	153
Table IEC-8.1: Hydraulic Parameters for Lower Lateral Drainage Layer.....	157
Table IEC-8.2: Vault 1 Lower Drainage Layer Darcy Velocity and Flow Budget	158
Table IEC-8.3: Vault 4 Lower Drainage Layer Darcy Velocity and Flow Budget	158
Table IEC-8.4: FDC Lower Drainage Layer Darcy Velocity and Flow Budget	159
Table SP-5.1: Saltstone ARP/MCU Simulant Grout Mixes Tested Without CSSX Solvent and Admixtures	171
Table SP-5.2: Measured Saturated Hydraulic Conductivity for ARP/MCU Simulated Saltstone Grout with Varying Water to Premix Ratio	172
Table SP-5.3: Saltstone Simulant ARP/MCU Grout Mixes Tested With CSSX Solvent and Admixtures	173
Table SP-5.4: Measured Saturated Hydraulic Conductivity for ARP/MCU Simulant Saltstone Grout with Organics and Admixtures	174
Table SP-5.5: Additional Saltstone Simulant Grout Mixes Tested.....	175
Table SP-5.6: Measured Hydraulic Conductivity for Additional Simulated ARP/MCU, DDA, and SWPF Saltstone Grout	176
Table SP-5.7: Linear and Logarithmic Regression Fits for Each Sample Set	178
Table SP-8.1: Minerals Allowed in GWB Simulations.....	183
Table SP-8.2: Mineralogy Input into GWB and the Re-calculated Mineralogy	185
Table SP-8.3: Alternative Mineralogy Calculated from the same Saltstone Formula	186
Table SP-8.4: Mineralogy of Similar Saltstone Formula with Different Bulk Densities	186
Table SP-8.5: E_h and pH Transitions in Pore Volumes for Different Bulk Densities and Porosities.....	189
Table SP-13.1: Selected K_d Value for All Elements Evaluated in the PA	199
Table SP-13.2: Selected K_d Value for All Elements Evaluated in Alternative Sensitivity Case K	201
Table SP-13.3: Radionuclide Ranking by Total Biosphere Influence	204
Table FFT-3.1: Z-Area Well pH Data Averaged by Year	248
Table FFT-3.2: Z-Area Well pH Data by Sampling Period.....	248
Table II-1.1: Darcy Velocity below a Disposal Unit at the Water Table.....	258

Table II-1.2: Peak Dose Contributors to the Chronic Intruder for the Base Case Near Vault 4 within 10,000 Years.....	259
Table II-1.3: Peak Dose Contributors to the Chronic Intruder for the Base Case Near an FDC within 10,000 Years.....	259
Table B-2.1: Bioaccumulation Factors for Vegetable, Milk, Beef, and Fish Pathways	269
Table B-2.2: Bioaccumulation Factors for Chicken and Egg Pathways.....	270
Table B-2.3: Ingestion Dose Conversion Factors.....	271
Table B-2.4: Peak Dose to the MOP in Sectors B and I from Egg and Chicken Ingestion for Base Case	272
Table B-2.5: Contribution to the Peak Dose in Sectors B and I from the Egg and Chicken Ingestion Pathways	273
Table B-2.6: Peak Dose to the MOP in Sectors B and I from Egg and Chicken Consumption Pathways with Dirt Consumption by Chickens	274
Table B-3.1: Soil Build-up Factors for Various Parameters	277
Table B-5.1: Peak Dose Comparison Based on 75 % and 87 % of the Water Ingested from the 100-Meter Well for the MOP in Sector B	282
Table B-5.2: Peak Dose Comparison Based on 75 % and 87 % of the Water Ingested from the 100-Meter Well for the MOP in Sector I.....	283
Table C-0.1: Status of Clarifying Question Comments for RAI-2009-01.....	287

ACRONYMS

ALARA	As Low As Reasonably Achievable
ARP	Actinide Removal Process
CPT	Cone Penetrometer Test
CSH	Calcium Silicate Hydrate
CSSX	Caustic Side Solvent Extraction
DBE	Design Basis Earthquake
DDA	Deliquification, Dissolution, and Adjustment
DF	Decontamination Factor
DOE	U.S. Department of Energy
EIS	Environmental Impact Statement
EPA	U.S. Environmental Protection Agency
FDC	Future Disposal Cell
FTF	F-Area Tank Farm
GCL	Geosynthetic Clay Liner
GSA	General Separations Area
GW	Groundwater
GWB	Geochemist's Workbench
HDPE	High Density Polyethylene
HELP	Hydrologic Evaluation of Landfill Performance Model
IAEA	International Atomic Energy Agency
LLDL	Lower Lateral Drainage Layer
LLW	Low-Level Waste
LW	Liquid Waste
MCC	Moisture Characteristic Curve
MCU	Modular Caustic Side Solvent Extraction Unit
MOP	Member of the Public
MSL	Mean Sea Level
NDAA	Ronald W Reagan National Defense Authorization Act (NDAA) for Fiscal Year 2005
NRC	U.S. Nuclear Regulatory Commission
NRMP	Natural Resources Management Plan
PA	Performance Assessment
PNNL	Pacific Northwest National Laboratory

PV	Pore Volume
PVC	Polyvinyl Chloride
QA/QC	Quality Assurance/Quality Control
RAI	Request for Additional Information
SA	Special Analysis
SCDHEC	South Carolina Department of Health and Environmental Control
SDF	Saltstone Disposal Facility
SPF	Saltstone Production Facility
SPT	Standard Penetration Test
SRR	Savannah River Remediation LLC
SRS	Savannah River Site
SWPF	Salt Waste Processing Facility
TER	Technical Evaluation Report
UDQE	Unreviewed Disposal Question Evaluation
ULDL	Upper Lateral Drainage Layer
USACE	U.S. Army Corp of Engineers
USDA	U.S. Department of Agriculture
UTR	Upper Three Runs
UTR-LZ	Upper Three Runs-Lower Zone
WAC	Waste Acceptance Criteria

Executive Summary

The *Performance Assessment for the Saltstone Disposal Facility at the Savannah River Site* (SRR-CWDA-2009-00017) was prepared to inform decisions regarding the pertinent requirements of the U.S. Department of Energy's Manual 435.1-1, *Radioactive Waste Management*, and Title 10 Code of Federal Regulations Part 61, *Licensing Requirements for Land Disposal of Radioactive Waste*, Subpart C as required by the *Ronald W. Reagan National Defense Authorization Act (NDAA) for Fiscal Year 2005*, Section 3116. Requirements in DOE M 435.1-1 and 10 CFR 61 stipulate that a PA should provide reasonable assurance that disposal of Low-Level Waste will comply with specified performance objectives. DOE M 435.1-1 also requires assessments for impacts to water resources. These assessments were performed to address a 10,000-year performance period after facility closure (which encompasses the DOE M 435.1-1 1,000-year compliance period).

The SDF PA serves as the primary long-term risk assessment tool to determine that performance objectives will be met following closure of the SDF. The SDF PA is a performance-based, risk-informed analysis of the fate and transport of SDF waste following final closure of SDF. The DOE used what is referred to as a "hybrid approach" involving a combination of deterministic and probabilistic models to develop this level of assurance. The foundation of the SDF assessment is the "Base Case" model, a deterministic analysis of post-SDF closure that utilizes the best-available, best-estimate values for the parameters within the SDF PORFLOW model. This deterministic analysis produces a single discrete value at each point of assessment that, in turn, can be compared directly to the 10 CFR 61.41 performance objective of 25 mrem/yr peak dose and the 10 CFR 61.42 inadvertent intruder dose. The understanding of the results of the SDF PA is further enhanced through an extensive series of uncertainty analyses and sensitivity analyses.

The deterministic Base Case of the SDF PA was developed using reasonably conservative, best-estimate assumptions (i.e., most probable modeling parameters) whenever possible. As a hybrid approach, the deterministic Base Case model is accompanied by the probabilistic model and deterministic alternative modeling cases, which are provided as tools to inform on uncertainty associated with the Base Case as a whole. These additional models employed assumptions that were possible on an individual assumption basis (although less probable than the Base Case and often non-mechanistic when coupled with other assumptions) to assess the effects of deviations from the best-estimate Base Case assumptions. The fact that Base Case values have uncertainty associated with them does not a priori make them incorrect or any less probable. Substituting only pessimistic values for every assumption to account for uncertainty would undercut the intent of the Base Case in supporting risk-based decision making and would likely result in little, if any, real risk reduction, in needless expenditures, exposure to the current SRS workforce, and delays in risk-reducing waste tank closure activities. The application of the hybrid approach to PA development (i.e., including a probabilistic model and deterministic alternative modeling cases) was to allow for the less probable, but still possible, assumptions to be modeled, improving overall understanding of the SDF system.

For the SDF system, a performance period of 10,000 years was considered reasonable when assessing compliance with the 10 CFR 61, Subpart C performance objectives related to future hypothetical members of the public and inadvertent intruders and is consistent with NRC guidance (NUREG-1854, page 4-3). To account for variability and uncertainty regarding the timing of barrier failures, DOE provided extensive discussion on doses for periods up to 20,000 years following closure of the SDF and performed analyses beyond 20,000 years to gain a better understanding of the closed system performance and radionuclide transport. DOE M

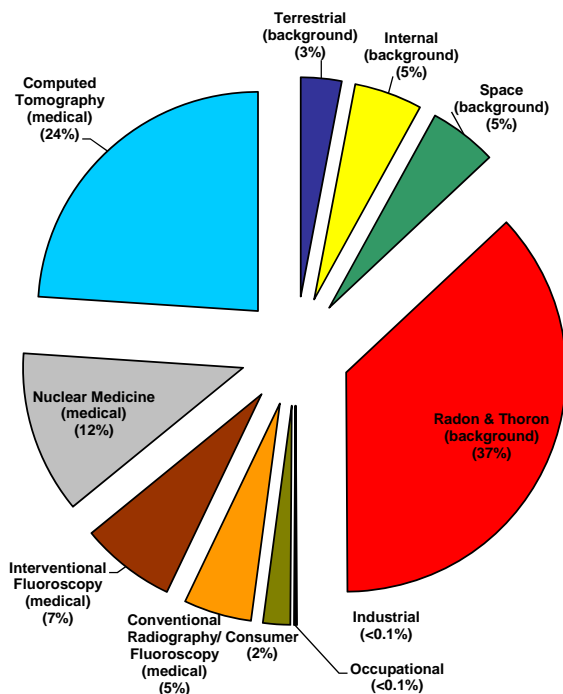
435.1-1 (page IV-11) requires PAs to “include calculations for a 1,000-year period after closure...”

As described above, in developing the deterministic Base Case assumptions, DOE sought to develop a conceptual model of the SDF system and surrounding General Separations Area that reflects the best available or best estimate values, and includes reasonably conservative modeling assumptions including inventory assignments. In developing these values, DOE did not seek to create artificially pessimistic assumptions that bound possible, but not probable, scenarios. Instead, DOE sought a risk-informed analysis that provides information to feed critical closure decisions associated with the SDF.

In support of the development of the SDF PA, DOE has made a significant investment in research and conceptual model development, utilizing nationally recognized experts in their respective fields including cementitious materials, hydrogeology, and modeling of environmental transport. The fate and transport modeling in the SDF PA reflects approximately 60 years of study of the subsurface of the GSA. It is this strong foundation of research and study that provides DOE reasonable assurance that the 10 CFR 61.41 and 10 CFR 61.42 performance objectives will be met during the 10,000-year performance period.

Some perspective should be put on the 25 mrem/yr dose objective used to demonstrate compliance with the performance objectives for the protection of the general population from releases of radioactivity (10 CFR 61.41). It should be noted that the average annual dose to a United States citizen in 2007 was 620 millirems, approximately 25 times higher than the 10 CFR 61.41 performance objectives. Figure EX-1 provides a breakdown of the exposure sources that make up the average dose of 620 millirems. If an individual moves from the area surrounding SRS to Denver, Colorado, their annual dose from just cosmic and terrestrial background radiation alone will increase by more than 100 millirem; a value four times the performance objective. [NCRP-160] Further, as noted in the NRC Fact Sheet on *Biological Effects on Radiation*, “Those people living in areas having high levels of background radiation – above 1,000 mrem (10 mSv) per year – such as Denver, Colorado, have shown no adverse biological effects.” [NRC_01-01-2011] A background dose of 1,000 mrem/yr represents a dose 40 times greater than the 10 CFR 61 performance objectives.

Figure EX-1: Major Sources of Radiation Exposure to the Average US Citizen



[NCRP-160]

The DOE response to RAI PA-8 provides additional discussion on the SDF PA approach and the uncertainty and sensitivity analyses modeling that were performed to provide additional potential system performance information. This response evaluates the impact on dose resulting from deviations from the Base Case through a non-mechanistic modeling case (Alternative Sensitivity Case K). This modeling case was developed as a supplement to the Single Parameter Sensitivity Analysis presented in SDF PA Section 5.6.6. Alternative Sensitivity Case K is not considered a likely alternate scenario; however, it was developed to provide additional information regarding the impacts when multiple barriers of concern are modified simultaneously following extensive discussions with the NRC. [WDPD-11-65] Alternative Sensitivity Case K should not be construed as representing an expected physical reality, but instead reflects the potential impact on system performance and the estimated contaminant release and resulting radiological dose when conservative, non-mechanistic degradation of barriers is postulated.

Alternative Sensitivity Case K is constructed in such a way as to improve the general understanding of the impacts due to physical degradation of cementitious materials through time, as well as other concerns raised by the NRC in the RAIs. The peak MOP dose within the 10,000-year period of performance for Alternative Sensitivity Case K is 13 mrem/yr around year 9,000 (see Figure PA-8.9). This peak dose is less than the 25 mrem/yr performance objective (10 CFR 61.41).

DOE acknowledges that the PA should contain adequate technical bases to support the Base Case, being the most likely modeling case and that the PA should appropriately reflect uncertainties to demonstrate with reasonable assurance that the performance objectives can be met. DOE believes that the PA provides information regarding both the expected (i.e., probable) results (reflected in the Base Case analyses) and the alternative cases (reflected in the sensitivity analyses). The SDF system has defense in depth through multiple barriers that

provide reasonable assurance that compliance with the performance objectives will be achieved. DOE clarifies that reasonable assurance is based on evaluations of how the facility is expected (i.e., most likely) to perform (Base Case, Case A) as well as alternative system performance evaluations (i.e., less likely) that encompass uncertainty and variability (uncertainty and sensitivity analyses, All Cases peak of the mean dose results).

The DOE M 435.1-1, *Radioactive Waste Management*, outlines a comprehensive program to maintain PAs. The program is in place to evaluate changes (e.g., new information, changing facility conditions) that could impact the inputs, results, or conclusions of a DOE PA such as the SDF PA. The program requires that PAs be formally reviewed on an annual basis and revised when changes in radionuclide inventories or facility design are identified or new information on key parameters becomes available through continued research and study. On an annual basis, the adequacy of the SDF PA will be assessed and, when warranted, will be revised and shared with the NRC through the NDAA Section 3116(b) monitoring protocols.

This document represents the second of two packages of responses to the comments transmitted via the *Second Request for Additional Information for the 2009 Performance Assessment for the Saltstone Disposal Facility at the Savannah River Site*, dated December 15, 2010. [ML103400571] The first package included the responses to the following RAIs:

PA-6	IN-5	SP-14	VP-5	FFT-1	B-1	C-8
PA-12	IN-6	SP-15		FFT-2	B-2	C-22
PA-13		SP-18			B-3	C-23
					B-4	
					B-5	

This second submittal, SRR-CWDA-2011-00044, Revision 1, includes responses to the remaining RAIs as well a few minor changes to some of the responses from the first submittal package incorporating direct feedback from the NRC staff.

Performance Assessment Methods (PA)

PA-1

Comment:

The contribution of individual radionuclides to the dose was not provided for several deterministic sensitivity cases.

NRC Response:

The answer to this RAI was adequate.

PA-2

Comment:

Probabilistic sensitivity analyses were not provided for cases representing bulk saltstone degradation.

NRC Response:

The answer to this RAI was adequate, but note that the NRC staff have concerns about the methodology used in the GoldSim analyses (see PA-11).

PA-3

Comment:

The determination of key radionuclides described in Section 5.2.2 of the PA may not have captured all of the risk significant radionuclides. The determination of key radionuclides is significant to the results of the PA because many of the analyses used to support the PA only include the key radionuclides (e.g., the PORFLOW analyses for Cases B-E).

NRC Response:

The NRC discussion on PA-3 has been combined with PA-4. See below for details.

PA-4

Comment:

Benchmarking based only on key radionuclides identified in the base case analysis does not provide adequate support for the interpretation of alternate-case GoldSim model results.

DOE Response Discussion:

In the DOE RAI response for PA-3, DOE indicated that the inventory list used in the GoldSim model included the less mobile radionuclides even if they were not determined to be key radionuclides. This aspect of the response was adequate.

However the response went on to indicate that the dose comparisons for the three key radionuclides Ra-226, Tc-99, and I-129 show good agreement, providing assurance that the behavior of additional radionuclides simulated in the GoldSim model for alternate cases is appropriate. NRC disagrees with this conclusion for two reasons. First, the code comparisons do not show particularly good agreement. The charts are presented with logarithmic scales starting from very low values. The many order of magnitude presentation of very low fluxes and concentrations makes the peak differences appear to be smaller. Examination of the flux curves for the radionuclides that have been benchmarked show differences of a factor of 10 to 30 or more, depending on the time period selected. The confidence in the non-benchmarked GoldSim radionuclides should necessarily be less than this, because they have not undergone the benchmarking exercise. Second, as discussed below for comment PA-5, the benchmarking process itself is not sufficiently transparent to allow NRC to have confidence in the adjustments that were made.

Path Forward:

The following options represent acceptable approaches to addressing this issue:

- 1) Perform a blind comparison of some radionuclides not included in the previous benchmarking (such as Np-237, Pb-210, U-234) for PORFLOW and GoldSim results for some alternate cases to demonstrate the level of confidence that should be assigned to non-benchmarked radionuclides. The blind comparison would be done by running each model for given radionuclides without iteration on benchmarking factors
- 2) Perform PORFLOW analyses with the additional radionuclides for the alternate cases.
- 3) Incorporate an appropriate amount of uncertainty in conclusions regarding the non-benchmarked radionuclides in the alternate cases (least recommended) that factors in the level of agreement achieved between the GoldSim and PORFLOW results and that the additional radionuclides will not have been benchmarked.

Response PA-4:

The initial responses to PA-3 and PA-4 focused on the results of the benchmarking analyses conducted during the development of the PA to justify the selection of the Key Radionuclides presented in SDF PA Section 5.2.2. Also included in the initial response to PA-4 was an analysis that evaluated the significant difference between the mean dose to the MOP for Case C computed via the GoldSim transport model, and the deterministic Case C dose result based on the PORFLOW model. This evaluation indicated that the much greater dose from the GoldSim transport model is attributed to the difference in the modeling of Case C between

GoldSim and PORFLOW and the selection of distribution coefficients (K_d values) in soil for plutonium during the stochastic analysis conducted within GoldSim.

To validate further the selection of radionuclides in SDF PA Section 5.2.2, DOE re-evaluated Case C with additional radionuclides via the PORFLOW model used in the SDF PA. The results of the sensitivity analysis presented in SDF PA Section 5.6.5.3 and SDF PA Table 5.6-15 indicate that K_d values associated with plutonium in soils are sensitive parameters to the MOP dose for Case C. However, the isotopes of plutonium were not considered key radionuclides in SDF PA Section 5.2.2. The focus of this RAI response is addressing concerns related to conclusions based on benchmarking results using only the key radionuclides; the response to PA-5 discusses the process used to develop the benchmark model.

Additional Radionuclides Considered

Originally (in the SDF PA), Case C was run with seven radionuclides as input, I-129, Np-237, Pu-238, Tc-99, Th-230, U-234, and U-235. For this new run, 20 radionuclides were used as input, Am-241, Am-243, Cm-244, Cm-245, Cs-135, I-129, Nb-93m, Np-237, Pu-238, Pu-239, Pu-240, Pu-241, Pu-244, Tc-99, Th-229, Th-230, U-233, U-234, U-235, and U-238. The additional radionuclides were chosen as input to the PORFLOW run for further comparison of the PORFLOW deterministic model to the benchmarked GoldSim transport model.

Table PA-4.1 provides a summary of the radionuclides considered. In this table, the initial inventory set is identified as “input” and the resulting output concentration set is identified as “output.” “PA Case C” refers to Case C described in SDF PA Section 4.4.2; and “PA-4 Case C” refers to the new runs performed for this analysis, as described below. Note that the PA-4 radionuclide sets do not include every radionuclide that was considered during the development of the Base Case (as described in Section 3.3 of the SDF PA). These radionuclide sets were determined based on the dose results from the GoldSim transport model that was run in deterministic mode for Case C.

Modeling Cases

In addition to the SDF PA Case C and the Benchmark Case C models, an additional GoldSim dose calculator model file was generated as part of this analysis. This additional model file used the PORFLOW concentration results based on PA-4 Case C. The GoldSim dose calculator model developed for the SDF PA is used in the PA-4 Case C analysis. For clarity, Table PA-4.2 defines each of these modeling cases.

Table PA-4.1: Radionuclide Summary for PA-4 Sensitivity Runs

Radionuclide	PA Case C Input	PA Case C Output	PA-4 Case C Input	PA-4 Case C Output
Ac-227		X		X
Am-241			X	X
Am-243			X	X
Cm-244			X	X
Cm-245			X	X
Cs-135			X	X
I-129	X	X	X	X
Nb-93m			X	X
Np-237	X	X	X	X
Pa-231		X		X
Pb-210		X		X
Pu-238	X	X	X	X
Pu-239			X	X
Pu-240			X	X
Pu-241			X	X
Pu-244			X	X
Ra-226		X		X
Ra-228				X
Rn-222		X		X
Tc-99	X	X	X	X
Th-229		X	X	X
Th-230	X	X	X	X
Th-232				X
U-233		X	X	X
U-234	X	X	X	X
U-235	X	X	X	X
U-236				X
U-238			X	X

Table PA-4.2: Case C Model Configurations for PA-4

Model Configuration	Description
PA Case	Recreates the deterministic PORFLOW results from PA Case C using the GoldSim dose calculator developed for the SDF PA.
PA-4 Case	Identical to PA Case C (above), but includes additional radionuclides as identified in Table PA-4.1.
Benchmark	The GoldSim transport model benchmarked to PORFLOW as described in PA Section 5.6.2.3 with dose results presented in PA Section 5.6.2.3.6.

Note: Although PORFLOW was run for all 12 sectors (A through L), the GoldSim dose calculator was only performed on six sectors (A, B, C, H, I, and J). Previous PORFLOW modeling indicated that the maximum doses were always from Sector B or Sector I (see SDF PA Table 5.6-16). Therefore, calculating dose from these two sectors along with their adjacent sectors captures the maximum peak dose.

The following discussion compares the Case C dose results from the deterministic PORFLOW models and the benchmarked GoldSim transport model that are defined in Table PA-4.2. Note that Section 5.6.2.1 of the SDF PA acknowledged that it is not expected that the PORFLOW model results and the benchmark model results “will be identical because there are fundamental differences in modeling platforms and differences in model approach.” Even with the fast flow paths modeled for Case C, these differences do not significantly influence the benchmarking results shown in SDF PA Figure 5.6-19 until approximately 16,000 years after closure, which is well beyond the 10,000-year period of performance.

Case C Comparisons, Sector B

Figure PA-4.1 provides a total MOP dose comparison in Sector B for Case C, based on the various model configurations described in Table PA-4.2. As expected, the PA-4 Case C results with the additional radionuclides (blue curve) show a much closer agreement to the Benchmark Case C results (red curve) than the initial PA Case C results (purple curve). As described in SDF PA Section 5.6.2.3.6, the “upswing” at the end of the dose curve shown in the Benchmarking model is from plutonium contributions to dose. The Benchmark Case C model assumes a direct mass transfer pathway from the saltstone waste form to the unsaturated zone; therefore, despite the high K_d value in the disposal unit wall and floor, plutonium is transported through the system much faster in the simplified benchmarking case (in GoldSim) than in the more complex PA-4 model (in PORFLOW). The PORFLOW model significantly retards transport as mass passes through the disposal unit wall and floor; however, the GoldSim model is conceptually different in that mass release from the saltstone bypasses the disposal unit wall and floor. As illustrated in Figure PA-4.1, the “upswing” in the dose also appears in the PA-4 Case as expected when additional radionuclides were included in the PORFLOW run.

Figure PA-4.1: Case C, Sector B Total Dose Comparison

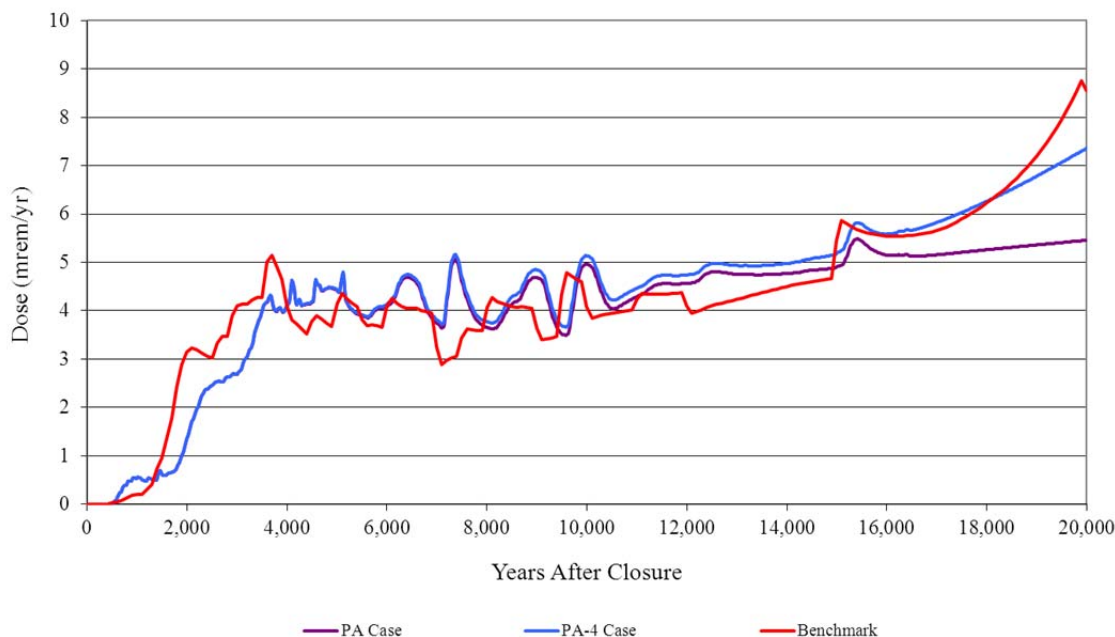


Figure PA-4.2 focuses on the time period after 14,000 years to illustrate the significant dose contributors to the PA-4 Case and compares the PA-4 total MOP dose to the total MOP dose from the Benchmark Case. Likewise, Figure PA-4.3 focuses on the time period after 14,000 years to illustrate the significant dose contributors to the Benchmark Case and compares the Benchmark total MOP dose to the total MOP dose from the PA-4 Case. Figure PA-4.2 illustrates that the results of the PORFLOW model are not significantly impacted by the inclusion of the additional radionuclides. Of the additional radionuclides analyzed in the PORFLOW PA-4 Case, only Pu-239 provides any appreciable additional contribution to the MOP dose. The remaining additional radionuclides analyzed in the PORFLOW PA-4 Case did not significantly contribute to the MOP dose.

Comparing Figures PA-4.2 and PA-4.3 illustrates that the difference between the PORFLOW results and the GoldSim results is indicative of the conceptual differences between the two models on the mass release path and not the exclusion of specific radionuclides in the PORFLOW analysis conducted in support of the SDF PA. Because of the mass release path modeled in GoldSim, the release of I-129 occurs earlier than in the PORFLOW model and thus does not appear in Figure PA-4.3 and Pu-240 appears in the GoldSim model (as seen in Figure PA-4.3) but it does not appear in the PORFLOW model (as seen in Figure PA-4.2).

Figure PA-4.2: Dose Contributors for PA-4 Case and Comparison of Total Dose with the Benchmark Case (Sector B)

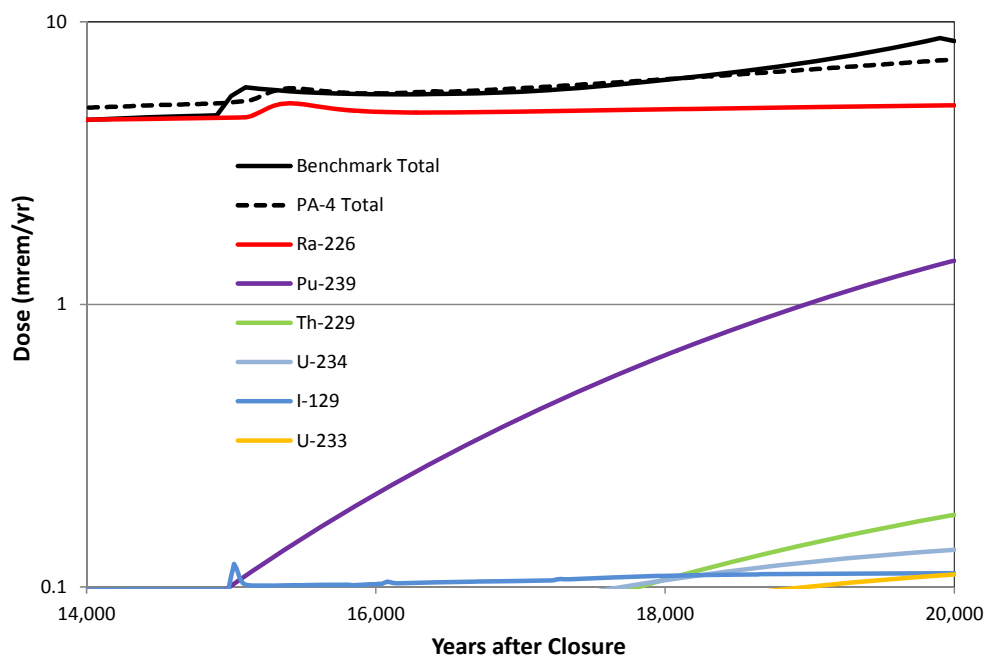
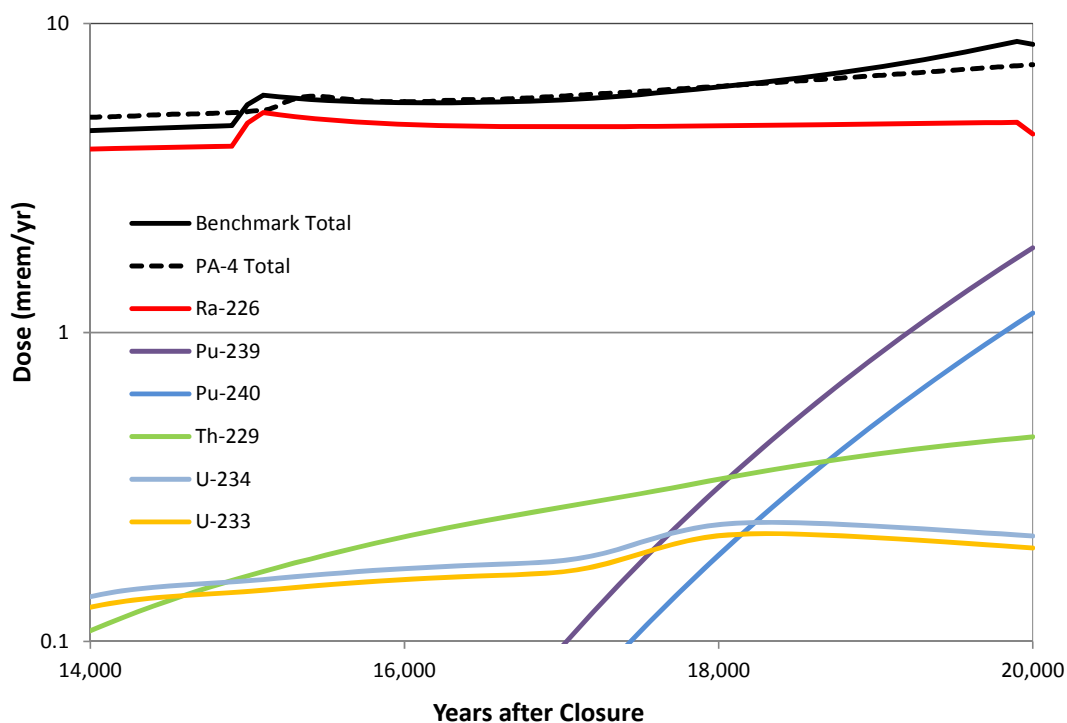


Figure PA-4.3: Dose Contributors for Benchmark Case and Comparison of Total Dose with the PA-4 Case (Sector B)



Case C Comparisons, Sector I

Figure PA-4.4 provides a total MOP dose comparison in Sector I for Case C, based on the various model configurations identified in Table PA-4.2. Unlike the results presented for Sector B, the inclusion of the additional radionuclides (PA-4 Case) has no appreciable impact on the MOP total dose in Sector I. The PA-4 Case C results with the additional radionuclides (blue curve) shows only a small increase in the dose presented for the initial PA Case C results (purple curve). The significant “upswing” of the total dose from the Benchmark Case C results (red curve) is not present in the PA-4 results with the additional radionuclides. The dose to the MOP in Sector I is dominated by the FDCs; therefore, the conceptual difference between the GoldSim and the PORFLOW models on the mass release path is accentuated by the multiple FDCs that contribute to the release. Thus, there is a significantly greater release of the slower moving radionuclides (e.g., Pu-239) from the GoldSim transport model compared to the PORFLOW model.

Figure PA-4.4: Case C, Sector I Total Dose Comparison

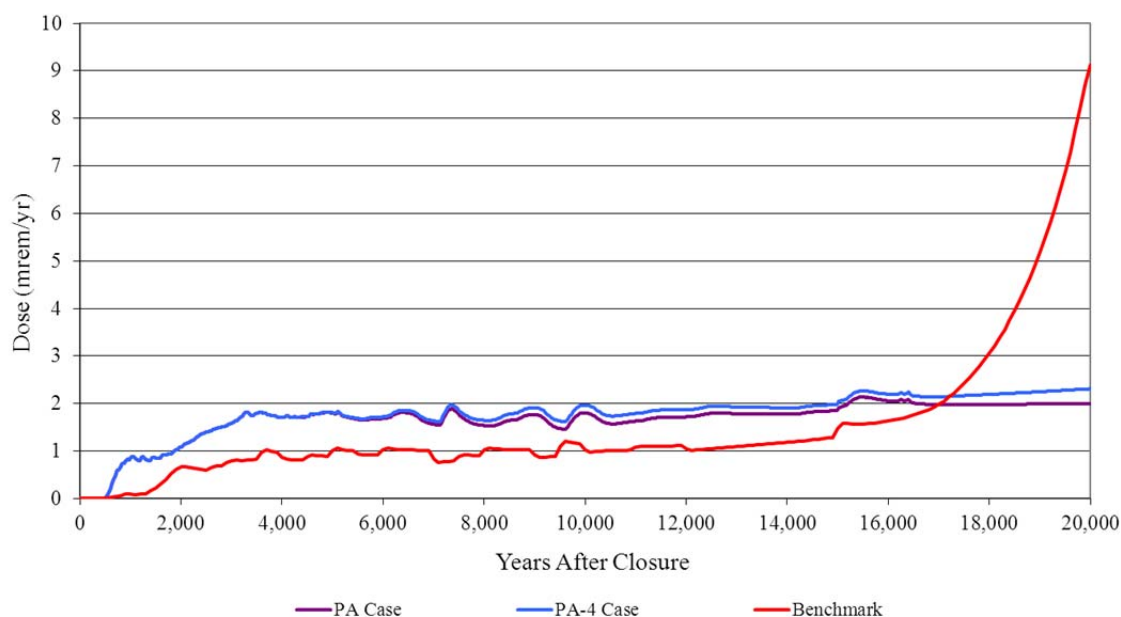


Figure PA-4.5 focuses on the time period after 14,000 years to illustrate the significant dose contributors to the PA-4 Case and compares the PA-4 total MOP dose to the total MOP dose from the Benchmark Case. Likewise, Figure PA-4.6 focuses on the time period after 14,000 years to illustrate the significant dose contributors to the Benchmark Case and compares the Benchmark total MOP dose to the total MOP dose from the PA-4 Case. Figures PA-4.4 and PA-4.5 illustrate that the results of the PORFLOW model are not significantly impacted by the inclusion of the additional radionuclides. Figure PA-4.5 indicates that Cs-135, Pu-239, and Th-229 provide the majority of the additional contribution to the MOP dose (approximately 0.3 mrem/yr additional dose of the total 2.3 mrem/yr at 20,000 years), with Ra-226 and I-129 still the major contributors to the dose. On the other hand, Figure PA-4.6 illustrates that Pu-239 and Pu-240 are the significant contributors to the MOP dose (approximately 7 mrem/yr of the total dose of approximately 9 mrem/yr) from the Benchmark run.

Comparing Figures PA-4.5 and PA-4.6 illustrates that the difference between the PORFLOW and the GoldSim results is indicative of the differences between the two models and not the exclusion of specific radionuclides in the PORFLOW analysis conducted in support of the SDF PA. Because of the mass release path modeled in GoldSim, the release of I-129, Cs-135, Pb-210, and Tc-99 occur earlier than in the PORFLOW model and thus they do not appear in Figure PA-4.6. The radionuclides with significant delay via large K_d values for the cementitious materials (e.g., plutonium and uranium) appear in the GoldSim model (as seen in Figure PA-4.6) but they do not appear in the PORFLOW model (as seen in Figure PA-4.5) because of the difference in the mass release path models between PORFLOW and GoldSim.

Figure PA-4.5: Dose Contributors for PA-4 Case and Comparison of Total Dose with the Benchmark Case (Sector I)

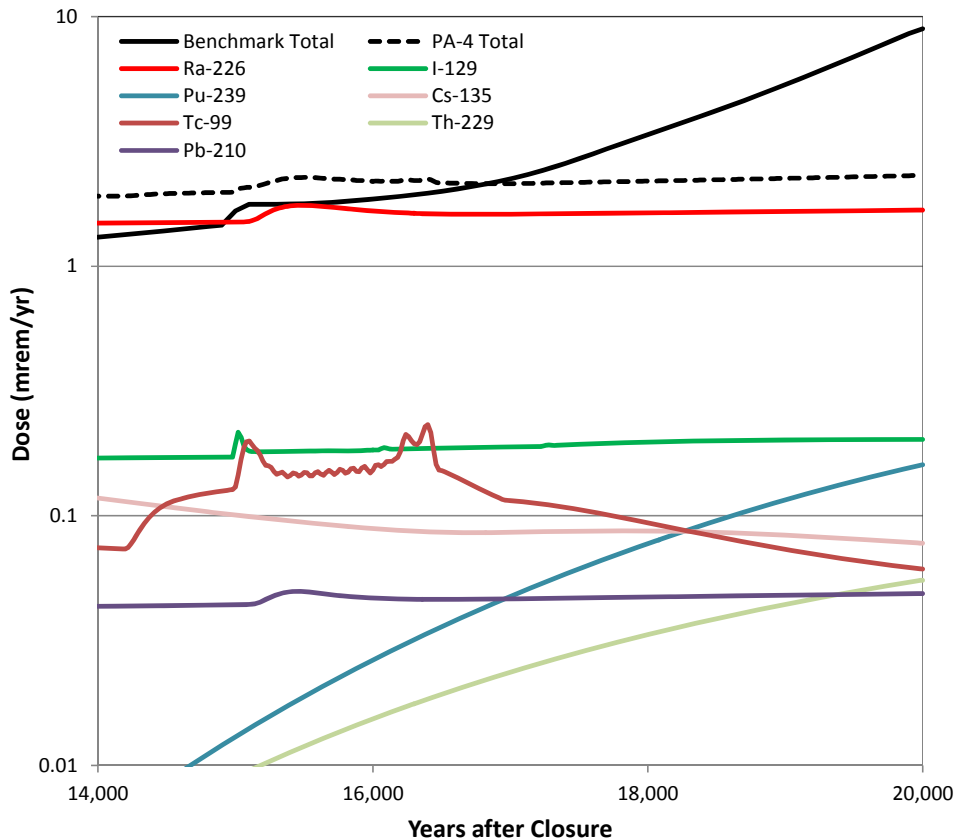
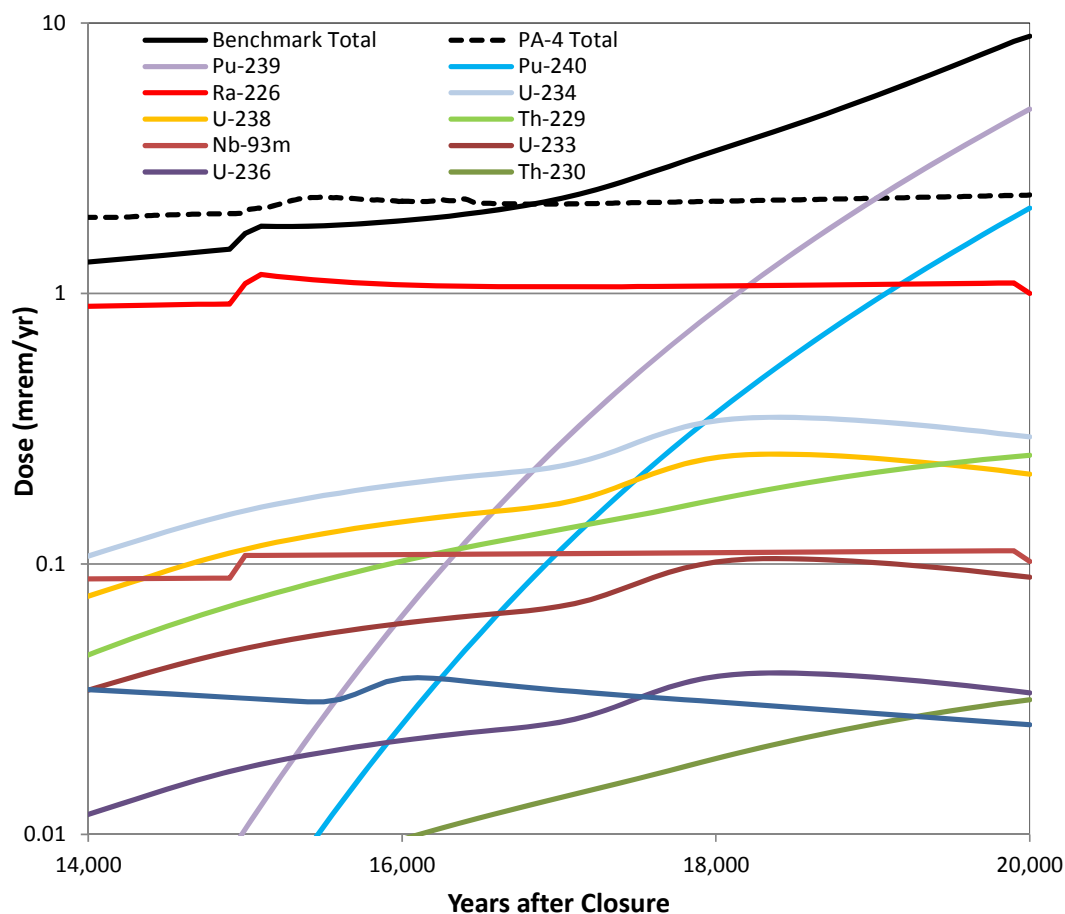


Figure PA-4.6: Dose Contributors for the Benchmark Case and Comparison of Total Dose with the PA-4 Case (Sector I)



Conclusions

The figures presented indicate that the variability between the modeled results was due to conceptual differences between the two models on the mass release path, rather than the selection of radionuclides modeled.

PA-5

Comment:

Additional information is needed about the benchmarking factors and other GoldSim parameter adjustments based on benchmarking to the PORFLOW model.

DOE Response Discussion:

DOE provided additional information discussing the changes that were made in the benchmarking exercise including the basis for some of the changes. The modifications made to account for the different release modeling of Tc was clear, as was the need to make modifications based on the different dimensionality of the flow fields. However, DOE did not sufficiently address the modifications to the saturated zone in reference to the PORFLOW “dilution” provided in the original NRC comment.

Although the PORFLOW model is being used for the base (compliance) case, the GoldSim model is used to understand the impact of key uncertainties. Some of those uncertainties, as discussed above, NRC believes should be represented in the base case. Conceptually, the benchmarking process was used to achieve better agreement between the results for the different models. The NRC concern is if the modifications cannot be clearly explained as having a physical basis tied to the conceptual representation of the two different models, then neither model representation may have sufficient predictive power of the future risks from the disposal facility. The benchmarking should increase confidence that each calculation appropriately represents the physical processes and therefore that the risks to future receptors has been appropriately estimated, and it should not be an exercise in getting the results of computer programs to match.

Path Forward:

Provide greater transparency in the benchmarking adjustments. For example, one acceptable approach would be to provide a comparison of the results (unbenchmarked) then a stepwise comparison after each benchmarking change, with each change linked to the conceptual model explaining the physical basis for the change. A diagram of the model, such as a cross section, with the benchmarking changes and the magnitude of the changes would be very useful to help the NRC develop the confidence in the benchmarked model results that the DOE has.

RESPONSE PA-5:

As stated in the Executive Summary, DOE believes that the PA provides information regarding both the expected (i.e., probable) results (reflected in the Base Case analyses) and the alternative cases (reflected in the sensitivity analyses). The SDF system has defense in depth through multiple barriers that provide reasonable assurance that compliance with the performance objectives will be achieved. DOE clarifies that reasonable assurance is based on evaluations of how the facility is expected (i.e., most likely) to perform (Base Case, Case A) as well as alternative system performance evaluations (i.e., less likely) that encompass uncertainty and variability. The GoldSim transport model is one of the tools used by DOE to conduct these alternative system performance evaluations.

NRC Comment PA-5 indicates that greater transparency is needed in the benchmarking exercise between the SDF sensitivity/uncertainty analysis GoldSim model and the SDF PORFLOW model. In support of the response to Comment PA-5, unbenchmarked results are presented along with a stepwise comparison after each benchmarking change. In addition, more detail is provided with respect to what differences in the two models could require these changes. The benchmarking process entailed the application of additional factors within the

GoldSim model in the attempt to reconcile fundamental modeling differences between the PORFLOW and GoldSim models. In the following discussion, the physical basis to support the value of a specific benchmarking factor is provided, when one exists. For a number of benchmarking factors their values were determined by trial and error to improve the comparison between unsaturated zone releases from the PORFLOW and GoldSim models. They were adjusted later to improve the comparisons between the dose results at the 100-meter boundary.

As noted in the previous comment response matrix for NRC RAIs on the SDF (SRR-CWDA-2010-00033 Revision 1), the benchmarking between the PORFLOW and GoldSim models was conducted in two phases. The two phases included: 1) comparing the radionuclide releases from the unsaturated zone into the saturated zone for each unit type and 2) comparing concentrations at the 100-meter boundary for each of the sectors. Note that for the saturated zone comparisons at the 100-meter boundary, the benchmarking factors used in the disposal unit and unsaturated zone transport calculations were left unchanged so that the saturated zone benchmarking analysis could be viewed in the same context that it was performed. In addition, note that the order with which the benchmarking factors are added back into the calculations does not necessarily reflect the order in which the benchmarking was actually performed. Table PA-5.1 contains the simulation file names used in this analysis, associated benchmark factors removed, and the figures generated from the simulation. The analysis simulations were generated by the removal of single or sets of benchmarking factors as noted in Table PA-5.1. For clarity, the analysis is described in the opposite order, starting from the simulation with all benchmarking factors removed.

Table PA-5-1: GoldSim Files Used in the Benchmarking Analysis

GoldSim Files (*.gsm)	Benchmarking Factors Removed	Figures
SRS Saltstone v2.009_nucs	None	PA-5.1-25 - PA-5.1-33; PA-5.2-7 - PA-5.2-8
SRS Saltstone v2.009_nucs_MinU	Upper zone flow multipliers	PA-5.1-19 - PA-5.1-24
SRS Saltstone v2.009_nucs_MinUW	Upper zone flow and wall flow multipliers	PA-5.1-13 - PA-5.1-18
SRS Saltstone v2.009_nucs_MinUWG	Upper zone flow, wall flow, and grout flow multipliers	PA-5.1-10 - PA-5.1-12
SRS Saltstone v2.009_nucs_MinUWGWf	Upper zone flow, wall flow, grout flow, and wall floor/soil multipliers	PA-5.1-1 - PA-5.1-9
SRS Saltstone v2.009_nucs_SatZ	Vault 4 contributions and Flow Divide multiplier	PA-5.2-5 - PA-5.2-6
SRS Saltstone v2.009_nucs_SatZby2	Vault 4 contributions, Flow Divide multiplier, and 0.5 benchmarking factors for the southern and northern sectors	PA-5.2-3 - PA-5.2-4
SRS Saltstone v2.009_nucs_SatZNBM	Vault 4 contributions, Flow Divide multiplier, 0.5 benchmarking factors for the southern and northern sectors, and the additional disposal unit contributions	PA-5.2-1 - PA-5.2-2

PA-5.1: Engineered Barrier and Unsaturated Zone

As indicated within the comment response matrix for NRC RAIs on the SDF (SRR-CWDA-2010-00033 Revision 1), the first phase of the benchmarking effort focused on the contaminant flux entering the water table below each of the three different disposal unit types (Vault 1, Vault 4, and FDCs). Each disposal unit type has differing disposal cell geometries and characteristics that result in different flow values that are computed by PORFLOW for each case. As stated in the SDF PA Section 5.6.2.3.1, and repeated below, the flow values abstracted from the PORFLOW runs are identified within the GoldSim model as:

- PF_Flowgrout – the flow of liquid through saltstone
- PF_FlowWall – the flow of liquid through the wall of the disposal unit
- PF_Flowdirt – the flow of liquid in the soil region adjacent to the wall
- PF_FlowUZ – the flow of liquid in the unsaturated zone below the disposal unit

For each case, Cases A through E, and each disposal unit type, the flow values for the saltstone, wall, and unsaturated zone were adjusted by use of multiplicative factors in an attempt to reproduce the flux behavior shown by PORFLOW. Note that the flow values for the soil adjacent to the wall (PF_FlowDirt) were not adjusted. The multiplicative factors can be found in Table PA-5.1-1, below. In addition, there is a benchmarking factor of 100, used in a series of fill cells used to help represent the complicated flow pattern in PORFLOW where the flow through the wall is diverted at the floor into the surrounding backfill and into the unsaturated zone beneath the engineered barrier. The factor is used to adjust the length of the pathway, which is not directly known. For this analysis, the flow multiplicative factors, and the fill pathway multiplicative factor are removed then added back in one at a time to show the degree of influence each one has. This breakdown of the benchmarking effort will be performed for the Base Case only. The benchmarked results for Base Case are shown in SDF PA Figures 5.6-1 through 5.6-9, but will also be presented here for convenience.

Table PA-5.1-1: Adjustment Multiplicative Factors for Flow Values

GoldSim Flow Value Parameter	Modeling Scenario Cases				
	Base Case	Case B	Case C	Case D	Case E
Vault 1					
PF_Flowgrout	1	1	1	1	1
PF_FlowWall	0.1	1	1	1	1
PF_FlowUZ	3	1	1	1	1
Vault 4					
PF_Flowgrout	0.8	0.3	1	1	0.9
PF_FlowWall	0.3	0.8	1	0.5	0.2
PF_FlowUZ	0.9	0.45	1.5	0.5	0.15
FDC					
PF_Flowgrout	10	0.15	1	1	1
PF_FlowWall	1	0.25	1	0.2	1
PF_FlowUZ	0.8	0.1	1	0.1	0.8

From PA Table 5.6-1

Benchmarking Analysis

In this analysis, all benchmarking factors were removed from the engineered barrier transport analysis. The benchmarking factors were then added back into the model, one category, or group of categories at a time, so that the influence of each type of benchmarking factor can be seen. The order in which the benchmarking factors were introduced back into the results are shown below. The associated GoldSim parameter name of the flow rate function with its implicit benchmarking factor or the name of the explicit benchmarking factors are shown in *italics* and within parentheses.

1. The wall floor/dirt pathway multiplicative factor for the FDCs (*benchmarkingaid*)
2. The flow multiplicative factors (for each disposal unit) for the saltstone grout (*PF_Flowgrout*)
3. The flow multiplicative factors (for each disposal unit) for the wall (*PF_FlowWall*)
4. The flow multiplicative factors (for each disposal unit) for the unsaturated zone (*PF_FlowUZ*)

Comparisons between the GoldSim and PORFLOW model unsaturated zone releases, evaluated without benchmarking factors, are presented by disposal unit type and radionuclide in Figures PA-5.1-1 to PA-5.1-9. The species, Ra-226, I-129, and Tc-99, were used in this analysis for consistency with the benchmarking effort described in SDF PA Section 5.6.2.2.

Figure PA-5.1-1: Vault 1 Ra-226 Release from the Unsaturated Zone without Benchmarking – Base Case

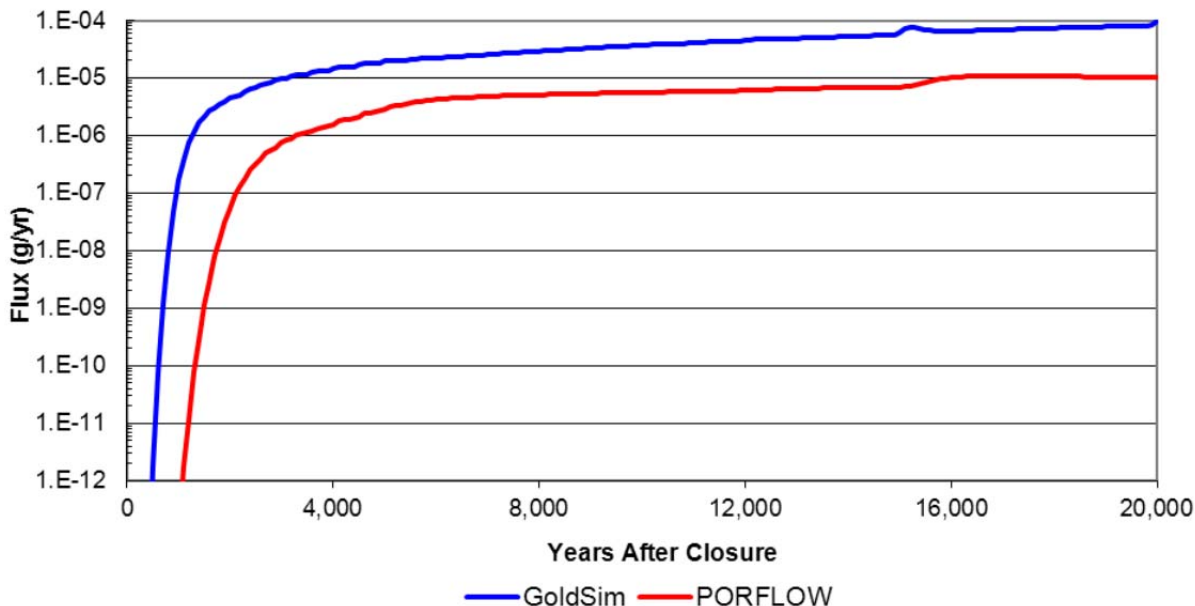


Figure PA-5.1-2: Vault 1 I-129 Release from the Unsaturated Zone without Benchmarking – Base Case

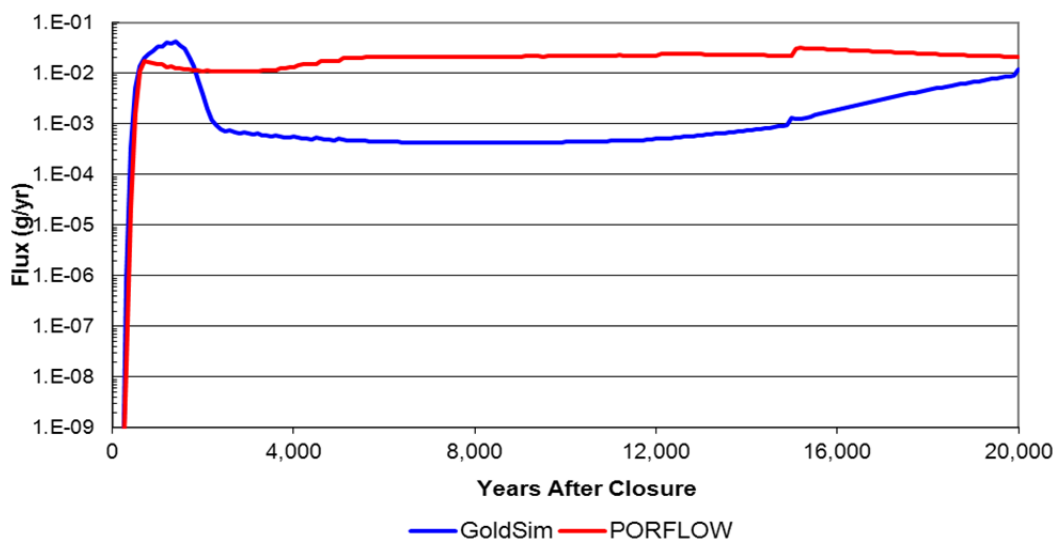


Figure PA-5.1-3: Vault 1 Tc-99 Release from the Unsaturated Zone without Benchmarking – Base Case

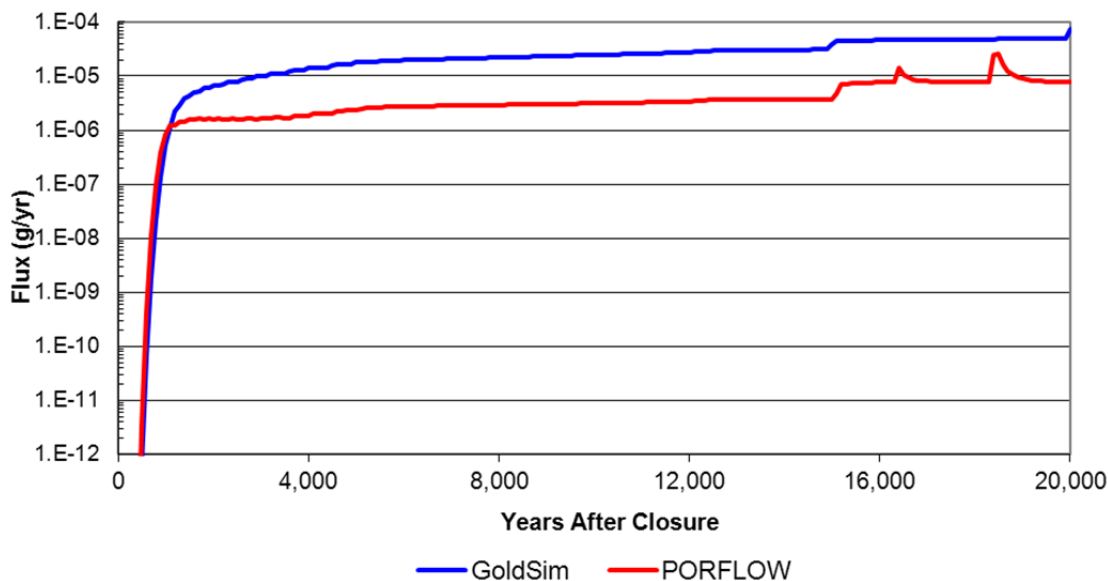


Figure PA-5.1-4: FDC Ra-226 Release from the Unsaturated Zone without Benchmarking – Base Case

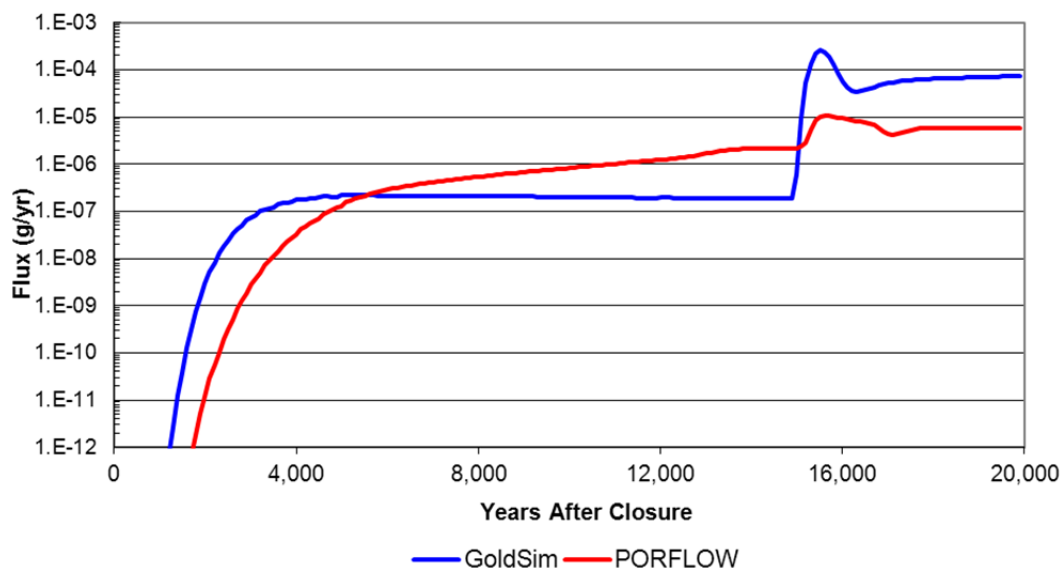


Figure PA-5.1-5: FDC I-129 Release from the Unsaturated Zone without Benchmarking – Base Case

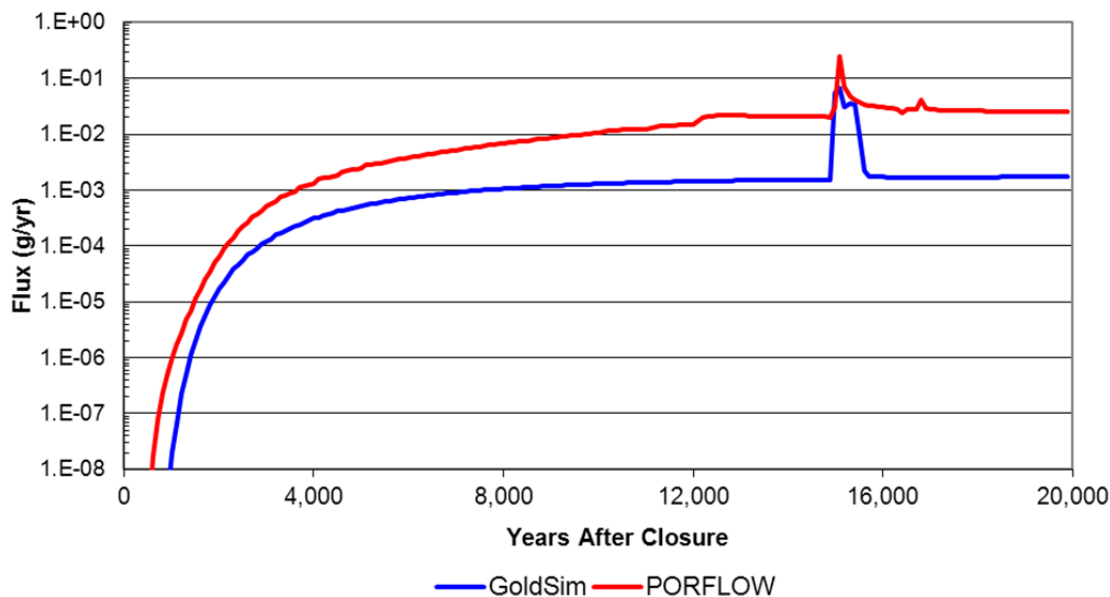


Figure PA-5.1-6: FDC Tc-99 Release from the Unsaturated Zone without Benchmarking – Base Case

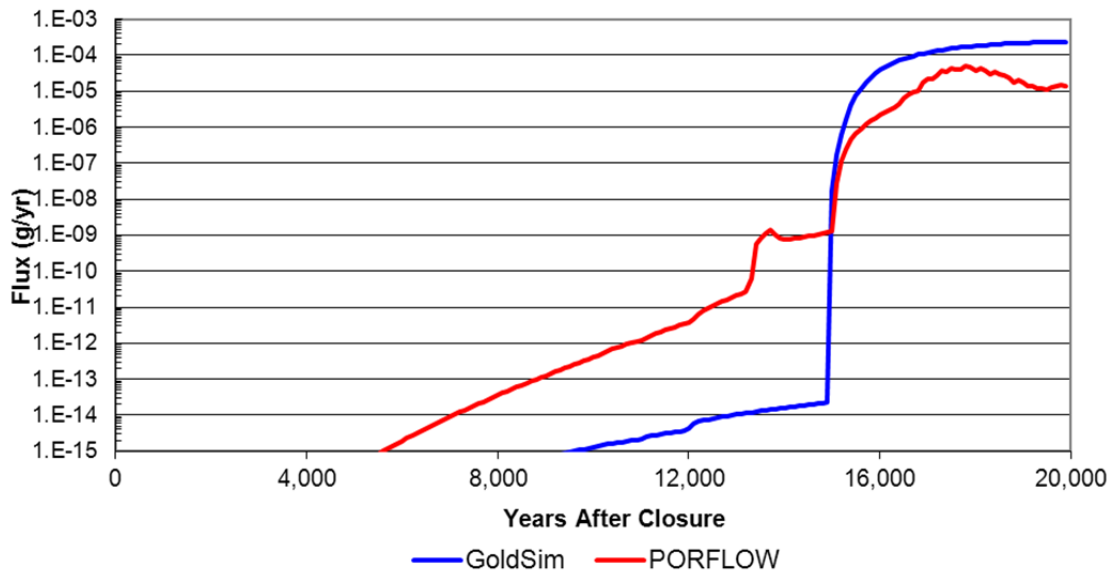


Figure PA-5.1-7: Vault 4 Ra-226 Release from the Unsaturated Zone without Benchmarking – Base Case

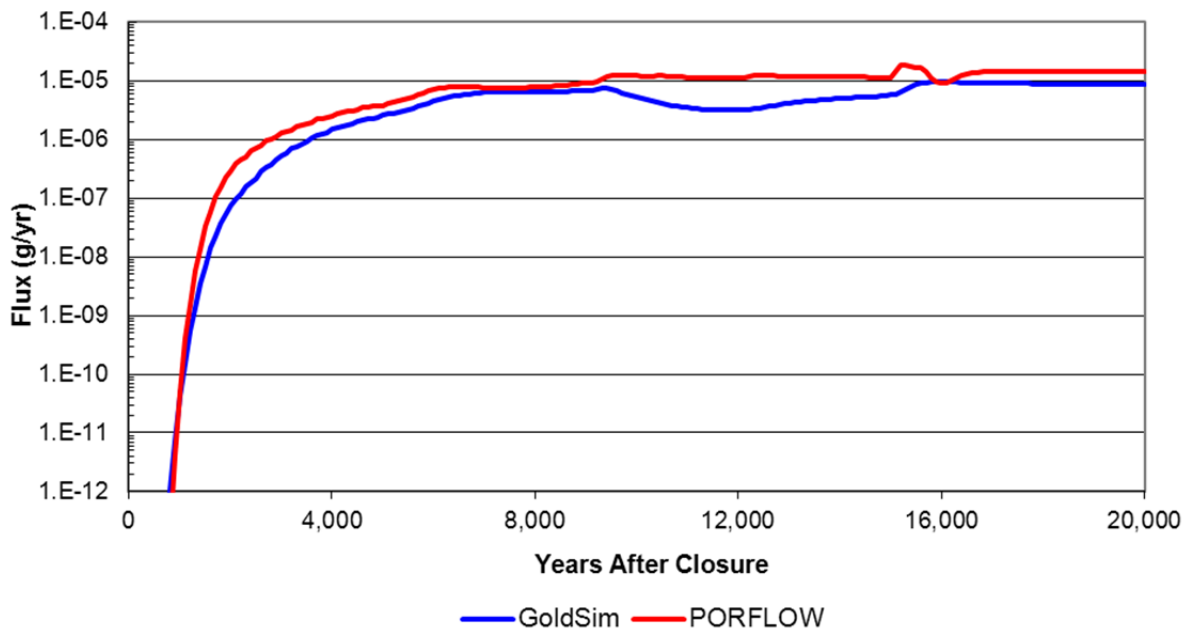


Figure PA-5.1-8: Vault 4 I-129 Release from the Unsaturated Zone without Benchmarking – Base Case

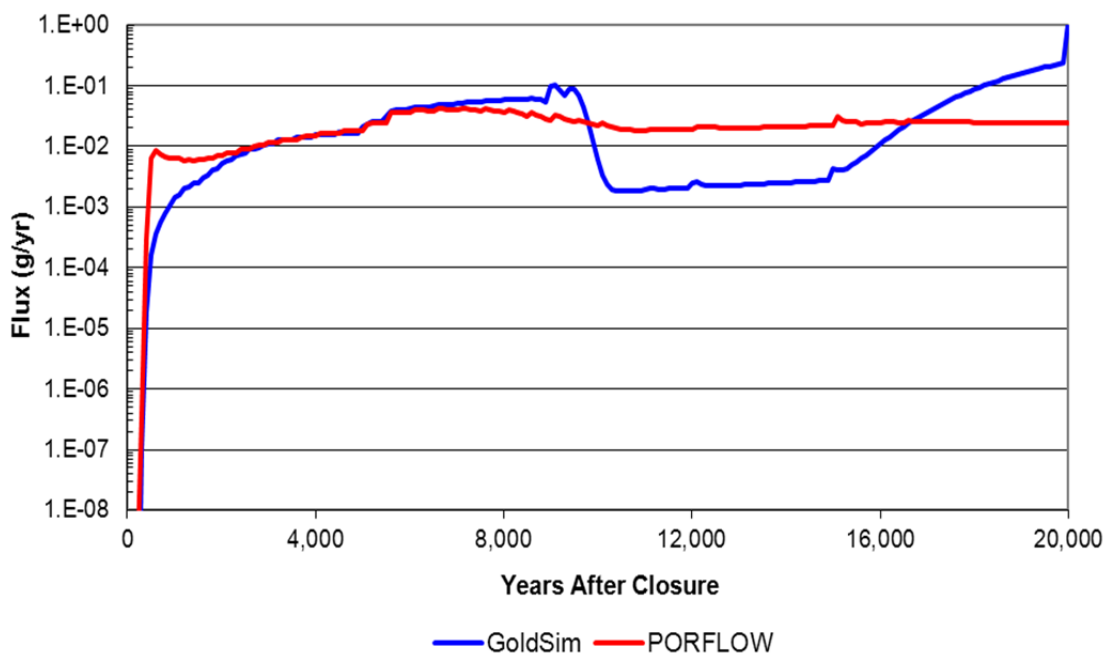
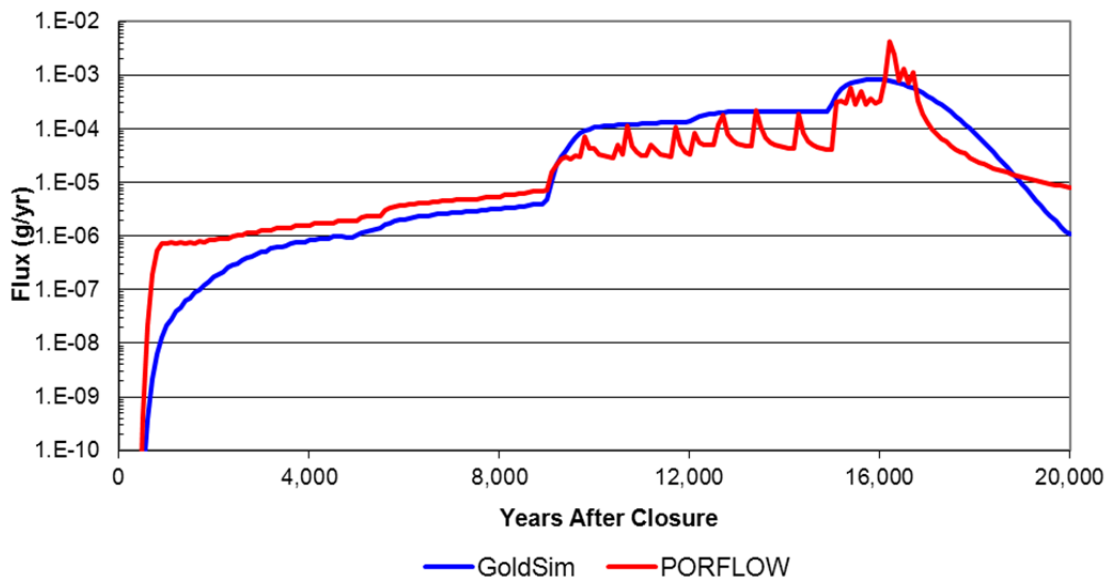


Figure PA-5.1-9: Vault 4 Tc-99 Release from the Unsaturated Zone without Benchmarking – Base Case



The first benchmarking factor added back into the disposal unit analysis is the wall floor/dirt pathway multiplicative factor (*benchmarkingaid*) (see Figures PA-5.1-10 through PA-5.1-12). This pathway multiplicative factor of 100 is used to account for the longer effective pathway taken by the radionuclides moving through the wall, as they are transported along the path of least resistance at the wall/floor contact. This path runs parallel to the floor, into the fill, and back under the floor in the unsaturated zone. The wall floor/soil pathway cells are only used for the FDCs in the GoldSim model therefore, only the FDC results are presented. Comparing Figures PA-5.1-10 through PA-5.1-12 to PA-5.1-4 through PA-5.1-6, respectively, shows the benchmarking factor has a slight retarding effect (relative to the time scale) for the two low-sorbing species I-129 and Tc-99. For Ra-226, which is more moderately sorbed, and is part of a decay chain including strongly sorbed species such as Th-230 and U-234, the use of the benchmarking factor dampens the release of Ra-226 at the time of the reducing environment to oxidizing environment transition in the wall (see Figures PA-5.1-10 and PA-5.1-4).

Figure PA-5.1-10: FDC Ra-226 Release from the Unsaturated Zone with Wall Floor/Soil Benchmarking Factor – Base Case

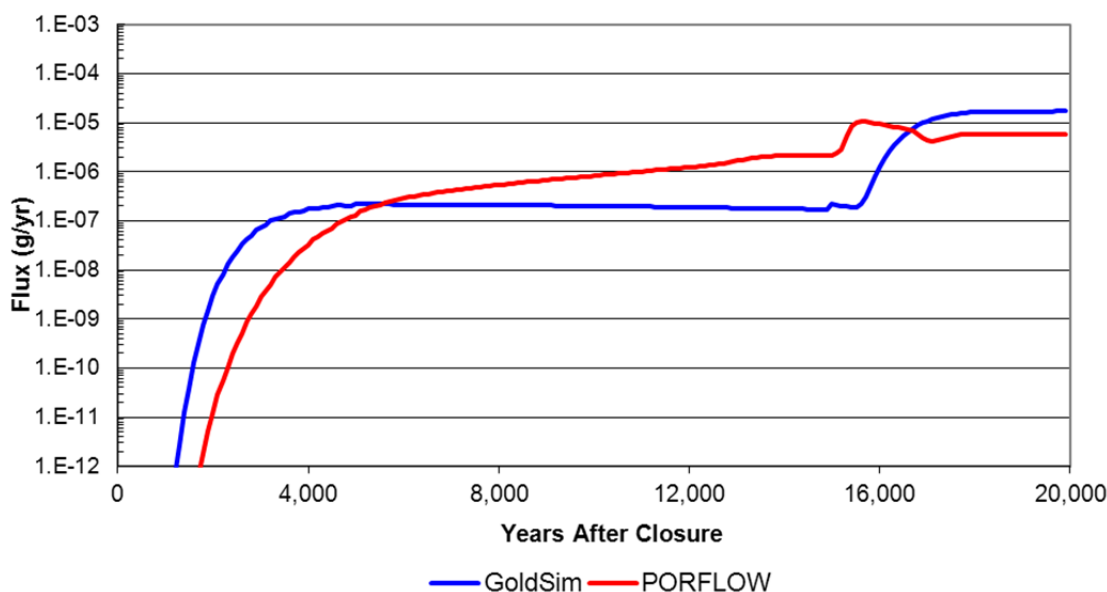


Figure PA-5.1-11: FDC I-129 Release from the Unsaturated Zone with Wall Floor/Soil Benchmarking Factor – Base Case

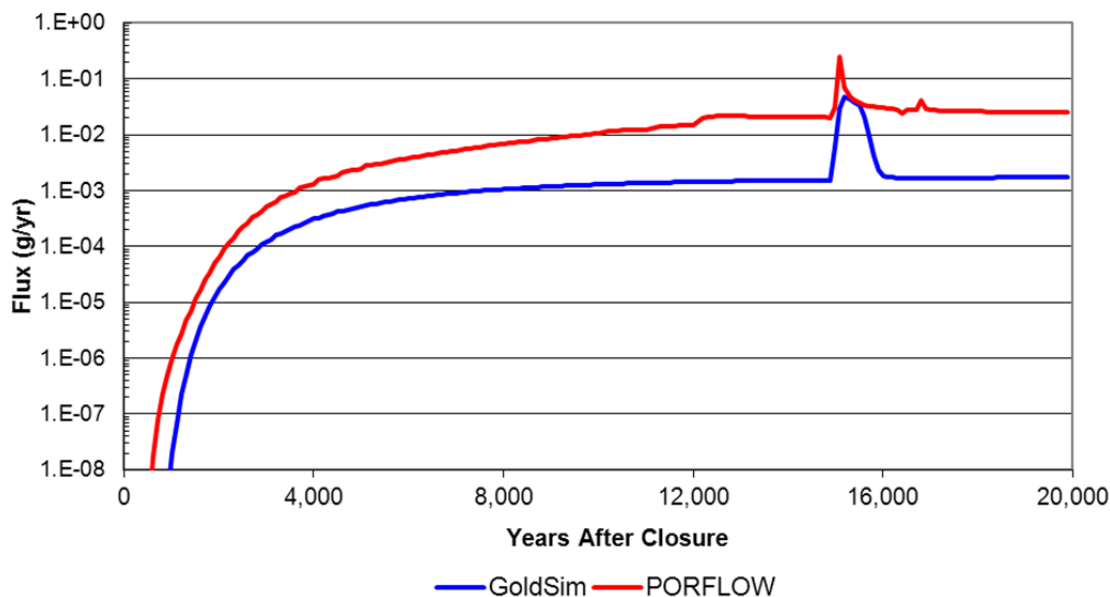
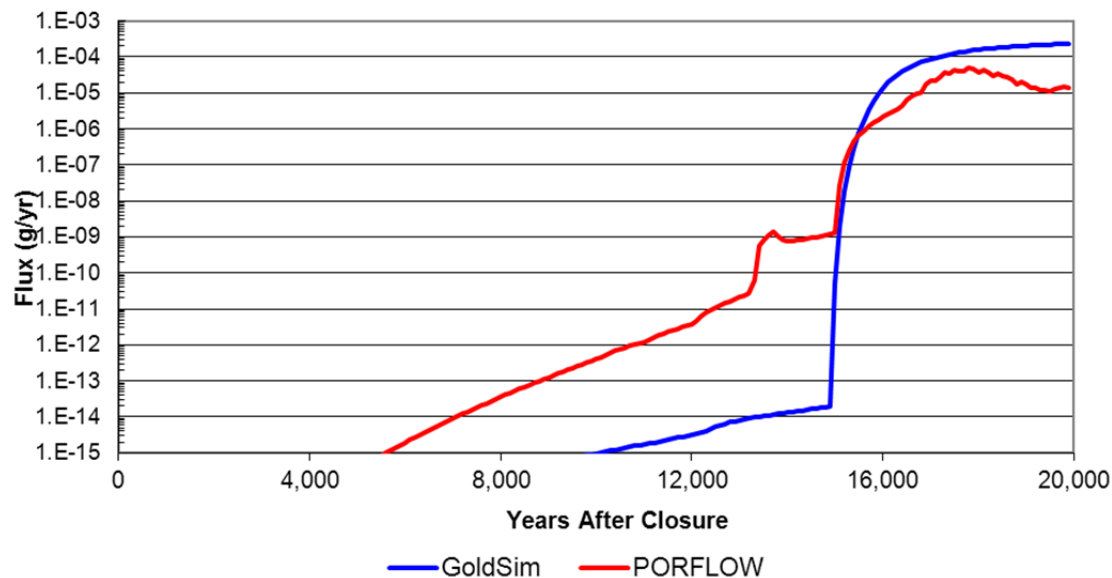


Figure PA-5.1-12: FDC Tc-99 Release from the Unsaturated Zone with Wall Floor/Soil Benchmarking Factor – Base Case



The next set of benchmark parameters added back in were the flow multiplicative factors for the saltstone flow rates (*PF_Grout*). As can be seen in Table PA-5.1-1, the grout flow multiplicative factor for Vault 1 is 1, so only the FDCs and Vault 4 will be examined herein (see Figures PA-5.1-13 through PA-5.1-18).

Comparing Figures PA-5.1-13 and PA-5.1-10, for the FDCs the increase in the Darcy velocity through the one-dimensional string of cells representing the saltstone (and the floor below which uses the bottom cell velocity for the grout) by a factor of 10, effectively increases the downward release of Ra-226 from the saltstone, which is originally understated. The degree to which the mass is released is conservative. A similar conservative increase is also seen for I-129 (see PA-5.1-14 and PA-5.1-11). Little change is seen for Tc-99 (see PA-5.1-15 and PA-5.1-12), indicating that the release of Tc-99 is mainly from the wall, as opposed to the downward flow through the saltstone. Although the percent of the saltstone (and other concrete) that is a reducing environment decreases over time, the saltstone is still mainly a reducing environment. For Vault 4, adding back in the saltstone flow multiplication factor of 0.8, there is no change in the Ra-226 and Tc-99 results (as seen by comparing Figure PA-5.1-16 to Figure PA-5.1-7 and Figure PA-5.1-18 to Figure PA-5.1-9), indicating the dominance of mass from the wall in the release. Later, around 18,000 years into the simulation, there is a slight decrease in the release for I-129 (as seen by comparing Figure PA-5.1-17 to Figure PA-5.1-8), which has a much lower sorptive capacity.

Figure PA-5.1-13: FDC Ra-226 Release from the Unsaturated Zone with Wall Floor/Soil and Grout Benchmarking Factors – Base Case

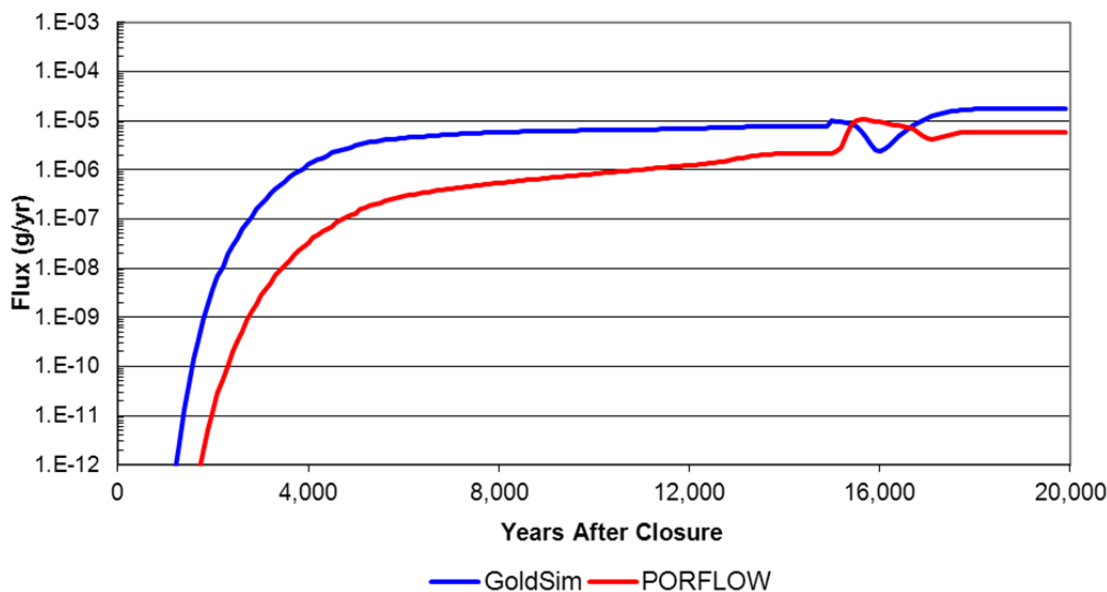


Figure PA-5.1-14: FDC I-129 Release from the Unsaturated Zone with Wall Floor/Soil and Grout Benchmarking Factors – Base Case

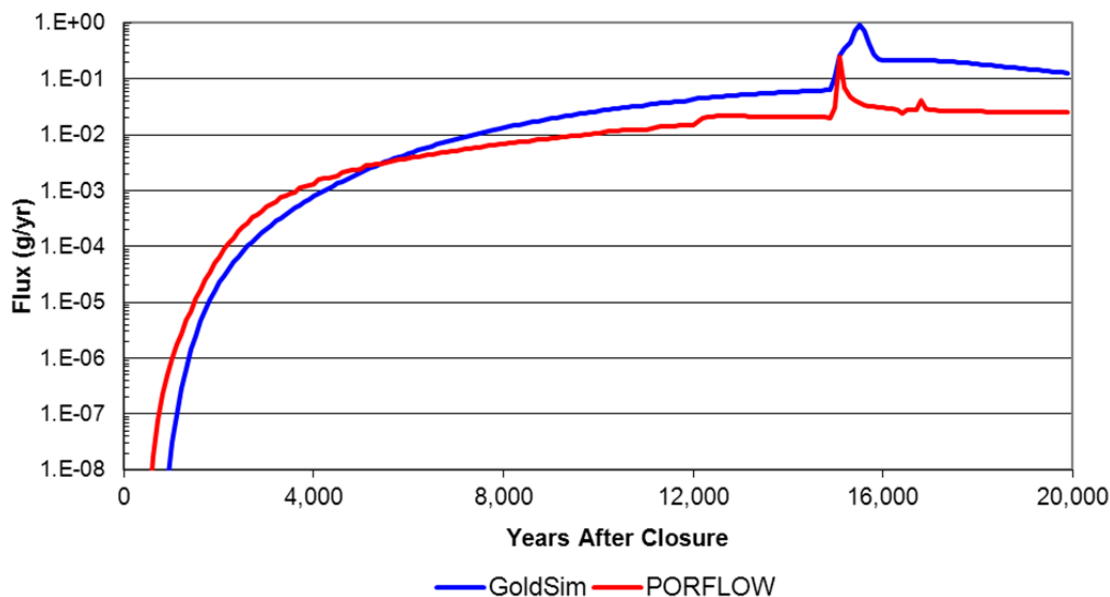


Figure PA-5.1-15: FDC Tc-99 Release from the Unsaturated Zone with Wall Floor/Soil and Grout Benchmarking Factors – Base Case

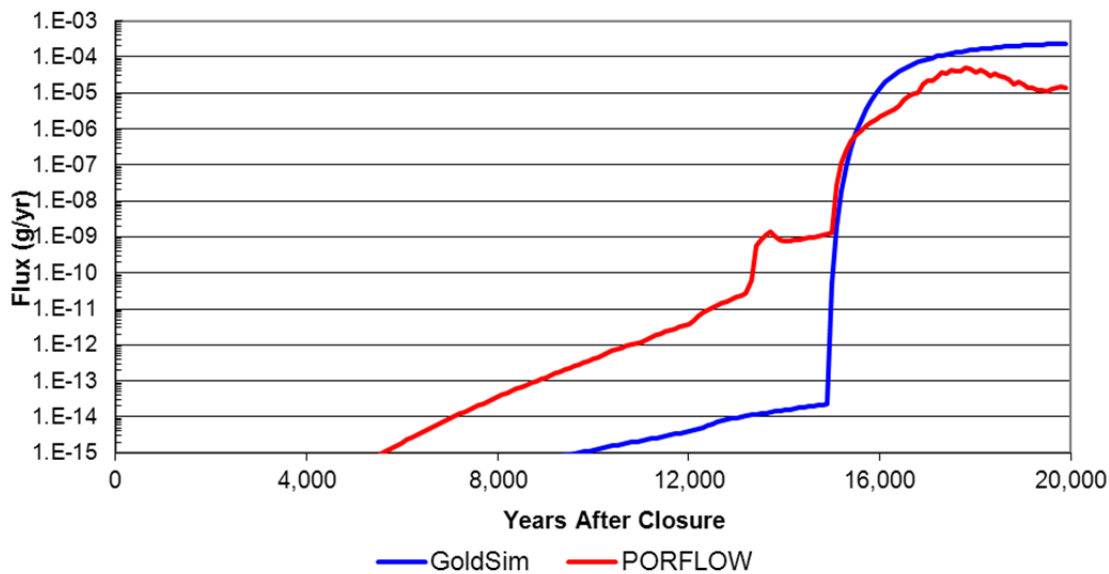


Figure PA-5.1-16: Vault 4 Ra-226 Release from the Unsaturated Zone with Wall Floor/Soil and Grout Benchmarking Factors – Base Case

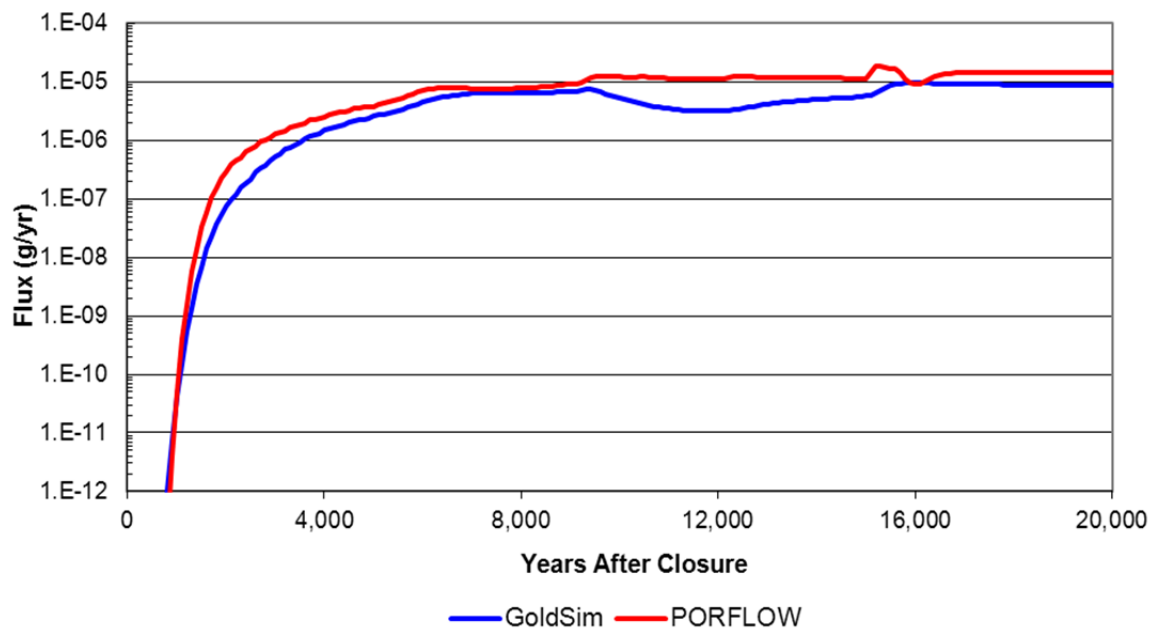


Figure PA-5.1-17: Vault 4 I-129 Release from the Unsaturated Zone with Wall Floor/Soil and Grout Benchmarking Factors – Base Case

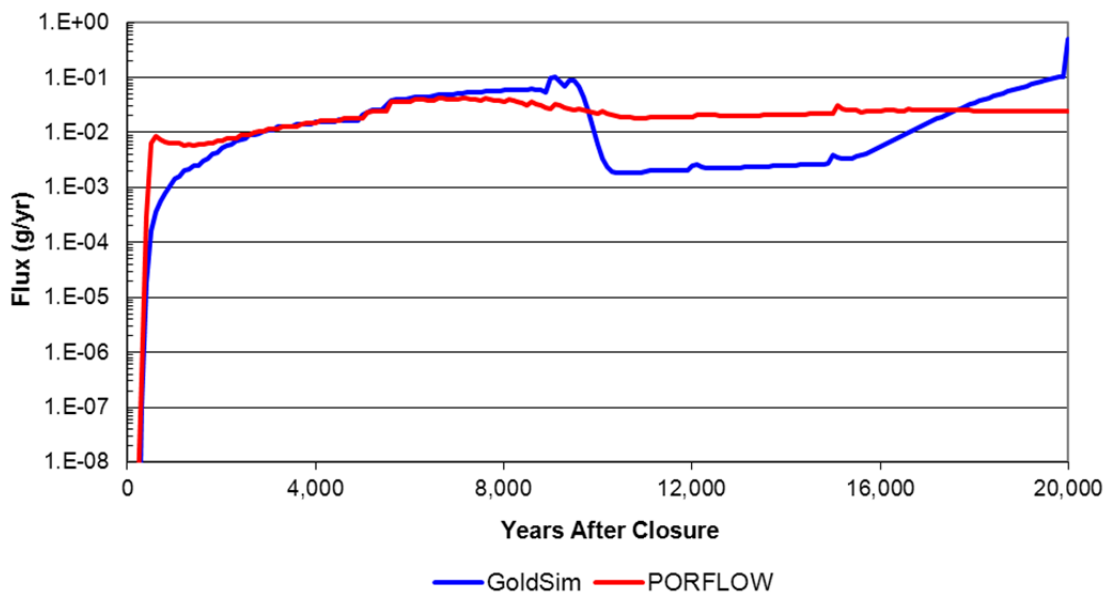
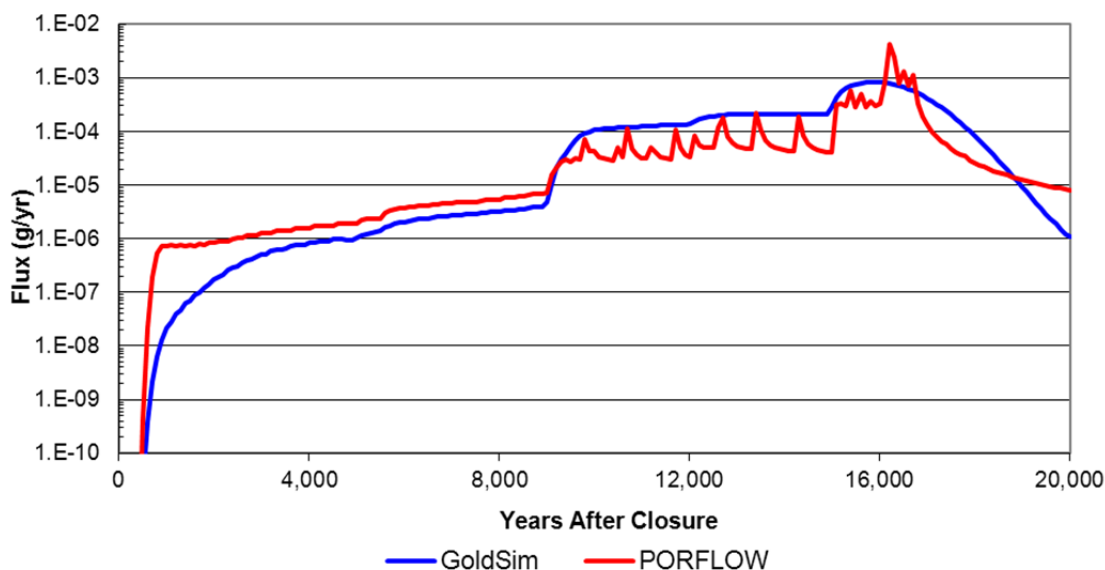


Figure PA-5.2-18: Vault 4 Tc-99 Release from the Unsaturated Zone with Wall Floor/Soil and Grout Benchmarking Factors – Base Case



The next set of benchmark parameters added back was the flow multiplicative factors for the wall (*PF_FlowWall*). As shown in Table PA-5.1-1, the wall flow multiplicative factor for FDCs is 1, so only Vault 1 and Vault 4 will be examined herein (see Figures PA-5.1-19 through PA-5.1-24). For Vault 1, the benchmarking factor is 0.1. Comparing the effect of the benchmarking factor on Ra-226 results (see Figures PA-5.1-19 and 5.1-1), shows that there is only a slight decrease in the release of Ra-226. Comparing the effect of the benchmarking factor on I-129 results (see Figures PA-5.1-20 and 5.1-2), it can be seen that the early time release of I-129 is more spread out improving the comparison between the GoldSim and PORFLOW results at early time. For Tc-99, comparing the effect of the benchmarking factor on the results (see Figures PA-5.1-21 and 5.1-3), the release is reduced creating a good match between the GoldSim and PORFLOW results except at early times. For Vault 4, the benchmarking factor is 0.3. Comparing the effect of the benchmarking factor on Ra-226 results (see Figures PA-5.1-22 and 5.1-16), it can be seen that there a decrease in the release of Ra-226, which makes the release lower than before, slightly diverging from the PORFLOW results. Comparing the effect of the benchmarking factor on I-129 results (see Figures PA-5.1-23 and 5.1-17), it can be seen that the early time GoldSim release of I-129 is lower diverging from the PORFLOW results. The peak results are retained for a longer period of time when the factor is included. For Tc-99, comparing the effect of the benchmarking factor the on results (see Figures PA-5.1-24 and 5.1-18), releases are decreased and generally make the GoldSim results lower than the PORFLOW results.

Figure PA-5.1-19: Vault 1 Ra-226 Release from the Unsaturated Zone with Wall Floor/Soil, Grout and Wall Benchmarking Factors – Base Case

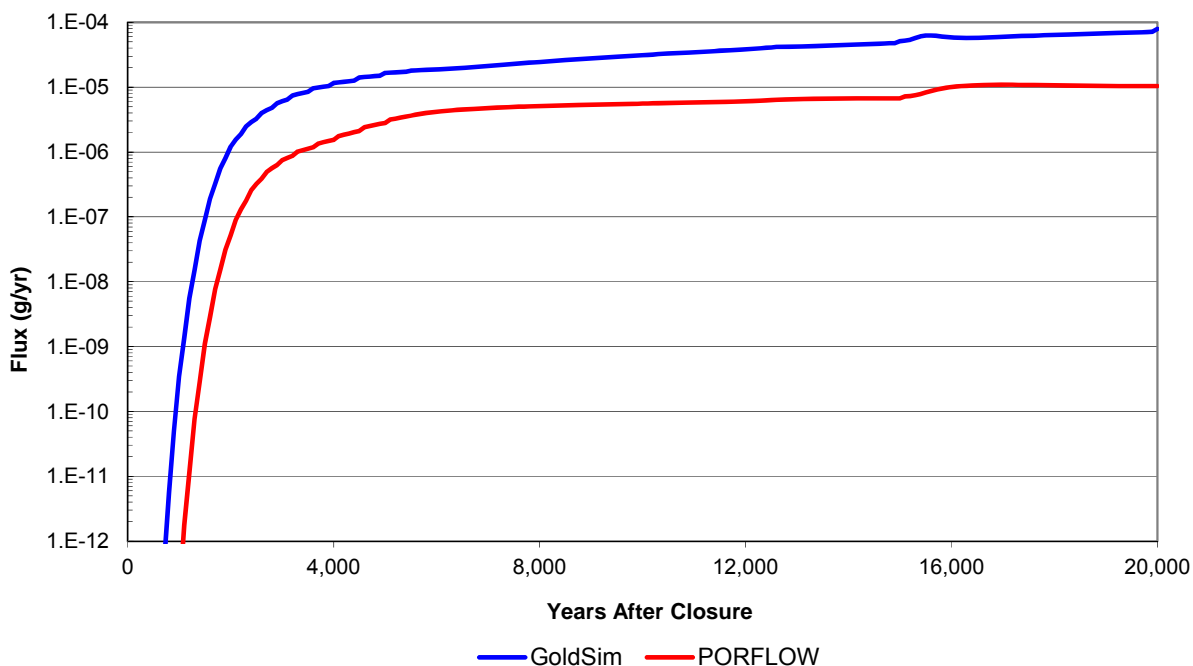


Figure PA-5.1-20: Vault 1 I-129 Release from the Unsaturated Zone with Wall Floor/Soil, Grout and Wall Benchmarking Factors – Base Case

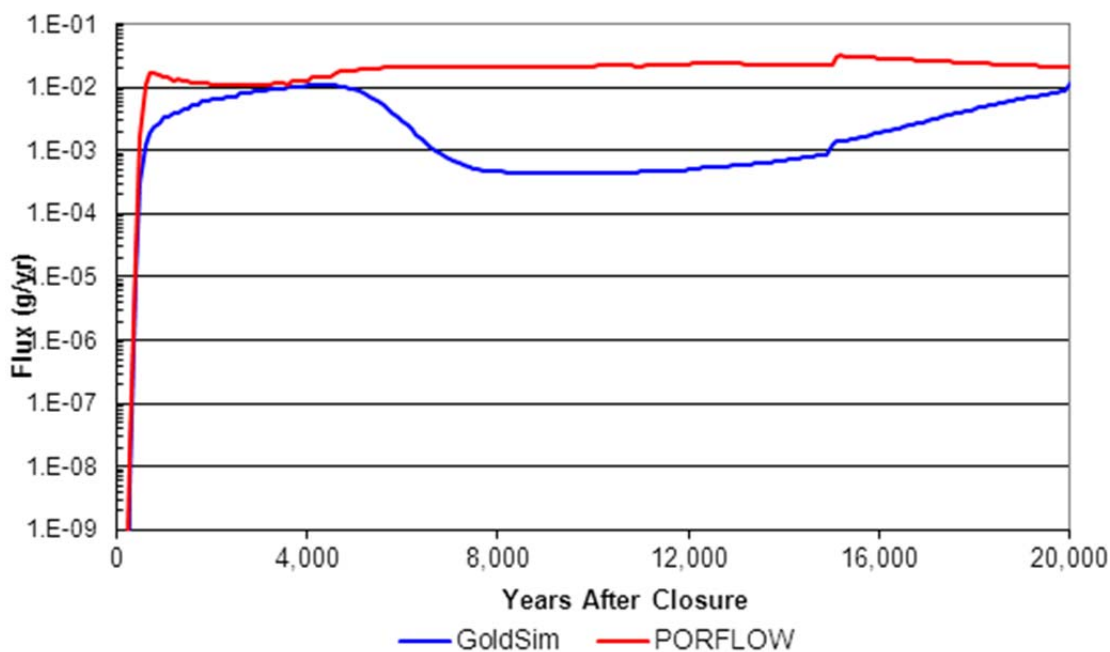


Figure PA-5.1-21: Vault 1 Tc-99 Release from the Unsaturated Zone with Wall Floor/Soil, Grout and Wall Benchmarking Factors – Base Case

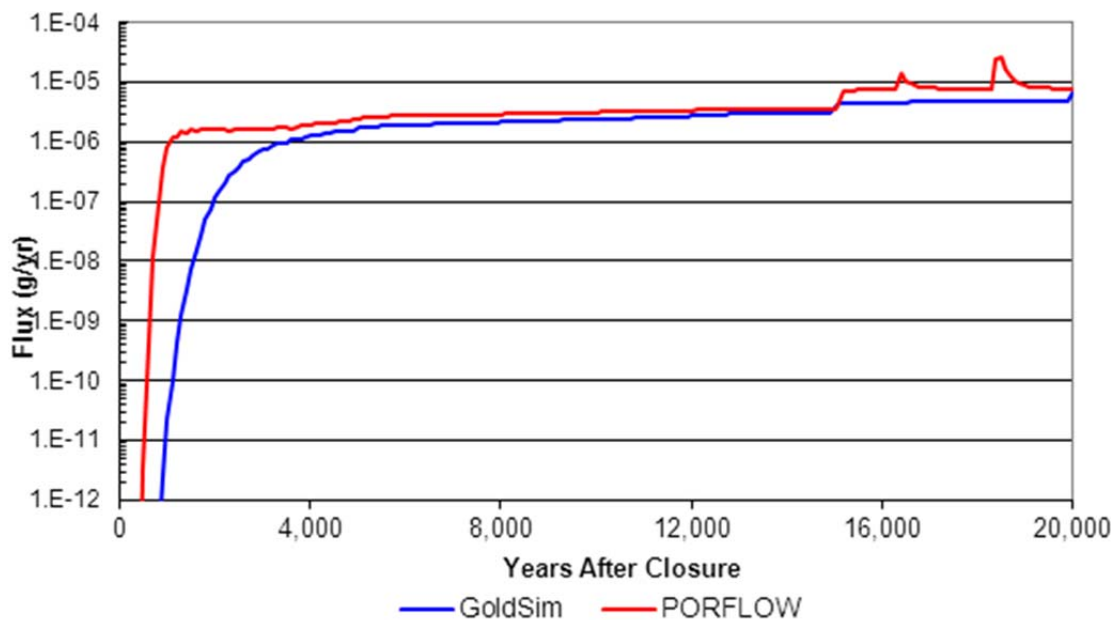


Figure PA-5.1-22: Vault 4 Ra-226 Release from the Unsaturated Zone with Wall Floor/Soil, Grout, and Wall Benchmarking Factors – Base Case

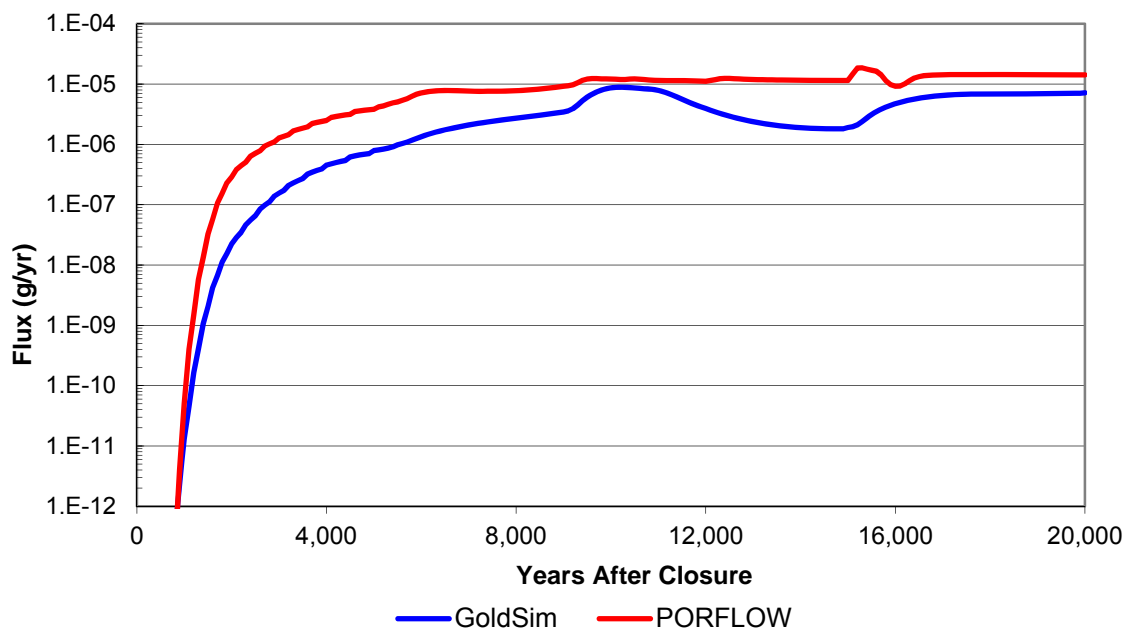


Figure PA-5.1-23: Vault 4 I-129 Release from the Unsaturated Zone with Wall Floor/Soil, Grout, and Wall Benchmarking Factors – Base Case

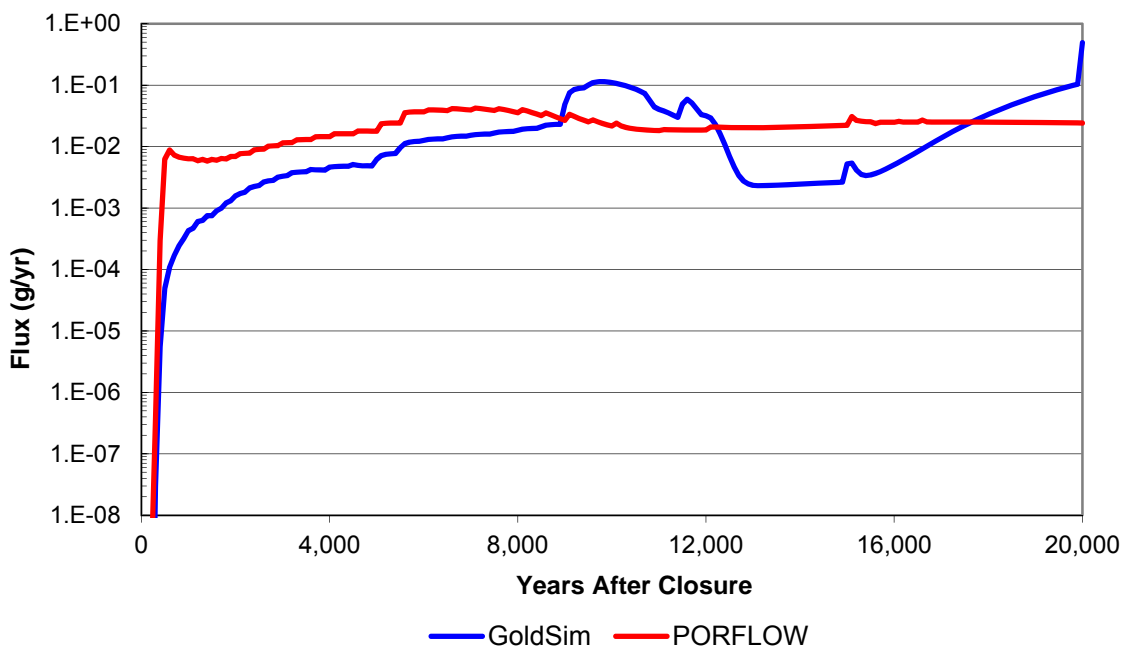
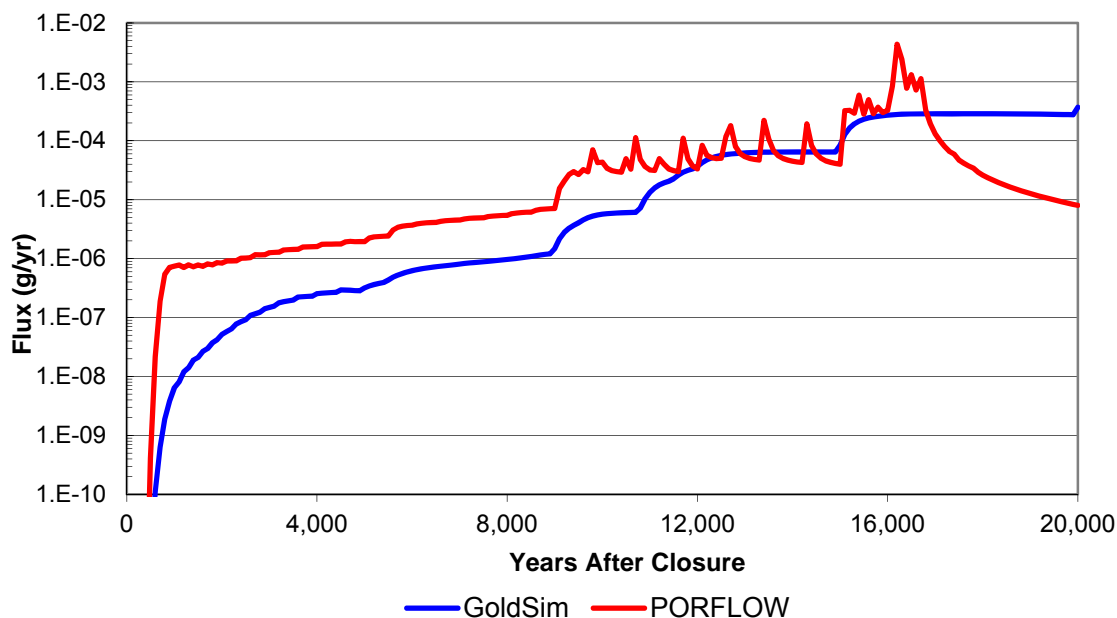


Figure PA-5.1-24: Vault 4 Tc-99 Release from the Unsaturated Zone with Wall Floor/Soil, Grout, and Wall Benchmarking Factors – Base Case



The last set of benchmark parameters added back was the flow multiplicative factors for the unsaturated zone (*PF_FlowUZ*). As can be seen in Table PA-5.1-1, the unsaturated zone flow multiplicative factors for Vault 1, the FDCs, and Vault 4 are 3.0, 0.9, and 0.8, respectively. As can be seen by comparing Figures PA-5.1-25 through PA-5.1-27 to PA-5.1-19 through PA-5.1-21 for Vault 1, Figures PA-5.1-28 through PA-5.1-30 to PA-5.1-13 through PA-5.1-15 for the FDCs, and PA-5.1-31 through PA-5.1-33 to PA-5.1-22 through PA-5.1-24 for Vault 4, the unsaturated zone benchmarking factors have little influence on the results.

Figure PA-5.1-25: Vault 1 Ra-226 Release from the Unsaturated Zone with All Benchmarking Factors – Base Case

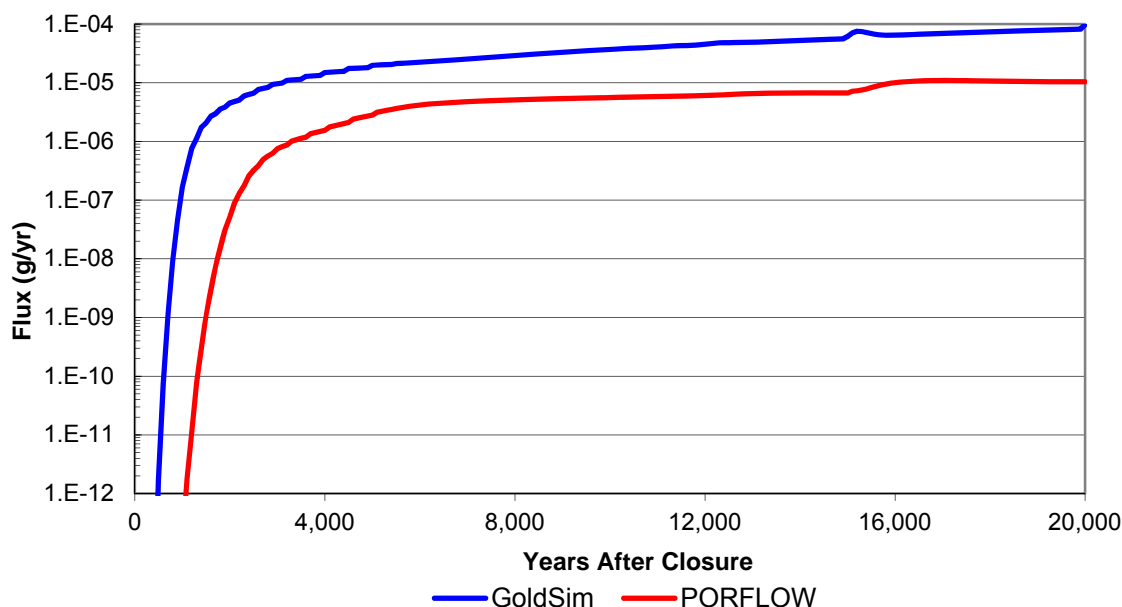


Figure PA-5.1-26: Vault 1 I-129 Release from the Unsaturated Zone with All Benchmarking Factors – Base Case

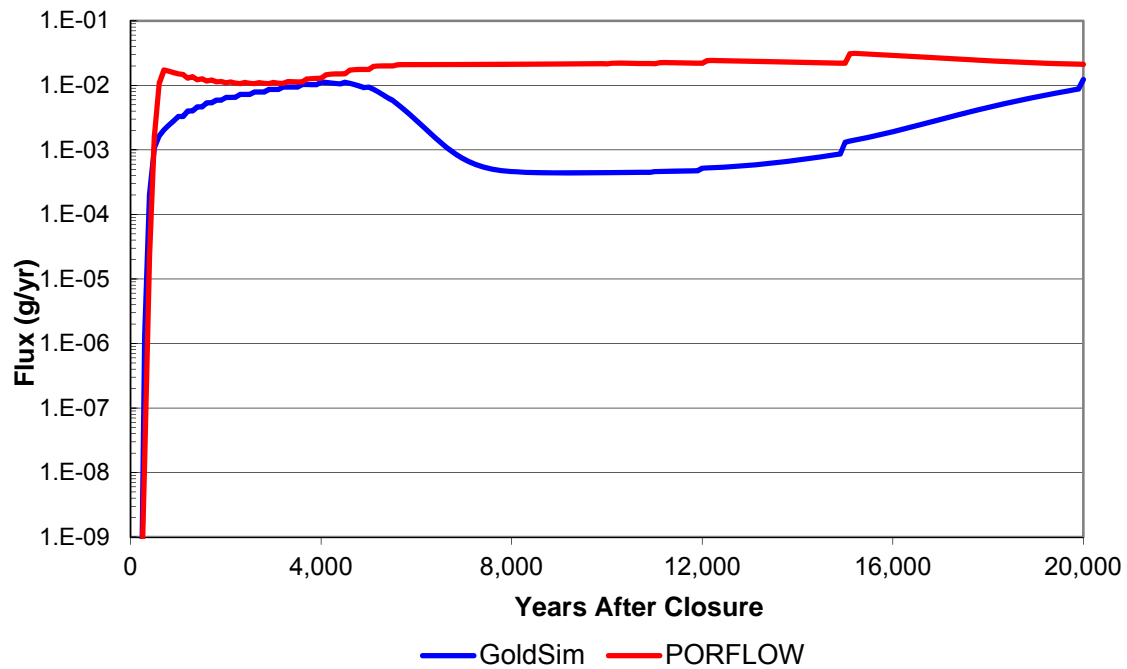


Figure PA-5.1-27: Vault 1 Tc-99 Release from the Unsaturated Zone with All Benchmarking Factors – Base Case

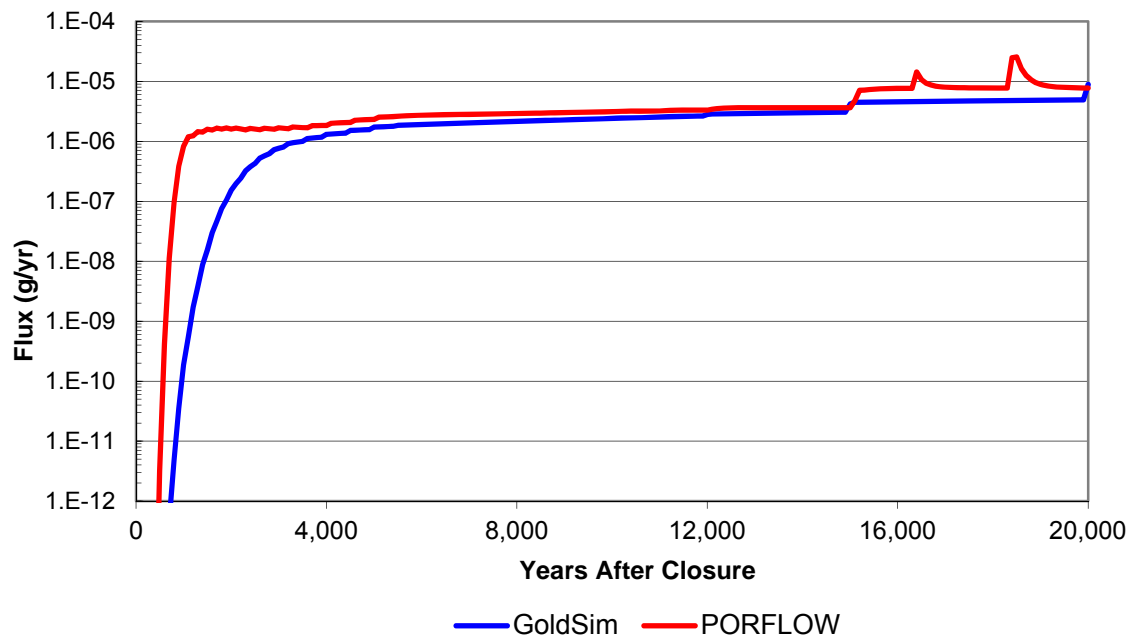


Figure PA-5.1-28: FDC Ra-226 Release from the Unsaturated Zone with All Benchmarking Factors – Base Case

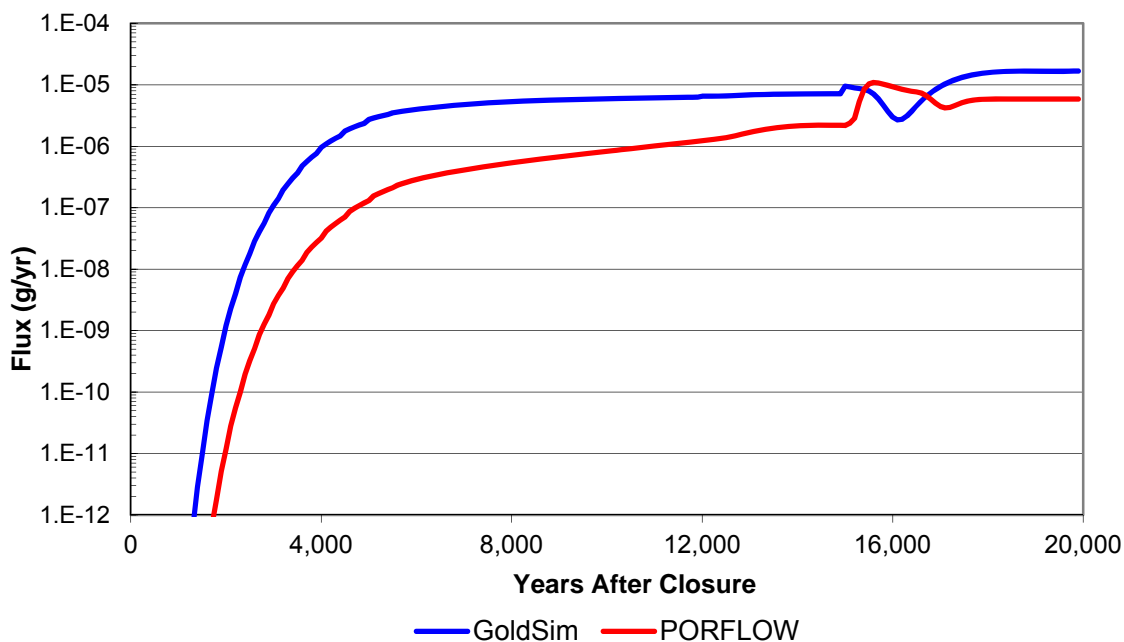


Figure PA-5.1-29: FDC I-129 Release from the Unsaturated Zone with All Benchmarking Factors – Base Case

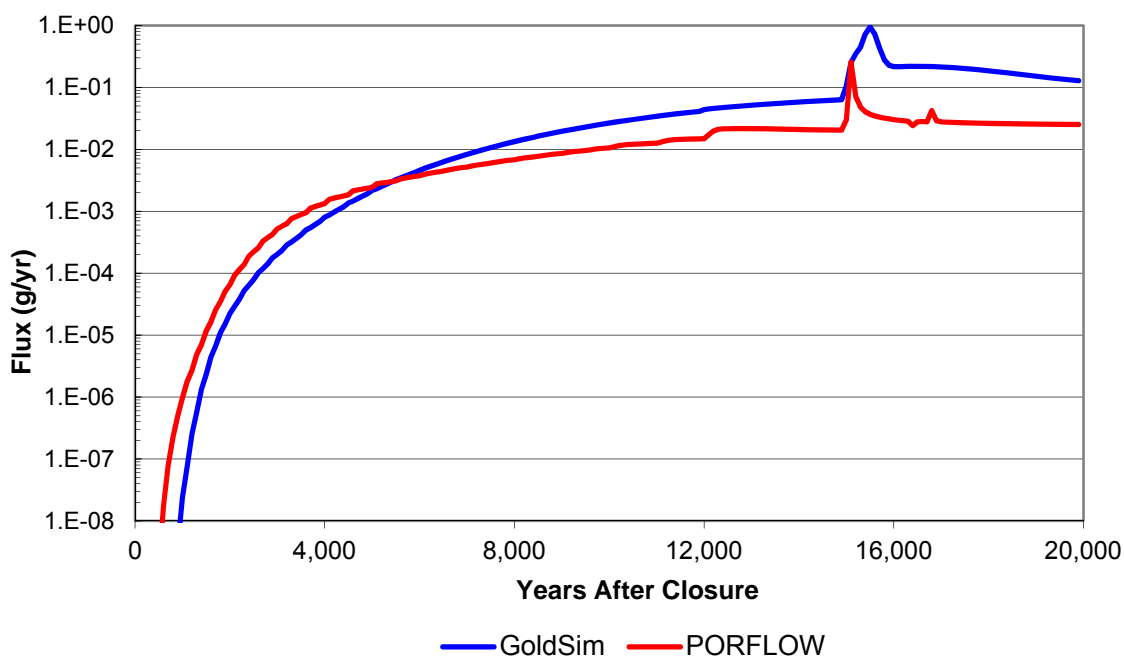


Figure PA-5.1-30: FDC Tc-99 Release from the Unsaturated Zone with All Benchmarking Factors – Base Case

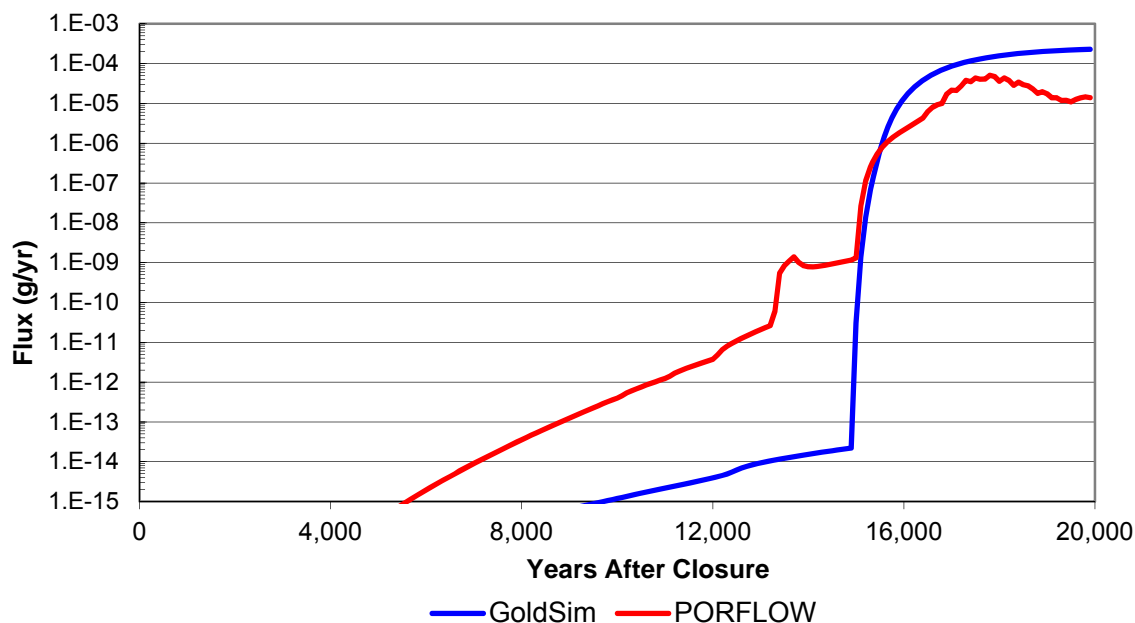


Figure PA-5.1-31: Vault 4 Ra-226 Release from the Unsaturated Zone with All Benchmarking Factors – Base Case

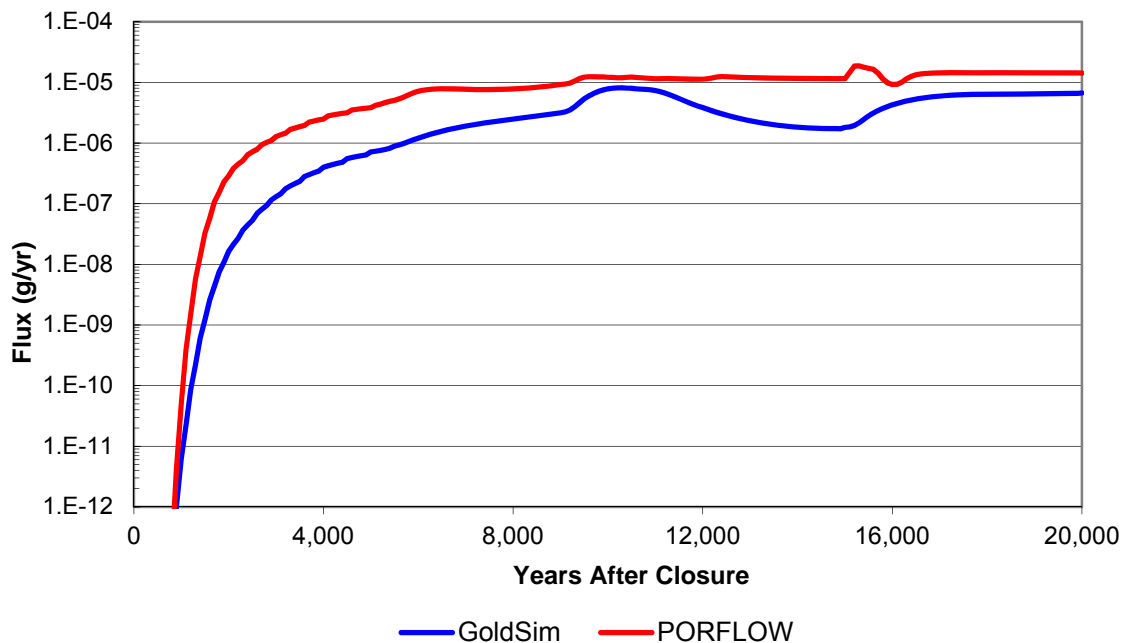


Figure PA-5.1-32: Vault 4 I-129 Release from the Unsaturated Zone with All Benchmarking Factors – Base Case

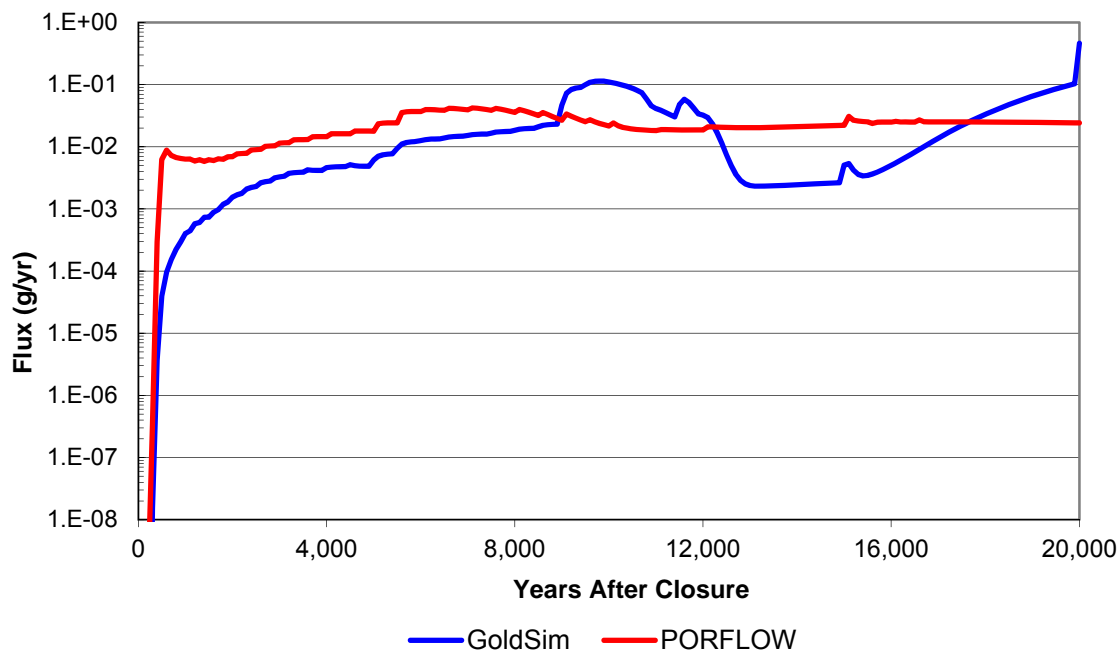
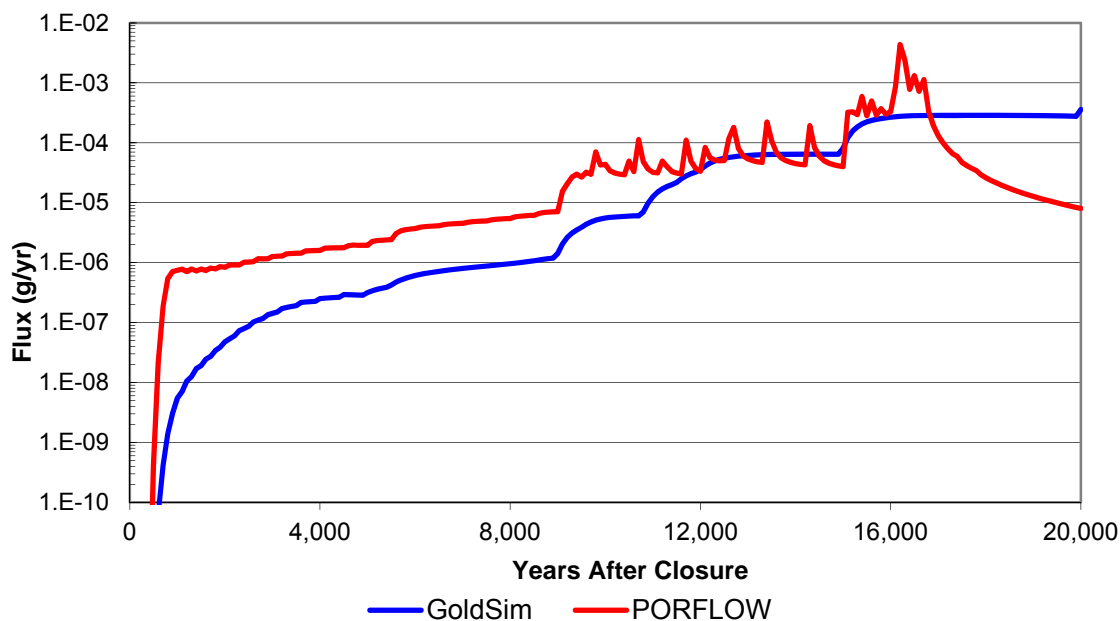


Figure PA-5.1-33: Vault 4 Tc-99 Release from the Unsaturated Zone with All Benchmarking Factors – Base Case



As can be seen by comparing GoldSim releases to PORFLOW releases for the GoldSim model prior to benchmarking (Figures PA-5.1-1 through PA-5.1-3 for Vault 1 and the Figures PA-5.1-4 through PA-5.1-6 for the FDCs) with the same releases when the GoldSim model is benchmarked (Figures PA-5.1-25 through PA-5.1-27 for Vault 1 and the Figures PA-5.1-28 through PA-5.1-30 for the FDCs) the similarity between GoldSim model and PORFLOW model results improves or is only slightly affected, depending on the radionuclide, after benchmarking for Vault 1 and the FDCs. For Vault 4, the opposite is seen (Figures PA-5.1-7 through PA-5.1-9 and Figures PA-5.1-31 through PA-5.1-33). Comparing Figure PA-5.1-7 to Figure PA-5.1-31, Figure PA-5.1-8 to Figure PA-5.1-32, and Figure PA-5.1-9 to Figure PA-5.1-33 it can be seen that there is a general lowering of the GoldSim generated releases after benchmarking. The benchmarking does improve the similarity between dose results. Although, the same effect could have been produced by changing the degree of dispersion in the saturated zone which is higher in the PORFLOW model since the GoldSim model limits vertical spreading, has a finer discretization along the flow line, and does not account for lateral spreading of the flow field. Radionuclide dependence can be seen by comparing the results presented in Figures PA-5.1-3 and PA-5.1-21. The wall benchmarking factor of 0.1, which is a velocity multiplier, improves the comparison. This is because for Vaults 1 and 4, the release of Tc-99, which is strongly sorbing, is dominated by the release of the initial inventory in the wall. It can also be seen by comparing the results presented in Figures PA-5.1-11 and PA-5.1-14 that the grout benchmarking factor of 10.0, which is a velocity multiplier, improves the comparison. This is because for a weakly sorbing species the mass released through the floor beneath the saltstone is important over the time period of interest. In the future, when improvements in GoldSim/PORFLOW model comparisons are warranted, adjustments to the GoldSim Model will be based on changes to specific GoldSim simplifications.

PA-5.2: Saturated Zone

Comment Response Matrix for NRC RAIs on the SDF PA (SRR-CWDA-2010-00033 Revision 1), discusses three types of benchmarking factors for the saturated zone analysis:

1. Adjustment for the Flow Divide

A benchmarking factor was applied to the contribution from Disposal Units 7A through 7D to Sector J concentrations to reflect the influence of the flow divide shown in SDF PA Figure 4.4-70. As can be seen by comparing the streamlines in SDF PA Figure 4.4-70 to the water table in SDF PA Figure 4.2-21, the contour intervals are much wider along the streamlines from FDCs 7A through 7D to Sector J, which most likely reflects a lower Darcy velocity and less water to mix with. Again, note that the degree of vertical mixing may also differ. This benchmarking factor multiplies the plume function value and thus the radionuclide concentration contribution from Disposal Units 7A through 7D to Sector J by a factor of 5.

2. Vault 4 Contributions in Sectors A, B, and C

Benchmarking factors were applied to the contributions from Vault 4 to the concentrations in Sectors A, B, and C. These benchmarking factors multiply the radionuclide concentration contributions from Vault 4 to the concentrations in Sectors A, B, and C by 70, 100, and 50, respectively. These specific adjustments to the Vault 4 contribution are included to offset the different amounts of water available for diluting the releases from Vault 4 in the PORFLOW and GoldSim models. This dilution effect is associated with the heterogeneous flow rates found in the three-dimensional PORFLOW model and the single-valued Darcy velocity used in the GoldSim model. The degree of vertical mixing is also a possible difference.

3. Additional Disposal Unit Contributions

An additional benchmarking effort conducted on the 100-meter concentrations was used to include contributions from specific disposal units to sectors that are not apparent based on the PORFLOW streamline paths shown in SDF PA Figure 4.4-70. The radionuclide concentrations in the Southern Sectors E and F were increased by adding a contribution from Vault 1. This additional contribution is 2 % from Vault 1 to Sector E and 1 % from Vault 1 to Sector F. These contributions may be reflective of a transverse dispersion effect not captured in the simplified GoldSim model. The radionuclide concentrations in the northern sectors, Sectors G through L, were increased by adding a contribution from the disposal units in the southern sectors. These contributions to the northern sectors were used to approximate the influence of northerly flow in the Gordon Aquifer. The northerly flow transports some of the mass released from the southern disposal units Sectors G through L, as shown in SDF PA Figure 4.4-71. The radionuclide concentrations in Sectors G and H were increased by adding a contribution from Vault 1. The concentrations in Sectors G and H include 4 % and 5 % of the radionuclide concentrations from Vault 1, respectively. For Sectors I through L the radionuclide concentrations include 5 % of the radionuclide concentrations computed in Sector A.

In addition to the three types of benchmarking factors for the saturated zone analysis described above, there is a fourth type consisting of two multiplication factors of 0.5 (one for the north and one for the south) which are used to decrease the concentrations. This factor helps offset the geometric differences between the two models, the PORFLOW model where the plume travels downward allowing for dispersion above and below the center of mass and the GoldSim model where the mass travels horizontally and only allows for dispersion below the center of mass.

Also, note that the benchmarking factors listed under the third category, *Additional Disposal Unit Contributions*, are only applied to concentrations used in the intruder scenario. The neglecting of these benchmarking factors in the MOP dose calculation is an unintentional result of the different logic (GoldSim elements and structure) used for the MOP and intruder dose calculations. Although neglecting these contributions in the MOP analysis is “non-conservative”, they represent a relatively small effect relative to the influence of the southern disposal units on Sectors A, B, and C and as such, have a negligible influence on dose results. These contributions are considered in this analysis because they were considered in all the past benchmarking documentations.

Benchmarking Analysis

In the present analysis, all benchmarking factors were removed from the saturated zone transport analysis. The benchmarking factors were then added back into the model, one category or group or categories at a time, so that the influence of each type of benchmarking factor can be seen. The order in which the benchmarking factors were introduced back into the results was:

1. The additional disposal unit contributions
2. The 0.5 benchmarking factors for the southern and northern sectors
3. Flow divide multiplier and Vault 4 contribution

Comparisons between the GoldSim and PORFLOW model 100-meter boundary concentrations evaluated without benchmarking factors are presented, by sector, in Figure PA-5.2-1, for the southern Sectors A through F. For the northern Sectors G through L, comparisons between the GoldSim and PORFLOW model 100-meter boundary concentrations, without benchmarking factors, are presented by sector in Figure PA-5.2-2. The first benchmarking factors added back into the saturated zone analysis are the contributions from the future disposal units (see Figures

PA-5.2-3 and PA-5.2-4). As noted above, these benchmarking factors are reflective of unaccounted dispersive effects in Sectors E and F, and transport of mass releases from the southern disposal units, northward in the Gordon Aquifer. Comparing Figures PA-5.2-1 and 5.2-3 it can be seen that for both Sectors E and F, much of the Ra-226 reaching these sectors is coming from Vault 1, which is not considered as a source for these two sectors in the more simplified GoldSim model. Although the streamlines in SDF PA Figure 4.4-70 indicate that mass from Vault 1 may not reach Sectors E and F, the process of dispersion must be considered. Note that the Vault 1 release also influences the degree to which Tc-99 reaches Sectors E and F. When considering the small component of the releases from disposal units in the southern sector that would be transported northward in the Gordon Aquifer, it can be seen, when comparing Figures PA-5.2-2 and PA-5.2-4 that the mass releases from the southern disposal units, especially Vaults 1 and 4, control the degree to which Ra-226 and Tc-99 reach the northern sectors. It can also be seen in SDF PA Figure 5.6-9, that until about 15,000 years into the simulation, the FDCs (which dominate the releases to the northern sectors) have little influence on the Tc-99 release to the saturated zone.

Figure PA-5.2-1: Southern Sectors Concentration Comparisons without Benchmarking – Base Case

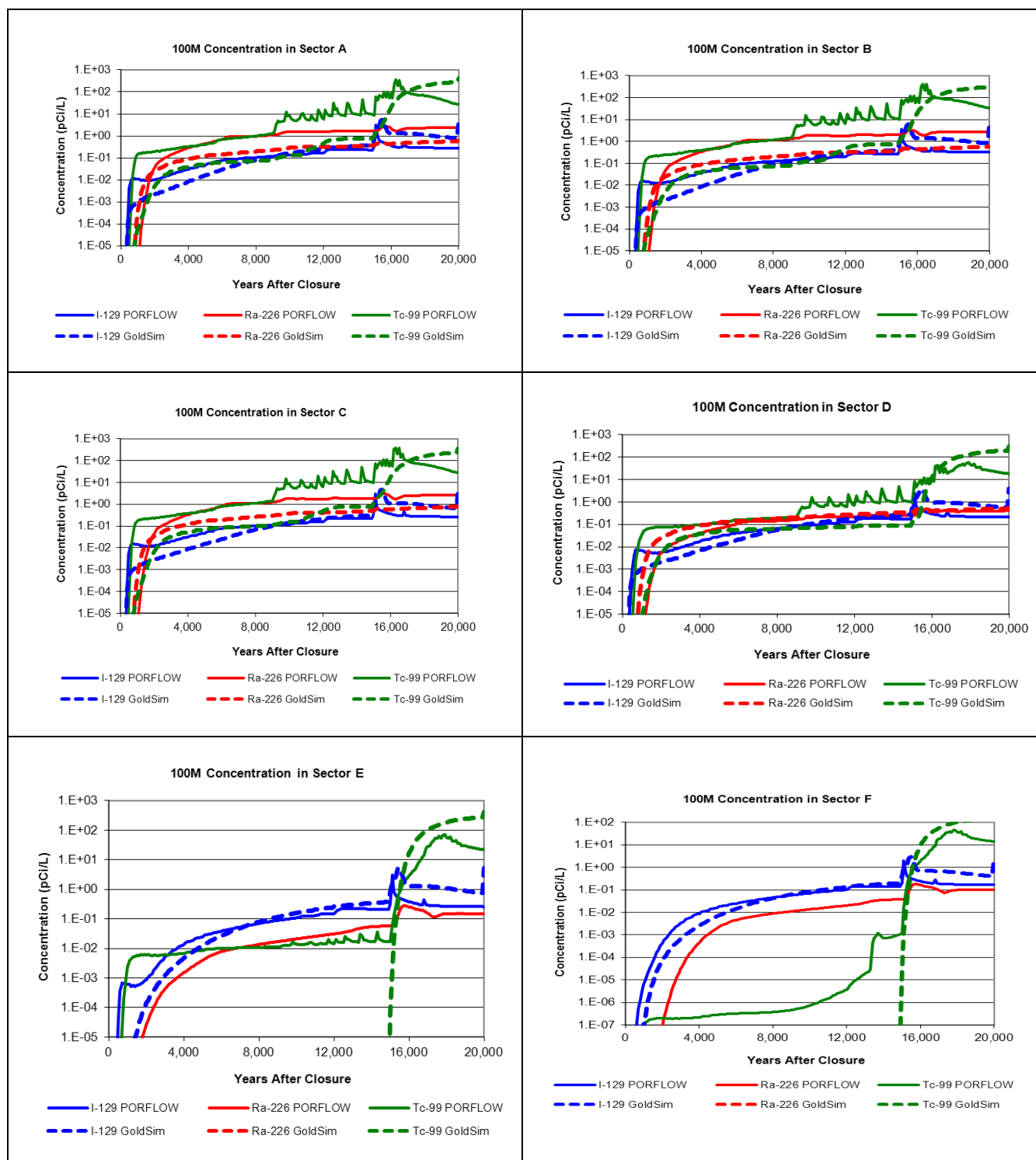


Figure PA-5.2-2: Northern Sectors Concentration Comparisons without Benchmarking – Base Case

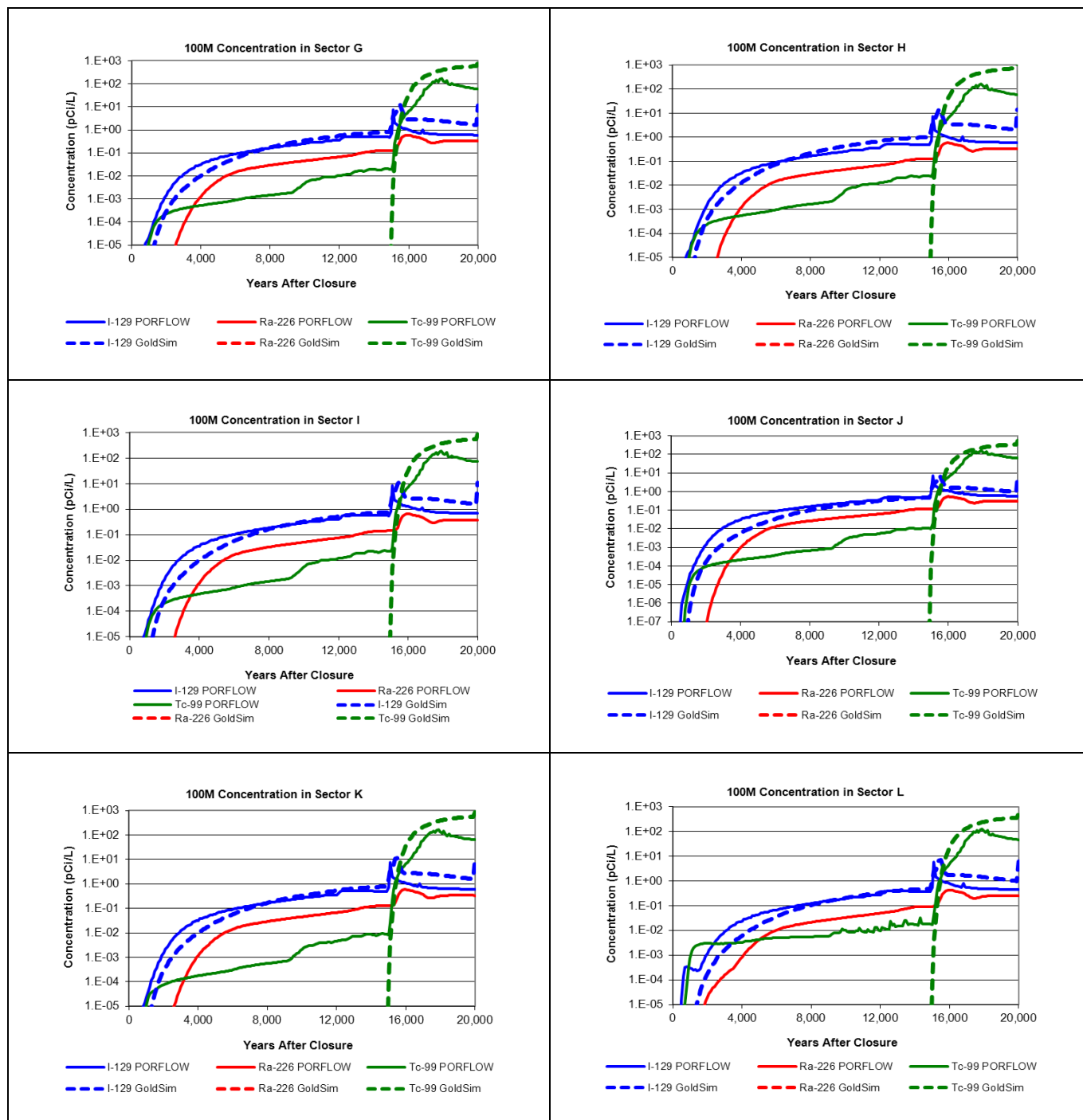


Figure PA-5.2-3: Southern Sectors Concentration Comparisons with Additional Disposal Unit Contributions – Base Case

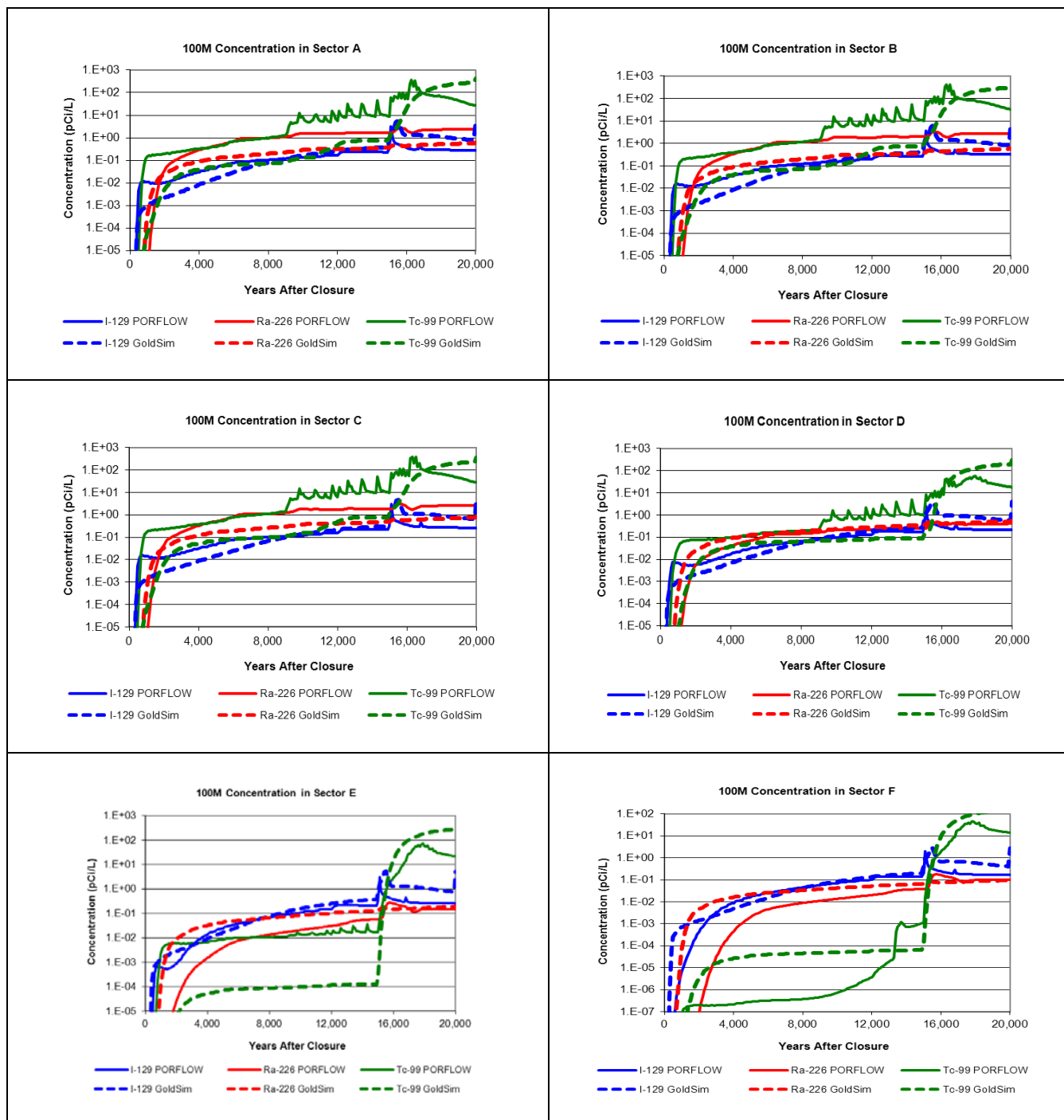
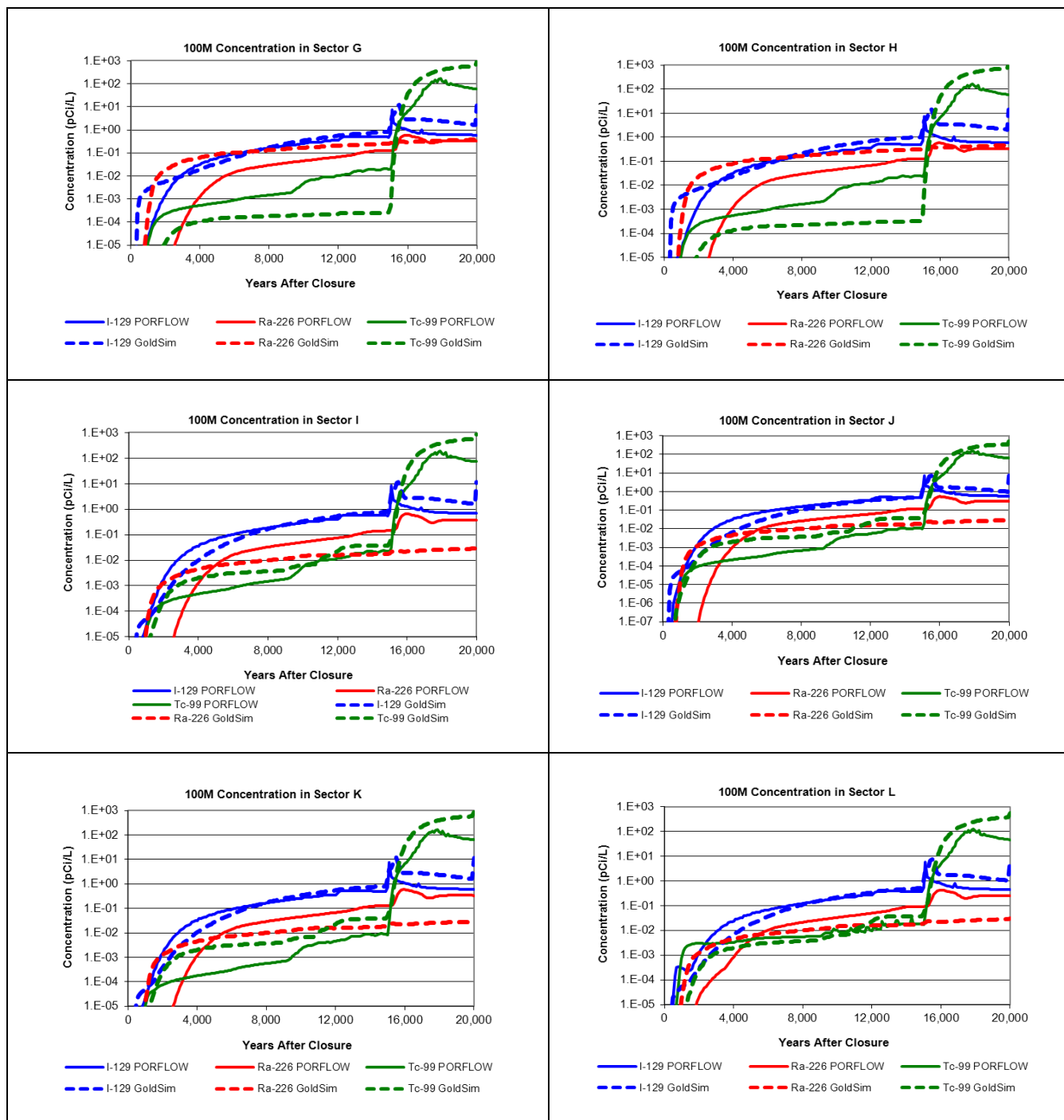


Figure PA-5.2-4: Northern Sectors Concentration Comparisons with Additional Disposal Unit Contributions – Base Case



The two benchmarking factors of 0.5 reduced all the concentrations at the 100-meter boundary by 0.5. Comparisons of Figures PA-5.2-3 and PA-5.2-5 and Figures PA-5.2-4 and PA-5.2-6, indicate that their main influence is with respect to the I-129 concentrations after 15,000 years, where they improve the matches. Although they have an effect when used in conjunction with other benchmarking factors that offset dilution effects, these two factors seem to offset the late-time FDC releases that are overestimated in the GoldSim model as shown in SDF PA Figure 5.6-8.

The final set of benchmark parameters described above as Categories 1 and 2, which influenced Sector J and Sectors A, B, and C, respectively were added back in the same run as they all effect different sectors. The 70, 100, and 50 factors used to multiply the Vault 4 releases reaching Sectors A, B, and C, respectively improved the match between the PORFLOW and GoldSim model concentrations before the 15,000 year time frame, a time period where the releases from Vault 4 are the dominant component of the of the concentrations in Sectors A, B, and C. This improved match can be seen for Tc-99, Ra-226 and I-129, when comparing Figures PA-5.2-5 and PA-5.2-7. This is most likely reflective of different dilution factors between the two models, associated with the use of heterogeneous versus spatially averaged flow fields. The benchmarking factor of 5 used to multiply the concentration components for Sector J from the FDCs may be associated with the differences in degree of dilution between models (see Figures PA-5.2-6 and PA-5.2-8), but this may not be the complete reason. Although the factor improves the Ra-229 comparison between the two models, it actually hurts the Tc-99 comparison. Either way, the use of the benchmarking factor is conservative.

Figure PA-5.2-5: Southern Sectors Concentration Comparisons with 0.5 Benchmarking Factor – Base Case

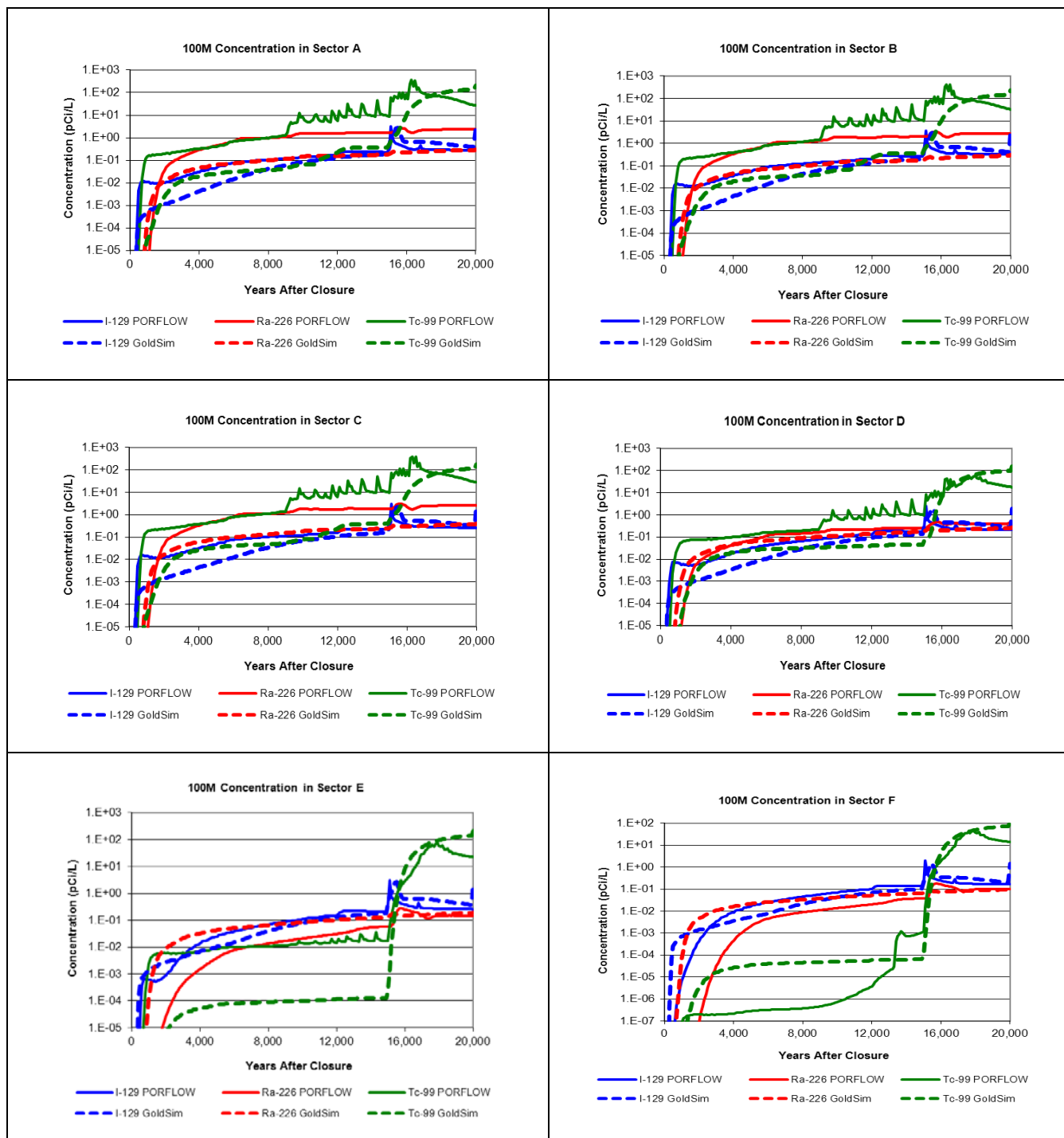


Figure PA-5.2-6: Northern Sectors Concentration Comparisons with 0.5 Benchmarking Factor – Base Case

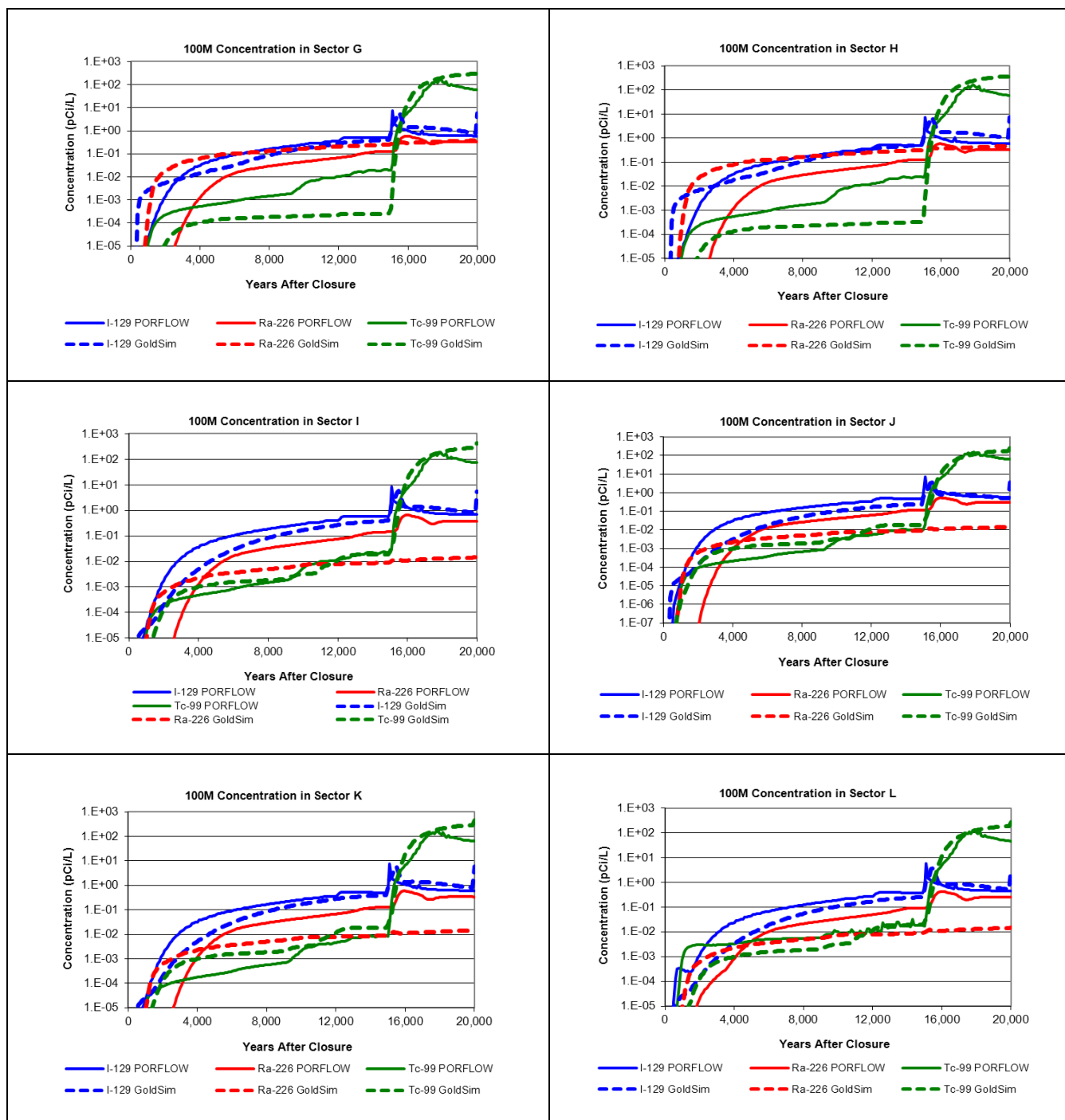


Figure PA-5.2-7: Southern Sectors Concentration Comparisons with Adjustment for the Flow Divide and Vault 4 Contributions – Base Case

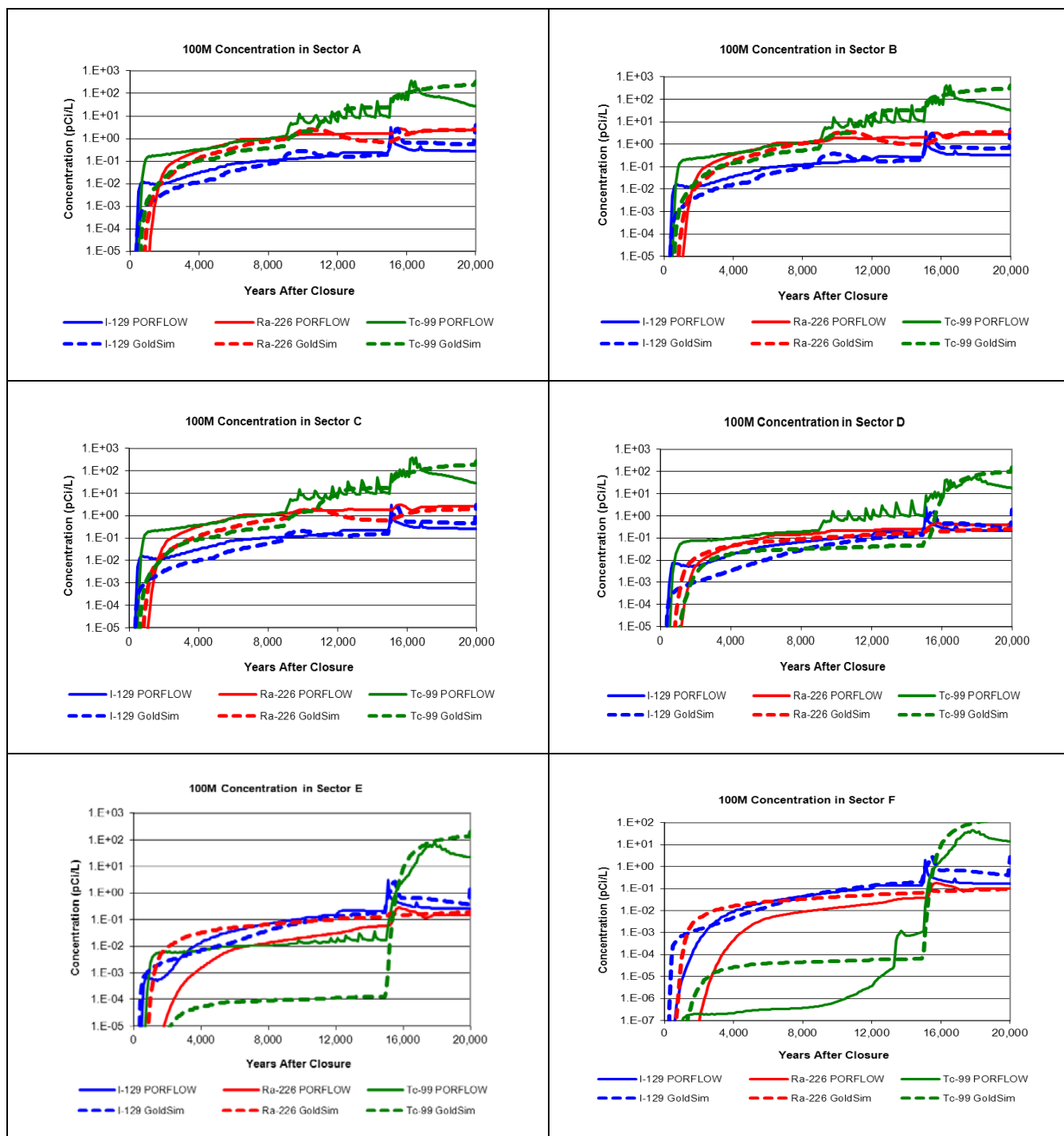
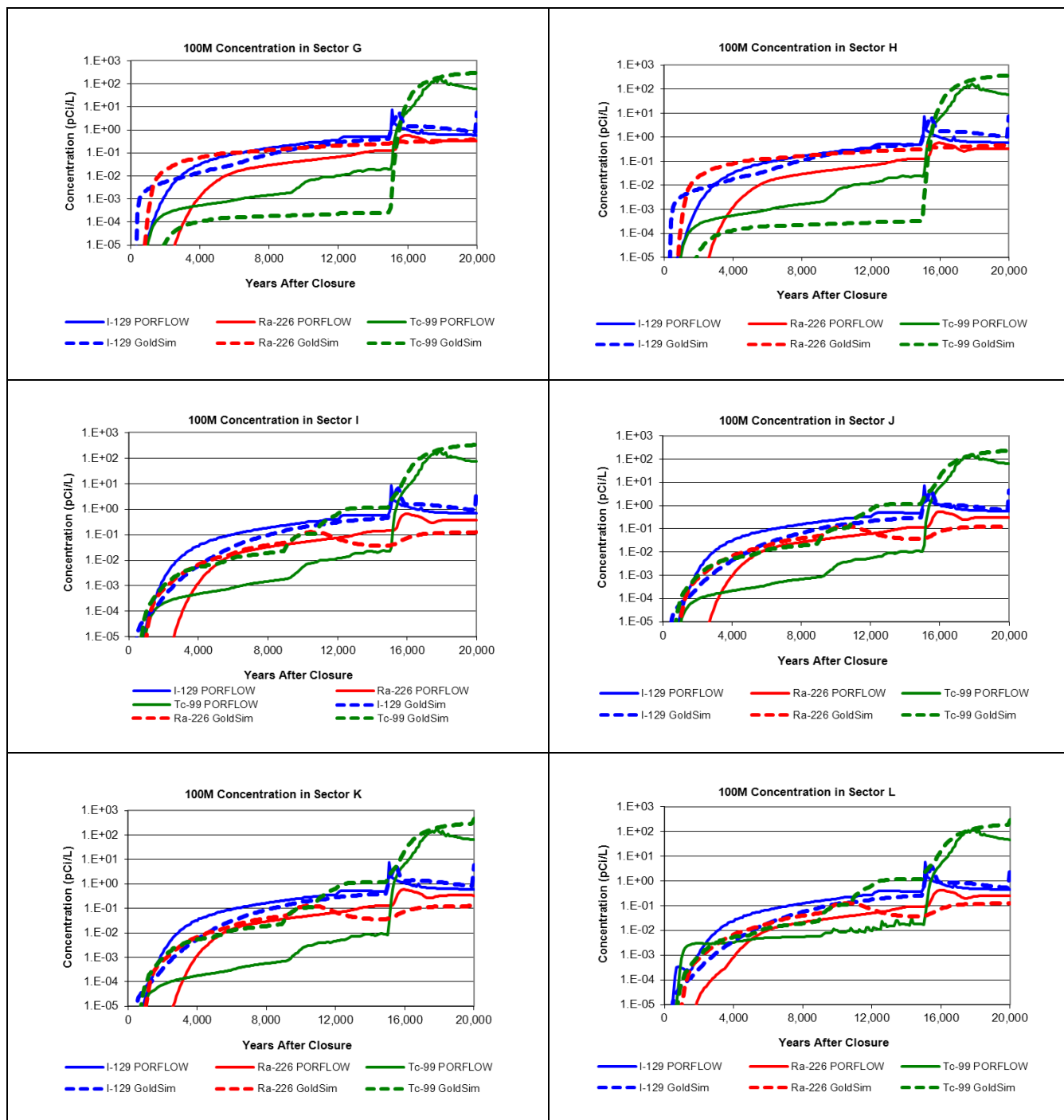


Figure PA-5.2-8: Northern Sectors Concentration Comparisons with Adjustment for the Flow Divide and Vault 4 Contributions – Base Case



When comparing sector based plots depicting GoldSim 100-meter concentrations for I-129, Ra-226, and Tc-99 prior to benchmarking and PORFLOW concentrations (Figure PA-5.2-1 for the southern sectors and Figure PA-5.2-2 for the northern sectors) with equivalent concentrations where the GoldSim model is benchmarked (Figure PA-5.2-7 for the southern sectors and Figure PA-5.2-8 for the northern sectors), the similarity between GoldSim and PORFLOW results increases after benchmarking. Adding contributions from Vault 1 to other sectors in the south to approximate the influence of transverse dispersion and contributions from the southern disposal units to the northern sectors helped to generate GoldSim results that were similar to PORFLOW results. These additional contributions were especially critical for Ra-226 and Tc-99 matching efforts involving Sectors E and F in the south and for all of the northern sectors.

PA-6

Comment:

Results of analyses run to times beyond or far beyond the performance period appear to underestimate dose by excluding radionuclides and pathways based on their contribution to the base case analysis at 10,000 or 20,000 years. Although an estimate of the dose at extremely long times is not likely to be necessary for a compliance determination, it is important to understand the basis for any reported results and, when reporting the information, to note important limitations.

DOE Response Discussion:

The answer to this RAI was mostly adequate, but NRC staff has one clarifying question about this RAI response. The first sentence in Section 5.5.1.5 of the PA states, "The peak groundwater pathways doses associated with key radionuclides are calculated for 40,000 years in order that the dose behavior well past the performance period can be evaluated". However, the RAI response implies that the calculation described in this section included all radionuclides. Although the dose at 40,000 years is outside of the period of compliance, the information presented in Figure 5.5-9 may be misleading if all radionuclides were not included in this PORFLOW calculation.

Path Forward

Please provide a list of the radionuclides that were included in the PORFLOW calculation described in Section 5.5.1.5.

RESPONSE PA-6:

The input to the PORFLOW analysis described in the SDF PA Section 5.5.1.5 includes the following radionuclides, I-129, Np-237, Pu-238, Tc-99, Th-230, U-234, and U-235. The principle dose contributing radionuclides, as identified in SDF PA Section 5.2.2, were captured by this analysis.

Based upon the modeling input identified above, concentrations for the following radionuclides were computed by PORFLOW:

- Ac-227 (from U-235 decay)
- I-129
- Np-237
- Pa-231 (from U-235 decay)
- Pb-210 (from decay of Th-230, Pu-238, and U-234)
- Pu-238
- Ra-226 (from decay of Th-230, Pu-238, and U-234)
- Tc-99
- Th-229 (from decay of Np-237)
- Th-230 (including decay of Pu-238 and U-234)
- U-233 (from decay of Np-237)
- U-234 (including decay of Pu-238)
- U-235

PA-7

Comment (New):

Model support for the PA is limited and plans for development of additional support are not provided.

Basis:

Model support is essential to developing confidence that the PA provides for decisions that are protective of public health and safety. Model support is intended to develop confidence that an appropriate model was used. DOE has done a much better job at explaining the calculations. However, with respect to model support, DOE has referenced ongoing research or provided sensitivity analyses. NRC acknowledges the ongoing research and is fully supportive of it. The sensitivity analysis is useful to understand how the results may change with changes in data or models. However they are of limited use in determining whether the current representation is appropriate and sufficient. The likelihood of making a poor decision increases if model support is limited. NUREG-1854 (NRC, 2007) provides information on appropriate forms of model support.

Path Forward:

Provide acceptable model support for the PA model. If research is ongoing, provide a description of the plans to develop model support including when the information is scheduled to be developed. Consult NUREG-1854 (NRC, 2007) for additional information regarding approaches acceptable to NRC.

Response PA-7:

The importance of model support is recognized and appreciated. Appropriately, activities to improve modeling confidence are ongoing. SDF PA Table 8.2-1 identified ongoing and planned activities to address, among other things, the eight factors resulting from NRC's TER on DOE's waste determination for salt waste disposal at SRS (ML053010225). Factor 3 specifically discussed model support activities.

The *FY2010 Annual Review Saltstone Disposal Facility (Z Area) Performance Assessment* (SRR-CWDA-2011-00055) discusses ongoing and planned studies designed to provide model support. Evaluations on work that has already been completed indicate that the results are supportive of PA results (SRR-CWDA-2011-00055, Section 3.3). Additional evaluations and other planned model support activities are discussed in *SRS Liquid Waste Facilities Performance Assessment Maintenance Program – FY2011 Implementation Plan* (SRR-CWDA-2011-00052).

Table PA-7.1 identifies the PA maintenance activities that address model support and cross-references these activities with the items in SRR-CWDA-2011-00052.

Consistent with the review procedures described in Section 4.2.5 of NUREG-1854, as these activities are completed the results from these various studies and observations will be evaluated against the results from the SDF PA. If results are not consistent with SDF PA results, the data shall be further evaluated and, if appropriate, the SDF PA may be revised to reflect the new information.

Table PA-7.1: PA Maintenance Activities to Address Model Support

Factor Description	Related PA Maintenance Activities	PA Maintenance Plan Sections
Adequate model support is essential to assessing whether the saltstone disposal facility can meet 10 CFR 61.41. The model support for (1) moisture flow through fractures in the concrete and saltstone located in the vadose zone, (2) realistic modeling of waste oxidation and release of technetium, (3) the extent and frequency of fractures in saltstone and disposal unit that will form over time, (4) the plugging rate of the lower drainage layer of the closure cap, and (5) the long-term performance of the engineering cap as an infiltration barrier is key to confirming performance assessment results.	(1) <u>Moisture Flow through Fractures</u> <ul style="list-style-type: none"> A long-range program plan for on-going testing of degradation mechanisms associated with cementitious hydraulic properties is being developed to identify additional field/lab testing and identify test methods and equipment. A future study will be performed to evaluate the rate of equilibration of saltstone water content. 	2.3.2.1 2.3.4.2 2.3.3.2 2.3.3.3
	(2) <u>Waste Oxidation and Technetium Release</u> <ul style="list-style-type: none"> A long-range program plan for on-going testing of waste oxidation and release of technetium is being developed to identify additional field/lab testing and identify test methods and equipment. 	2.3.1 2.3.1.6 2.3.1.4 2.3.1.5 2.3.3.5
	(3) <u>Extent and Frequency of Fractures</u> <ul style="list-style-type: none"> A long-range program plan for on-going testing of the extent and frequency of fractures is being developed to identify additional field/lab testing and identify test methods and equipment. 	2.3.3.6 2.3.3.7
	(4) <u>Plugging Rate of lower Drainage Layer</u> <ul style="list-style-type: none"> A long-range program plan for evaluating the plugging rate of the lower drainage layer is being developed to identify additional field/lab testing and identify test methods and equipment. Evaluation of a replacement for the HELP code is currently planned. 	Future work (no current maintenance activities)
	(5) <u>Long-Term Performance of Closure Cap</u> <ul style="list-style-type: none"> A long-range program plan for evaluating the long-term performance of the closure cap is being developed to identify additional field/lab testing and identify test methods and equipment. 	Future work (no current maintenance activities)

[SRR-CWDA-2009-00017 Table 8.2-1]

PA-8

Comment (New):

The base case does not represent the current and reasonably expected future conditions.

Basis:

The PA base case scenario is unrealistic and non-conservative in that it (i) does not reflect relevant known conditions, (ii) does not adequately account for uncertainty and variability, and (iii) does not have adequate technical bases.

The base case model is inconsistent with known conditions. Significant site characteristics that have not been adequately incorporated into the model include the following:

- Fractured saltstone is not considered in the base case even though fracturing of saltstone has been observed. In addition, shrinkage has been observed and is not included in the model. (Comment SP-2)
- The PA models appear to be inconsistent with observed, advective contaminant releases from Vault 4. (Comments SP-6)
- Material interfaces have shown to be relevant to performance; however they are not considered in the PORFLOW model. (Comment VP-5)

The base case model does not adequately account for uncertainty in initial, temporal, and spatial conditions. NRC concerns with parameter and conceptual model uncertainty include the following:

- The hydraulic conductivity and effective diffusion coefficient for saltstone are time-invariant as the base case model does not adequately account for temporal variation. (Comment SP-1; SP-6)
- The initial hydraulic conductivity of saltstone does not fully account for uncertainty in scaling from laboratory conditions to full-scale, as-emplaced saltstone. (Comment SP-5)
- The PA does not account for uncertainty in the predictions of Eh-pH evolution for cementitious materials. (Comment SP-12)
- The PA does not account for uncertainty with respect to vault degradation mechanisms. (Comment VP-2)

The base case does not have adequate technical bases. NRC concerns with limited model support include the following:

- Model support for geotextile filter fabrics and the lateral drainage layers is not commensurate with their expected long-term performance and risk significance. (Comment IEC-8)
- The moisture characteristic curves implemented in the base case for intact and fractured cementitious materials, which significantly reduce flow, lack adequate support considering their risk significance. (Comments SP-3; SP-4)
- The chemical stability of saltstone provides a significant barrier to transport; however, the basis for the Eh-pH evolution of cementitious materials is very limited. (Comment SP-12)
- The basis for the adopted technetium pseudo-K_d of 1,000 mL/g is inaccurate and insufficient. (Comment SP-15)
- The selected biotic transfer factors lack site-specific data and have very limited support. (Comment B-1)
- There is not a sufficient technical basis to exclude the chicken and egg pathway. (Comment B-2)

- The effects of radionuclide build-up in irrigated soils may be underestimated. (Comment B-3)
- The soil to plant transfer factors may be too low due to the elimination of the leafy plant component. (Comment B-4)

DOE has supported the base case with alternative scenarios and one-off sensitivity analyses. Alternative scenarios can be considered towards compliance determination; however, limitations with the assumptions and parameterization make the conservatism of the alternate cases and the synergistic case unclear (see Comment PA-9).

DOE has used one-off sensitivity analyses to evaluate the risk significance of certain parameters that are not incorporated into the base case model to demonstrate that the individual parameters do not appreciably impact the estimated dose to the Member of the Public (MOP) during the compliance period. However, this type of analysis, which may result in an insignificant increase in the base case dose, will only identify local sensitivity within the parameter space. When (i) many uncertainties exist, (ii) the margin between compliance and the base case dose is relatively small, and (iii) it is not clear how all of the uncertainties are interrelated, then the resultant dose from the inclusion of these uncertainties could be significant on a cumulative basis even if the increases for individual one-off analyses are insignificant on an absolute basis.

Path Forward:

DOE should establish a base case that has adequate technical bases and appropriately reflects uncertainties to demonstrate with reasonable assurance that the performance objectives can be met.

Response PA-8:

NRC Comment PA-8 indicates that the SDF PA Base Case does not represent the current and reasonably expected future conditions. In support of the response to this broad comment, information is provided related to topical areas that crosscut comments contained in multiple individual RAIs. These areas include:

1. The fundamental PA concepts that guided the SDF PA development
2. The results of an additional non-mechanistic sensitivity analysis, referred to as "Alternative Sensitivity Case K"

Discussion is provided in other RAI responses to address more narrowly focused comments and questions provided by the NRC. Our evaluation indicates that nothing in the issues raised by the NRC significantly challenge the overall reasonableness of maintaining Case A as the Base Case. In summary, DOE maintains that the current approach and design of the PA as informed by the Base Case and associated uncertainty and sensitivity analyses results, provide reasonable assurance that closure of SDF disposal units will be in compliance with the performance objectives described in 10 CFR 61, Subpart C.

SDF PA Development

Development of the SDF PA was predicated on several fundamental PA precepts that guided the approach used and the results presented. Two such precepts, 1) development of a Base Case using best-estimate deterministic assumptions and 2) use of a risk-informed approach, are discussed below.

Base Case

The deterministic Base Case of the SDF PA includes a combination of reasonably conservative and best-estimate assumptions (i.e., most probable modeling parameters). The deterministic Base Case model is accompanied by a probabilistic model of uncertainty and deterministic alternative modeling cases, which are provided as tools to identify uncertainty associated with the Base Case. This combination of deterministic and probabilistic analyses is referred to as a hybrid approach. Analyses provided in addition to the Base Case evaluated the risk significance of assumptions that were possible although less probable than the Base Case assumptions and often were even considered non-mechanistic when coupled with other assumptions. An assumption is considered non-mechanistic when there is no set of physical causative conditions that can provide a basis for the conditions used to implement the assumption. Though unlikely to occur, the results of modeling using non-mechanistic assumptions can further identify risk significant modeling parameters.

The Base Case uses a thoughtful combination of probable and conservative assumptions that taken together provides a result that is reasonably conservative. Clearly, substituting mostly pessimistic values for every assumption to account for uncertainty would undercut the intent of the Base Case in supporting risk-based decision-making and would likely result in needless expenditures and delays in waste treatment and stabilization activities while resulting in little to no real risk reduction. The application of the hybrid approach to PA development (i.e., including a probabilistic model and alternative modeling cases) was to allow for the less probable assumptions to be modeled, improving overall understanding of the SDF system. DOE decisions pertaining to system performance and reasonable assurance of compliance with performance objectives are based on both the Base Case and uncertainty/sensitivity analyses results.

In addition, when given a set of possible risk-significant values there seems to be a predilection for the development of the Base Case primarily using the perceived “conservative” values, without due consideration of the combined impact of such an approach. DOE maintains that uncertainty/sensitivity analyses are the appropriate mechanisms for developing a risk-informed understanding of the dose impact of low probability combinations of conservative assumptions. Basing compliance considerations solely on the results of uncertainty analysis, regardless of the best-estimate assumptions reflected in the Base Case creates the perception that the Base Case results do not necessarily reflect the most probable modeling case. The fact that using a more pessimistic modeling value can cause the Base Case peak dose results to increase does not make that modeling value more valid or more appropriate for use in the Base Case. A risk-informed PA utilizes this fact to determine where uncertainty is most significant and where additional modeling emphasis should be placed. Alternatively, basing compliance decisions solely on the Base Case analysis does not appropriately consider potential variability in system performance.

All physical systems are simplified to some degree when they are modeled. The goal is to capture the major features and components of the system at a level of detail that provides a reasonable estimate of performance within the domain under consideration. Application of modeling assumptions and/or specifications that do not reflect a one-to-one match to real-world physical conditions does not invalidate the model. With the Base Case, approaches or parameters were often selected because they represented a reasonable modeling simplification for the highly complex SDF system, not because they explicitly reflected a perceived future outcome. In fact, multiple competing assumptions make decisions regarding implementation of perceived “conservative” assumptions challenging. For example, when considering transient releases of mass into the saturated zone an increase in longitudinal dispersion and associated

spreading of the release would be expected to decrease the maximum contribution to dose for a specific radionuclide. This is often true, but for a decaying species, the amount of mass that reaches the point of assessment also depends on a combination of the retarded seepage velocity and the half-life of the species. The dispersion of a fast decaying mass may increase the mass that actually reaches the assessment point.

Modeling parameters were selected to reflect closely the best available information and real-world physical conditions wherever possible, but when parameters could not specifically reflect such conditions appropriate modeling simplifications were selected based upon modeling conventions and expert judgment. Enhancements to the Base Case will be made as knowledge is acquired. If new information regarding modeling assumptions show a different approach or value is more probable or appropriate (e.g., new moisture characteristic curves, or new K_d values), updates to the Base Case will be considered and applied as appropriate. This can have implications that are both conservative and non-conservative with respect to dose. There are modeling approaches and assumptions that have been identified that potentially reduce the peak doses that are not currently incorporated within the Base Case, such as refinements to inventory estimates for Ra-226 and its parents and updates to the dose calculation methodology, as described in the responses to B-2, B-3 and B-4. As required by DOE Manual 435.1-1, maintenance of the SDF PA will include future updates to incorporate new information, update model codes, analysis of actual residual inventories, etc., as appropriate.

Risk-Informed Approach

In developing the deterministic Base Case assumptions and its parameterization, DOE developed a conceptual model of the SDF system and surrounding GSA that captures the major features of the system and incorporates a total level of conservatism considered reasonable. The level of conservatism for each subsystem was dependent on the state of knowledge of each, respectively. In developing assumptions and parameter values, DOE did not seek to create artificial pessimistic assumptions that bound possible, but not probable, scenarios. Instead, DOE sought a risk-informed analysis (through both reasonably conservative and variable system performance) that provides information to feed critical closure decisions associated with the disposal units in the SDF.

In support of the development of the SDF PA, DOE consulted and used nationally recognized experts in their respective fields including cementitious materials, geochemistry, hydrogeology, and modeling of environmental fate and transport phenomena. The fate and transport modeling in the SDF PA reflects results and conclusions from approximately 60 years of study of subsurface conditions of the GSA. It is this strong foundation of research and study that provides DOE reasonable assurance that the 10 CFR 61.41 and 10 CFR 61.42 performance objectives will be met during the 10,000-year compliance period. The Base Case analysis, extensive uncertainty analysis/sensitivity analyses, and the responses to these NRC comments, further inform this assessment.

It can be inferred that the writers of the 10 CFR 61 factored in the risk and associated level of pessimism when projecting a dose to a hypothetical MOP thousands of years into the future in selecting a value as low as 25 mrem/yr. While understanding the level of pessimism reflected in the 25 mrem/yr worst case or peak dose value, please note the following:

- The average annual dose to a United States citizen in 2007 was 620 millirem; approximately 25 times higher than the 10 CFR 61.41 performance objectives. If an individual moves from the area surrounding SRS to Denver, Colorado, their annual dose from just cosmic and terrestrial background radiation alone will increase greater than 100 millirem; a value four times the performance objective. [NCRP-160] Further, as

noted in the NRC, Fact Sheet on *Biological Effects on Radiation*, “Those people living in areas having high levels of background radiation – above 1,000 mrem (10 mSv) per year – such as Denver, Colorado, have shown no adverse biological effects.” [NRC_01-01-2011] A background dose of 1,000 mrem/yr represents a dose 40 times greater than the 10 CFR 61 performance objectives.

- Today a MOP living on the site boundary can receive 100 millirem each year and non-occupational worker including a MOP visiting the site can receive this same 100-millirem dose, either chronic or acute. This value is also four times higher than 10 CFR 61.41 performance objectives.
- An occupational worker at a DOE site, such as SRS, or a commercial nuclear facility regulated by the NRC can receive 5,000 mrem/yr; a value 200 times greater than the 10 CFR 61.41 performance objectives. [10 CFR 835, 10 CFR 20]

To support this reasonably conservative, risk-informed SDF PA, DOE used many possible, though not likely, assumptions to describe a future individual who serves as a hypothetical dose receptor. First, the individual is permitted to homestead unabated in the former location of the SDF. It is assumed that all knowledge of the SRS is lost including both public records and any indicators of the previous activities, such as designed markers of the closed facilities. It is then assumed that the individual drills a well just 100 meters from the outermost disposal unit. The depth of the well does not reflect the optimal depth consistent with local drilling practices but rather selects a depth that would maximize the resultant doses. Further, as a conservative modeling assumption, DOE selected maximum concentrations of contaminants across relatively large “sectors” and assumed these were concentrations at a single “well” location. The scenarios developed for evaluating the groundwater dose also have the benefit of inherent conservatism. For example, the doses calculated using water from a well for domestic purposes tend to maximize the number of functions for which a single well (with the maximum source of contamination) is utilized. The individual is assumed to use this well as the principle source of non-public drinking water (approximately 75 % of all fluid intake), and also use the well to supply an unspecified irrigation system for both a garden (from which individual is supplied vegetables) and for livestock water and fodder (from which the individual is subsequently exposed to contaminated milk and meat).

Given the designed conservatism in the SDF PA modeling approach described in SDF PA Section 7.2, DOE believes that the selected assumptions and parameter values is based on sound science and engineering principles for both engineered and natural barriers, and is appropriate for understanding the risk of closure activities on future human health and the environment.

Non-Mechanistic Sensitivity Analysis

As explained in the Base Case discussion (above), uncertainty around the Base Case is addressed in the SDF PA via additional, supporting assessments (i.e., alternate modeling cases and probabilistic analyses). These additional analyses provide insights into the Base Case results and overall system performance. Several RAI responses provide additional information in these areas, such as IN-2 (pertaining to the uncertainty distributions of the radionuclide inventories in the FDCs).

Section 4.4.2 of the SDF PA explains that the alternative modeling cases represent postulated conditions that may be present, without regard to the mechanism that led to those conditions. There are varieties of mechanisms that can lead to early degradation times, relative to the Base Case. In closed SDF conditions, these mechanisms may be possible, although not likely. In

other words, the alternate modeling cases should not be interpreted as representing a specific mechanism for grout/concrete degradation or taken as belief that a given or set of conditions would actually be present in a closed system at some point in the future. The failure times modeled in Cases B, C, D, and E encompass various mechanisms and provide information on the risk-significance of early failure, relative to the Base Case, as well as providing understanding of system performance while considering uncertainty and variability.

ALTERNATIVE SENSITIVITY CASE K

To evaluate further the impact on dose due to deviations from the Base Case, a non-mechanistic modeling case (Alternative Sensitivity Case K) has been developed as a supplement to the Single Parameter Sensitivity Analysis presented in SDF PA Section 5.6.6). Following lengthy discussions with the NRC as documented in DOE Letter to the NRC, WDPD-11-65, dated May 20, 2011 the parameters associated with Alternative Sensitivity Case K were finalized. Alternative Sensitivity Case K is not considered a likely alternate scenario; however, it was developed to provide additional information regarding the impacts when select barriers of concern (addressed below) are pessimistically modified simultaneously. Alternative Sensitivity Case K cannot be construed as representing an expected physical reality, but instead reflects the potential impact on system performance and the estimated contaminant release and resulting radiological dose when conservative, non-mechanistic degradation of barriers is postulated.

Alternative Sensitivity Case K is constructed in such a way as to provide additional understanding of the impacts due to physical degradation of cementitious materials through time, as well as other concerns raised by the NRC in the other RAIs cited in the Basis for this RAI. This sensitivity modeling case was developed by modifying the SDF Base Case model from the PA.

The following discussion provides a description of the methodology applied to develop and implement Alternative Sensitivity Case K and an analysis of the results.

ALTERNATIVE SENSITIVITY CASE K METHODOLOGY

Table PA-8.1 provides a brief summary of the modeling approach developed as Alternative Sensitivity Case K. The changes to these modeling attributes are discussed in detail below. Alternative Sensitivity Case K applies updated input data (as appropriate) and significantly exaggerates the degradation of cementitious materials.

Table PA-8.1: Summary of Alternative Sensitivity Case K Attributes

Modeling Attributes	Change from Base Case (associated RAI)	Impact on Base Case
Saltstone Physical Degradation	Complete degradation occurred within 10,000 years with degraded saltstone having a saturated hydraulic conductivity of $1.0\text{E-}06$ cm/sec and an effective diffusion coefficient of $5.0\text{E-}06$ cm ² /sec. Final degradation values are representative of soil properties (SP-1, SP-2, SP-7, and SP-17).	Increases the flow through the closure system and the release of contaminants
Moisture Characteristic Curves	MCCs were not used for cementitious material. Relative permeability and saturation were set equal to 1.0 for all suction levels for saltstone, clean cap, and disposal unit concrete (SP-3).	Increases the flow through the closure system and the release of contaminants
Saturated hydraulic conductivity for intact saltstone	Assumed to be $1.0\text{E-}08$ cm/sec, largest value reported using simulants with a minimum of 90-day curing time and nominal curing temperature (SP-5).	Increases the flow through the closure system and the release of contaminants
Effective diffusivity of saltstone	For intact saltstone and clean cap the initial value was unchanged from the Base Case but increased to $5.0\text{E-}06$ cm ² /sec as the saltstone and clean cap degrade within 10,000 years (SP-6).	Increases the release of contaminants
Pore volumes required to initiate E_h and pH transitions	E_h transition volume changed to 18 % of the Base Case value based on arbitrarily reducing by a factor of four, the reduction capacity of saltstone and applying a porosity correction. pH transition volume changed to 73 % of the Base Case value based on a porosity correction (SP-12).	Increases the release of the majority of contaminants
Technetium release via shrinking core model	Modified using a single porosity model that is based on the ISBN: 1-55899-189-1 approach; and using a semi-log fracture growth relationship with a final fracture spacing of 10 centimeters. Pertinent parameters (SP-13) are: <ul style="list-style-type: none"> Constant diffusion coefficient of intact matrix of $1.0\text{E-}07$ cm²/sec Reduction capacity of 0.206 meq e-/g (0.25 of Base Case value) Dissolved oxygen concentration at fracture face is 1.06 meq e-/L 	Increases surface area for oxygen diffusion and increases the oxidation of saltstone which accelerates the release of technetium from saltstone

Table PA-8.1: Summary of Alternative Sensitivity Case K Attributes (Continued)

Modeling Attributes	Change from Base Case (associated RAI)	Impact on Base Case
Drainage layer performance	No Change (IEC-8) Time periods refined to capture significant changes to model parameters (C-22)	Increases flow into the closure system and contaminant release
Degradation of disposal unit concrete	Concrete fully degrades to representative soil properties with a saturated hydraulic conductivity of 1.0E-06 cm/sec and an effective diffusion coefficient of 5.0E-06 cm ² /sec <ul style="list-style-type: none"> Initially for walls of Vaults 1 and 4 (VP-6) Within 3,500 years for the roof of Vault 4 Within 10,000 years for other disposal unit concrete (VP-2 and VP-3) Non-degraded properties provided in PA Table 4.2-16 	Increases flow through the closure system without potentially diverting water away from saltstone caused by highly degraded walls in Vaults 1 and 4
Dose to the chronic intruder in vicinity of disposal units	Dose estimated based on water concentrations below Vault 4 and an FDC (II-2)	Increases potential dose to the intruder
Radionuclides analyzed	No change; all radionuclides identified in PA Section 3.3.	No impact
Inventory	Vault 4 inventory reduced from the PA Table 3.3-3 for Pu-238, Ra-226, Th-230, and U-234. FDC inventory reduced from the PA Table 3.3-5 for Ra-226 and Th-230 (IN-5).	Reduces the impact of radionuclides identified
K _d values for saltstone, disposal unit concrete, and soil	Values updated based on latest issued reports (SP-10, SP-14, SP-15, FFT-2, and FFT-3)	Changes the impact of specific radionuclides
Dose methodology	Biotic transfer factors updated based on latest information (B-1) Inclusion of chicken and egg pathway (B-2) 25-year buildup of radionuclides in irrigated soil (B-3) Inclusion of leafy portion in plant transfer factor (B-4)	Changes the impact of specific radionuclides

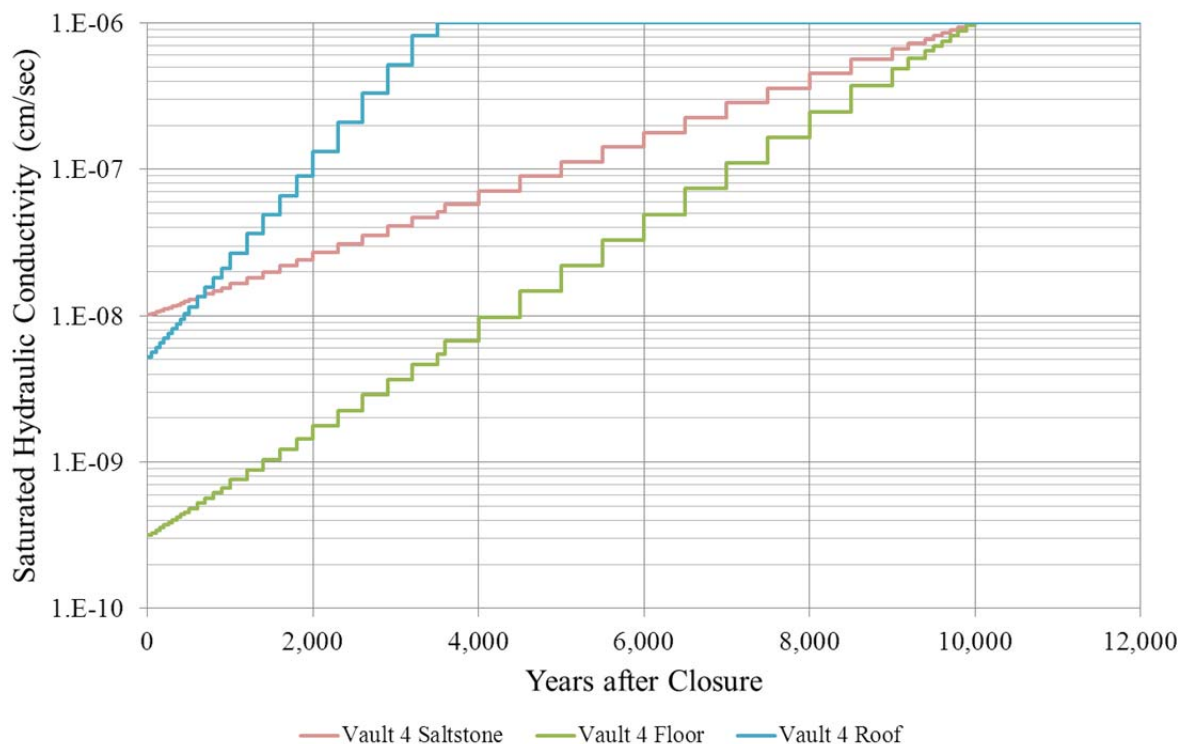
For this case, the cementitious materials hydraulically degrade non-mechanistically such that the final hydraulic conductivity is on the same order of magnitude as the surrounding unsaturated soil. Realistically, this amount of degradation is highly pessimistic within the timeframe modeled (i.e., 10,000 years after closure). It is reasonable to assume that a cementitious monolith buried within SRS soil is likely to still be a cementitious monolith after 10,000 years (i.e., it is not realistic to assume that the entire monolith would degrade to soil properties within 10,000 years). Therefore, applying such high values of hydraulic conductivity is a highly conservative approach, which would greatly exaggerate flow through the closure system and increase the release of contaminants.

Specific attributes of the model used for the Alternative Sensitivity Case K are discussed below.

Cementitious Material Degradation: Hydraulic Conductivity

Saturated hydraulic conductivity (K_{sat}), or the velocity of water flowing through saturated materials subjected to a unit hydraulic head gradient, is a material property that increases as a material degrades: the more degraded the material, the higher the K_{sat} and the greater the flow. Figure PA-8.1 illustrates the change in K_{sat} over time for selected Vault 4 cementitious materials. Other cementitious materials follow the same rate of degradation; only the initial value may be different as indicated in PA Table 4.2-16.

Figure PA-8.1: Example of Hydraulic Degradation for Vault 4 Cementitious Materials in Alternative Sensitivity Case K



As shown, the hydraulic conductivities at the initial time of closure are the same as the Base Case model, except for saltstone, which uses a higher initial K_{sat} of 1.0E-08 cm/sec for Alternative Sensitivity Case K, as opposed to 2.0E-09 cm/sec in the Base Case. The hydraulic conductivities of the materials then degrade, following a log-linear (or semi-log) relationship,

until the full degradation rate of 1.0E-06 cm/sec is achieved and is then held constant (see Equation 1). Specifically, the changes in the saturated hydraulic conductivities for the cementitious materials are assumed to vary through time according to the relationship:

$$\log_{10}(K_{sat,t}) = \begin{cases} \log_{10}(K_{sat,t0\%}) & t \leq t_{0\%} \\ \frac{\log_{10}(K_{sat,t100\%}) - \log_{10}(K_{sat,t0\%})}{t_{100\%} - t_{0\%}}(t - t_{0\%}) + \log_{10}(K_{sat,t0\%}) & t_{0\%} < t < t_{100\%} \\ \log_{10}(K_{sat,t100\%}) & t \geq t_{100\%} \end{cases} \quad (\text{Eq. 1})$$

where:

- $K_{sat,t}$ = the saturated conductivity (cm/sec) at the evaluation time t
- $K_{sat,t0\%}$ = the initial saturated conductivity (cm/sec) as defined in Table PA-8.2
- $K_{sat,t100\%}$ = the final saturated conductivity (1.0E-06 cm/sec)
- t = the evaluation time (yr) and the subscripts refer to 0 % and 100 % degradation

For the purpose of Alternative Sensitivity Case K, the hydraulic degradation is based on non-mechanistic assumed failure times (see Table PA-8.2).

Table PA-8.2: Initial Hydraulic Conductivities and Assumed Degradation Times of Cementitious Materials for Alternative Sensitivity Case K

Cementitious Material	Initial Hydraulic Conductivities (cm/sec)			Assumed Degradation Times (yr)		
	Vault 1	Vault 4	FDCs	Vault 1	Vault 4	FDCs
Disposal Unit Roof	5.0E-09	5.0E-09	9.4E-11	10-10,000	10-3,500	10-10,000
Saltstone	1.0E-08	1.0E-08	1.0E-08	10-10,000	10-10,000	10-10,000
Disposal Unit Wall	1.0E-06	1.0E-06	9.4E-11	1-5	1-5	10-10,000
Disposal Unit Floor	3.1E-10	3.1E-10	9.4E-11	10-10,000	10-10,000	10-10,000
Disposal Unit Upper Mud Mat	N/A	N/A	9.4E-11	N/A	N/A	10-10,000
Disposal Unit Lower Mud Mat	N/A	N/A	1.0E-08	N/A	N/A	10-10,000

[Source: SDF PA Table 4.2-16. Note that the final hydraulic conductivities for all cementitious materials at the assumed failure times are 1.0E-06 cm/sec.]

This simplified approach for determining saturated hydraulic conductivity is pessimistic. Actual degradation rates and failure times are expected to vary over time for the different disposal units. By failing multiple materials from multiple disposal units at the same time, the effect of cementitious degradation has a net non-mechanistic cumulative effect with respect to contaminant releases.

Cementitious Materials Degradation: Effective Diffusion Coefficients

For diffusive transport of all contaminant species (not only Tc-99), the effective diffusion coefficient (D_e) for the homogenized system increases over time in a semi-log manner over the same time period as the hydraulic conductivity increases.

$$\log_{10}(D_e) = \begin{cases} \log_{10}(D_{e0\%}) & t \leq t_{0\%} \\ \frac{\log_{10}(D_{e100\%}) - \log_{10}(D_{e0\%})}{t_{100\%} - t_{0\%}}(t - t_{0\%}) + \log_{10}(D_{e0\%}) & t_{0\%} < t < t_{100\%} \\ \log_{10}(D_{e100\%}) & t \geq t_{100\%} \end{cases} \quad (\text{Eq. 2})$$

The initial value ($D_{e0\%}$) for the cementitious materials is provided in SDF PA Table 4.2-16. The fully degraded value ($D_{e100\%}$) is $5.0\text{E-}06 \text{ cm}^2/\text{s}$. Note that this value is representative of the soils surrounding disposal cells; SDF PA Section 4.2.3.2.5 defines the effective diffusion coefficient of the sandy saturated zone soils as $5.3\text{E-}06 \text{ cm}^2/\text{s}$ and the clayey saturated soils as $4.0\text{E-}06 \text{ cm}^2/\text{s}$ and Table 4.2-14 defines the effective diffusion coefficient of the vadose zone soils as $5.3\text{E-}06 \text{ cm}^2/\text{s}$. This increase in the diffusion coefficient significantly increases contaminant release when compared to the Base Case.

Cementitious Material Degradation: Fracture Spacing and Oxidation

With respect to oxidation of slag-bearing grout and concrete in Tc-99 transport modeling, Alternative Sensitivity Case K assumes that the saltstone grout will undergo increased fracturing (cracking) over time. As with the saturated hydraulic conductivity, fracture spacing also varies non-mechanistic with time in a semi-log (log-linear) manner.

$$\log_{10}(B) = \begin{cases} \infty & t \leq t_{0\%} \\ \frac{\log_{10}(B_{100\%}) - \log_{10}(B_{0\%})}{t_{100\%} - t_{0\%}}(t - t_{0\%}) + \log_{10}(B_{0\%}) & t_{0\%} < t < t_{100\%} \\ \log_{10}(BK_{100\%}) & t \geq t_{100\%} \end{cases} \quad (\text{Eq. 3})$$

where:

B = fracture spacing

t = time

(the subscripts refer to degree of physical degradation)

The relationships between fracture spacing (m), fracture frequency (m^{-1}), and time (years) are illustrated in Figure PA-8.2 for the example of a 10-meter initial spacing and 0.1-meter final spacing. In Figure PA-8.2 the red line represents decreasing space between fractures over time and the blue line represents the increasing frequency of fractures over time. Increased fracturing is conceptually modeled by decreasing the fracture spacing, or the distance between cracks in the saltstone. The initial fracture spacing for the saltstone and the other cementitious materials are provided in Table PA-8.3.

Figure PA-8.2: Example of Progressive Fracturing Through Time

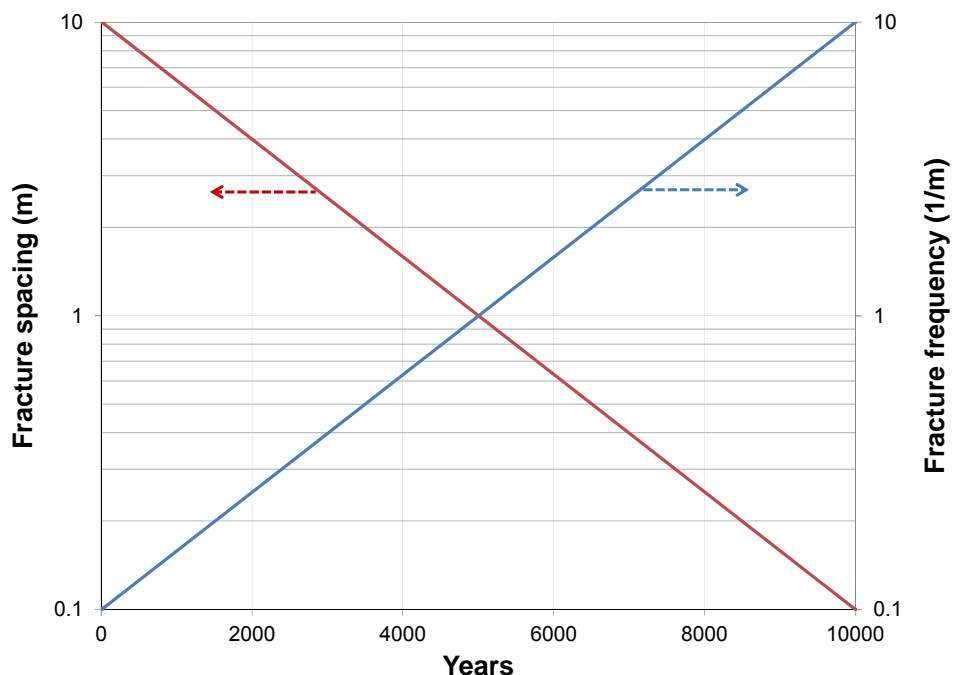
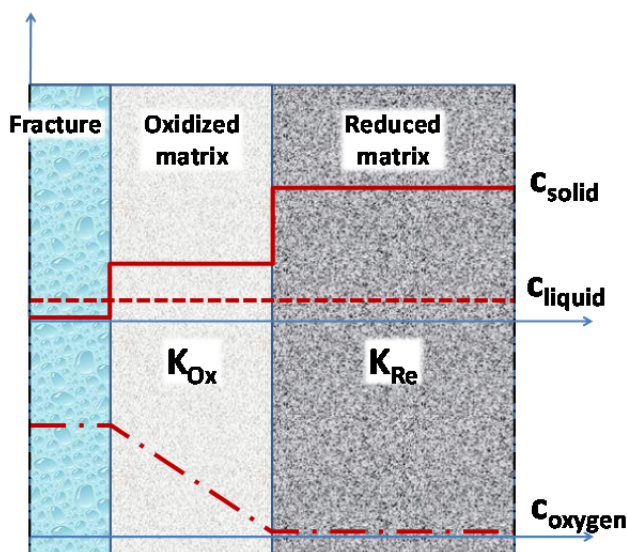


Table PA-8.3: Initial Fracture Spacing of Cementitious Materials Assumed for Alternative Sensitivity Case K

Cementitious Material	Initial Fracture Spacing (m)		
	Vault 1	Vault 4	FDCs
Disposal Unit Roof	10	10	41
Saltstone	30	61	41
Disposal Unit Wall	10	10	7
Disposal Unit Floor	10	10	41

Figure PA-8.3 illustrates the conceptual model of degraded (fractured and partially oxidized) cementitious material for Alternative Sensitivity Case K. Local equilibrium of aqueous concentrations across fractures and matrix is assumed, except for dissolved oxygen, which exhibits a linear profile across the oxidized subzone following ISBN: 1-55899-189-1.

Figure PA-8.3: Conceptual Model of a Degraded Cementitious Material Assuming Equilibrium of Dissolved Species

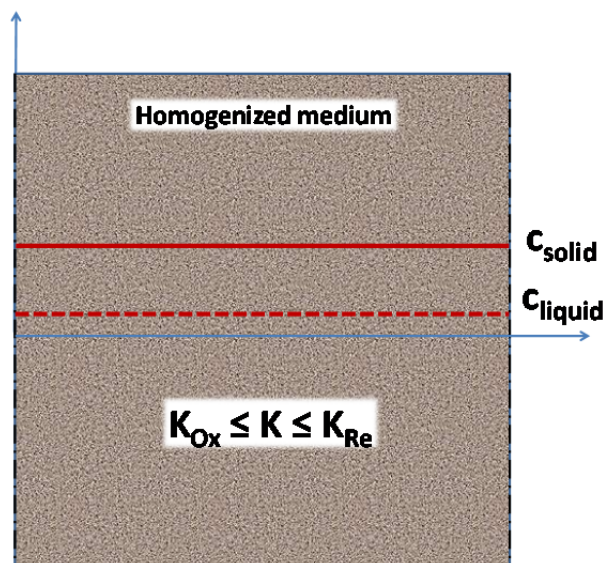


Alternative Sensitivity Case K applies fracture spacing as small as 0.1 meters (approximately 4 inches). Due to model size and runtime limitations, explicit representation of fractures with spacing less than 1 meter was not feasible with the current SDF PORFLOW model. Therefore, to implement very small fracture spacing, Alternative Sensitivity Case K applies a single-continuum/effective porous medium model. The single-continuum approach is more computationally efficient than discrete fracture models, and feasible for system-level simulations. With respect to solute transport, the single-continuum approach implicitly assumes local chemical equilibrium between fractures and matrix. This assumption is reasonable for fracture spacing approaching the final value of 0.1 meters when peak Tc-99 releases occur. [SRR-CWDA-2011-00114]

Sorption is assumed to be negligible in the fracture (distribution coefficient, $K_d = 0$), and generally differs in the oxidized and reduced sub-regions of the matrix (i.e., $K_{d,Ox} \neq K_{d,Re}$). Thus, while the liquid concentration is uniform, the solid concentration may vary.

Figure PA-8.4 illustrates a homogenized representation of the system depicted in Figure PA-8.3 for numerical implementation using PORFLOW.

Figure PA-8.4: Single Continuum Model Representation



Additional details about the implementation of this single-continuum model are discussed below, under *Technetium Release via Shrinking Core Model*.

Moisture Characteristic Curves and Unsaturated Hydraulic Conductivity of Cementitious Materials

The PA Base Case model used moisture characteristic curves to define the unsaturated conductivity of cementitious materials as a function of the suction head (see SDF PA Figures 4.2-23 to 4.2-27). However, throughout the simulated period, saturation of the saltstone was nearly complete (between 95 % and 100 %). Therefore, Alternative Sensitivity Case K applies a simplified, conservative assumption that the saltstone and concrete are always fully saturated. Assuming fully saturated conditions maximizes flow that would otherwise be restricted because of unsaturated conditions. This simplification negates the need to define values for unsaturated hydraulic conductivity, so no moisture characteristic curves are needed. With saturation set to 100 %, the relative permeability is also set to a value of 1.0 for all suction levels ($S = k_r = 1.0$).

Saturated Hydraulic Conductivity for Intact Saltstone

As indicated in the response to RAI SP-5, the largest value for saturated hydraulic conductivity measured from samples analogous to saltstone (with a minimum of 90-day curing time and nominal curing temperature) was 1.0E-08 cm/sec. For conservatism, this saturated hydraulic conductivity is assumed for Alternative Sensitivity Case K.

Effective Diffusion Coefficients of Saltstone

As discussed above for cementitious materials, the effective diffusivity of intact saltstone is initially unchanged (relative to the Base Case) then increases to maximum of 5.0E-06 cm²/sec as the saltstone degrades within 10,000 years, using the semi-log relationship defined by Equation 2. This increase in the diffusion coefficient increases contaminant release from the Base Case.

Pore Volumes Required to Initiate E_h and pH Transitions

RAI SP-12 indicates that support is needed for the process used to predict the E_h -pH evolution for cementitious materials in the PA. As indicated in the response to RAI SP-12, one area of future work is further support for the source term release model that is dependent on the pore volumes required to initiate E_h and pH transitions within saltstone. Alternative Sensitivity Case K modifies saltstone and clean grout transition times, but makes no change to the material properties of the disposal unit concrete, relative to the Base Case. To access conservatively the amount of reducing capacity in saltstone, the reducing capacity of saltstone used in the Base Case (based on calculations presented in SRNS-STI-2008-00045, 0.822 meq e-/g) is reduced by a factor of four to represent the percentage of blast furnace slag present in the saltstone. Thus, for the Alternative Sensitivity Case K, the reducing capacity of saltstone is conservatively estimated to be 0.206 meq e-/g. The transition volume calculations presented in SRNL-TR-2008-00283 were based on an effective porosity of 42.3 % for saltstone. For the Base Case PA modeling, the porosity of saltstone is 58 % based on data presented in SRNL-STI-2008-00421. Thus, for Alternative Sensitivity Case K to reflect the modeling value of 58 % for saltstone porosity, the transition volumes calculated in SRNL-TR-2008-00283 are reduced by 73 % ($= 0.423/0.58$) to account for the difference in the saltstone porosity. The E_h transition volume for saltstone grout for Alternative Sensitivity Case K was reduced to 18 % of the Base Case transition volume (0.25×0.73) where 0.25 represents a reduction by a factor of four on the reducing capacity and 0.73 represents the porosity adjustment. Similarly, the pH transition volume was reduced to 73 % of the Base Case transition volume. For example, SDF PA Table 4.2-9 cites a saltstone E_h transition volume of 2,806 and pH transition volume of 10,422. For Alternative Sensitivity Case K, these transitions are 505 and 7,608, respectively. The response to RAI SP-8 provides additional discussion of E_h and pH transition volumes.

It is recognized that the transition volume for E_h in saltstone used in this Alternative Sensitivity Case K is not indicative of the expected value. As indicated in the response to RAI SP-8, the corrected, expected value is 1,653, more than three times greater than the value used in Alternative Sensitivity Case K.

Technetium Release via Shrinking Core Model

The technetium release model was modified to use a single porosity, shrinking core model. Note that this model was mentioned above, with respect to fracture spacing, as a "single-continuum/effective porous medium model". The Alternative Sensitivity Case K approach utilizes the fracture growth model with a final fracture spacing of 10.0 centimeters (approximately 4 inches) to define time-dependent sorption coefficient values (K_d s) for technetium.

The groundwater pathway of the PA model generally focused on liquid phase transport processes in the vadose and aquifer zones. However, gas phase transport of oxygen through fractures is a controlling process for slag and Tc-99 oxidation in reducing grouts. Simulation of combined gas and liquid phase transport is not supported by currently available versions of PORFLOW, and explicit representation of fractures is not feasible except for special cases involving a relatively small number of fractures. To overcome these limitations, the analytical approach in *The Role of Oxygen Diffusion in the Release of Technetium from Reducing Cementitious Waste Forms* (ISBN: 1-55899-189-1) was used to predict transient oxidation external to PORFLOW. The results of this analysis provide an effective Tc-99 sorption coefficient reflecting varying oxidation through time. The derived sorption coefficient can then be used in a conventional liquid phase only PORFLOW simulation, thus implicitly accounting for both gas and liquid phase oxygen transport in fractured cementitious materials.

Oxidation is assumed to occur as multiple one-dimensional moving fronts across the reducing material, emanating from multiple exposure faces. Fractions of oxidized and reduced material may be denoted by x_{Ox} and x_{Re} , respectively, such that

$$x_{Ox} + x_{Re} = 1 \quad (\text{Eq. 4})$$

The total mass kilogram per mole (M) of a species in a porous medium with sorption is

$$M = Vnc + V(1-n)\rho_s c_s \quad (\text{Eq. 5})$$

where:

V	=	the volume (cm ³ or mL)
n	=	the porosity (%)
ρ_s	=	the density (g/mL)
c	=	the liquid concentration (mol/mL)
c_s	=	the solid concentration (mol/mL)

For linear sorption:

$$c_s = K_d c \quad (\text{Eq. 6})$$

where:

K_d	=	sorption coefficient
-------	---	----------------------

Equation 6 becomes:

$$\begin{aligned} M &= Vnc + V(1-n)\rho_s K_d c \\ &= Vnc \left[1 + \frac{(1-n)\rho_s K_d}{n} \right] \\ &= VncR \end{aligned} \quad (\text{Eq. 7})$$

The retardation factor R is defined by:

$$R = 1 + \frac{(1-n)\rho_s K_d}{n} \quad (\text{Eq. 8})$$

Therefore, the total species mass in the oxidized and reduced regions is:

$$VncR = x_{Ox}VncR_{Ox} + x_{Re}VncR_{Re} \quad (\text{Eq. 9})$$

where the liquid concentration has been assumed to be in equilibrium between the oxidized and reduced regions and R is the effective retardation for the composite of oxidized and reduced material. Equation 9 simplifies to:

$$R = x_{Ox}R_{Ox} + x_{Re}R_{Re} \quad (\text{Eq. 10})$$

The composite sorption coefficient is derived as

$$\begin{aligned} R - 1 &= x_{Ox}R_{Ox} + x_{Re}R_{Re} - (x_{Ox} + x_{Re}) \\ \frac{(1-n)\rho_s K_d}{n} &= x_{Ox} \frac{(1-n)\rho_s K_{d,Ox}}{n} + x_{Re} \frac{(1-n)\rho_s K_{d,Re}}{n} \end{aligned}$$

$$K_d = x_{Ox}K_{d,Ox} + x_{Re}K_{d,Re} \quad (\text{Eq. 11})$$

As discussed above, fracture spacing varies over time (see Equation 3). Decreasing the fracture spacing increases the number of fractures, thus increasing the surface area of exposed surfaces on the saltstone. Counting both left and right boundaries, the number of exposure faces N for a material zone of dimension W (transverse to cracking) is:

$$N = 2 \frac{W}{B} \quad (\text{Eq. 12})$$

The intact matrix between exposure faces is assumed to have sufficiently low permeability that oxygen transport is by diffusion only within the matrix. Fractures are assumed to air-filled, except for thin liquid films on each exposure face, such that the concentration of dissolved oxygen is held constant at its saturation value (1.06 meq e-/L) at each face. The oxidation process is then independent of the flow through fractures (i.e., the system flow model). The oxidation front advances at a rate defined by the differential equation (ISBN: 1-55899-189-1):

$$r_{Ox}\rho_b \frac{d\delta}{dt} = \frac{nD_e c_{Ox}}{\delta} \quad (\text{Eq. 13})$$

where:

r_{Ox}	=	the reduction capacity of solid (meq e-/g)
ρ_b	=	the bulk density of solid (g/mL)
δ	=	the distance of oxidation front from the exposure face (cm)
t	=	time (s)
n	=	the porosity (%)
D_e	=	the effective diffusion coefficient (cm ² /s)
c_{Ox}	=	is the dissolved oxygen concentration at the exposure face (meq e-/mL)

The reduction capacity, as defined in the E_h -pH pore volume transitions discussion (above), is conservatively set to 0.206 meq e-/g. For the intact matrix, a constant diffusion coefficient of 1.0E-07cm²/s is applied. The analytic solution to determine the oxidation front position from Equation 13 is

$$\delta(t) = \left[\frac{2nD_e c_{Ox}}{r_{Ox}\rho_b} t \right]^{1/2} \quad (\text{Eq. 14})$$

For exposure faces created at different discrete times, the cumulative oxidation thickness is the convolution

$$\delta_T = N_1 \cdot \delta(t - \tau_1) + (N_2 - N_1) \cdot \delta(t - \tau_2) + (N_3 - N_2) \cdot \delta(t - \tau_3) + \quad (\text{Eq. 15})$$

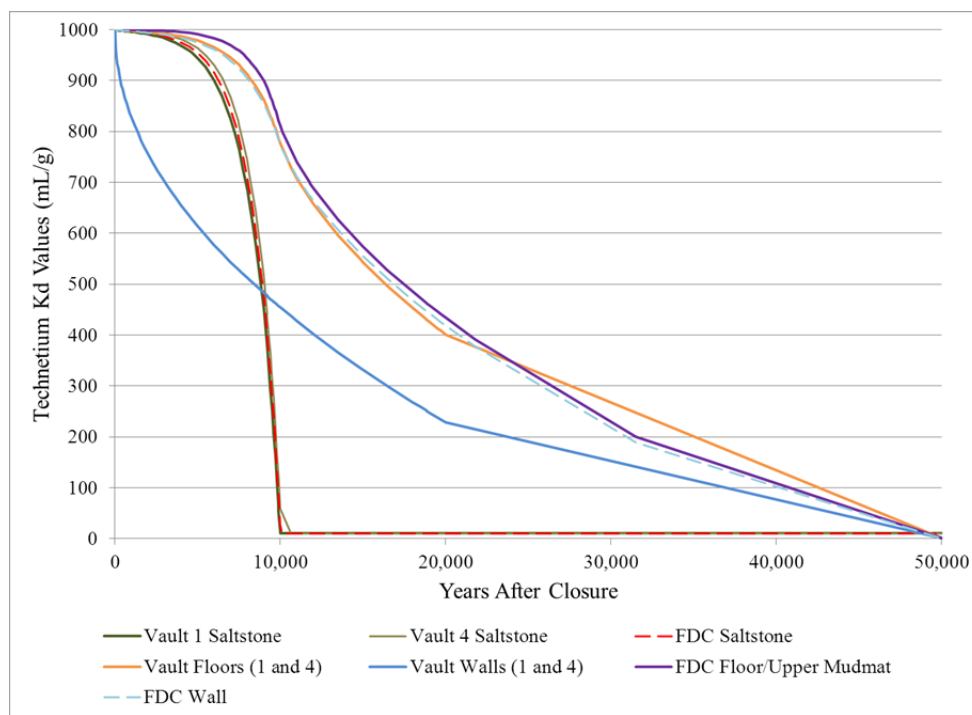
where N_i = total exposure faces through time τ_i . Equation 16 assumes that each new fracture exposes fresh material and each oxidation front advances independent of others. The fraction of material oxidized becomes

$$x_{Ox} = \min \left[\frac{\delta_T}{W}, 1 \right] \quad (\text{Eq. 16})$$

The effective sorption coefficient can then be determined from Equation 11. Assuming the log-linear fracture-spacing relationship given by Equation 3, Figure PA-8.5 illustrates the resulting homogenized technetium K_d values for cementitious materials. For saltstone, this assumes $t_{0\%} = 5$ yr, $t_{100\%} = 10,000$ yr, $B_{0\%} = 10$ m, $B_{100\%} = 0.1$ m, $K_{d,Ox} = 10$ mL/g, and $K_{d,Re} = 1,000$ mL/g.

In the response to RAI SP-19, the sensitivity of the Tc-99 release to the assumed bounding values for $K_{d,Ox}$ and $K_{d,Re}$ is investigated and shown not to significantly impact the resulting doses to the MOP.

Figure PA-8.5: Effective Sorption Coefficients for Technetium in Partially Oxidized Cementitious Materials

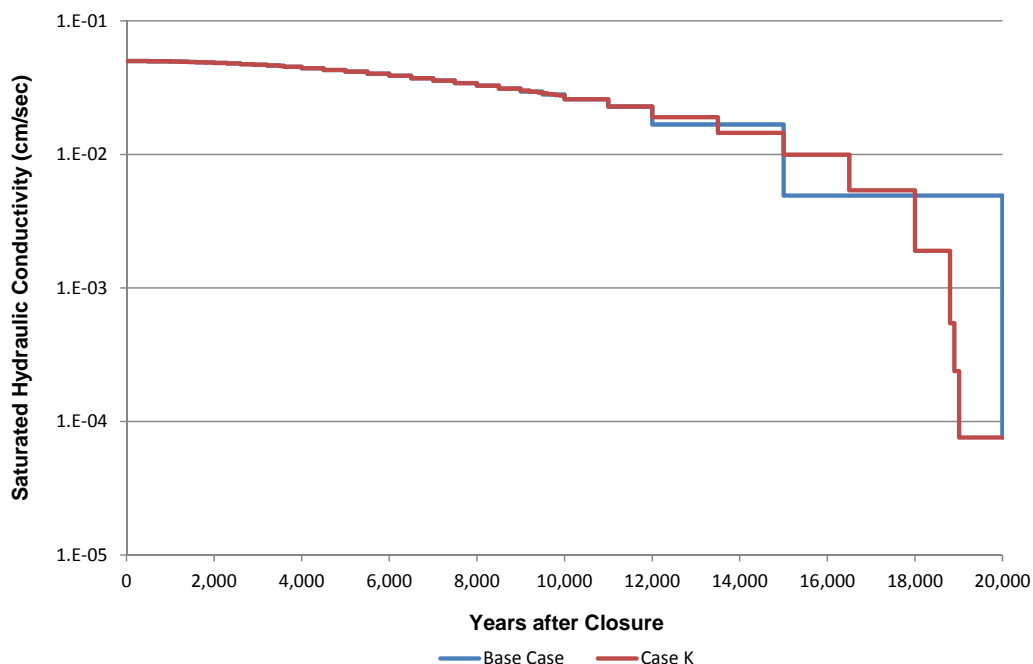


Further discussion and numerical analysis of the shrinking core model is provided in SRNL-L4321-2011-00004.

Drainage Layer Performance

In the Base Case (Case A), the saturated hydraulic conductivity was modeled using coarse time stepping at later years. As a modeling improvement, Alternative Sensitivity Case K applies more discrete time steps (from 44 flow periods to 59). This better captures significant changes to the drainage layer performance (see Figure PA-8.6).

Figure PA-8.6: Comparison of Saturated Hydraulic Conductivities of the Lower Lateral Drainage Layer Using Base Case and Case K Time Steps



Additionally, it should be noted that, as a conservative modeling simplification, the vertical hydraulic conductivity of the degraded lower lateral drainage layer has been set equal to the horizontal hydraulic conductivity of the degraded sand drainage layer (i.e., $K_v = K_h = 7.6E-05$ cm/sec).

Degradation of Disposal Unit Concrete

Changes to the degradation of cementitious materials (including the disposal unit concrete) were discussed above (see the discussion of *Cementitious Degradation: Hydraulic Conductivity, Effective Diffusion Coefficient, Fracture Spacing and Oxidation*; and Table PA-8.2). Undegraded material properties are consistent with values provided in SDF PA Table 4.2-16.

Dose to the Chronic Intruder in Vicinity of Disposal Units

The chronic intruder dose from Alternative Sensitivity Case K applies the same approach as used in the sensitivity analyses discussed in the response to RAI II-2. These chronic intruder doses are estimated based on water concentrations beneath the disposal units, which is more conservative than basing the water concentrations at 1 meter from the SDF boundary that were used in the Base Case.

Radionuclides Analyzed

The suite of radionuclides analyzed for Alternative Sensitivity Case K is the same as the Base Case. This is not a change from the Base Case, but it is important to note that this is a change relative to the other alternative modeling scenarios and sensitivity analyses presented in the PA, which used only key radionuclides defined in SDF PA Section 5.2.2. Refer to the responses to RAIs PA-4 and PA-9, which address the inclusion of additional radionuclides from the set of key radionuclides.

Inventory

Inventory values have been reduced since the SDF PA to reflect new sampling analysis data from Tank 50 samples. Based upon this new analysis, there is no change to the Vault 1 inventory. For Vault 4, the inventories for the following radionuclides have been changed: Pu-238 (from 9,300 curie to 1,000 curie), U-234 (from 26 curie to 10 curie), Th-230 (from 7.5 curie to 0.01 curie), and Ra-226 (from 4.1 curie to 0.001 curie). The FDCs inventories have been changed for Th-230 (0.19 curie to 1.3E-04 curie) and Ra-226 (from 7.8E-07 curie to 1.3E-05 curie). No other inventories have changed from the Base Case. [SRR-CWDA-2011-00115]

K_d Values for Saltstone, Disposal Unit Concrete, and Soil

K_d values have been updated since the development of the SDF PA Base Case. These latest values reflect new site-specific data and new analysis data. Tables PA-8.4, PA-8.5, and PA-8.6 show K_ds for both the Base Case and Alternative Sensitivity Case K.

Table PA-8.4: Updated K_d Values for Backfill and the Vadose Zone

Element	Material	PA K_d (mL/g)	PA Value Reference	Current K_d (mL/g)	Current Value Reference	Location in Reference
Ba	Clay (Backfill Soil)	17	Table 4.2-15	101	SRNL-STI-2011-00011	Table 2-2
C	Clay (Backfill Soil)	0	Table 4.2-15	400	SRNL-STI-2009-00473	Table 16
Ce	Clay (Backfill Soil)	1,500	Table 4.2-15	8,500	SRNL-STI-2009-00473	Table 16
Cl	Clay (Backfill Soil)	0	Table 4.2-15	8.0	SRNL-STI-2010-00493	Table 9
Co	Clay (Backfill Soil)	30	Table 4.2-15	100	SRNL-STI-2009-00473	Table 16
Cs	Clay (Backfill Soil)	250	Table 4.2-15	50	SRNL-STI-2009-00473	Table 16
I	Clay (Backfill Soil)	0.6	Table 4.2-15	0.9	SRNL-STI-2009-00473	Table 16
K	Clay (Backfill Soil)	60	Table 4.2-15	25	SRNL-STI-2009-00473	Table 16
Np	Clay (Backfill Soil)	35	Table 4.2-15	9.0	SRNL-STI-2009-00473	Table 16
Pa	Clay (Backfill Soil)	35	Table 4.2-15	9.0	SRNL-STI-2009-00473	Table 16
Pt	Clay (Backfill Soil)	0	Table 4.2-15	30	SRNL-STI-2009-00473	Table 16
Pu	Clay (Backfill Soil)	5,900	Table 4.2-15	5,950	SRNL-STI-2009-00473	Table 16
Ra	Clay (Backfill Soil)	17	Table 4.2-15	185	SRNL-STI-2011-00011	Table 2-2
U	Clay (Backfill Soil)	300	Table 4.2-15	400	SRNL-STI-2010-00493	Table 8
Y	Clay (Backfill Soil)	0	Table 4.2-15	8,500	SRNL-STI-2009-00473	Table 16
Ba	Sand (Vadose Zone Soil)	5	Table 4.2-15	15	SRNL-STI-2011-00011	Table 2-2
C	Sand (Vadose Zone Soil)	0	Table 4.2-15	10	SRNL-STI-2009-00473	Table 16
Ce	Sand (Vadose Zone Soil)	1,000	Table 4.2-15	1,100	SRNL-STI-2009-00473	Table 16
Cl	Sand (Vadose Zone Soil)	0	Table 4.2-15	1.0	SRNL-STI-2010-00493	Table 9
Co	Sand (Vadose Zone Soil)	7	Table 4.2-15	40	SRNL-STI-2009-00473	Table 16
Cs	Sand (Vadose Zone Soil)	50	Table 4.2-15	10	SRNL-STI-2009-00473	Table 16
I	Sand (Vadose Zone Soil)	0	Table 4.2-15	0.3	SRNL-STI-2009-00473	Table 16
K	Sand (Vadose Zone Soil)	10	Table 4.2-15	5.0	SRNL-STI-2009-00473	Table 16
Np	Sand (Vadose Zone Soil)	0.6	Table 4.2-15	3.0	SRNL-STI-2009-00473	Table 16
Pa	Sand (Vadose Zone Soil)	0.6	Table 4.2-15	3.0	SRNL-STI-2009-00473	Table 16
Pt	Sand (Vadose Zone Soil)	0	Table 4.2-15	7.0	SRNL-STI-2009-00473	Table 16
Pu	Sand (Vadose Zone Soil)	270	Table 4.2-15	290	SRNL-STI-2009-00473	Table 16
Ra	Sand (Vadose Zone Soil)	5	Table 4.2-15	25	SRNL-STI-2011-00011	Table 2-2
U	Sand (Vadose Zone Soil)	200	Table 4.2-15	300	SRNL-STI-2010-00493	Table 8
Y	Sand (Vadose Zone Soil)	0	Table 4.2-15	1,100	SRNL-STI-2009-00473	Table 16

Table PA-8.5: Saltstone Specific K_d Values

Element	Ox/Re	Age	PA K_d (mL/g)	PA Value Reference	Current K_d (mL/g)	Reference for Current Value	Location in Reference
Ba	Re	Young	0.5	Table 4.2-18	6,000	SRNL-STI-2010-00667	Table 2
Ba	Re	Middle	3	Table 4.2-18	6,000	SRNL-STI-2010-00667	Table 2
Sr	Re	Young	0.5	Table 4.2-18	1,000	SRNL-STI-2010-00667	Table 2
Sr	Re	Middle	3	Table 4.2-18	1,000	SRNL-STI-2010-00667	Table 2
Tc ^a	Re	Young	5000	Table 4.2-18	1,000	SRNL-STI-2010-00667	Table 2
Tc ^a	Re	Middle	5000	Table 4.2-18	1,000	SRNL-STI-2010-00667	Table 2
Ba	Ox	Young	100	Table 4.2-18	6,000	SRNL-STI-2010-00667	Table 1
Ba	Ox	Middle	100	Table 4.2-18	6,000	SRNL-STI-2010-00667	Table 1
Sr	Ox	Young	3	Table 4.2-18	1,000	SRNL-STI-2010-00667	Table 1
Sr	Ox	Middle	30	Table 4.2-18	1,000	SRNL-STI-2010-00667	Table 1
Tc ^a	Ox	Young	0.8	Table 4.2-18	10	SRNL-STI-2010-00667	Table 1
Tc ^a	Ox	Middle	0.8	Table 4.2-18	10	SRNL-STI-2010-00667	Table 1

a) For the Alternative Sensitivity Case K analysis, the technetium values are used as bounding values for shrinking core model calculations.

Re = Reducing

Ox = Oxidizing

Table PA-8.6: Updated K_d Values for Reducing Cementitious Materials

Element	Age	PA K_d (mL/g)	PA Value Reference	Current K_d (mL/g)	Reference for Current Value	Location in Reference
Ac	Young	5,000	Table 4.2-18	7,000	SRNL-STI-2009-00473	Table 18
Ac	Middle	5,000	Table 4.2-18	7,000	SRNL-STI-2009-00473	Table 18
Ac	Old	1,000	Table 4.2-18	1,000	SRNL-STI-2009-00473	Table 18
Al	Young	5,000	Table 4.2-18	7,000	SRNL-STI-2009-00473	Table 18
Al	Middle	5,000	Table 4.2-18	7,000	SRNL-STI-2009-00473	Table 18
Al	Old	1,000	Table 4.2-18	1,000	SRNL-STI-2009-00473	Table 18
Am	Young	5,000	Table 4.2-18	7,000	SRNL-STI-2009-00473	Table 18
Am	Middle	5,000	Table 4.2-18	7,000	SRNL-STI-2009-00473	Table 18
Am	Old	1,000	Table 4.2-18	1,000	SRNL-STI-2009-00473	Table 18
Ba	Young	0.5	Table 4.2-18	100	SRNL-STI-2010-00667	Table 2
Ba	Middle	3	Table 4.2-18	100	SRNL-STI-2010-00667	Table 2
Ba	Old	20	Table 4.2-18	70	SRNL-STI-2009-00473	Table 18
Bk	Young	5,000	Table 4.2-18	7,000	SRNL-STI-2009-00473	Table 18
Bk	Middle	5,000	Table 4.2-18	7,000	SRNL-STI-2009-00473	Table 18
Bk	Old	1,000	Table 4.2-18	1,000	SRNL-STI-2009-00473	Table 18
C	Young	20	Table 4.2-18	3,000	SRNL-STI-2009-00473	Table 18
C	Middle	10	Table 4.2-18	3,000	SRNL-STI-2009-00473	Table 18
C	Old	0	Table 4.2-18	300	SRNL-STI-2009-00473	Table 18
Ce	Young	5,000	Table 4.2-18	7,000	SRNL-STI-2009-00473	Table 18
Ce	Middle	5,000	Table 4.2-18	7,000	SRNL-STI-2009-00473	Table 18
Ce	Old	1,000	Table 4.2-18	1,000	SRNL-STI-2009-00473	Table 18
Cf	Young	5,000	Table 4.2-18	7,000	SRNL-STI-2009-00473	Table 18
Cf	Middle	5,000	Table 4.2-18	7,000	SRNL-STI-2009-00473	Table 18
Cf	Old	1,000	Table 4.2-18	1,000	SRNL-STI-2009-00473	Table 18
Cl	Young	20	Table 4.2-18	10	SRNL-STI-2009-00473	Table 18
Cl	Middle	20	Table 4.2-18	10	SRNL-STI-2009-00473	Table 18
Cl	Old	2	Table 4.2-18	1.0	SRNL-STI-2009-00473	Table 18
Cm	Young	5,000	Table 4.2-18	7,000	SRNL-STI-2009-00473	Table 18
Cm	Middle	5,000	Table 4.2-18	7,000	SRNL-STI-2009-00473	Table 18
Cm	Old	1,000	Table 4.2-18	1,000	SRNL-STI-2009-00473	Table 18
Cs	Young	0	Table 4.2-18	2.0	SRNL-STI-2009-00473	Table 18
Cs	Middle	2	Table 4.2-18	20	SRNL-STI-2009-00473	Table 18
Cs	Old	10	Table 4.2-18	10	SRNL-STI-2009-00473	Table 18

Table PA-8.6: Updated K_d Values for Reducing Cementitious Materials (Continued)

Element	Age	PA K_d (mL/g)	PA Value Reference	Current K_d (mL/g)	Reference for Current Value	Location in Reference
Eu	Young	5,000	Table 4.2-18	7,000	SRNL-STI-2009-00473	Table 18
Eu	Middle	5,000	Table 4.2-18	7,000	SRNL-STI-2009-00473	Table 18
Eu	Old	1,000	Table 4.2-18	1,000	SRNL-STI-2009-00473	Table 18
I	Young	5	Table 4.2-18	5.0	SRNL-STI-2009-00473	Table 18
I	Middle	9	Table 4.2-18	9.0	SRNL-STI-2009-00473	Table 18
I	Old	0	Table 4.2-18	4.0	SRNL-STI-2009-00473	Table 18
K	Young	0	Table 4.2-18	2.0	SRNL-STI-2009-00473	Table 18
K	Middle	2	Table 4.2-18	20	SRNL-STI-2009-00473	Table 18
K	Old	10	Table 4.2-18	10	SRNL-STI-2009-00473	Table 18
Ni	Young	5,000	Table 4.2-18	4,000	SRNL-STI-2009-00473	Table 18
Ni	Middle	5,000	Table 4.2-18	4,000	SRNL-STI-2009-00473	Table 18
Ni	Old	1,000	Table 4.2-18	400	SRNL-STI-2009-00473	Table 18
Np	Young	4,000	Table 4.2-18	10,000	SRNL-STI-2009-00473	Table 18
Np	Middle	4,000	Table 4.2-18	10,000	SRNL-STI-2009-00473	Table 18
Np	Old	3,000	Table 4.2-18	5,000	SRNL-STI-2009-00473	Table 18
Pa	Young	5,000	Table 4.2-18	10,000	SRNL-STI-2009-00473	Table 18
Pa	Middle	5,000	Table 4.2-18	10,000	SRNL-STI-2009-00473	Table 18
Pa	Old	500	Table 4.2-18	5,000	SRNL-STI-2009-00473	Table 18
Pb	Young	500	Table 4.2-18	5,000	SRNL-STI-2009-00473	Table 18
Pb	Middle	500	Table 4.2-18	5,000	SRNL-STI-2009-00473	Table 18
Pb	Old	250	Table 4.2-18	1,000	SRNL-STI-2009-00473	Table 18
Pt	Young	0	Table 4.2-18	5,000	SRNL-STI-2009-00473	Table 18
Pt	Middle	0	Table 4.2-18	5,000	SRNL-STI-2009-00473	Table 18
Pt	Old	0	Table 4.2-18	1,000	SRNL-STI-2009-00473	Table 18
Pu	Young	10,000	Table 4.2-18	10,000	SRNL-STI-2009-00473	Table 18
Pu	Middle	10,000	Table 4.2-18	10,000	SRNL-STI-2009-00473	Table 18
Pu	Old	10,000	Table 4.2-18	2,000	SRNL-STI-2009-00473	Table 18
Ra	Young	0.5	Table 4.2-18	100	SRNL-STI-2009-00473	Table 18
Ra	Middle	3	Table 4.2-18	100	SRNL-STI-2009-00473	Table 18
Ra	Old	20	Table 4.2-18	70	SRNL-STI-2009-00473	Table 18
Sb	Young	5,000	Table 4.2-18	1,000	SRNL-STI-2009-00473	Table 18
Sb	Middle	5,000	Table 4.2-18	1,000	SRNL-STI-2009-00473	Table 18
Sb	Old	1,000	Table 4.2-18	100	SRNL-STI-2009-00473	Table 18
Se	Young	300	Table 4.2-18	300	SRNL-STI-2009-00473	Table 18

Table PA-8.6: Updated K_d Values for Reducing Cementitious Materials (Continued)

Element	Age	PA K_d (mL/g)	PA Value Reference	Current K_d (mL/g)	Reference for Current Value	Location in Reference
Se	Middle	300	Table 4.2-18	300	SRNL-STI-2009-00473	Table 18
Se	Old	300	Table 4.2-18	150	SRNL-STI-2009-00473	Table 18
Sm	Young	5,000	Table 4.2-18	7,000	SRNL-STI-2009-00473	Table 18
Sm	Middle	5,000	Table 4.2-18	7,000	SRNL-STI-2009-00473	Table 18
Sm	Old	1,000	Table 4.2-18	1,000	SRNL-STI-2009-00473	Table 18
Sn	Young	5,000	Table 4.2-18	5,000	SRNL-STI-2009-00473	Table 18
Sn	Middle	5,000	Table 4.2-18	5,000	SRNL-STI-2009-00473	Table 18
Sn	Old	2,000	Table 4.2-18	500	SRNL-STI-2009-00473	Table 18
Sr	Young	0.5	Table 4.2-18	15	SRNL-STI-2010-00667	Table 2
Sr	Middle	3	Table 4.2-18	15	SRNL-STI-2010-00667	Table 2
Sr	Old	20	Table 4.2-18	5.0	SRNL-STI-2009-00473	Table 18
Tc ^a	Young	5,000	Table 4.2-18	1,000	SRNL-STI-2010-00667	Table 2
Tc ^a	Middle	5,000	Table 4.2-18	1,000	SRNL-STI-2010-00667	Table 2
Tc ^a	Old	5,000	Table 4.2-18	1,000	SRNL-STI-2009-00473	Table 18
Y	Young	5,000	Table 4.2-18	7,000	SRNL-STI-2009-00473	Table 18
Y	Middle	5,000	Table 4.2-18	7,000	SRNL-STI-2009-00473	Table 18
Y	Old	1,000	Table 4.2-18	1,000	SRNL-STI-2009-00473	Table 18

- a) For the Alternative Sensitivity Case K analysis, the technetium values are used as bounding values for shrinking core model calculations.

Prior to the development of Alternative Sensitivity Case K, the same K_d values assigned to cementitious materials were assigned to the saltstone (see Tables PA-8.6 and PA-8.7). New, site-specific studies have yielded saltstone-specific recommended K_d values for three elements, barium, strontium, and technetium. These values are documented in Table PA-8.5. Also, note that the Alternative Sensitivity Case K run will use the technetium K_d values from Figure PA-8.5 which are based on the shrinking core model calculations.

Table PA-8.7: Updated K_d Values for Oxidizing Cementitious Materials

Element	Age	PA K_d (mL/g)	PA Value Reference	Current K_d (mL/g)	Reference for Current Value	Location in Reference
C	Young	20	Table 4.2-18	3,000	SRNL-STI-2009-00473	Table 17
C	Middle	10	Table 4.2-18	3,000	SRNL-STI-2009-00473	Table 17
C	Old	0	Table 4.2-18	300	SRNL-STI-2009-00473	Table 17
Cl	Young	20	Table 4.2-18	10	SRNL-STI-2009-00473	Table 17
Cl	Middle	20	Table 4.2-18	10	SRNL-STI-2009-00473	Table 17
Cl	Old	2	Table 4.2-18	1.0	SRNL-STI-2009-00473	Table 17
Co	Young	4,000	Table 4.2-18	4,000	SRNL-STI-2009-00473	Table 17
Co	Middle	4,000	Table 4.2-18	4,000	SRNL-STI-2009-00473	Table 17
Co	Old	1,000	Table 4.2-18	400	SRNL-STI-2009-00473	Table 17
Ni	Young	4,000	Table 4.2-18	4,000	SRNL-STI-2009-00473	Table 17
Ni	Middle	4,000	Table 4.2-18	4,000	SRNL-STI-2009-00473	Table 17
Ni	Old	1,000	Table 4.2-18	400	SRNL-STI-2009-00473	Table 17
Np	Young	1,600	Table 4.2-18	10,000	SRNL-STI-2009-00473	Table 17
Np	Middle	1,600	Table 4.2-18	10,000	SRNL-STI-2009-00473	Table 17
Np	Old	250	Table 4.2-18	5,000	SRNL-STI-2009-00473	Table 17
Pa	Young	1,600	Table 4.2-18	10,000	SRNL-STI-2009-00473	Table 17
Pa	Middle	1,600	Table 4.2-18	10,000	SRNL-STI-2009-00473	Table 17
Pa	Old	250	Table 4.2-18	5,000	SRNL-STI-2009-00473	Table 17
Pb	Young	500	Table 4.2-18	300	SRNL-STI-2009-00473	Table 17
Pb	Middle	500	Table 4.2-18	300	SRNL-STI-2009-00473	Table 17
Pb	Old	250	Table 4.2-18	100	SRNL-STI-2009-00473	Table 17
Pd	Young	4,000	Table 4.2-18	4,000	SRNL-STI-2009-00473	Table 17
Pd	Middle	4,000	Table 4.2-18	4,000	SRNL-STI-2009-00473	Table 17
Pd	Old	1,000	Table 4.2-18	400	SRNL-STI-2009-00473	Table 17
Pt	Young	0	Table 4.2-18	4,000	SRNL-STI-2009-00473	Table 17
Pt	Middle	0	Table 4.2-18	4,000	SRNL-STI-2009-00473	Table 17
Pt	Old	0	Table 4.2-18	400	SRNL-STI-2009-00473	Table 17
Pu	Young	10,000	Table 4.2-18	10,000	SRNL-STI-2009-00473	Table 17
Pu	Middle	10,000	Table 4.2-18	10,000	SRNL-STI-2009-00473	Table 17
Pu	Old	1,000	Table 4.2-18	2,000	SRNL-STI-2009-00473	Table 17
Sb	Young	100	Table 4.2-18	1,000	SRNL-STI-2009-00473	Table 17
Sb	Middle	100	Table 4.2-18	1,000	SRNL-STI-2009-00473	Table 17
Sb	Old	2	Table 4.2-18	100	SRNL-STI-2009-00473	Table 17
Se	Young	300	Table 4.2-18	300	SRNL-STI-2009-00473	Table 17

Table PA-8.7: Updated K_d Values for Oxidizing Cementitious Materials (Continued)

Element	Age	PA K_d (mL/g)	PA Value Reference	Current K_d (mL/g)	Reference for Current Value	Location in Reference
Se	Middle	300	Table 4.2-18	300	SRNL-STI-2009-00473	Table 17
Se ^b	Old	150	Table 4.2-18	150	SRNL-STI-2009-00473	Table 17
Sr	Young	3	Table 4.2-18	15	SRNL-STI-2010-00667	Table 1
Sr	Middle	30	Table 4.2-18	15	SRNL-STI-2010-00667	Table 1
Sr	Old	15	Table 4.2-18	5.0	SRNL-STI-2009-00473	Table 17
Tc ^a	Young	0.8	Table 4.2-18	0.8	SRNL-STI-2010-00667	Table 1
Tc ^a	Middle	0.8	Table 4.2-18	0.8	SRNL-STI-2010-00667	Table 1
Tc ^a	Old	0.5	Table 4.2-18	0.5	SRNL-STI-2009-00473	Table 17
Th	Young	5,000	Table 4.2-18	10,000	SRNL-STI-2009-00473	Table 17
Th	Middle	5,000	Table 4.2-18	10,000	SRNL-STI-2009-00473	Table 17
Th	Old	500	Table 4.2-18	2,000	SRNL-STI-2009-00473	Table 17
U	Young	250	Table 4.2-18	1,000	SRNL-STI-2010-00493	Table 8
U	Middle	250	Table 4.2-18	1,000	SRNL-STI-2010-00493	Table 8
U	Old	70	Table 4.2-18	100	SRNL-STI-2010-00493	Table 8
Y	Young	5,000	Table 4.2-18	6,000	SRNL-STI-2009-00473	Table 17
Y	Middle	5,000	Table 4.2-18	6,000	SRNL-STI-2009-00473	Table 17
Y	Old	500	Table 4.2-18	600	SRNL-STI-2009-00473	Table 17
Zr	Young	5,000	Table 4.2-18	10,000	SRNL-STI-2009-00473	Table 17
Zr	Middle	5,000	Table 4.2-18	10,000	SRNL-STI-2009-00473	Table 17
Zr	Old	500	Table 4.2-18	2,000	SRNL-STI-2009-00473	Table 17

- a) For the Alternative Sensitivity Case K analysis, the technetium values are used as bounding values for shrinking core model calculations.
- b) For old aged oxidized cementitious materials, a different K_d value was applied for Se-79 in the Alternative Sensitivity Case K analysis. Instead of using the value of 150, a value of 30 was applied which reduces the retardation of selenium and increases its water concentration which will increase the dose from selenium.

In Tables PA-8.4 through PA-8.7, pink cells indicate that the newer K_d value is slower (higher) than the value used in the SDF PA; green values indicate faster (lower) K_d values. Note that in addition to impacting radionuclide transport calculations, these updated K_d values in sandy soil also impact dose calculations, consistent with the soil build-up factor methodology provided in the response to RAI B-3.

Dose Methodology

The dose calculations for Alternative Sensitivity Case K reflect the updated dose methodology presented in the responses to RAIs B-1, B-2, B-3, and B-4 but with the updated K_d values in sandy soil provided in Table PA-8.4. For more information, refer to those responses.

ANALYSIS OF RESULTS

Consistent with the settings described above, and with the model process flow description provided in SDF PA Section 4.4.2, Tables PA-8.8 through PA-8.10 provide timelines associated with various modeled components for the Base Case and the Alternative Sensitivity Case K model. The following discussion of the dose results from Alternative Sensitivity Case K reflects the transition and degradation times provided by these tables.

Note that Table 5.6-16 of the SDF PA demonstrated that peak doses always resulted from Sectors B and I. Therefore, this analysis focuses on those two sectors as well as the immediately adjacent sectors (i.e., the Alternative Sensitivity Case K analysis examines the results from Sectors A, B, C, H, I, and J). Consistent with this observation, the peak dose for Alternative Sensitivity Case K occurs in Sector I.

Table PA-8.8: Occurrences of Model Changes by Case for Vault 1

Change in Model Parameters	Time of Occurrence for Given Case (years after closure)	
	Base Case	Case K
Degradation of closure cap	5,500	5,500
Floor concrete transitions from reducing to oxidizing	40,000+ ^a	7,740
Floor concrete transitions from middle age to old age	40,000+ ^a	8,227
Wall concrete transitions from reducing to oxidizing	20,781	8,297
Wall concrete transitions from middle age to old age	21,043	9,545
Vault roof hydraulically degrades to soil conditions	50,000	10,000
Vault walls hydraulically degrade to soil properties	Initially greater than soil properties	10,000
Vault floor hydraulically degrades to soil properties	50,000+ ^a	10,000
Saltstone hydraulically degrades to soil properties	50,000+ ^a	10,000
Saltstone transitions from reducing to oxidizing	50,000+ ^a	14,196
Lateral drainage layer degrades to soil properties	20,000	19,013

[Source: SDF PA Table 4.4-7, Base Case, and Alternative Sensitivity Case K PORFLOW result files]

a) Transition times occur beyond the time indicated.

Table PA-8.9: Occurrences of Model Changes by Case for Vault 4

Change in Model Parameters	Time of Occurrence for Given Case (years after closure)	
	Base Case	Case K
Vault roof hydraulically degrades to soil properties	10,000	3,500
Degradation of closure cap	5,500	5,500
Floor concrete transitions from reducing to oxidizing	40,000 ^a	7,635
Floor concrete transitions from middle age to old age	40,000 ^a	8,141
Wall concrete transitions from reducing to oxidizing	15,519	9,219
Vault walls hydraulically degrade to soil properties	Initially greater than soil properties	10,000
Vault floor hydraulically degrades to soil properties	50,000 ^a	10,000
Saltstone hydraulically degrades to soil properties	50,000 ^a	10,000
Wall concrete transitions from middle age to old age	16,018	10,671
Saltstone transitions from reducing to oxidizing	40,000 ^a	14,844
Lateral drainage layer degrades to backfill properties	20,000	19,013

[Source: SDF PA Table 4.4-7, Base Case, and Alternative Sensitivity Case K PORFLOW result files]

a) Transition times occur beyond the time indicated.

Table PA-8.10: Occurrences of Model Changes by Case for FDCs

Change in Model Parameters	Time of Occurrence for Given Case (years after closure)	
	Base Case	Case K
Complete degradation of closure cap	5,500	5,500
Degradation of HDPE layer outside FDC wall	6,000	6,000
Upper mud mat transitions from reducing to oxidizing	22,177	6,915
Degradation of HDPE/GCL above and below FDCs	7,500	7,000
Upper mud mat transitions from middle age to old age	22,871	7,361
Wall concrete transitions from reducing to oxidizing	16,344	7,756
Floor concrete transitions from reducing to oxidizing	22,498	7,970
Wall concrete transitions from middle age to old age	16,753	8,232
Floor concrete transitions from middle age to old age	23,274	8,462
Roof hydraulically degrades to backfill properties	20,000	10,000
Walls hydraulically degrade to backfill properties	20,000	10,000
Floor and upper mud mat hydraulically degrade to soil properties	20,000	10,000
Saltstone hydraulically degrades to soil properties	50,000 ^a	10,000
Lateral drainage layer degrades to backfill properties	20,000	19,013
Saltstone transitions from reducing to oxidizing	40,000 ^a	20,000 ^a

[Source: SDF PA Table 4.4-7, Base Case, Alternative Sensitivity Case K PORFLOW result files]

a) Transition times occur beyond the time indicated.

MOP Dose Results

Three figures depict the results of this analysis. Figure PA-8.7 shows the Alternative Sensitivity Case K dose results, by sector. This figure demonstrates that the doses in Sector I dominate throughout most of the simulated period. Figures PA-8.8 and PA-8.9 present the individual radionuclide dose contributions for Alternative Sensitivity Case K within the 20,000-year simulated period for Sectors B and I, respectively.

Figure PA-8.7: Alternative Sensitivity Case K 100-Meter Peak Groundwater Pathways Dose by Sector

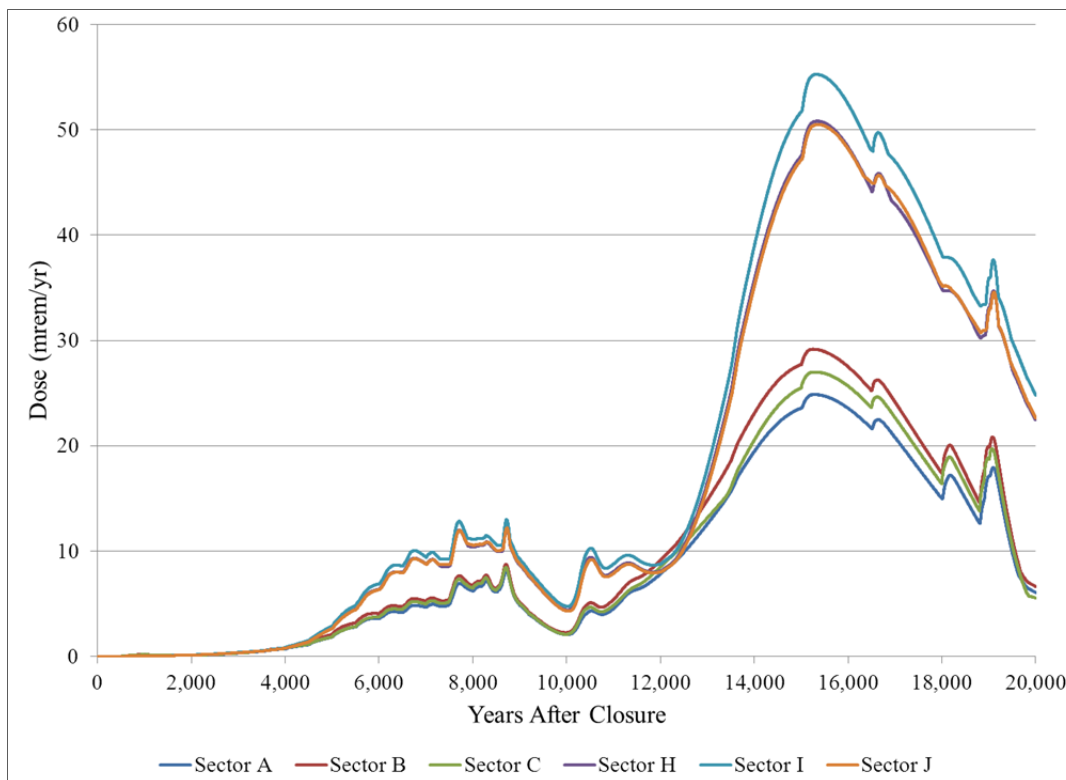


Figure PA-8.8: Alternative Sensitivity Case K Contributors to the Sector B 100-Meter Peak Groundwater Pathways Dose, 20,000 Years

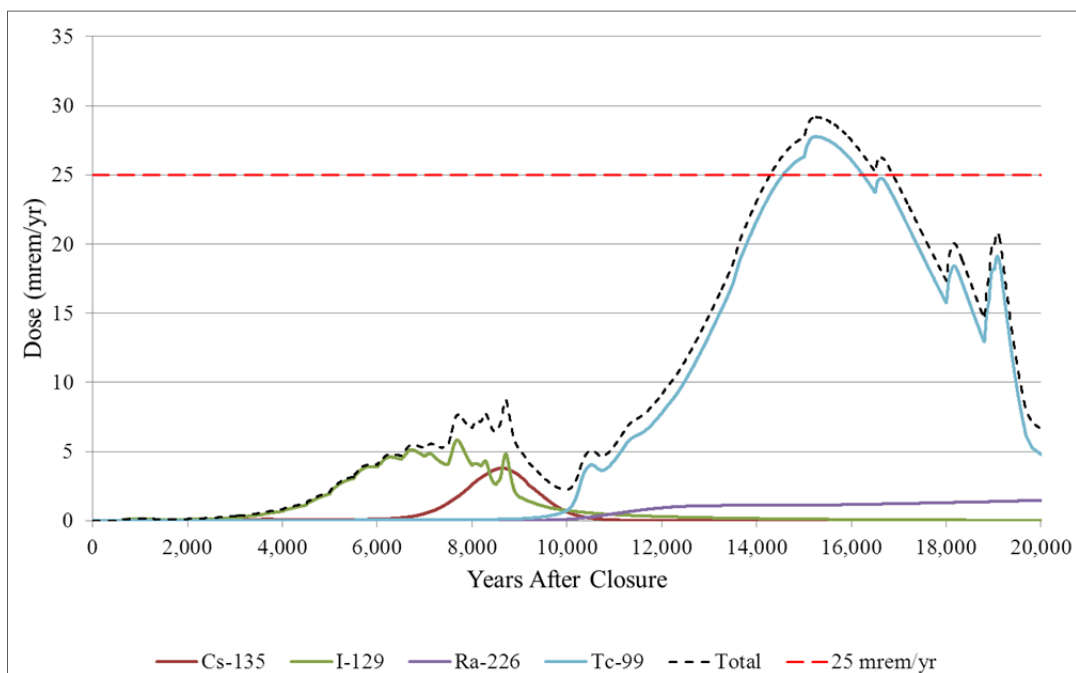
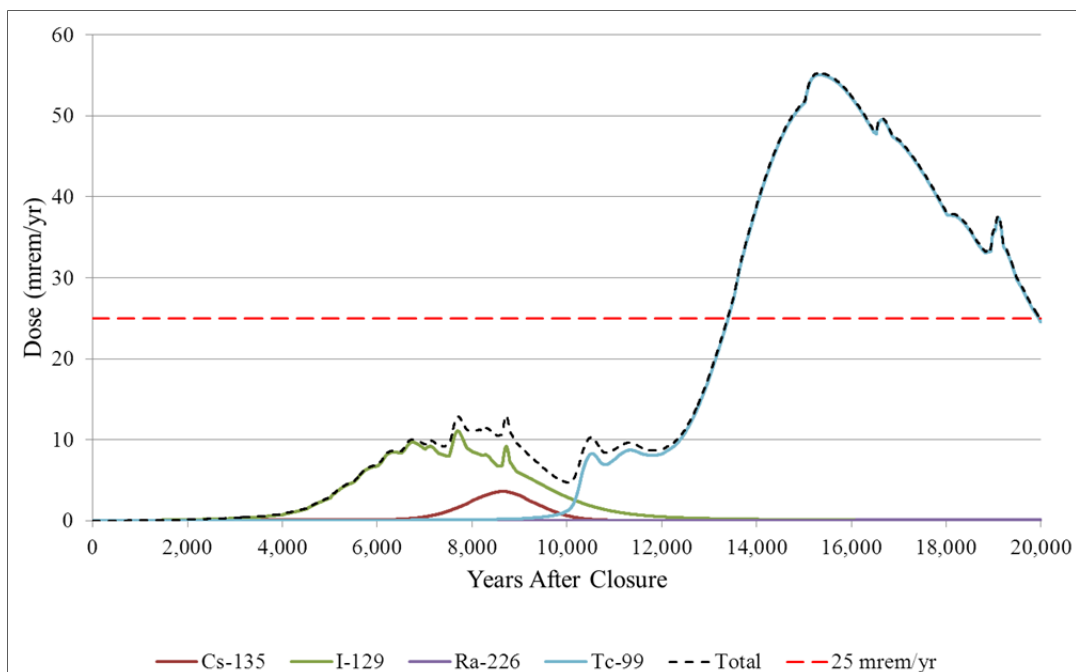


Figure PA-8.9: Alternative Sensitivity Case K Contributors to the Sector I 100-Meter Peak Groundwater Pathways Dose, 20,000 Years



The peak dose within the 10,000-year period of performance is 13.0 mrem/yr at year 8,720 (see Figure PA-8.7). This is less than the 25 mrem/yr performance objective (10 CFR 61.41). Even given the conservative, non-mechanistic assumption of premature cementitious degradation, the peak dose does not exceed 25 mrem/yr until 13,390 years after closure.

Table PA-8.11 compares the peak 100-meter groundwater pathway doses from the Base Case to the doses from Alternative Sensitivity Case K within both 10,000 and 20,000 years for the six 100-meter sectors included in this analysis. In calculating the peak groundwater pathways dose, the highest radionuclide concentration within the vertical computational meshes is used from each of the six-sectors modeled. The sectors are depicted in SDF PA Figure 5.2-1.

Table PA-8.11: 100-Meter MOP Peak Groundwater Pathways Dose by Sector

Sector	Base Case		Alternative Sensitivity Case K	
	Peak Dose in 10,000 Years	Peak Dose in 20,000 Years	Peak Dose in 10,000 Years	Peak Dose in 20,000 Years
A	1.2 mrem/yr (year 10,000)	2.6 mrem/yr (year 15,080)	8.1 mrem/yr (year 8,718)	24.9 mrem/yr (year 15,276)
B	1.4 mrem/yr (year 10,000)	2.9 mrem/yr (year 15,080)	8.8 mrem/yr (year 8,710)	29.2 mrem/yr (year 15,258)
C	0.7 mrem/yr (year 10,000)	2.0 mrem/yr (year 15,080)	8.5 mrem/yr (year 8,706)	27.0 mrem/yr (year 15,302)
H	0.4 mrem/yr (year 10,000)	2.8 mrem/yr (year 15,080)	12.3 mrem/yr (year 8,718)	50.8 mrem/yr (year 15,348)
I	0.4 mrem/yr (year 10,000)	3.1 mrem/yr (year 15,080)	13.0 mrem/yr (year 8,720)	55.3 mrem/yr (year 15,348)
J	0.4 mrem/yr (year 10,000)	2.7 mrem/yr (year 15,080)	12.2 mrem/yr (year 8,728)	50.5 mrem/yr (year 15,352)

[Source: SDF PA Table 5.5-1 and Alternative Sensitivity Case K PORFLOW result files]

Tables PA-8.12 and PA-8.13 compare the radionuclide-specific dose contributions from the Base Case to those from Alternative Sensitivity Case K at the time of peak groundwater doses. For Table PA-8.12, the peak Base Case dose comes from Sector B during the first 10,000 years after closure whereas the peak Alternative Sensitivity Case K dose comes from Sector I. During the first 10,000 years after closure, the peak Alternative Sensitivity Case K dose is driven by releases from two radionuclides, I-129, and Cs-135. Doses from Ra-226 no longer play a significant role within the period of performance as the inventories for Ra-226 and its parent radionuclides (Th-230 and U-234) have been updated to reflect more accurate inventory estimates based on inventory reports. After the first 10,000 years, Tc-99 quickly becomes the dominant dose contributor, overwhelming the contributions from all other radionuclides.

Table PA-8.12: 100-Meter MOP Peak Groundwater Pathways Dose in 10,000 Years

Radionuclide	Base Case, Sector B		Alternative Sensitivity Case K, Sector I	
	Peak Dose Contribution at Year 10,000 (mrem/yr)	Percentage of Total Peak Dose (%)	Peak Dose Contribution at Year 8,710 (mrem/yr)	Percentage of Total Peak Dose (%)
Cs-135	<0.05	<1	3.6	28
I-129	1.3	94	9.2	71
Ra-226	0.05	4	<0.05	<1
Tc-99	<0.05	<1	0.21	1.6
Others	<0.05 each	<1 total	<0.05 each	<1 total
Total	1.4	100	13.0	100

[Source: SDF PA Table 5.5-2 and Alternative Sensitivity Case K PORFLOW result files.]

Note: Values may not sum to total due to rounding.

Table PA-8.13: 100-Meter MOP Peak Groundwater Pathways Dose in 20,000 Years

Radionuclide	Base Case, Sector I		Alternative Sensitivity Case K, Sector I	
	Peak Dose Contribution at Year 15,080 (mrem/yr)	Percentage of Total Peak Dose (%)	Peak Dose Contribution at Year 15,348 (mrem/yr)	Percentage of Total Peak Dose (%)
I-129	2.7	87	0.1	<1
Ra-226	0.3	13	0.06	<1
Tc-99	<0.05	<1	55.1	99.6
Others	<0.01 each	<1 total	<0.01 each	<1 total
Total	3.1	100	55.3	100

[Source: SDF PA Table 5.5-3 and Alternative Sensitivity Case K PORFLOW result files.]

Note: Values may not sum to total due to rounding.

The most dose-significant radionuclide at the time of the peak dose within the 10,000-year period of performance (year 8,720) is I-129. This radionuclide contributes about 71 % of the total dose for Sector I. The second most significant contributor is Cs-135, with about 28 % of the dose, followed by Tc-99 that contributes less than 2 % of the dose. The pessimistic modeling assumptions for degradation of the cementitious materials cause the greater and earlier releases of I-129 and Cs-135 when the Alternative Case K is compared to the Base Case. The significant reduction in dose from Ra-226 when the Alternative Case K is compared to the Base Case is caused by the reduction of the inventories of Ra-226 and some of its parent radionuclides

The significant dose pathway contributors to this peak dose are the water ingestion pathway (49 %), the fish ingestion pathway (40 %) and the vegetable consumption pathway (8 %). The dominate contributor is I-129 to the water ingestion pathway (98 %) and the vegetable consumption pathway (95 %) with Tc-99 contributing the remaining dose to these pathways. Contributing 70 % of the fish ingestion pathway is Cs-135 with I-129 contributing the vast majority of the remaining fish consumption dose.

For time periods out to 20,000 years, the only radionuclide that contributes significantly to the peak MOP dose for the Alternative Case K is Tc-99, as shown in Table PA-8.13. In contrast, I-

129 and Ra-226 are the principal dose contributors for the Base Case. The earlier and greater release of I-129 and the reduced inventory for Ra-226 and some of its parent radionuclides explain why the dose from these radionuclides are significantly less for the Alternative Case K than for the Base Case. The significant increase in the dose from Tc-99 is attributed to the pessimistic assumptions for degradation of cementitious materials and the reduction of the reducing capacity for saltstone assumed in the Alternative Sensitivity Case K.

Alternative Sensitivity Case K is not considered a likely alternate scenario; however, it was developed to provide additional information regarding the impacts when multiple barriers of concern are modified simultaneously following extensive discussions with the NRC. [WDPD-11-65] Alternative Sensitivity Case K should not be construed as representing an expected physical reality, but instead reflects the potential impact on system performance and the estimated contaminant release and resulting radiological dose when conservative, non-mechanistic degradation of barriers is postulated.

Alternative Sensitivity Case K is constructed in such a way as to improve the general understanding of the impacts due to physical degradation of cementitious materials through time, as well as other concerns raised by the NRC in the RAIs. Nonetheless, the peak MOP dose within the 10,000-year period of performance for Alternative Sensitivity Case K is 13 mrem/yr. This peak dose is less than the 25 mrem/yr performance objective (10 CFR 61.41).

Intruder Dose Results

As discussed in SDF PA Section 6.1, the peak dose to the chronic intruder was calculated using the highest concentration at one meter from the SDF boundary for each radionuclide regardless of sector. Alternatively, for Alternative Sensitivity Case K, the concentrations were obtained directly from PORFLOW results at locations where the contaminants enter the water table below the disposal units. Note that plume spreading from other SDF sources contributes to the respective disposal unit concentrations at these locations. Further note that for the FDC the concentrations are conservatively determined based on the maximum concentrations per radionuclide, regardless of the specific FDC modeled. The dose to the chronic intruder also includes the dose from the stream concentrations (for fish ingestion, swimming and boating exposures) from all SDF sources, as described in the response to RAI II-1. The response to RAI II-1 also describes how Darcy velocities associated with the disposal units were used to determine concentrations for use in the dose calculations below Vault 4 and an FDC.

Additionally, the intruder dose for Alternative Case K was determined by applying changes to the SDF PA dose calculations based on the approaches described in the responses to RAIs B-2 (inclusion of the chicken and egg pathway and updated transfer factors), B-3 (25-year build-up of radionuclides in irrigated soil), and B-4 (inclusion of the leafy plant component in the soil-to-plant transfer factor). The updated K_d values for sandy soil provided in Table PA-8.4 were used in the dose calculations.

The estimated peak dose to the chronic intruder within 10,000 years after closure, based on the Alternative Sensitivity Case K, is less than 8.1 mrem/yr within the vicinity of Vault 4 and less than 53 mrem/yr within the vicinity of an FDC. This compares to the Base Case results, shown in the response to RAI II-1, of less than 49 mrem/yr for Vault 4, and less than 1 mrem/yr for an FDC. The Vault 4 doses are lower due to the change in the inventory (Ra-226 previously dominated the peak doses) whereas the FDCs are higher due to the increased releases of I-129 resulting from the cementitious material degradation and the methodology of selecting the maximum radionuclide concentration below an FDC described above. The major radionuclide and dose pathway contributors to the chronic intruder dose are presented in Tables PA-8.14 and PA-8.15 for the intruder within the vicinity of Vault 4 and to an FDC, respectively.

Table PA-8.14: Peak 10,000 Year Chronic Intruder Dose, Vault 4 Contributors

Radionuclide Contributors			Dose Pathway Contributors		
Isotope	Dose (mrem/yr)		Dose Pathway	Dose (mrem/yr)	
Cs-135	4.9E+00	60.2 %	Fish Consumption	5.10E+00	63.3 %
I-129	2.8E+00	34.4 %	Water Ingestion	2.1E+00	26.2 %
Pa-231	1.6E-02	0.2 %	Vegetable Consumption	6.0E-01	7.4 %
Pb-210	1.9E-02	0.2 %	Milk Consumption	8.4E-02	1.0 %
Ra-226	2.4E-01	3.0 %	Beef Consumption	7.9E-02	1.0 %
Tc-99	1.4E-01	1.7 %	Chicken Consumption	2.7E-02	0.3 %
Remainder	1.7E-02	0.2 %	Egg Consumption	2.5E-02	0.3 %
Total	8.1E+00	N/A	Remainder	3.0E-02	<0.4 %
			Total	8.1E+00	N/A

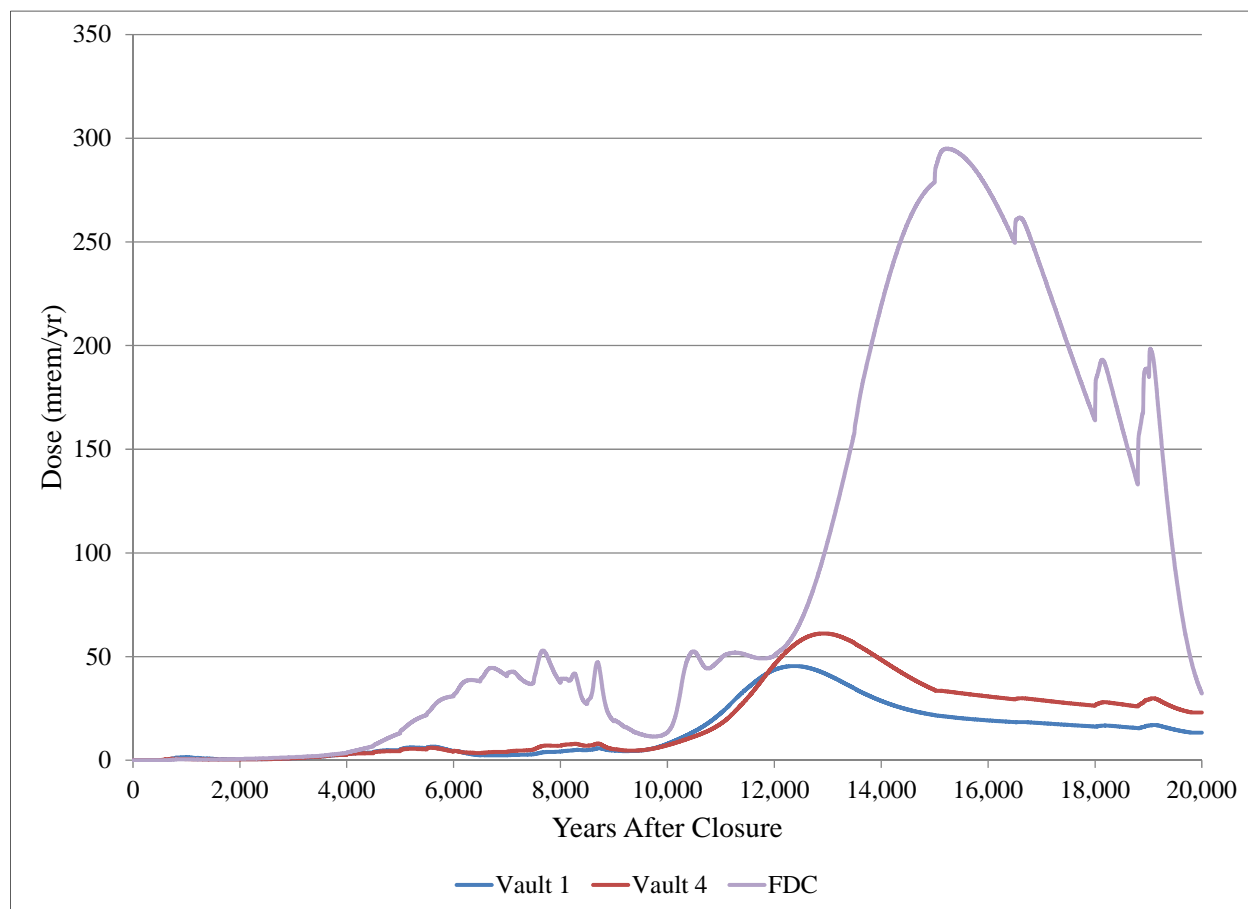
Table PA-8.15: Peak 10,000 Year Chronic Intruder Dose, FDC Contributors

Radionuclide Contributors			Dose Pathway Contributors		
Isotope	Dose (mrem/yr)		Dose Pathway	Dose (mrem/yr)	
Cs-135	2.0E+00	3.7 %	Water Ingestion	3.6E+01	68.7 %
I-129	5.0E+01	94.9 %	Vegetable Consumption	9.9E+00	18.8 %
K-40	1.1E-02	< 0.1 %	Fish Consumption	3.4E+00	6.4 %
Pb-210	8.2E-03	< 0.1 %	Milk Consumption	1.7E+00	3.2 %
Ra-226	1.0E-01	0.2 %	Beef Consumption	7.2E-01	1.4 %
Tc-99	6.2E-01	1.2 %	Egg Consumption	7.2E-01	1.4 %
Remainder	8.0E-03	< 0.1 %	Chicken Consumption	1.2E-02	< 0.1 %
Total	5.3E+01	N/A	Remainder	9.6E-02	<0.2 %
			Total	5.3E+01	N/A

These dose results demonstrate that, given conservative assumptions, the peak intruder dose still meets the performance objectives described in 10 CFR 61, Subpart C, for the Alternative Sensitivity Case K.

Figure PA-8.10 shows the 20,000-year dose curves resulting from concentrations sampled beneath each of the SDF disposal units for the Alternative Sensitivity Case K. This figure shows that FDC dominates the chronic intruder dose.

Figure PA-8.10: Alternative Sensitivity Case K Chronic Intruder Dose at the Vicinity of an SDF Disposal Unit, 20,000 Years



PA-9

Comment (New):

Conclusions about the conservatism of the synergistic case are not clear as certain assumptions appear to be overly optimistic, while other assumptions are potentially conservative.

Basis:

The synergistic case was developed by DOE, based on comments received from the LFRG, to evaluate the impact of simultaneously changing multiple material parameters to account for several potential increased degradation mechanisms from the base case. The PA describes this case as pessimistic. However, NRC staff believes that certain assumptions within the synergistic case render the degree of pessimism or conservatism indeterminate.

NRC staff is unable to assess the adequacy of the synergistic case without additional understanding of the balance between (i) the potential conservatism of the flow through the cracked saltstone and (ii) the model limitations that are applicable to all of the cases in the PA. The general limitations of the PA cases include the following: flow through the vaults and saltstone (see Comments PA-10; IEC-8; SP-1; SP-2; SP-3; SP-4; SP-5; SP-6; VP-3; and VP-6); chemical stability of cementitious materials (see Comment SP-12); and appropriateness of the biosphere calculations (see Comments B-1; B-2; B-3; B-4; and B-5). In addition, the synergistic case appears to only include the key radionuclides determined in the base case. Differences in the conceptualization between the synergistic case and the base case could change the key radionuclides (e.g., short-lived radionuclides may be risk significant in the synergistic case with the earlier degradation of the closure cap and the presence of fast pathways and the advective flow present in the synergistic case could result in a set of key radionuclides that differs from the diffusion-dominated base case.)

Path Forward:

The appropriateness of the synergistic case depends on the extent that DOE relies on the synergistic case to demonstrate compliance with the performance objectives. If compliance determination rests heavily on the synergistic case (i.e., the synergistic case is used to estimate the impact from key uncertainties, lack of model support, limited information), DOE should (i) provide discussion on the balance between potential optimisms and conservatisms within the synergistic case, (ii) address the limitations applicable to all of the cases in the PA, and (iii) address the potentially limited subset of radionuclides.

Response PA-9:

Comment PA-9 requests that DOE (i) discuss “the balance between potential optimisms and conservatisms within the synergistic case, (ii) address the limitations applicable to all of the cases in the PA, and (iii) address the potentially limited subset of radionuclides.”

Prior to addressing each of these issues, it is important to discern the roles between the different models presented within the SDF PA document. The Synergistic Case plays a different role than does the Base Case with respect to the demonstration of compliance. The deterministic Base Case model was designed using the “best estimate” values, where appropriate, coupled with conservative values whenever formulating these “best estimate” values was complicated by uncertainty or parameter sensitivity. Alternatively, as indicated in SDF PA Section 5.6.6.5, the Synergistic Case “was used to determine the impact of changing multiple material parameters to account for several potential increased degradation

mechanisms from the Base Case.” Although the Synergistic Case provides useful insights into the system behavior, this model is not designed exclusively to demonstrate compliance. As stated in the Executive Summary, DOE provides reasonable assurance based on evaluations of how the facility is expected (i.e., most likely) to perform (Base Case) as well as alternative system performance evaluations (i.e., less likely) that encompass uncertainty and variability via additional modeling cases, such as this Synergistic Case, and uncertainty and sensitivity analyses. Despite the varied purposes of these different modeling approaches, this RAI response shall speak to the issues raised by RAI PA-9.

Optimisms versus Conservatisms within the Synergistic Modeling Case

RAI PA-9 indicates, “certain assumptions within the Synergistic Case render the degree of... conservatism indeterminate.” The DOE agrees that the specific impact of each assumption is difficult to assess independently given the complexity of the model. The Synergistic Case was not developed with the intention of serving as a “one-off” analysis (i.e., a sensitivity model providing insights into the effects of a single, specific parameter or submodel); rather, the Synergistic Case demonstrates the synergistic effect of applying multiple, simultaneous assumptions to simulate the increase of flow through cracked saltstone.

The comparison of the doses between the Base Case and the Synergistic Case (see SDF PA Table 5.6-20 and SDF PA Figure 5.6-83) provides the basis for asserting that the Synergistic Case is pessimistic. The Base Case was developed using “best-estimate” assumptions, wherever possible. On the other hand, the alternative assumptions used in the Synergistic Case (see SDF PA Section 5.6.6.5) resulted in significantly higher doses. Therefore, the collective assumptions applied to the Synergistic Case were generally conservative relative to the “best-estimate” approach of the Base Case; hence, the Synergistic Case is pessimistic. In other words, the Synergistic Case is considered pessimistic because of the higher dose results, and not due to any single, specific assumption.

Limitations Applicable to All of the Cases in the PA

As indicated by RAI PA-9, the general model limitations of the PA are considered and discussed within several other RAI comments. These limitations are addressed within the respective RAI comment responses (see responses to B-1; B-2, B-3, B-4, B-5, IEC-8, PA-10, SP-1, SP-2, SP-3, SP-4, SP-5, SP-6, SP-12, VP-3, and VP-6). Further, the response to RAI PA-8 offers additional insight into the limitations of the modeling cases and provides additional technical bases.

Additional Radionuclides Considered

In support of RAI PA-9, the DOE performed a PORFLOW run using additional radionuclides and applying the Synergistic Case settings (as described in PA Section 5.6.6.5).

Initially, the Synergistic Case in the PA was run with seven radionuclides as inventory input: I-129, Np-237, Pu-238, Tc-99, Th-230, U-234, and U-238. For this new run, the following 13 additional radionuclides were input to the PORFLOW model, Am-241, Am-243, Cm-244, Cm-245, Cs-135, Nb-93m, Pu-239, Pu-240, Pu-241, Pu-244, Th-229, U-233, and U-235.

Table PA-9.1 provides a summary of the radionuclides considered. In this table, the initial inventory set is identified as “input” and the resulting concentration set is identified as “output”. “PA Synergistic Case” refers to the Synergistic Case described in SDF PA Section 5.6.6.5; and “PA-9 Analysis” refers to the new run performed for the analysis described below. Note that the PA-9 radionuclide sets do not include every radionuclide that was considered during the

development of the Base Case (as described in the SDF PA), but this set is identical to the radionuclide set developed in the response to RAI PA-4.

Table PA-9.1: Radionuclide Summary for PA-9 Sensitivity Runs

Radionuclide	PA Synergistic Case Input	PA Synergistic Case Output	PA-9 Analysis Input	PA-9 Analysis Output
Ac-227		X		X
Am-241			X	X
Am-243			X	X
Cm-244			X	X
Cm-245			X	X
Cs-135			X	X
I-129	X	X	X	X
Nb-93m			X	X
Np-237	X	X	X	X
Pa-231		X		X
Pb-210		X		X
Pu-238	X	X	X	X
Pu-239			X	X
Pu-240			X	X
Pu-241			X	X
Pu-244			X	X
Ra-226		X		X
Ra-228				X
Rn-222		X		X
Tc-99	X	X	X	X
Th-229		X	X	X
Th-230	X	X	X	X
Th-232				X
U-233		X	X	X
U-234	X	X	X	X
U-235	X	X	X	X
U-236				X
U-238			X	X

Modeling Cases

Two GoldSim model files were used as part of this analysis and both models use the PORFLOW concentration results based on the PA-9 Analysis output. The first GoldSim dose calculator model was developed for the SDF PA. The second GoldSim dose calculator model has been updated to incorporate the dose methodology and dose parameters provided in the responses to RAIs B-1, B-2, B-3, and B-4. For clarity, Table PA-9.2 defines each of these modeling cases.

Table PA-9.2: Model Configurations for PA-9

Model Configuration	Description
PA Synergistic Case	Recreates the Synergistic Case deterministic PORFLOW results from the SDF PA
PA-9 Analysis	Identical to the SDF PA Synergistic Case (above), but includes additional radionuclides identified in Table PA-9.1.
Updated PA-9 Analysis	Uses the same concentrations as the PA-9 Analysis (above), but utilizes updated dose methodology as described in responses to RAIs B-1 through B-4.

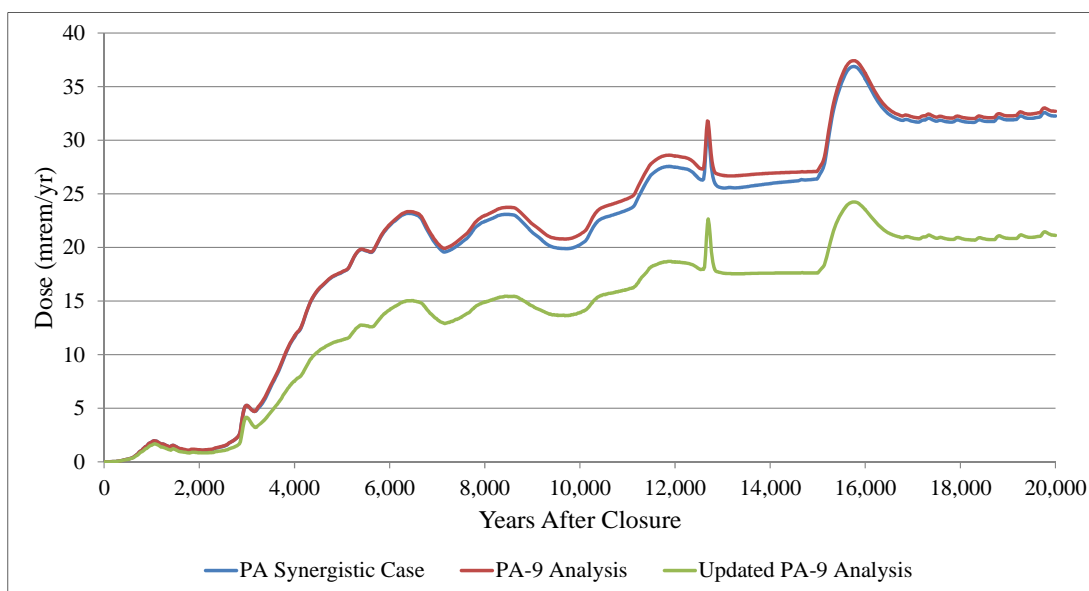
Note, although PORFLOW was run for all 12 sectors (A through L) the GoldSim dose calculator was only performed on six sectors (A, B, C, H, I, and J). Previous PORFLOW modeling indicated that the maximum doses were always from Sector B or Sector I (see SDF PA Tables 5.6-16 and 5.6-20). Therefore, calculating dose from these two sectors along with their adjacent sectors captures the maximum peak dose.

The following discussion compares Synergistic Case dose results from the PA (presented in SDF PA Section 5.6.6.5) to the Synergistic Case dose results from running the GoldSim dose calculator model with additional radionuclides and an updated dose methodology.

Synergistic Case Comparisons, Sector B

Figure PA-9.1 provides a total dose comparison for the Synergistic Case, Sector B results. As expected, the PA Synergistic Case results (blue curve) show a close agreement to the PA-9 Analysis results (red curve). This indicates that the limited radionuclides initially used for the Synergistic Case presented in the SDF PA represented the most risk significant radionuclides, as modeling additional radionuclides had a minimal impact on the total dose.

Figure PA-9.1: Synergistic Case, Sector B Total Dose Comparison



The updated PA-9 results (green curve) applied an updated dose methodology (as described in the responses to RAIs B-1, B-2, B-3, and B-4). This configuration applies the Synergistic Case assumptions (which are implicitly pessimistic), includes the more robust set of radionuclides (from Table PA-9.1), and uses the updated dose methodology. The result is a 30 % to 40 % reduction of the total dose based on the PA dose methodology with the peak dose less than 25 mrem/yr even out to 20,000 years after closure. The pathway contributions to the MOP dose are dominated by water consumption (approximately 47 %), fish consumption (approximately 25 %), and vegetable consumption (approximately 21 %) at the peaks within 10,000 years and 20,000 years. The updated dose methodology has no impact on the water ingestion dose; however, the water-to-fish transfer factors have been updated from the SDF PA for a number of elements as shown in Table RAI B-2.1 of the response to RAI B-2. Most notably, the updated water-to-fish transfer factor for radium has been reduced from 50 L/kg to 4 L/kg. Because Ra-226 contributes greater than 80 % of the dose from fish consumption, the reduction of its water-to-fish transfer factor significantly reduces the dose to the MOP from this pathway. In addition, the updated dose methodology considers a garden productivity (or vegetation production) yield of 2.2 kg/m² which is greater than the value of 0.7 kg/m² used in the SDF PA analysis. This increase in the garden productivity yield will reduce the dose from the vegetable consumption pathway.

Figures PA-9.2 and PA-9.3 show the Sector B individual radionuclide dose contributions for the PA Synergistic Case and the PA-9 Analysis Case, respectively. These figures are presented on a logarithmic y-axis scale to provide detail of the dose contributions from radionuclides of relatively lower risk-significance. A number of radionuclides that contributed to dose with peak magnitudes less than 1.0E-05 mrem/yr are not presented within these figures.

Figure PA-9.2: PA Synergistic Case, Sector B Radionuclide Doses

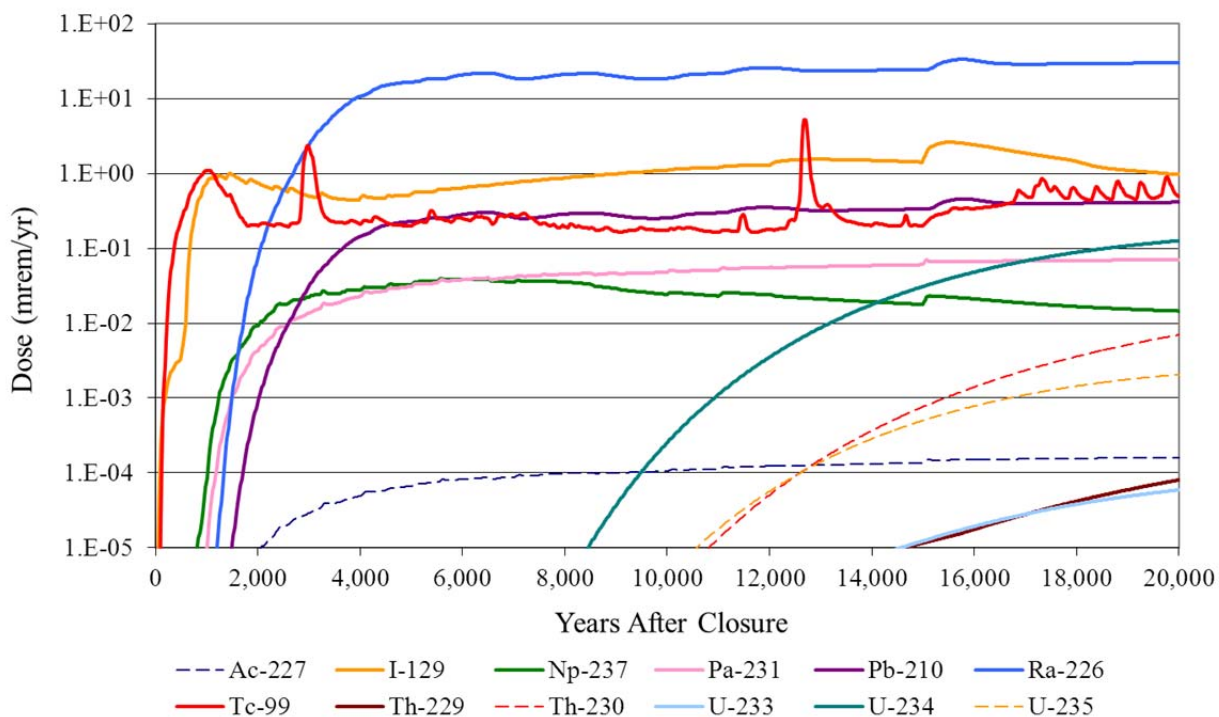
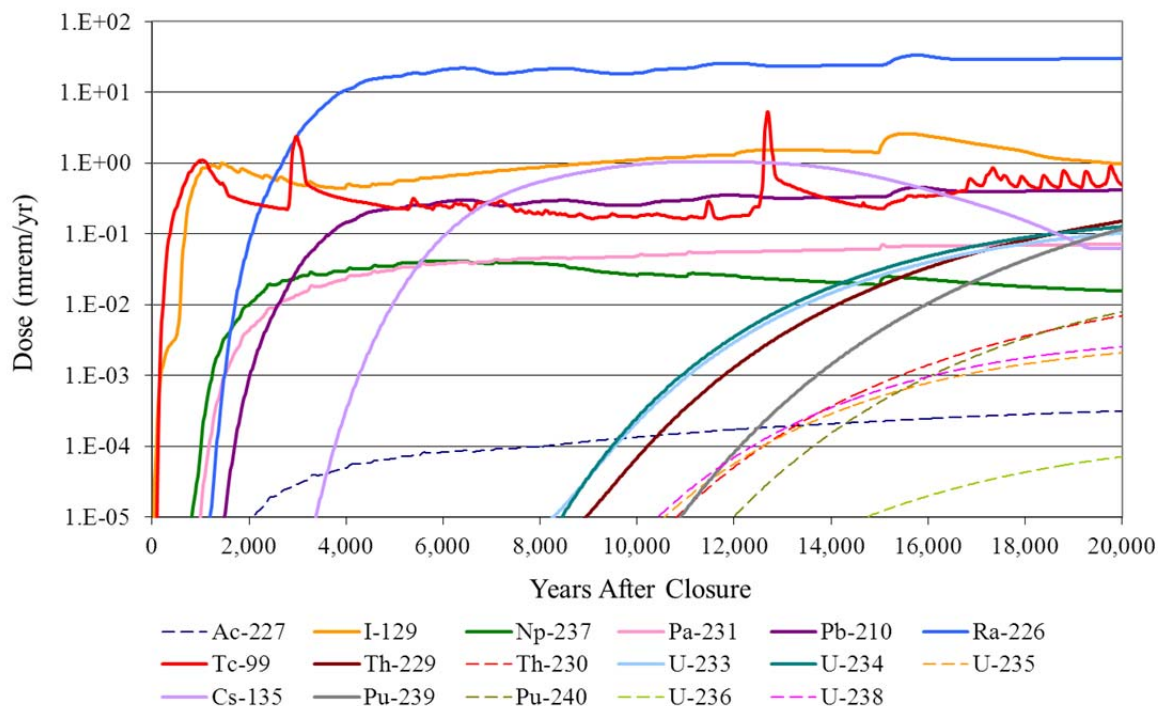


Figure PA-9.3: PA-9 Analysis Case, Sector B Radionuclide Doses



These figures show that the inclusion of additional radionuclides does not represent an appreciable increase to the total dose. The most significant difference was the dose contribution from Cs-135, which peaked with a maximum dose of 1 mrem/yr around year 11,600 (see the light purple curve in Figure PA-9.3). However, Cs-135 represents less than 3 % of the dose contribution to the peak dose within 10,000 years and less than 1.5 % of the dose contribution to the peak dose within 20,000 years. Further, more than 93 % of the Cs-135 dose contribution in Sector B comes from the aquatic food (fish) ingestion dose pathway, which is independent of sector and is a highly pessimistic assumption for this pathway.

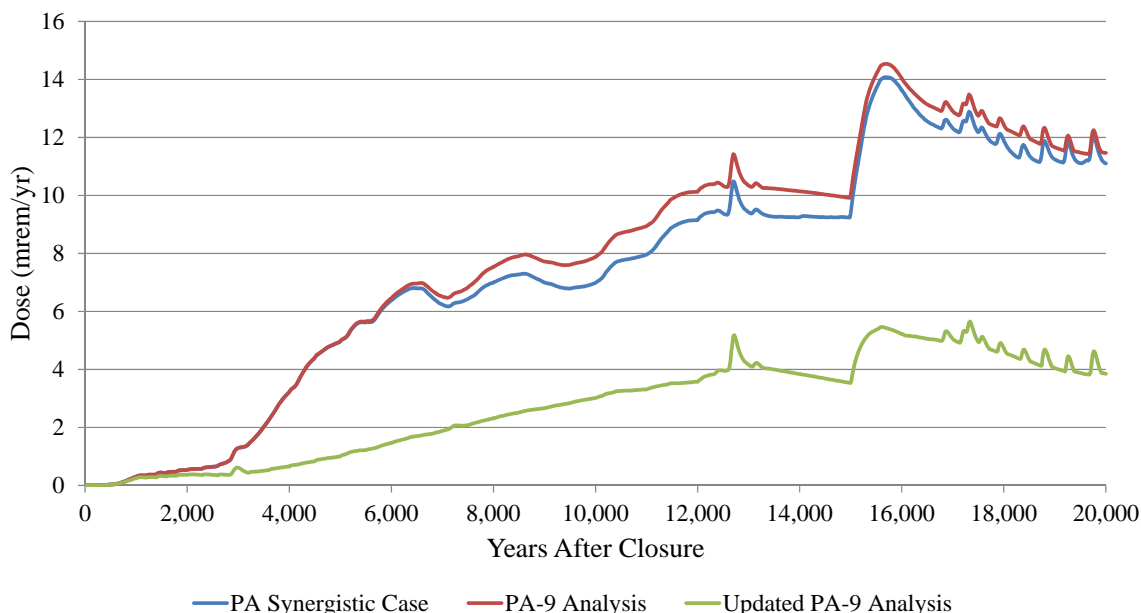
Synergistic Case Comparisons, Sector I

Figure PA-9.4 provides a total dose comparison for the Synergistic Case, Sector I results. As with the Sector B results, the PA Synergistic Case results (blue curve) show a close agreement to the PA-9 Analysis results (red curve). Again, this indicates that the limited radionuclides initially used for the Synergistic Case in the SDF PA represented the most risk significant radionuclides. Modeling additional radionuclides has a minimal impact on the total dose.

The updated PA-9 results (green curve) applied updated dose methodology (as described in the responses to RAIs B-1, B-2, B-3, and B-4). This configuration applies the Synergistic Case assumptions (which are implicitly pessimistic), includes the more robust set of radionuclides (from Table PA-9.1), and uses the updated dose methodology. The result is a 50 % to 70 % reduction of the total dose based on the SDF PA dose methodology. The pathway contributions to the MOP dose are dominated by fish consumption (78 % to 65 %), water consumption (12 % to 20 %), and vegetable consumption (6 % to 9 %) at the peaks within 10,000 years and 20,000 years, respectively. Because of the relatively large contribution to the total dose from the fish consumption pathway; and the greater than 80 % contribution of Ra-226 to the dose from the

fish consumption pathway, the updated water-to-fish transfer factor for radium, addressed above, significantly reduces the dose to the MOP. In addition, the updated value for the garden productivity yield, addressed above, also reduces the dose to the MOP from the vegetable consumption pathway.

Figure PA-9.4: Synergistic Case, Sector I Total Dose Comparison



The Sector I individual radionuclide dose contributions for the SDF PA Synergistic Case and the PA-9 Analysis Case are shown in Figures PA-9.5 and PA-9.6, respectively. These figures are presented on a logarithmic y-axis scale to provide detail of the dose contributions from radionuclides of relatively lower risk-significance. A number of radionuclides that contributed to the dose with peak magnitudes less than 1.0E-05 mrem/yr are not presented within these figures.

Figure PA-9.5: PA Synergistic Case, Sector I Radionuclide Doses

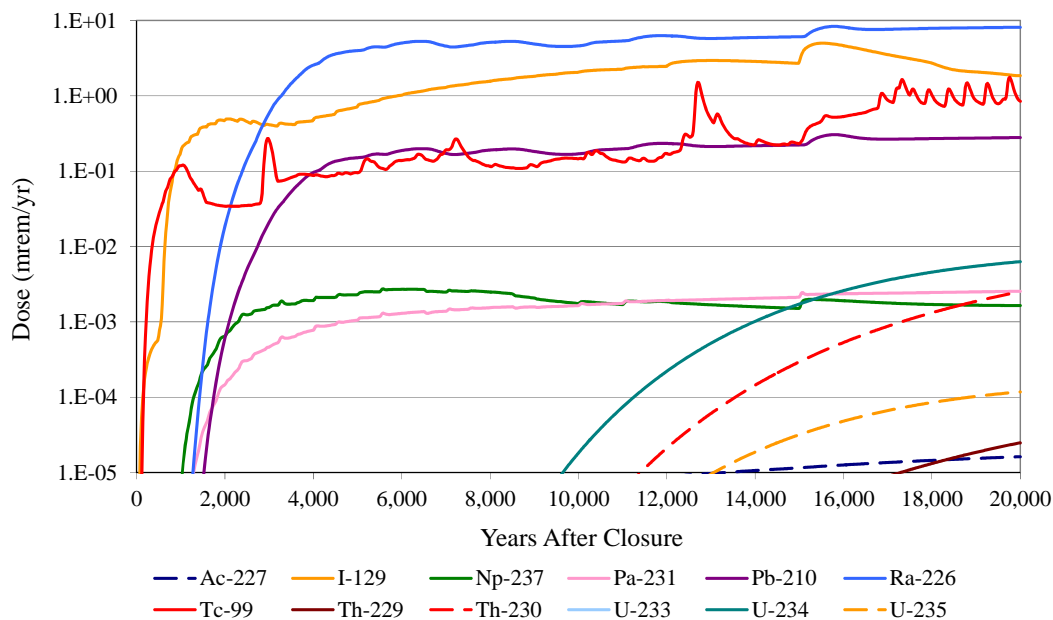
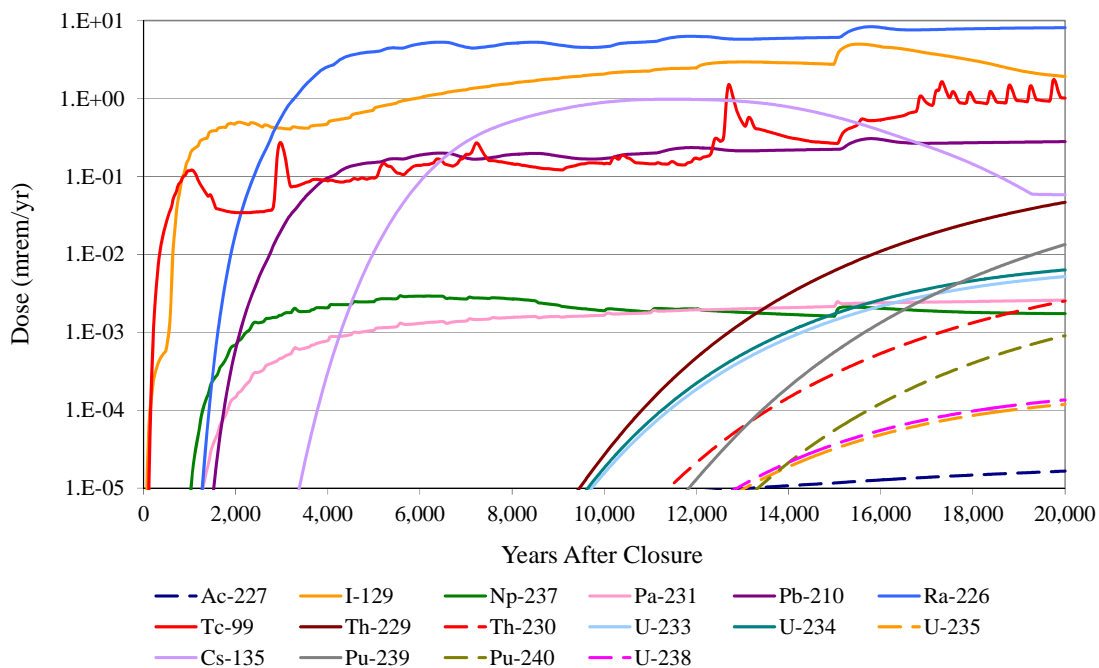


Figure PA-9.6: PA-9 Analysis Case, Sector I Radionuclide Doses



These figures show that the inclusion of additional radionuclides does not represent an appreciable increase to the total dose. The most significant difference was the dose contribution from Cs-135, which approached 1 mrem/yr at approximately 11,400 years (see the light purple curve in Figure PA-9.6). The dose contribution from Cs-135 in Sector I is exclusively from the fish ingestion dose pathway and represents approximately 8 % of the dose contribution to the peak dose within 10,000 years and approximately 3 % of the dose contribution to the peak dose within 20,000 years.

Conclusion

The Synergistic Case was developed to inform compliance-based decisions on the potential effects of significant departures from the Base Case including saltstone cracking and early degradation of the vault concrete and the closure cap, which are expected to be unlikely. Comparison of the dose results from the Synergistic Case, relative to the Base Case, shows that the Synergistic Case is pessimistic. The selected set of radionuclides used in the Synergistic Case provided a sufficient set of results; any increases in dose due to including additional radionuclides are negligible and are negated by applying the updated dose methodology. Given the intended purpose of this modeling case, and the low likelihood for such conditions (e.g., all disposal units failing simultaneously), the Synergistic Case provides an appropriate level of detail for informing compliance-based decisions, and Figure PA-9.4 illustrates results that are less than the performance objectives within 10,000 years.

PA-10

Comment (New):

Assumptions in the PA regarding the conceptual model and parameterization may result in unsupported modeled flow rates through saltstone.

Basis:

Several engineered barriers in the PA provide a significant and long-term impediment to the flow of water through the saltstone wasteform. However, DOE has very limited data to support the performance of several of these key barrier components, which include:

- Hydraulic conductivity of saltstone being hydraulically undegraded for 20,000 years in the base case. (See Comment SP-1)
- Saltstone as not being fractured in the base case. (See Comment SP-2)
- Moisture characteristic curves that are implemented for intact saltstone. (See Comment SP-3)
- Moisture characteristic curves that are implemented for fractured saltstone and concrete. (See Comment SP-4)
- Initial hydraulic conductivity of saltstone that does not adequately account for uncertainty. (See Comment SP-5)
- Geotextile filter fabrics and the lateral drainage layers that provide long-term shedding of water around the vaults. (See Comment IEC-8)
- Neglecting disposal unit degradation mechanisms other than sulfate attack. (See Comment VP-2)
- Degradation of the vault walls that can result in the bypassing of flow around the saltstone as a potential modeling artifact. (See Comment VP-6)

Model support for these flow-related components is limited, however DOE assumptions and parameter selections indicate a consistent bias towards constrained flow through the saltstone wasteform that is unsupported. Reducing the flow of water through the modeled Saltstone system has a compounded effect in that less water is available for the transport of contaminants and the lifespan of reducing conditions in the cementitious materials is prolonged. The timing of the chemical transitions for the walls, floors, and saltstone are dependent on the number of pore volumes that pass through these cementitious materials. Higher flow rates would result in more rapid chemical transitions and generally a more rapid release of redox sensitive radioelements (e.g., Tc-99).

As a scoping calculation, NRC staff determined that the flow through saltstone, the floors, and the walls would be more than a factor of 10 higher at the 500 year time period, if the geotextile filter fabric fails at 500 years (i.e., the lower lateral drainage layer has properties similar to the overlying backfill) and the moisture characteristic curves for saltstone and fractured cementitious are comparable to literature values. As a first order approximation, the dose would increase by this factor based on the increased flow rate through saltstone and the floors. However, the contaminant release is compounded due to a more rapid change in chemical transitions for cementitious materials. The timing of these chemical transitions for these cementitious materials would be less than 1/10 of the time assumed in the PA. It appears that the chemical transitions for saltstone, the floors, and the walls would occur well before the 10,000 year compliance period. This result would have a significant dose impact as transitions for saltstone, the floors, and the walls are assumed in the PA to occur beyond the 10,000 year compliance period. It should be noted that these scoping calculations still likely contain significant optimisms; for example, the assumption of intact saltstone in the base case, the

assumed hydraulic conductivity of saltstone, the limited degradation mechanisms for the disposal units, and the assumption that 100% of the blast furnace slag is available for reaction with the infiltrating water (WSRC-TR-2008-00283).

Path Forward:

Verify that the modeled flow rates are (i) physically reasonable and (ii) consistent with the conceptual models for the various cases.

Provide a level of data support for flow through the Saltstone system commensurate with the risk significance of this topic, or use parameter values that are technically defensible. If research is ongoing, provide a description of the plans to develop model support including when the information is scheduled to be developed. Even if research is ongoing, the compliance case needs to be adequately supported based on information that is available at the time the compliance case is developed.

Response PA-10:

The flow through the saltstone matrix is dependent on the hydraulic parameters of the various components of the SDF disposal units and the infiltration rate entering the disposal units based on the expected performance of the proposed closure cap and the lower lateral drainage layer. The performance of the disposal units, as dictated by the hydraulic properties of the components of the disposal units, is discussed in the responses to the following RAIs:

- Saltstone performance – responses to SP-1, SP-2, SP-3, SP-4, and SP-5
- Disposal unit concrete performance – responses to SP-4, VP-2, and VP-6
- Geotextile filter fabric and the lateral drainage layers – response to IEC-8

Alternative Sensitivity Case K is described in the response to RAI PA-8 and shows that for postulated conservative, non-mechanistic degradation of cementitious material barriers (saltstone and disposal unit concrete), the resultant dose consequences to the MOP and the intruder are less than the 10 CFR 61.41 performance objectives. The increased flow through the SDF closure system in Case K causes more rapid chemical transitions in saltstone and the disposal unit concrete as shown in Tables PA-8.8, PA-8.9, and PA-8.10 of the response to PA-8. These more rapid transitions do significantly increase the dose to the MOP as compared to the Base Case (as shown in Table PA-8.11); however, the increased dose is approximately 50 % of the 10 CFR 61.41 performance objectives in the compliance period. To respond to this RAI additional sensitivity runs were performed in PORFLOW to estimate the flow through the saltstone grout based on changing hydraulic parameters associated with the performance of the saltstone grout, disposal unit concrete, and the geotextile filter fabric and the lateral drainage layers. Four cases were considered for this analysis:

- Case PA – using parameters described in the SDF PA Base Case
- Case K – using parameters described in the response to PA-8
- Case PA x 2 – same as Case PA except that the drainage layers degrade faster (described below)
- Case K x 2 – same as Case K except that the drainage layers degrade faster (as described below)

Faster Degradation of the Drainage Layers

The response to RAI IEC-8 discusses that the performance of the geotextile filter fabric and the migration of clay and silt are conservatively assessed for the performance of the ULDL within the closure cap and of the LLDL above the individual disposal units. However, to examine the

risk significance of the performance of the geotextile filter fabric the rate of clay migration in both drainage layers is doubled from that assumed in the Base Case PA analysis (Case PA x 2) and the Alternative Sensitivity Case K analysis (Case K x 2). Doubling the rate of clay migration into the ULDL hastens the degradation of the ULDL and reduces the time it takes to achieve the maximum infiltration rate. The reduction of time to achieve the maximum infiltration rate, coupled with the doubling of the clay migration rate in the LLDL, further hastens the degradation of the LLDL. Figure PA-10.1 illustrates the infiltration rate from the closure cap for the PA analysis and for the greater clay migration rate (PA x 2) analysis. Figure PA-10.2 illustrates the horizontal conductivity of the LLDL for the PA analysis and the Case K analysis along with the modified analyses (with the greater clay migration rates; i.e., PA x 2 and Case K x 2). The Case K values differ from the SDF PA analysis values because of the refined time steps used in the Case K analysis.

Figure PA-10.1: Infiltration Rate from Closure Cap

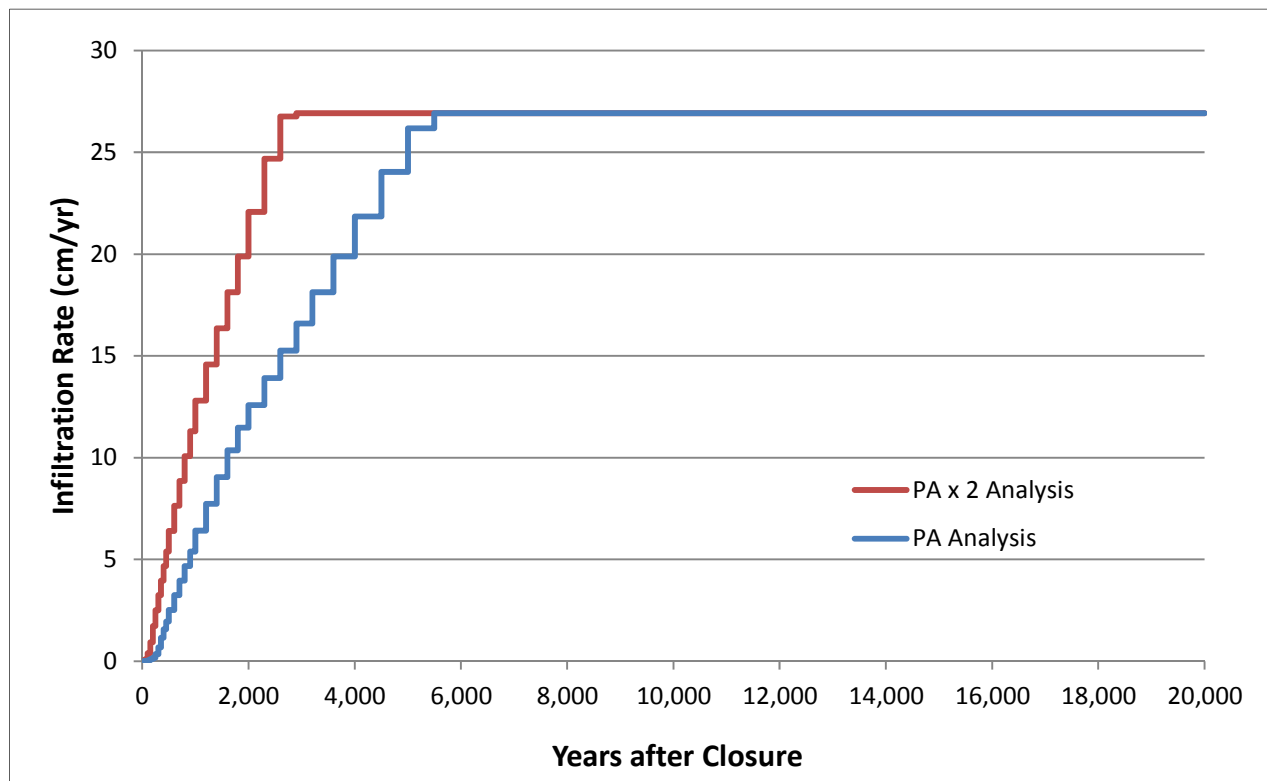
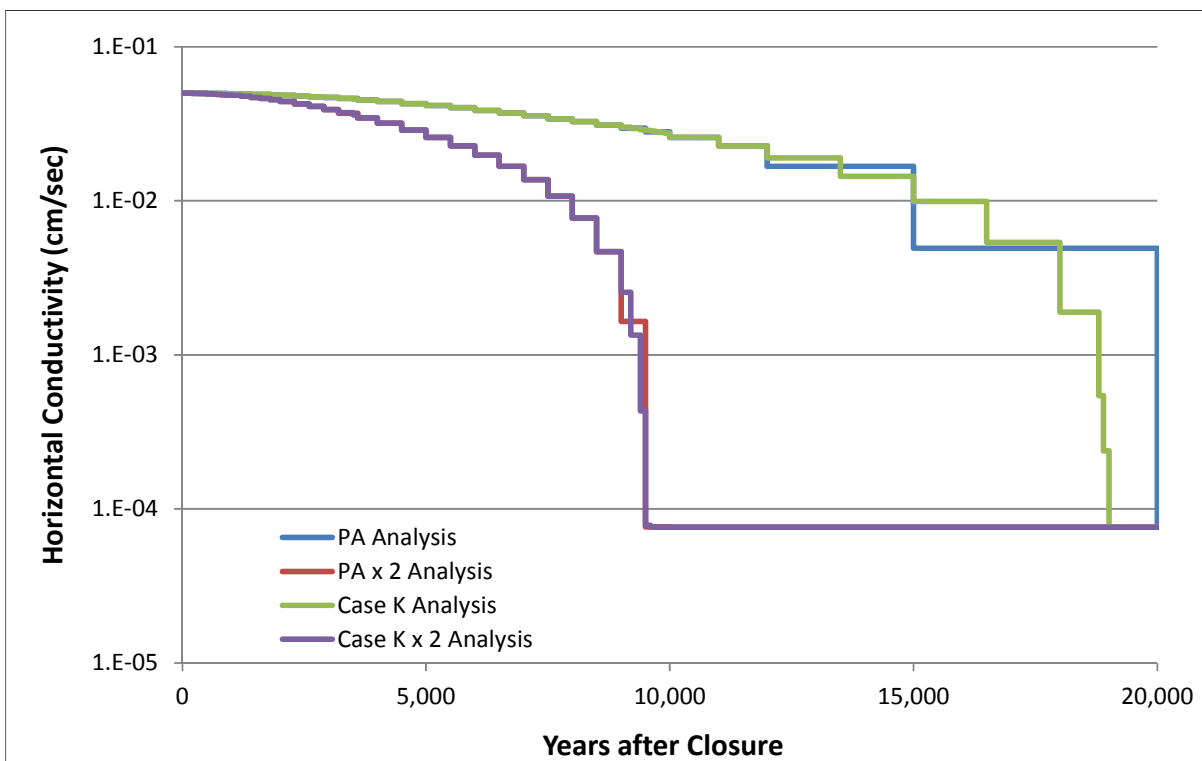


Figure PA-10.2: LLDL Hydraulic Conductivity



PORFLOW runs were performed for the four cases described above to determine the flow rates for Vault 4 and an FDC. Flow budget files were generated from PORFLOW output to obtain the flow crossing the faces of a modeling cell coinciding with the saltstone wastefrom. Flows across the upper, lower, and right boundaries of the saltstone-modeling cell were captured from these PORFLOW runs. The value at the upper part of the saltstone-modeling cell is the total flow entering the top of the cell, and the value at the lower part of the saltstone-modeling cell is the total flow leaving from the bottom of the cell. The flow across the right side of the saltstone-modeling cell is leaving the saltstone-modeling cell if a positive value or entering the saltstone-modeling cell if a negative value from the horizontal direction. These flow rates were then converted to fluxes (Darcy velocity) by dividing by flow area.

Figure PA-10.3 illustrates the water flux, or Darcy velocity, through the saltstone grout for Vault 4 for the four cases analyzed and the infiltration rate. The flux through the saltstone is based on the flux leaving the bottom of the modeling cell described above. Examination of Figure PA-10.3 indicates that the severe degradation of the vault concrete and saltstone (Case K versus Case PA) has a much more significant impact on the flux through the saltstone grout than the greater degradation of the drainage layers ("Case PA x 2" versus Case PA). Indeed, comparing the results between "Case K x 2" and Case K there is essentially no impact on the flux through the saltstone from greater degradation of the drainage layers when the Vault 4 concrete and saltstone are severely degraded. Thus, for Vault 4, the performance of the geotextile filter fabric and the drainage layers are not risk significant when compared to the degradation of the vault concrete and the saltstone.

Figure PA-10.3: Infiltration Rate and Flux through the Saltstone for Vault 4

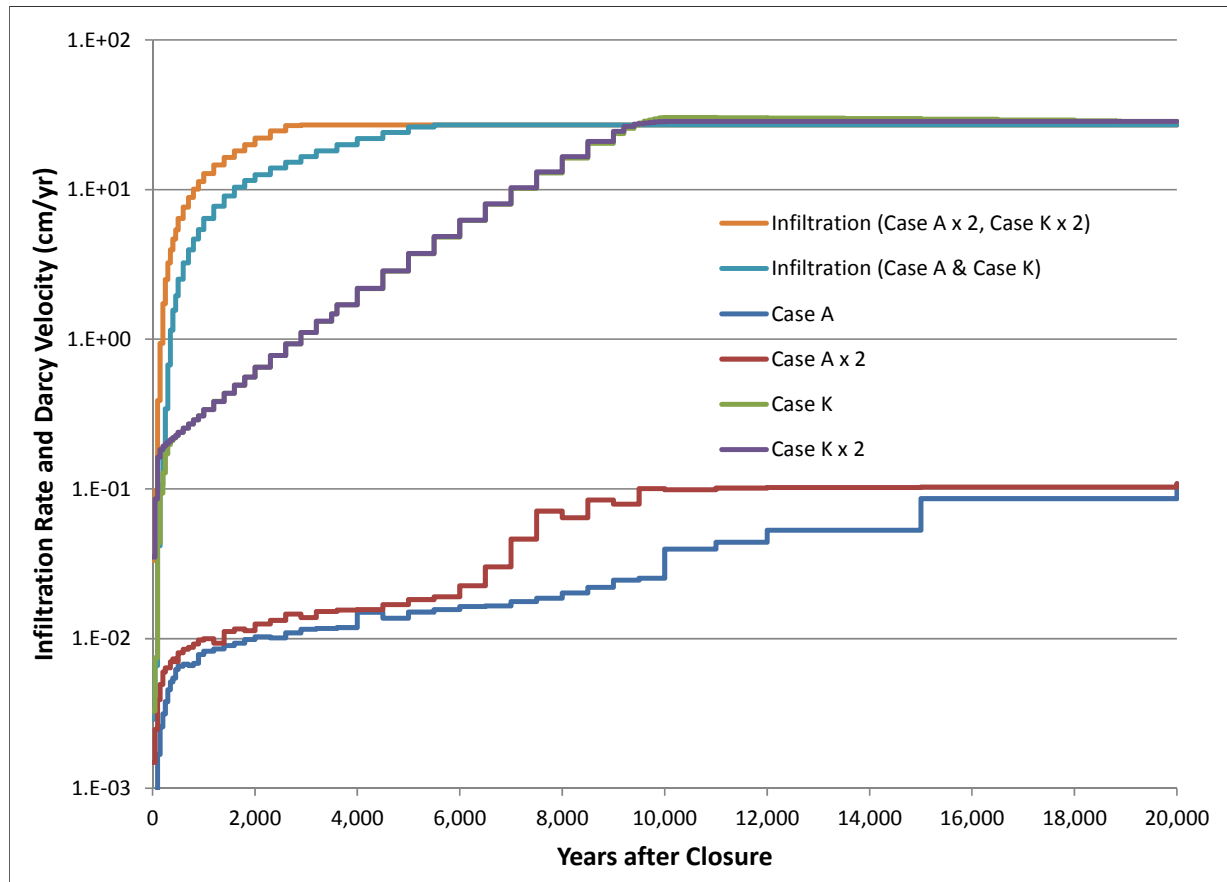
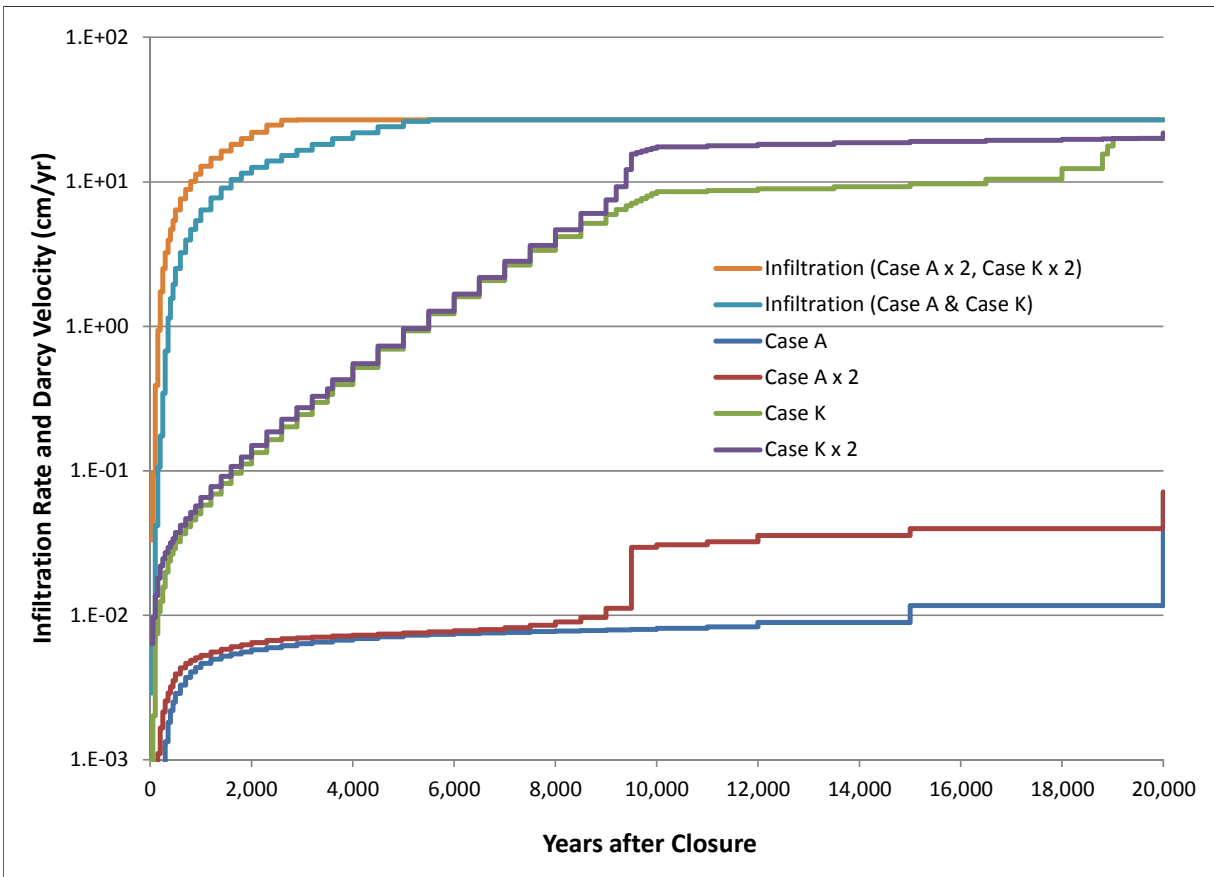


Figure PA-10.4 illustrates the infiltration rate and the flux through the saltstone for an FDC for the four cases analyzed. Examination of Figure PA-10.4 indicates, as shown earlier for Vault 4, that the severe degradation of the FDC concrete and saltstone (Case K versus Case PA) has a much more significant impact on the flux through the saltstone grout than the greater degradation of the drainage layers ("Case PA x 2" versus Case PA). Comparing the results between "Case K x 2" and Case K there is a noticeable impact on the flux through the saltstone when the LLDL has fully degraded. This impact is not as significant (a factor of two between "Case K x 2" and Case K versus a factor of 1,000 between Case K and Case PA). This impact is attributed to the presence of the HDPE-GCL layer that will overlay the FDC roof at closure. This layer provides additional support to the LLDL by allowing water to shed away from the roof. As in the case for Vault 4, the performance of the geotextile filter fabric and the drainage layers are not risk significant when compared to the degradation of the FDC concrete and the saltstone.

Figure PA-10.4: Infiltration Rate and Flux through the Saltstone for an FDC



In conclusion, the geotextile filter fabric has been shown not to be risk significant to the flow through the saltstone for varying conditions of the disposal unit concrete and the saltstone, and thus not risk significant to the MOP dose. Therefore, model support on the performance of the disposal unit concrete and saltstone, which are risk significant features of the SDF closure system, are appropriate, and will continue as described in the responses to RAIs SP-1 and VP-2.

PA-11

Comment (New):

The GoldSim probabilistic model used for sensitivity and uncertainty analyses is not adequately supported.

Basis:

NRC staff has several concerns with the methodology used in the GoldSim calculations:

- 1) NRC staff has numerous concerns with the implementation of the PORFLOW calculations that provide the input into the GoldSim Calculations (see e.g., PA-8 and PA-10).
- 2) The GoldSim model incorporates all five cases (Case A-E), and the assumed probability of each case occurring is considered in the uncertainty calculations. NRC staff believes that the probabilities of each case provided in Table 5.6-3 of the PA are unrealistic. For example, the actual probability of Case A is essentially 0 for Vaults 1 and 4 because this case assumes that the saltstone does not crack during the performance period and the saltstone is already known to have cracks. However, in Table 5.6-3, the probability assumed for Case A is 95% for Vault 1 and 85% for Vault 4.
- 3) The results of the GoldSim model may not be applicable to radionuclides other than the ones that the benchmarking was performed for (see PA-4 and PA-5). In addition, there does not appear to be a good correlation between the PORFLOW and GoldSim results even for the radionuclides that were benchmarked (see Figures 5.6-1 to 5.6-25 in PA and PA-5).
- 4) It is not clear that there is adequate basis for the uncertainty distributions used (e.g., the uncertainty distributions for inventory [see IN-2] and the uncertainty distributions for K_d values [see SP-18]).

Because the GoldSim model was not used as the basis for demonstrating compliance, the NRC staff did not review these calculations to the same extent as the compliance case (Case A) was reviewed. If DOE decides to use this case to demonstrate compliance, the NRC staff will focus more on these calculations and new questions may be identified.

Path Forward:

The concerns listed above need to be addressed. The amount of information needed for this comment depends on the extent to which the GoldSim model will be relied on to demonstrate compliance with the performance objectives of 10 CFR 61. These concerns need to be addressed to the degree that this model is not used to demonstrate compliance or for model support.

Response PA-11:

When reviewing the SDF PA modeling methodology, it is important to discern the roles between the different models presented within the PA document. The probabilistic Case A model plays a different role than does the deterministic Base Case model, with respect to the demonstration of compliance. As discussed in the response to RAI PA-8, the deterministic Base Case model was designed using the “best estimate” values, where appropriate, coupled with conservative values whenever formulating these “best estimate” values was complicated by uncertainty or parameter sensitivity. Alternatively, as indicated in SDF PA Section 4.4.4.2, the probabilistic model was used “to address uncertainty and sensitivity of the modeling of the SDF.” The probabilistic

models were designed with the intention of identifying parameters with the greatest impact on system performance and do not necessarily reflect “best estimate” values; therefore, although the probabilistic models provide useful insights into the system behavior, these models are not designed to represent compliance configurations.

Note: Although the SDF PA used the terms “Base Case,” “Case A,” and “Configuration A” interchangeably when referring to both the deterministic and the probabilistic models, the deterministic Base Case is not identical to the probabilistic Base Case. The two models are intentionally very similar, hence the ambiguity in terminology, but there are noted differences in the model implementation (e.g., the deterministic PORFLOW model is two-dimensional and models flow, whereas the probabilistic GoldSim model is one-dimensional and relies on flow data provided by PORFLOW). These variations in implementation are consistent with the varying roles between the models. The following text speaks to the key concerns identified within the NRC’s Basis for RAI PA-11.

PORFLOW Calculations as GoldSim Input

Item 1 is a broad concern that is addressed broadly by this RAI response package, as a whole, including the responses to PA-8 and PA-10.

Assignment of Probabilities to the Various Cases in GoldSim

As indicated by the response to RAI SP-2, the probabilistic Case A model assumed that the observed cracking does not adversely impact the vault performance. In other words, the cracks are assumed to be surficial and not indicative of cracks that penetrate into the saltstone monolith resulting in fast flow paths. Work is on-going to improve the general understanding of saltstone material degradation and the effects that such degradation may have on flow. The response to RAI SP-1 explains that additional research into saltstone degradation is planned and that the first phase of the long-range testing has been completed. Similarly, the wall concrete for Vaults 1 and 4 is also modeled as intact for Case A (i.e., without fast flow paths through the cracks). These assumptions are appropriate for the probabilistic modeling approach because, 1) the effects of cracking is expected to be significantly mitigated by sealants and by the installation of drain systems (see SDF PA Sections 3.2.1.1.1 and 3.2.1.2.1, and the response to RAI PA-13), 2) non-conservative assumptions are balanced by the conservative assumption that the pore spaces of the vault walls are initially filled with pore fluid containing the same concentration of contaminants as in the vault cells and the walls are modeled with a greater hydraulic conductivity and moisture characteristic curves associated with fractured concrete (see SDF PA Sections 4.4.1.1, 4.4.1.2, and 4.2.3.2.4), and 3) fast flow paths through the wall cracks are included in the suite of uncertainty analyses via Cases B and C.

Provided below is discussion of the rationale that was used to assign the probabilities of occurrence for the five probabilistic modeling cases described in PA Section 5.6.3.1. The intent, when assigning these probabilities, was not to demonstrate compliance. The intent of this probabilistic approach was to generate a model that could facilitate analysis of the uncertainty within the model and provide insights into the sensitivities of parameters with respect to overall performance of the system.

The rationale for assignment of probabilities used a qualitative but informed approach because a quantitative estimation was not directly possible due to significant uncertainty. These probability values were selected because they represented a reasonable modeling simplification based upon the perceived relative likelihood for occurrence, and not based upon future outcomes, which cannot be predicted with certainty.

Rationale for the Likelihood of Each Configuration

A small group of engineers and scientists from the PA development team (the PA preparer bios are provided in Section 9.0 of the SDF PA) was assembled to first develop the appropriate alternative disposal unit modeling cases and associated pessimistic assumptions in support of the SDF PA uncertainty analyses. A systematic, step-by-step approach was used to assign the probability values for each modeling case according to disposal unit type. The first step was to rank each of the modeling cases based upon the perceived likelihood of occurrence for each disposal unit type. Following the relative probability rankings, each modeling case was considered and probabilities were designated.

Case A was considered the most likely, or nominal, scenario. This assessment is intuitive because most of the Case A assumptions represent the best estimate for each assumption as informed by currently available information and engineering judgment. Case A marks the starting point for the probability determination, and is ranked first for all three different disposal unit types.

As described in SDF PA Section 5.6.3.1, Cases B and D address potential impacts to the sheet drain systems in Vault 4 and the FDCs. Vault 1 does not include a drainwater collection system, therefore these modeling cases are not considered with respect to Vault 1.

Cases B, C, D, and E are all considered to be much less likely than Case A, as discussed in Section 5.6.3.1 and summarized as follows:

- Case B is unlikely, relative to Case A, because of the low likelihood that the deterioration of the sheet drain would develop the specific fast flow path analyzed.
- Case C is unlikely, relative to Case A, because “straight line” cracks are not anticipated to occur in the cementitious materials. Any degradation of the cementitious materials that does occur is expected to result in small cracks (which cause increased flow through hydraulic conductivity changes) rather than void spaces as modeled in Case C.
- Case D is unlikely, relative to Case A, because of the low likelihood that the sheet drain present in Vault 4 and the FDCs would form a capillary break between the saltstone monolith and the disposal unit walls.
- Case E is unlikely, relative to Case A, because (as documented in WSRC-STI-2008-00236) the fracturing initiated by expansive phase precipitation is unlikely to occur in saltstone.

Preliminary Rationale for the Likelihood of Each Case

During the initial development of the probabilistic modeling approach, only Cases A, B, C, and D were considered. Without extensive analysis of the statistical likelihood for the various failure mechanisms, Cases B, C, and D were initially considered to be equally unlikely, relative to Case A. thus Configuration A was ranked “1” and the other cases were tied as “2.” At this time, a minimum value of 5 % was selected as the minimum probability for all modeling cases ranked “2.” This probability value was considered conservative; however, it was appropriate given the desire to obtain a reasonable sample size for uncertainty analysis. The balance was assigned to the Case A approach, such that the total probabilities for each disposal unit type was 100 %.

Table PA-11.1 presents the preliminary results of the ranking approach, as based upon the above assessments. This information reflects the qualitative discussion provided in Section 5.6.3.1 of the SDF PA.

Table PA-11.1: Preliminary SDF PA Alternate Modeling Case Probabilities

Case	Probability Ranking (and Weights) by Tank Type		
	Vault 1	Vault 4	FDCs
A	1 (95 %)	1 (85 %)	1 (85 %)
B	N/A	2 (5 %)	2 (5 %)
C	2 (5 %)	2 (5 %)	2 (5 %)
D	N/A	2 (5 %)	2 (5 %)

N/A = Not applicable. Vault 1 does not have a sheet drain system.

Final Rationale for the Likelihood of Each Case

Later, when Case E was added to the suite of alternative modeling cases, the rankings and probabilities (as depicted in Table PA-11.1) were reassessed. Case E was ranked the least likely, relative to the other modeling cases. Analysis supports the assertion that fracturing initiated “in pores by expansive phase precipitation is unlikely to occur in saltstone” (WSRC-STI-2008-00236). This modeling case was assigned a much lower probability (0.1 %) to represent the very low likelihood of this failure mechanism.

Cases B and D simulate adverse performance resulting from potential interactions between the sheet drainage system and the saltstone. Without sufficient data to weight one modeling case over the other, Cases B and D were considered equally unlikely, thus ranked equally. Case C is considered less likely than Cases B and D because the “void space” modeling approach to address cracks in the cementitious materials is considered overly conservative.

Considering the qualitative ranking considerations discussed above, the probability of Case C was reduced by 0.1 % to accommodate the new modeling case. The results of this probability assignment approach are provided in Table PA-11.2. This information reflects the qualitative discussion provided in Section 5.6.3.1 of the SDF PA.

Table PA-11.2: Final SDF PA Alternate Modeling Case Probabilities

Case	Probability Rankings (and Weights) by Disposal Unit Type		
	Vault 1	Vault 4	FDCs
A	1 (95 %)	1 (85 %)	1 (85 %)
B	N/A (0 %)	2 (5 %)	2 (5 %)
C	2 (4.9 %)	3 (4.9 %)	3 (4.9 %)
D	N/A (0 %)	2 (5 %)	2 (5 %)
E	3 (0.1 %)	4 (0.1 %)	4 (0.1 %)

N/A = Not applicable

Vault 1 does not have a sheet drain system.

Radionuclide Benchmarking Concerns

Item 3 is a blanket concern asking for greater transparency with respect to benchmarking and the applicability of the benchmarking with respect to radionuclides, given a lack of excellent correlation between the Base Case model and the benchmarking results. The benchmarking approach and results are discussed in the response to PA-5.

Basis for Uncertainty Distributions

Item 4 is a blanket concern asking for clarification of the basis for uncertainty distributions used within the probabilistic model. The uncertainty distributions for inventory values and for K_d values are discussed in the responses to IN-2 and SP-18, respectively. The development of the uncertainty parameters for modeling cases is discussed in this RAI response (above). Aside from these parameters, there are 43 variable stochastic elements within the probabilistic SDF model. Table PA-11.3 identifies these stochastic elements by their name within the GoldSim SDF probabilistic model, the parameters as identified in the SDF PA, and the PA reference, which cites the data associated with the stochastic elements.

Table PA-11.3: Remaining Stochastic Elements within the Probabilistic SDF Model

Element	Parameter	SDF PA Reference
Path within GoldSim Model File: \DoseAssessment\DoseParameters\IRRIDOSE_Factors		
CattleWaterConsumptionBeef	Water Beef Cow Consumption	Table 5.6-11
CattleWaterConsumptionMilk	Water Milk Cow Consumption	Table 5.6-11
ConsumptionFodderBeef	Fodder Beef Cow Consumption	Table 5.6-11
ConsumptionFodderMilk	Fodder Milk Cow Consumption	Table 5.6-11
FodderFractionBeef	Fraction of Beef Cow intake from pasture	Table 5.6-11
FodderFractionMilk	Fraction of Milk Cow intake from pasture	Table 5.6-11
FracYearIrrigate	Fraction of Year Garden Irrigated	Table 5.6-10
IrrigationRate	Garden Irrigation Rate	Table 5.6-10
SoilBuildupTime	Soil exposure time period to irrigation	Table 5.6-9
VegetationProductionYield	Vegetable Crop Yield Productivity	Table 5.6-9
VeggieExposureTime	Vegetable crop exposure times to irrigation	Table 5.6-9
Path within GoldSim Model File: \DoseAssessment\Doses_by_Sector\Inhalation		
ExposureFractionShower	Showering Exposure Time	Table 5.6-11
Path within GoldSim Model File: \DoseAssessment\Doses_by_Sector\IRRIDOSE		
FracLocalBeef_MOP	MOP Fraction of Meat Produced Locally	Table 5.6-9
FracLocalMilk_MOP	MOP Fraction of Milk Produced Locally	Table 5.6-9
Path within GoldSim Model File: \DoseAssessment\Doses_by_Sector\IRRIDOSE\LeeValues		
Beef	Annual Beef Consumption	Table 5.6-11
Leafy	Annual Leafy Veggie Consumption	Table 5.6-11
LocalGrown	MOP Fraction of Vegetables Produced Locally	Table 5.6-9
Milk	Annual Milk Consumption	Table 5.6-11
Veg	Annual Other Veggie Consumption	Table 5.6-11
Path within GoldSim Model File: \DoseAssessment\Doses_by_Sector\LADTAP_Sectors		
AnnualAquaticFoodConsumption	Annual Finfish Food Consumption	Table 5.6-11
WaterConsumptionRate	Water Consumption Rate	Table 5.6-11
Path within GoldSim Model File: \DoseAssessment\ExposureMediaConc\WellCompletionDepth		
CompletionStratum	Probability of Well Driller Exposure by Aquifer	Table 5.6-7
Path within GoldSim Model File: \DoseAssessment\IHI		
AirIntake	Annual Breathing Rate	Table 5.6-11
ConsumptionVeggies	Annual Other Veggie Consumption	Table 5.6-11
ConsumptionWater	Water Consumption Rate	Table 5.6-11
FracLocalMeat	Intruder Fraction of Meat Produced Locally	Table 5.6-9
FracLocalMilk	Intruder Fraction of Milk Produced Locally	Table 5.6-9
FracLocalVeggie	Intruder Fraction of Vegetables Produced Locally	Table 5.6-9
Path within GoldSim Model File: \DoseAssessment\IHI\ResidentScenario		
FractionInGarden	Fraction of Year In Garden – Intruder	Table 5.6-11
GardenSize	Garden Size	Table 5.6-10
TillDepth	Depth of Garden	Table 5.6-10

**Table PA-11.3: Remaining Stochastic Elements within the Probabilistic SDF Model
(Continued)**

Element	Parameter	SDF PA Reference
Path within GoldSim Model File: \\Inventory\\Tank_to_Vault\\TankAndVaultRandomization\\VaultRandomizerLoop		
TankIndexer	Source variation of filling a disposal unit	Section 5.6.3.2
VaultIndexer	Location variation of disposal unit filling	Section 5.6.3.2
Path within GoldSim Model File: \\TheVaults\\Vault_1\\SiteGeometry		
SatWidth	Width of Saturated Zone for Vault 1	Section 5.6.3.8.1
Path within GoldSim Model File: \\TheVaults\\Vault_2\\SiteGeometry		
SatWidth	Width of Saturated Zone for an FDC	Section 5.6.3.8.1
Path within GoldSim Model File: \\TheVaults\\Vault_4\\SiteGeometry		
SatWidth	Width of Saturated Zone for Vault 4	Section 5.6.3.8.1
Path within GoldSim Model File: \\TheVaults\\VaultData\\PoreFlushes		
Flushes_1stc	Pore Volume Transition from Region II Reducing to Region II Oxidizing for Concrete	Table 5.6-6
Flushes_1stss	Pore Volume Transition from Reducing Region II to Oxidizing Region II for Saltstone Grout	Table 5.6-6
Flushes_2ndc	Pore Volume Transition from Region II Oxidizing to Region III Oxidizing for Concrete	Table 5.6-6
Flushes_2ndss	Pore Volume Transition from Region II Oxidizing to Region III Oxidizing for Saltstone Grout	Table 5.6-6
Path within GoldSim Model File: \\TheVaults\\VaultData\\UZ_Thickness		
UZthicknessDist	Vadose Zone Thickness Below the Disposal Units	Section 5.6.3.5
Path within GoldSim Model File: \\Transport\\WaterTransport		
SatThickness	Aquifer Thickness	Section 5.6.3.8.1
SatZoneDarcyVelDist	Darcy Velocity of Saturated Zone	Section 5.6.3.8.2

PA-12

Comment (New)

The dose consequences from the disposal of containerized Vault 4 waste in Vault 1 should be evaluated.

Basis

The NDAA states that, "(t)he Commission shall, in coordination with the covered State, monitor disposal actions taken by the Department of Energy". As part of this coordination, SCDHEC and NRC staff discussed a letter written by SCDHEC to the DOE regarding the potential disposal of containerized Vault 4 waste in Vault 1 (SCDHEC, 2010). In this letter, a request for the disposal of containerized waste from Vault 4 operations and soil remediation is described.

The NRC staff requires more information about this waste in order to assess compliance with the performance objectives of 10 CFR 61. In particular, the NRC staff must understand the origin and amount of this material. This is possibly important to monitoring the performance of Vault 4 because if this waste primarily consists of soil that has become contaminated due to seeps from Vault 4, then this might show that Vault 4 is not performing as expected. It also would be useful to evaluate whether the PORFLOW model accurately predicts the inventory that has seeped out of Vault 4. If the amount of inventory that has reached the outside of Vault 4 and the surrounding soil is significant, this may indicate that the model underestimates the release from this vault. Also, if any residual radioactivity remains in the soil surrounding Vault 4 following this remediation, this radioactivity could move through the subsurface more rapidly than predicted, especially since the site does not yet have a cover to limit the infiltration.

NRC staff is also interested in the effect of this additional waste on the expected dose from Vault 1. In particular, NRC staff is interested in how much additional inventory will be placed in Vault 1 and the effect of this inventory on the expected dose. It is possible that the long-term performance of containerized waste will be different than the long-term performance of grout. An evaluation of the potential effect of the containerized waste on long-term performance should be performed.

Path Forward

Please provide the following information:

- 1) The inventory of radionuclides that has seeped from Vault 4, including the amount (concentrations and total activity) and location of this inventory.
- 2) A comparison of the inventory that has seeped from Vault 4 to the inventory predicted by the PORFLOW model to be released from the vault to confirm that the modeling calculations are accurate.
- 3) An assessment of the dose due to residual radioactivity remaining outside of Vault 4, if any.
- 4) The inventory in the additional waste that will be added to Vault 1 and the expected dose from this inventory.
- 5) An evaluation of whether the presence of containerized waste is consistent with the assumptions in the PA for Vault 1 and the potential effect of this waste on the calculated dose.

RESPONSE PA-12:

Please note that the condition of the Vault 4 walls have been previously evaluated with respect to the 1992 PA (WSRC-RP-92-1360) and the Composite Analysis (WSRC-RP-97-311) in the UDQE *Evaluation of Liquid Weeping from Saltstone Vault 4 Exterior Walls*, SRS-REG-2007-00041 Revision 1. In addition, the NRC has concluded in their observation report that there is reasonable assurance that Vault 4 can meet the performance objectives in spite of the observed vault conditions if the system is emptied of liquids prior to closure. [ML081290367] The containerized Vault 4 waste is the contaminated soil removed following the weeping from the Vault 4 exterior walls.

The referenced letter from SCDHEC to DOE regarding the potential disposal of containerized Vault 4 waste in Vault 1 is part of an ongoing discussion to determine the appropriate path forward with respect to the disposition of the soil that mixed with liquid from Vault 4. As acknowledged in the referenced letter, several studies “must be completed before it will be known if Vault 1 is an acceptable disposal location for the containerized wastes.” [DHEC_09-30-2010] These studies include geotechnical investigations and inventory studies of the waste generated from Vault 4 soil remediation activities. These studies are ongoing, thus no final decision has been made with respect to the final disposition of the contaminated soil. If the decision is made to proceed forward with disposal in Vault 1, a UDQE will be performed to determine the potential impact of the disposal action including an evaluation of the inventory in the remediated soil. DOE will provide any additional information fully addressing items 1, 4, and 5 of the Path Forward to the NRC when decisions are made and the information is available to support the NRC’s monitoring role related to disposal actions at the SDF.

Although the inventory of the contaminants within the containerized Vault 4 waste has not yet been characterized (as requested by item 1 of the Path Forward), studies were performed on the soils prior to remediation that provide insight into the inventories and the impact of the contamination. Prior to cleanup activities, the contaminated soils were sampled and the inventory was characterized. [ERD-EN-2008-0056; ERD-EN-2008-0083] The resulting inventories from these soil analyses are expected to be representative of the containerized waste. A comparison of the doses from the sampled inventories against dose results from an analytical model demonstrated that the inventories (based on the sampled soils) were bound by those of the analytical model. Therefore, doses from the soils could be expected to be below the doses resulting from the analytical model (which had results that were negligible with respect to the SDF PA). The containerized waste only includes soils and plastic used to line the containers.

As mentioned above, prior to any final disposition, the inventory of the waste will be characterized and evaluated against relevant information (e.g., the 2009 SDF PA). Based upon such evaluations, changes to the SDF PA (SRR-CWDA-2009-00017) model will be made as deemed appropriate.

Concerning item 2 of the Path Forward, the operational conditions (e.g., bleed water weeping through vault walls) is not representative of the closure conditions (e.g., inventory leaching from cured saltstone) and therefore comparison to the SDF PA (SRR-CWDA-2009-00017) closure modeling is not appropriate. The 2009 PA does account for flush/bleed water that may have seeped into the Vault 4 walls during vault filling operations and is present at the time of closure. The seepage during vault filling operations was evaluated in a UDQE and found to not impact the conclusions of the PA. [SRS-REG-2007-00041] The SDF PA (SRR-CWDA-2009-00017) accounts for this seepage during vault filling operations by including radionuclide inventory in the walls of Vault 1 and Vault 4 as described in SDF PA Section 4.4.1.1 for Vault 1 and SDF PA Section 4.4.1.2 for Vault 4. [SRR-CWDA-2009-00017] Furthermore, the observed condition of the Vault 1 walls and the Vault 4 walls is modeled in the SDF PA by considering an initial saturated hydraulic conductivity of 0.17 cm/sec (as shown in SDF PA Table 4.2-16) with characteristic curves developed for "fractured concrete" as shown in SDF PA Figure 4.2-26.

Concerning item 3, the facility is still in an operational condition so any current inventory within the existing containments, but outside Vault 4 is not representative of the final closure condition. Therefore, no assessments of this source are planned at this time. However, DOE will continue to inform the NRC under monitoring.

PA-13

Comment (New)

The dose consequence from early releases from the vaults prior to completion of the closure cap is not considered.

Basis

The performance assessment calculations assume that the closure cap will result in a significant [sic] reduction in the infiltration reaching the vaults starting at the first year of the model. However, the closure cap is not expected to be constructed until the end of the operational period, and there will be no reduction in the amount of precipitation reaching the vault roofs and walls before that time. The reported average precipitation rate for the site is 49 in/yr (124 cm/yr), which is significantly higher than the assumed initial infiltration rate (0.00042 in/yr [0.0011 cm/yr]). It is likely that the amount of leaching will be higher before the closure cap is installed because more water could contact the saltstone during this time. This is especially true for Vaults 1 and 4 because these vaults have had problems with water leaking through the roof and cracks forming in the walls. It is important to understand the potential for early releases to the environment during the time between the placement of the saltstone and the installation of the closure cap and the potential future dose from these releases because these releases could be significant compared to future releases.

In addition, the rate of degradation of the vaults might be higher before the backfill and cover are installed. For example, the larger amount of water reaching the vaults during this time could cause the concrete to age more rapidly. Also, the vaults will be exposed to more of the freeze/thaw cycle prior to the backfill being placed around the vaults. The saltstone wasteform would likely experience faster rates of oxidation due to higher rates of oxygen transport associated with air movement through the system compared to post-closure configurations.

Path Forward

Provide an assessment of the dose consequences from the increased amount of water the vaults will be exposed to prior to completion of the closure cap. Also, provide an assessment of the effect of the vaults being initially uncovered on the integrity of the vaults and the oxidation of saltstone.

RESPONSE PA-13:

As described in SRR-CWDA-2009-00017 Sections 3.2.1.2.6 and 3.2.1.3.4, Vault 4 and FDC's will have ventilation ports installed in the roof. Filters for contamination control are installed on the ventilation ports and any condensation is returned to the cell. The ventilation ports allow air exhaust during cell filling as well as natural air exchange. The ventilation ports and other access ports will be permanently sealed with the installation of the clean grout cap and permanent roof closure.

As described in SRR-CWDA-2009-00017 Sections 3.2.1.1.4, 3.2.1.2.4, 3.2.1.2.6, 3.2.1.3.4, and 3.2.1.3.5, the vaults and future disposal cells contain walls and a roof, which prevent the intrusion of water into the cell. Vaults 1 and 4, however, have experienced water intrusion and leakage. Corrective actions were implemented on Vault 1 to prevent the entry of rainwater through the roof and to remove water between the vault wall and saltstone using a pipe and drain valve. Vault 4 Cells A, C, G, and I were partially to completely filled when rainwater intrusion into Cells A and G was detected. Similar corrective actions were implemented to remove water using a pipe and drain valve and to prevent rainwater entry through the roof.

Cells C and I were only partially filled, and have not experienced the same issues. [ESH-WPG-2006-00132] To prevent recurrence, a sheet drain system was installed in Vault 4 Cells B, D, E, F, H, J, K, and L (SRR-CWDA-2009-00017 Section 3.2.1.2.5). Future disposal cells will have a sheet drain system to remove free liquid in the cells during the operational period (SRR-CWDA-2009-00017 Section 3.2.1.3.5). In addition, operational control of the disposal units includes the timely removal of bleed water associated with saltstone curing, flush water following saltstone emplacement, as well as any potential infiltrating water. Timely removal of water from the disposal units minimizes water intrusion into the saltstone monolith. The drain systems will be maintained until the individual units are closed.

The closure of an individual disposal unit includes the emplacement of a clean grout cap covering the saltstone monolith having similar hydraulic properties as saltstone, filling the remaining volume to the roof, and the sealing of disposal unit penetrations. These closure activities may be conducted when the disposal unit is at the end of its operational life and will effectively isolate the saltstone monolith from water intrusion. The time between the end of the operational life for a disposal unit and the time of closure is expected to be relatively short. In fact, the closure of all of the SDF disposal units is expected to occur within 20 years.

Because (1 the disposal units are designed to preclude water ponding (i.e., sloped roofs), (2 normal operations would identify rainwater infiltration and implement preventative measures, and (3 the prompt removal of water through the sheet drain system, limited water would be available to impact the disposal cells during freezing conditions. Furthermore, South Carolina is located in a temperate climate where freezing conditions are typically limited to overnight hours and do not penetrate the ground surface. Therefore, the freezing conditions and potential impacts would be limited to the disposal unit walls and would not penetrate to the saltstone. The walls of the FDCs will be backfilled with soil and impacts from freeze-thaw cycles will not be expected. The outer walls of Vaults 1 and 4 are open to the atmosphere and would be subjected to freezing conditions. The Vaults 1 and 4 outer-wall concrete is a high strength material that would be resistant to freeze-thaw cycle impacts. This is currently evidenced by the lack of freeze-thaw cycle impacts on the Vaults 1 and 4 walls. Because of the prompt water removal, the temperate climate of South Carolina, and the strength of the disposal unit walls, freeze-thaw cycle impacts to the disposal cells are expected to be negligible.

With the introduction of operational clean caps and the low diffusion coefficients of the concrete, the impacts of any potential increased oxygen are not risk-significant to the PA results. For example, SRR-CWDA-2009-00017 Section 5.6.6.6 presents a sensitivity case in which the assumption for Vaults 1 and 4 concrete is that it will be oxidized at closure. The results indicate that there is an impact to the timing of the peak dose but a decrease in the magnitude of the peak. Thus, sensitivity of the disposal units to oxidation and other degradation mechanisms prior to the placement of the closure cap is not considered significant and would have a negligible impact on the current performance analysis. To support this position, oxygen diffusion into the saltstone and vault walls was calculated using the methodology presented in the response to RAI PA-8. Equation 14 (from the response to RAI PA-8) establishes a method to determine the oxidation front position. The reduction capacity of the concrete was obtained from SRNS-STI-2008-00045, using 50-year old concrete as a surrogate for Vault 1 and 4 roof and walls. The cementitious material parameters used in Equation 14 are presented in Table PA-13.1.

Table PA-13.1: Cementitious Material Parameters

Cementitious Material	Reduction Capacity of Solid^a (meq e-/g)	Bulk Density of Solid^b (g/cm³)	Concrete Porosity^b (%)	Effective Diffusion Coefficient^b (cm²/sec)	Dissolved Oxygen Concentration at Exposure Face^c (meq e-/L)
Vault 1 Roof	0.0855	2.2	14.5	1.0E-07	1.06
Vault 4 Roof	0.0855	2.21	13.6	1.0E-07	1.06
Vault 1 & 4 Walls	0.0855	2.24	12	5.0E-08	1.06
FDC	0.2398	2.22	11	5.0E-08	1.06
Saltstone and Clean Cap	0.8218	1.01	58	1.0E-07	1.06

a. SRNS-STI-2008-00045, Table 8

b. SRR-CWDA-2009-00017, Table 4.2-16

c. SRR-CWDA-2009-00017, Section 4.2.3.2.4

The saltstone would be contained on each side by the walls and floor, but would be open to the atmosphere through the ventilation ports during pouring and prior to the installation of the clean grout cap. The timeframe would typically be 3 to 6 months between the saltstone pour and the installation of the clean grout cap. The oxygen diffusion during a 6-month period was calculated using Equation 14 to be negligible (0.48 millimeters) for the 24-foot thick saltstone monolith.

To determine the impact of oxygen diffusion prior to the emplacement of the closure cap, the time required for the oxygen diffusion to penetrate the walls or roof of the disposal units was determined. Equation 14 was solved for time using the thickness of the wall, roof, and clean cap for each of the disposal unit designs. The results are provided in Table PA-13.2.

Table PA-13.2: Time for Oxygen Diffusion through Saltstone and Vault Concrete

	Vault 1		Vault 4		FDC	
	Cementitious Material Thickness (in)	Time for Oxygen Diffusion (yr)	Cementitious Material Thickness (in)	Time for Oxygen Diffusion (yr)	Cementitious Material Thickness (in)	Time for Oxygen Diffusion (yr)
Wall	18	998,000	18	998,000	8	598,000
Roof	6	45,100	4	21,500	8	598,000
Clean Cap	6	49,700	15	311,000	24	795,000

As shown in Table PA-13.2, oxygen diffusion and penetration through the cementitious material of the wall, roof, or clean cap of the disposal units would be minimal during the time period prior to the emplacement of the closure cap while the disposal units are exposed to the atmosphere.

PA-14

Comment (New):

The PA does not discuss the existence or implications of calcareous material, or soft zones, underlying Z-Area.

Basis:

Two supporting PA documents (K-ESR-Z-00001; K-ESR-Z-00002) addressed geotechnical issues regarding the calcareous zones at Z-Area that support 10 CFR Part 61.44. In addition to potential stability impacts, these zones have potential implications for other aspects of the future performance of the SDF (e.g. cover integrity, saltstone integrity, and far-field flow and transport [see Comment FFT-4]). It is not clear how these features were or were not considered. As NRC staff only recently became aware of these features, additional information may be requested.

Path Forward:

Provide any additional documentation of calcareous features at

Z-Area, including any documentation regarding how these features were addressed in the PA as well as data or analyses from any core, geophysical logs, cone penetrometer test logs and geotechnical borings.

Response PA-14:

As stated in the geotechnical evaluation report for Disposal Unit 2, K-ESR-Z-00001, soft zones are defined as intervals with a CPT tip resistance less than 15 ton/ft² over a continuous interval of two feet or greater. Ground elevation at Disposal Unit 2 is approximately 305 feet above MSL. A soft zone approximately 14-feet thick was identified in one CPT below Disposal Unit 2 designated CP-15, centered at an elevation of 170 feet above MSL (approximately 135 feet below ground surface). Looking at the tip resistance for CP-15 (K-ESR-Z-00001 Figure 2), the interval identified is represented by a tip pressure of less than 15 ton/ft², but does not appear to represent a void, as there is still tip resistance apparent on the CPT log. This would indicate a zone of underconsolidation as opposed to an actual void. As indicated in Appendix A of K-ESR-Z-00001, three other borings surrounding CP-15, all approximately 75 feet away laterally, did not indicate the presence of soft zones, limiting the potential lateral extent of the zone.

The amount of potential Disposal Unit 2 settlement due to a DBE (a peak ground acceleration of 0.21 g), has been calculated and summarized in Section 5.3.3 of K-ESR-Z-00001. The results of this analysis indicate potential compression of the soft zone represented at ground surface due to a DBE would only be a maximum of 1 inch.

In addition, geotechnical evaluation report K-ESR-Z-00002, which summarizes the results of subsurface characterization below future SDF Disposal Units 3A, 3B, 5A, and 5B (located approximately as shown in SDF PA Figure 3.2-2 as Disposal Units 7A through 7D), did not identify any soft zones, which indicates that soft zones are infrequent and laterally discontinuous.

Although various early documents describe voids, drilling fluid losses, and grout takes associated with the Santee Formation (Calcareous Zone, Lower Aquifer Zone, etc.), there is in fact no evidence of subsurface voids, karst, or caves that would act as open flow conduits in the GSA. In historical and recent literature, no documentation was found of void spaces or other phenomena that would influence contaminant migration in a manner not already captured by the SDF Flow Model.

Conclusions from early SRS investigations and research are presented in the response to RAI FFT-4 (Item 1) and are not reiterated here. Additional information from other sources is provided below.

Soft zones have been the subject of many general and facility-specific investigations, the conclusions of which are summarized below and referenced (unless otherwise noted) in a comprehensive review of soft zones. [WSRC-TR-99-4083]

- The existence of under consolidated soft zones (in the Santee Formation) beneath SRS was documented by the USACE during characterization in the early 1950s. The USACE identified these zones as a concern for foundation design, and recommended and carried out a program of injection grouting to remediate foundation conditions in F, H, C, K, L, P, and R Areas. Grouting prior to construction of sensitive facilities continued as a standard engineering practice at SRS through the 1980s.
- Historically, soft zones in the Santee Formation have been identified by various field parameters including loss of drilling fluid, low resistance to drill penetration, and drill rod drops. Currently, soft zones are delineated quantitatively through various geotechnical field criteria including CPT (tip stress less than 15 ton/ft²) and SPT (blow counts less than 5), both carry a criterion for soft zone minimum vertical thickness of two feet.
- The compendium of literature on SRS soft zones describes them not as actual cavities or caves but as zones of loose, weak, saturated sediments with a honeycomb or sponge-like structure and having substantial structural competence.
- The mechanisms of soft zone formation and preservation are subjects of debate, but the association with mixed carbonate/clastic sediments of the Santee Formation is clear and well documented. Frequently presented hypotheses for soft zone formation include dissolution of carbonate material by meteoric water under shallow/vadose conditions, and/or partial replacement of carbonate minerals with amorphous silica. The existence of cemented hardpan zones in shallow vadose and transitional phreatic environments may offer a modern analog for the very hard, indurated strata often encountered just above soft zones in the Santee Formation.
- Zones of hard, cemented sediments are commonly encountered in conjunction with soft zones, usually just above, and sometimes above and below soft zones. The physical properties and engineering behavior of these more competent layers has led to their characterization as competent bridges that redistribute geostatic stresses around the underlying soft zones; this soil-arch phenomenon appears to take place even in semi- and non-indurated sands overlying soft zones.
- Soft zones have been encountered beneath most of SRS, but are less common in the northwest (updip) and more common in the southeastern (downdip) regions. This distribution appears to correlate with the well-documented pattern of increasing carbonate content in the Santee Formation to the southeast. This lateral variation in carbonate content reflects the original range of depositional environments, from nearshore and inner shelf environments with primarily terrigenous input in the northwest, to quiet water, outer shelf conditions of carbonate accumulation in the southeast. In the GSA the Santee Formation is composed of mixed clastic and carbonate materials, with clastic material being dominant; the interpreted depositional scenario is a moderate energy, middle shelf environment, with input of both clastic and carbonate sediments. Lithologic and petrographic studies have divided the Santee Formation in the GSA into eight microfacies, quartz sand (stone), terrigenous mud (stone), skeletal lime mudstone,

skeletal wackestone, skeletal packstone, skeletal grainstone, microsparite, and siliceous mudstone. [WSRC-RP-94-54] In the GSA, three facies have been interpreted in soft zone sediments, sandy biomoldic chert, siliceous sandy mud, and terrigenous sand. [SAIC 1999]

- Soft zone geometries have been studied in great detail by CPT/SPT characterization across the entire SRS. Apart from the observation that soft zones cluster in two zones within the Santee Formation (approximately 140 feet MSL and approximately 170 feet MSL in the GSA), these efforts have otherwise shown soft zones to be isolated, discrete, poorly connected, non-uniformly distributed, random features. Although their sizes and shapes vary greatly, their average thickness is generally a few feet, with a postulated maximum lateral dimension of about 10 to 20 feet or less. [K-ESR-G-00013]
- Confirmatory borings and careful study of previously grouted zones (especially in K Area) revealed no significant thicknesses of grout (contrary to what would be expected if large volumes of grout had filled open cavities). Instead, grout was found to have thoroughly mixed with the formation sediment. Grout was often distributed in thin ribbons, leading some to conclude that the grouting program may have had the unintentional effect of fracturing the target formation. Therefore, soft zones that existed before grouting were still present after grouting.
- Efforts to detect soft zones with remote or minimally invasive techniques have not been successful. Soft zones have not been found with ground penetrating radar or with any other surface electrical method (resistivity, magnetics, or gravity) that relies on detection of physical property contrasts. Borehole P-wave tomography may be more successful, but it relies on advance knowledge of soft zone distribution requires installation or existence of appropriately arrayed boreholes. [WSRC-TR-96-0041]

In addition, response to RAI FFT-4 (Item 3) provides a summary of 23 soil borings for characterization of the subsurface for the SDF, including soft zone evaluations and recommended that no type of grouting program for the voids or soft zones was necessary to stabilize the subsurface in the SDF area to minimize potential for future subsidence. [87814-PT1]

In summary, soft zones and carbonates are generally represented by very small and infrequent pockets in the UTR-LZ that do not continuously run the length of the flow path of the plume, are located near the base of the UTR-LZ, and appear to be filled in with fine sand from the surrounding formation. [WSRC-TR-94-0369] As such, to assume the effects of the presence of carbonate material and soft zones on mobility should be spread across the entire aquifer is not reasonable. Any localized increase in mobility would be very short relative to the total distance of transport.

Inventory (IN)

IN-1

Comment:

The reported inventory of some of the radionuclides disposed of in Vaults 1 and 4 as of March 31, 2009 (X-CLC-Z-00027) exceeds the total inventory of these radionuclides assumed in the PA for these vaults (Tables 3.3-1 and 3.3-3 in the PA), even when accounting for the decay of these radionuclides to the year 2030.

NRC Response:

The answer to this RAI was adequate.

IN-2

Comment:

More information is needed about the basis for the uncertainty distributions for the radionuclide inventories used in the GoldSim calculations.

DOE Response Discussion:

In the PA, it is stated that “(t)he source variation deals with variability associated with the ability to predict inventories. This source variation not only includes material variability within the waste tanks, but also includes process treatment uncertainty and analytical uncertainty.” The ratios of the measured saltcake concentration to the concentration predicted by the Waste Characterization System (WCS) calculations were used as the basis for developing these distributions. The previous NRC comment addressed the basis of using the ratio information for a subset of the radionuclides and applying the ratio for the distributions for all radionuclides.

In the response to this comment, DOE stated that the exclusive use of C-14, Cs-137, Pu-239, Sr-90, and U-238 ratio information in developing the uncertainty distributions was due to the lack of data for the other radionuclides.

NRC staff understands that limited information is available on these ratios, but the uncertainty distributions are not adequately justified and may not be appropriate for the following reasons:

- 1) The basis for using salt concentration ratios to represent uncertainty in the supernate is not provided.
- 2) It is not clear how the uncertainty in removal efficiencies is being represented by uncertainty in the WCS predictions.
- 3) The basis for using the same uncertainty distributions for radionuclides that are expected to be removed during treatment and those that are not (e.g., Tc) is not clear.
- 4) It is not clear why the inventory uncertainty factors are used for Vaults 1 and 4. Most of the inventory for these vaults has already been placed into the vaults, so there should not be significant uncertainty associated with either the WCS predictions or the treatment removal efficiency since the inventory in this waste has already been directly measured.

The uncertainty distributions assumed for Sr-90, Cs-137, and U-238 are biased towards being less than one such that the use of these uncertainty distributions would result in the mean inventory in the calculations being decreased. This could cause the dose calculated in the GoldSim model for these radionuclides to be underestimated (biased in an arbitrary way to low values).

Path Forward:

As was true for PA-11, the amount of additional information needed on this topic depends on the extent to which DOE intends to use the GoldSim model results for compliance or model support. If the GoldSim model is going to be used for compliance, the basis for the ranges is not adequate. In that case, either more information is needed to justify the distributions, or the distributions should be changed to distributions that are defensible.

Response IN-2:

In response, each of the reasons provided in the discussion above are addressed below to justify the inventory distributions currently used in the GoldSim transport model.

1. Salt concentration uncertainties are used because supernate is generated from dissolved salt. Therefore, the uncertainty in the salt concentrations directly effects the supernate concentrations. Since the process used to dissolve the salt involves a significant amount of mixing, the expectation is that the uncertainties used are bounding and that the actual variability will be less than that seen in the salt. In addition, since the concentrations of the radionuclides in the salt is expected to be higher than the concentrations once the salt is dissolved, relative uncertainties were used, explained in more detail in item 3 below.
2. Bounding conservative removal efficiencies were used in both the deterministic and probabilistic cases. The removal efficiency had no uncertainty assigned to it. Limited data was available at the time on the range of efficiencies, so estimating the uncertainty was problematic. For this reason, bounding conservative efficiencies were used in all cases (i.e., a DF of only 12 for cesium and no DF for all other elements).
3. The uncertainties used a multiplier method, the uncertainty multiplier times the inventory, such that the uncertainty is not an absolute value but rather relative to the inventory. Whether the radionuclide is removed or not is reflected in the inventory estimate, not the uncertainty multiplier. The range of uncertainty for those radionuclides that are removed would be reduced based on the inventory being reduced, while the relative uncertainty is not expected to change.
4. The material projected (post 2008) to be disposed in Vaults 1 and 4 is different from the material currently disposed (pre 2008). In general, the material projected to be disposed of in these vaults has a higher activity content than that which is currently disposed. Therefore, the projected vaults inventories were based in a greater portion on the future material. This material is associated with the projected uncertainties and was used as the basis for inclusion with the Vaults 1 and 4 inventories.

Further, the uncertainty distributions for those radionuclides (for Sr-90 and U-238) less than one will reduce the mean inventory to less than the estimated inventory. These uncertainty distributions suggest the estimated inventory is an overestimate, not that the GoldSim model would underestimate the inventory. The uncertainty distributions would cause the mean to be biased, but it would be biased based on actual sample results, which would not be arbitrary.

IN-3

Comment:

Information is needed on the process that will be used to ensure that the inventory will be distributed among the FDCs in a configuration that provides reasonable assurance that the performance objectives will be met.

DOE Response Discussion:

The DOE response to this comment stated that the probabilistic model incorporated the variability in the disposal sequence of the waste. As noted in (PA-11 and IN-2) NRC staff has concerns with the methodology used in the GoldSim probabilistic model, including the uncertainty distributions used for the inventory.

The DOE response stated that the process of moving the waste through the tank farm to the SPF would tend to move the concentrations of radionuclides in the waste towards the average due to mixing of the waste. NRC staff agrees with this assessment, but there will still be some variability in the concentrations of radionuclides in the different FDCs. Because the compliance case is based on all of the FDCs having a concentration at the average concentration, it would be necessary for the NRC staff to monitor the inventory in each FDC to the average concentration. Information on the methodology that will be used by DOE to assess the actual configuration of inventory in the FDCs would be extremely useful for the NRC to have when writing the updated monitoring plan.

Path Forward:

Provide a description of the strategy that will be used to assess the dose from the actual inventory disposed of in the FDCs.

Response IN-3:

The following is a description of the anticipated process to assess the actual inventory disposed in FDCs. As part of the implementation of the SDF PA, new values will be developed for the WAC in order to protect the assumptions made concerning FDC inventories. Characterization of salt batches prior to treatment will continue, as will sampling and characterization of Tank 50, the SDF feed tank. As waste material is disposed in each FDC, the inventory quantities will be monitored and tracked. If the disposed inventory is projected to be greater than the estimated inventory for an FDC, an evaluation of this information on the performance of the disposal system will be conducted. Once an FDC is filled, the inventory of the FDC will be finalized, and any new information will be analyzed as necessary. This strategy and implementing procedures are in the process of development. Once completed, the specifics of the strategy will be provided to the NRC.

IN-4

Comment:

More information is needed about the inventory expected to remain in the sheet drain systems for Vault 4 and the FDCs and the inventory expected to remain in the transfer lines at the time of closure.

DOE Response Discussion:

In the response to this comment, DOE staff stated that a cold cap containing clean water will be placed over the saltstone monolith and that the sheet drain system will therefore be filled with clean water at the time of closure. DOE also stated that the drainwater system will be emptied to the maximum extent practical prior to closure.

NRC staff agrees that the bleed water from the clean grout will likely dilute the concentration of material in the feed water collection system, but the system will likely still contain some residual amount of radionuclides because the system is likely to respond like a stirred tank reactor and not with plug flow dynamics. NRC staff is interested in understanding the volume and possible concentration of radionuclides remaining in these systems.

The DOE response also stated that the transfer lines will be removed and disposed of as LLW, so they will not contribute to dose. NRC staff finds that this portion of the response is adequate

Path Forward:

Provide information on the volume of liquid that is expected to remain in the drain water collection system for Vault 1, Vault 4, and the FDCs. Provide an estimate of the inventory that could remain in these systems at the time of closure.

Response IN-4:

No, or negligible, inventory is expected to be present in the drainwater system (i.e., sheet drains and drainage piping) at the completion of a vault's or cell's use. As bleed water makes its way to the sheet drains, the concentration of radionuclides is roughly expected to be a diluted representation of the feed stream. Once the bleed water reaches the sheet drains, the flow out of the drain system is expected to behave similar to plug flow dynamics, not stirred tank reactor dynamics. This expectation is based on the dimensions of the sheet drains. The sheet drain is a narrow gap between the vault wall and the saltstone waste form. The bleed water descends the side of the wall to the piping system before it is removed and transferred back to SPF, for treatment in the next saltstone batch to the next vault or cell. Based on these dimensions, free mixing is severely hindered causing the flow profile to resemble plug flow characteristics.

As the cold cap is added to the top of the monolith, clean water will enter at the upper end of the sheet drain. Based on the plug flow behavior, little mixing will occur with the clean water and this generally clean water will be the last material exiting the collection piping of the vaults. In addition, the sheet drain will be emptied and filled with clean grout. Therefore, if any volume of material remains, it is expected to be negligible in mass as well as low in the concentration of radionuclides, especially relative to the inventory in the saltstone.

For the purpose of completeness, the volumes of the sheet drains and drainage piping for Vault 4 and a FDC are included below in Table IN-4.1. Note Vault 1 does not contain a drainwater collection system.

Table IN-4.1: Vault 4 and FDC Drainage System Volumes

	Vault 4	FDC
Sheet Drain (gal)	18,000	1,000
Drain Piping (gal)	1,600	2,800

Based on these volumes and bounding the possible inventory by assuming that these volumes are filled with undiluted salt solution, the total inventory in the sheet drains and drainage piping would be less than 0.15 % of the SDF PA Table 3.3-3 inventory in Vault 4 and less than 0.3 % of the SDF PA Table 3.3-5 inventory in each of the FDCs.

IN-5

Comment (New):

Additional information is needed about the Th-230 inventory assumed for Vault 4 and the process used to confirm that all risk-significant radionuclides have been identified as key radionuclides as waste is disposed and final inventory information becomes available.

Basis

One of the key radionuclides identified in the current PA is Ra-226, which is created by ingrowth from Th-230. Neither of these radionuclides was identified as key radionuclides in the 2005 PA. Because of this, the NRC staff is concerned that the process used to predict the inventory for the purpose of the PA may not be capturing all risk-significant radionuclides. Key uncertainties in DOE's ability to estimate disposal inventories may not be adequately accounted for in the estimates. When updated inventory information is developed as waste is disposed, it is important to verify that any changes between the predicted and actual inventory do not result in significant changes to the predicted dose or to the list of key radionuclides. NRC staff is interested in the process used by DOE to confirm this.

Additionally, NRC staff would like information on the basis for the assumed inventory of Th-230 in Vault 4 (i.e., was this inventory based on measurements or a calculated value) and NRC staff would like more information on the reason for the underestimation of the Th-230 and Ra-226 inventory in the 2005 PA. This information would help the NRC staff to better understand the cause of this and to have confidence that this type of problem will not occur in the future.

Path Forward

Provide a description of the process that will be used to verify that all key radionuclides have been identified as additional waste is disposed and a more certain inventory is developed. Provide information on the cause of the underestimation of Th-230 and Ra-226 inventory in the previous PA.

RESPONSE IN-5:

The inventories of Th-230 and Ra-226 were not estimated in the 2005 SA (WSRC-TR-2005-00074). In an effort to ensure all risk significant radionuclides were identified for this SDF PA revision (SRR-CWDA-2009-00017), a conservative approach was used to set the radionuclide screening criteria for the SDF PA as described in SRNS-J2100-2008-00004 Section 2 including the identification of key daughter products. Based on the conservative criteria, DOE is confident that the sufficient constituents have been evaluated. Using these conservative criteria, both Th-230 and Ra-226 were selected for an initial inventory estimate. Based on experience to that point, these two radionuclides were not expected to be risk significant and therefore the method chosen to estimate their initial inventory was a bounding one. Both Th-230 and Ra-226 were estimated to be in equilibrium with their parent U-234 which is a significant conservatism. For example, at a 10,000-year decay time, the Th-230 is actually less than 10 % of the U-234 inventory due to the long half-lives of both the U-234 and Th-230 as presented in CBU-PIT-2005-00040. The same estimate method was used for Th-230 and Ra-226 in the FTF PA Revision 0 (SRS-REG-2007-00002_Superseded) inventories. Using this conservative methodology, the results from the dose calculations showed Ra-226 to be a significant dose driver. To avoid an over estimate of the risk significance of Ra-226, or Th-230 and U-234, an adjustment was made in developing the inventory estimates for the FTF PA Revision 1 (SRS-REG-2007-00002) to remove the significant conservatisms in the Th-230 and Ra-226 inventory estimates and replace them with more realistic estimates. [SRR-CWDA-2009-00045]

In the future, the inventories of the risk-significant radionuclides in the SDF disposal units will be primarily based upon laboratory analyses of samples from Tank 50 and not on the conservative methods discussed above. The material sent to the SDF will continue to be sampled and analyzed for radiological constituents and the sample results used as the primary means for inventory determinations. This methodology will ensure that risk-significant radionuclides are identified and proper comparisons can be made to inventories modeled in the SDF PA. Note, the inventory developed in response to comment PA-8 (Case K) included this more realistic approach to Ra-226 and Th-230 inventory estimates and resulted in a significant reduction in the modeled inventories.

IN-6

Comment (New):

Additional information is needed about potential changes to the salt solution feed batch preparation tanks and the sampling methodology that will be used for these tanks.

Basis

As part of the coordination with the State required by the NDAA, the NRC and SCDHEC staff discussed a copy of a letter from SCDHEC to the Department of Energy regarding the replacement of Tank 50 as the feed tank for the SPF (SRR-ESH-2010-00030). According to this letter, DOE is proposing to install two 60,000-gallon (2.3E5 L) Salt Solution Receipt Tanks at the SPF as a replacement for Tank 50 as the feed tank.

NRC staff would like information on the sampling approach that will be used for these tanks to assess the inventory of radionuclides that will be disposed of at the SDF. Because the proposed tanks are much smaller than Tank 50 (60,000 gallons [2.3e5 L] instead of 1.3 Mgal [4.9e6 L]), a smaller amount of waste will be mixed in each tank, and the cycle of filling and emptying the tanks will occur more often. The sampling strategy for these tanks may need to be different than for Tank 50. More frequent sampling may be required, particularly if the waste entering these tanks is heterogeneous and there is significant inter-batch variability.

This information would be useful for NRC staff in the preparation of the updated plan for monitoring the disposal of salt waste disposal at the SRS.

Path Forward

If Tank 50 is going to be replaced as the salt solution feed tank, please provide updated information on the sampling approach that will be used to verify the inventory that is sent to the SDF.

RESPONSE IN-6:

Consistent with the recently issued Revision 16 of the SRS *Liquid Waste System Plan* (SRR-LWP-2009-00001), current plans are to continue to utilize Tank 50 in low-level waste service and to serve as the collection tank within the H-Tank Farm for the low-level waste streams destined for ultimate disposal in the SDF. Tank 50 will continue to be the sample location for this consolidate low-level waste stream that is the feed stream of the SPF. The Executive Summary (Section 1) of SRR-LWP-2009-00001 states, in part: "projects Tank 50 utilization as the feed tank for the Saltstone Production Facility (SPF) for the duration of the LW program." Discussions had previously been held with SCDHEC on the possibility of using alternative tank(s) to collect the low-level waste streams and feed the SPF so that Tank 50 could be placed in high-activity liquid waste service. Due to the advantage of continued use of Tank 50 in its current service, alternative plans have been placed on hold.

Infiltration and Erosion Control (IEC)

IEC-1

Comment:

The PA does not describe what portion of the water entering the perimeter drainage channel will infiltrate back into the native soil or backfill, or what, if any, effect such infiltration will have on vadose zone or saturated zone flow.

NRC Response:

The DOE response is adequate. The comment will be tracked with monitoring of the final closure cap design.

IEC-2

Comment:

The cross-sections of disposal units in WSRC-STI-2008-00244 illustrate the lower backfill layer and other materials in the closure cap covering the cells, but do not indicate what materials will be used to backfill around the cells.

NRC Response:

The DOE response is adequate.

IEC-3

Comment:

Additional information is needed to support conclusions about the long-term performance of the side slopes of the closure cap.

NRC Response:

No additional information is requested, the final cap design will be tracked in monitoring.

IEC-4

Comment:

During the transition from Bahia grass to a pine tree forest the closure cap could be affected by external factors such as drought or fire, thus changing the assumptions required for the stability calculation.

NRC Response:

The DOE response is adequate. The comment will be tracked with monitoring of the final closure cap design.

IEC-5

Comment:

Differential settlement could occur due to the presence of the relatively rigid disposal cells within the lower backfill and non-uniform thickness of the backfill. This could affect the drainage efficiency of the upper drainage layer and the integrity of the geomembrane layer.

NRC Response:

The DOE response is adequate. The comment will be tracked with monitoring of the final closure cap design.

IEC-6

Comment:

Additional justification is needed for the hydraulic conductivity assigned to the foundation layer of the infiltration and erosion cap.

NRC Response:

The DOE response is adequate.

IEC-7

Comment (New):

The PA should evaluate the potential implications of saturated conditions above the lateral drainage layer in the closure cap.

Basis

Table 47 in WSRC-STI-2008-00244 indicates that beyond 3,200 years the lateral drainage layer is unable to remove a large portion of the infiltrating water, the system saturates above the filter fabric layer, and runoff increases. If saturation occurs, pore pressure build-up in the overlying closure cap layers could directly affect cover stability, vegetation, hydraulic performance of cover materials, and erosion.

Path Forward

Provide (i) the saturation for individual cover layers with respect to time and (ii) the average head on top of each layer for all time periods. If saturated conditions are physically reasonable, provide discussion of the effects of closure cap saturation on stability, vegetation, erosion, and the performance of cover materials under hydrostatic pressure.

RESPONSE IEC-7:

WSRC-STI-2008-00244 provides the following in association with the SDF future closure cap:

- An SDF closure cap scoping level concept with sufficient information to evaluate the closure cap configuration relative to its constructability and functionality
- Utilization of the HELP model to provide conservative infiltration estimates over time, as the upper boundary condition for 2-dimensional PORFLOW SDF vadose zone flow and transport modeling

The HELP model considers precipitation, runoff, evapotranspiration, and lateral drainage in estimating infiltration through the composite barrier layer, HDPE geomembrane overlaying a GCL, of the SDF closure cap at each time step modeled. [WSRC-STI-2008-00244 Table 47] The initial moisture storage of soil layers designated as either a vertical percolation layer or a lateral drainage layer was conservatively set at the maximum field capacity of the soil. The HELP model assigns the saturated state for the GCL based upon its model designation as a barrier soil liner. Table IEC-7.1 provides the nominal saturation extracted from the HELP model output for individual closure cap layers associated with each of the time steps used for SDF PA modeling. [WSRC-STI-2008-00244] Based upon the HELP modeling results, Table IEC-7.1 indicates that the upper backfill, erosion barrier, middle backfill, and lateral drainage layer may become completely saturated in year 5,412 and after.

Table IEC-7.1: SDF Closure Cap Layer Nominal Saturation with Time

Year	Topsoil (6 in)	Upper Backfill (30 in)	Erosion Barrier (12 in)	Middle Backfill (12 in min)	Lateral Drainage Layer (12 in)	HDPE (60 mil)	GCL (0.2 in)	Foundation Layer (12 in)	Lower Backfill Layer (12 in min)
0	0.527	0.911	0.860	0.959	0.566	N/A	1.000	0.720	0.720
100	0.529	0.907	0.860	0.951	0.592	N/A	1.000	0.718	0.718
180	0.532	0.906	0.860	0.952	0.601	N/A	1.000	0.767	0.715
220	0.533	0.908	0.852	0.948	0.608	N/A	1.000	0.772	0.717
300	0.534	0.911	0.859	0.950	0.608	N/A	1.000	0.815	0.722
380	0.534	0.912	0.857	0.952	0.614	N/A	1.000	0.843	0.741
460	0.533	0.913	0.855	0.952	0.622	N/A	1.000	0.856	0.750
560	0.529	0.913	0.850	0.954	0.635	N/A	1.000	0.867	0.759
1,000	0.531	0.908	0.849	0.953	0.704	N/A	1.000	0.896	0.780
1,800	0.534	0.906	0.853	0.951	0.822	N/A	1.000	0.923	0.799
3,200	0.539	0.926	0.821	0.982	0.985	N/A	1.000	0.961	0.813
5,412	0.812	1.000	1.000	1.000	1.000	N/A	1.000	0.978	0.823
5,600	0.813	1.000	1.000	1.000	1.000	N/A	1.000	0.978	0.822
10,000	0.844	1.000	1.000	1.000	1.000	N/A	1.000	0.984	0.822

Note Initial layer thicknesses shown in parenthesis.

Table IEC-7.2 provides the predicted average annual head on the HDPE geomembrane extracted from the HELP model output associated with each of the time steps. The predicted HDPE geomembrane head increases with time through year 5,412 due to the assumed SDF closure cap degradation, particularly that of the upper lateral drainage layer. The predicted average annual hydraulic head of the overlying layers remains low and insignificant until the upper lateral drainage layer is fully degraded. After year 5,412, the head begins to decrease because complete degradation of the upper lateral drainage layer has occurred while degradation of the underlying HDPE geomembrane continues. At its greatest, the predicted HELP model HDPE geomembrane head extends partially into the upper backfill. The saturation and head estimates values are bounding and conservative.

Table IEC-7.2: Average Annual Head on SDF Closure Cap HDPE Geomembrane

Year	Average Annual Head on HDPE (inch)
0	3.755
100	3.865
180	3.919
220	3.961
300	4.026
380	3.973
460	3.954
560	3.965
1,000	4.158
1,800	4.860
3,200	8.796
5,412	39.545
5,600	39.511
10,000	38.978

Several assumptions were made to produce the conservative saturation and head estimates, including:

- An evaporative zone depth of 22 inches was utilized within the closure cap modeling, based upon HELP model guidance, which lists this depth as a “fair” depth for Augusta, Georgia. [WSRC-STI-2008-00244 Section 5.2] This is a conservative maximum zone depth for evapotranspiration due to the anticipated capillarity associated with the surficial soil types (i.e., topsoil and upper backfill) and the anticipated root depths.
- “Silting-in” of the 1-foot thick upper lateral drainage layer is assumed to occur due to a percolating water flux of approximately 16 in/yr, containing 63 mg/L colloidal clay. A percolation rate of 16 in/yr into the lateral drainage layer represents an upper end of the background infiltration. A colloidal clay content of 63 mg/L represents an upper end colloidal clay concentration. [WSRC-STI-2008-00244 Section 6.5.1 and Appendix I] This is a conservative approach since it assumes all colloids entering the lateral drainage layer are deposited and accumulated within the drainage layer resulting in a decrease in saturated hydraulic conductivity and lateral drainage over time. It takes no credit for colloid mobilization and flushing from the lateral drainage layer.
- The HELP modeling assumed that the middle backfill was only 12 inches thick, whereas the current SDF closure cap conceptual design has the middle backfill ranging in thickness from a minimum of 12 inches at the closure cap crest to a maximum of 20.6 feet thick at the closure cap side-slopes. This greater thickness indicates that the middle backfill will likely provide significantly more water storage capacity and lateral transport potential than indicated in the current HELP model results thus the overlying surficial layers are less likely to approach saturation.

A discussion is provided below to address potential implications of saturated conditions above the lateral drainage layer for the recommended SDF closure cap configuration.

Stability

Within the conceptualized SDF closure cap, the lateral drainage layer and composite barrier layers are on a 4 % slope. It is possible for head to build-up above the composite barrier layer, if the lateral drainage layer does not adequately drain. As conceptualized, the top slope of the closure cap is at a maximum 1.5 %, and therefore slope stability should not be an issue even with a build-up of head above the composite barrier layer. A significant build-up of head should not be possible within the side slopes due to their slope (i.e., maximum 33.3 % slope). [WSRC-STI-2008-00244 Section 4.2]

As outlined within WSRC-STI-2008-00244 (Section 4.2), the erosion barrier, side slope, and toe of the side slope have been conceptually designed for physical stability per NUREG-1623. These closure cap components have been conceptually designed to prevent any riprap movement during a probable maximum precipitation event. This means that these closure cap components will remain physically stable when subject to the much lower typical historic range of SRS precipitation (i.e., 35 to 72 in/yr) and associated possible head build-up.

As outlined within WSRC-STI-2008-00244 (Section 6.7.1), fully hydrated (i.e., saturated) GCLs can be placed on up to 10 % slopes without the need for internal reinforcement or slope stability analysis. The GCL within the SDF closure cap will be placed on a maximum 4 % slope; therefore, the SDF closure cap GCL is considered physically stable.

Table IEC-7.1 saturations should not negatively impact the physical stability of the closure cap erosion barrier, side slope, toe of the side slope, and GCL.

Vegetation

As outlined within WSRC-STI-2008-00244 (Section 6.2), most plant roots (i.e., grass, herbaceous vine, scrubs, suppressed mixed hardwood, and loblolly pine) will be located within the top 24 inches of the ground surface within the topsoil and upper backfill layers. Deeper roots will be associated with the suppressed mixed hardwoods and loblolly pine. Some of the deeper hardwood and pine roots may penetrate through the backfill and upper lateral drainage layers, and reach the HDPE geomembrane (i.e., 6 feet deep). Only the pines have roots that could potentially extend deeper than the geomembrane; however, deeper roots could only penetrate below the geomembrane in locations of existing geomembrane cracks or holes.

None of the nominal saturations listed in Table IEC-7.1 pose a problem to plant health either in terms of fully saturated conditions (i.e., root drowning) or in terms of wilting point (i.e., inability of plants to extract water). The anticipated root distribution does mean that the actual zone of evapotranspiration will likely extend deeper within the closure cap profile than the 22-inch depth assumed in the HELP modeling. The middle backfill varies in thickness from a minimum 1 foot to greater than 20 feet. It is possible that the evapotranspiration zone depth will extend to the HDPE geomembrane (i.e., 6 feet deep) in areas where the middle backfill is thinnest.

Bamboo could be planted as the final vegetative cover at the end of the 100-year institutional control period, and maintained into the post-closure compliance period until a dense bamboo ground cover has been established over the entire area. [WSRC-STI-2008-00244] Bamboo is a shallow-rooted species, which evapotranspires year-round in the SRS climate, minimizes erosion, and can sustain growth with minimal maintenance. If an alternative cap vegetation strategy, such as use of bamboo as the final vegetation cover were pursued to increase evapotranspiration and reduce the degradation of the GCL, the amount of infiltration through the composite barrier layer would be reduced.

The minimum depth to the lower lateral drainage layer overlying each disposal cell is 13 feet, root penetration is assumed to not exceed 12 feet, therefore, roots are unable to penetrate the lower lateral drainage layer overlying each disposal cell as they may the upper lateral drainage layer in the SDF closure cap (see WSRC-STI-2008-00244 Section 7.4 and Appendix I). The long-term performance of the lower drainage layer is described in the response to RAI IEC-8.

Erosion

As outlined within WSRC-STI-2008-00244 (Section 4.4.13), the soil above the erosion barrier was considered as a SDF closure cap degradation mechanism for modeling purposes. As defined by NUREG-1623, the slope (maximum 1.5 %) and slope-length (maximum 825 feet) of these soil layers has been conceptually designed to prevent the initiation of gully erosion during a probable maximum precipitation event. Also outlined within WSRC-STI-2008-00244 (Section 4.2), the erosion barrier, side slope, and toe of the side slope have been conceptually designed to prevent any riprap movement during a probable maximum precipitation event. The only type of soil erosion applicable to the SDF closure cap is sheet erosion. Therefore, the soil above the erosion barrier will not be subject to significant erosion due to the much lower typical historic range of SRS precipitation (i.e., 35 to 72 in/yr) and associated possible head build-up.

Eight background water balance studies that were conducted in and around SRS were evaluated within WSRC-STI-2008-00244 (Section 3.2). They included both field and modeling studies and ranged in scale from 55-gallon drum lysimeters to entire watersheds. Runoff was seen to range from 0.1 to 4 in/yr with a median of 1.6 in/yr and a mode of 2 in/yr for the eight studies. The estimated runoffs for the proposed SDF closure cap fall within this range of background values (see WSRC-STI-2008-00244 Table 47).

The saturation values, shown in Table IEC-7.1, are typical of SRS surficial soils; thus, since the closure cap has been conceptually designed to resist extreme precipitation events, and the closure cap runoff is typical of background condition, excessive closure cap erosion should be precluded.

Performance of Cover Materials under Hydrostatic Pressure

The conservative assumptions for evaporative zone depth and absence of colloid mobilization and flushing tend to restrict modeled evapotranspiration and lateral drainage from the closure cap, and thus increase infiltration through the composite barrier layer. Therefore, the HELP model infiltration and saturation is expected to be greater than what would occur in the field. Therefore it is unlikely that the upper backfill, erosion barrier, and middle backfill will become saturated by year 5,412, or that geomembrane head increases with time through year 5,412. Concerns relative to the potential impact of the closure cap saturation on stability, vegetation, erosion, and the performance of cover materials under hydrostatic pressure should be minimal.

Utilization of the HELP model provides conservative saturation and infiltration estimates over time, as the upper boundary condition for 2-dimensional PORFLOW SDF vadose zone flow and transport modeling. A long-range program plan for evaluating the long-term performance of the closure cap is being developed to identify additional field/lab testing and identify test methods and equipment (SDF PA Section 8.2). All work in association with the closure cap shall be performed in accordance with the approved drawings, plans, and specifications of the final closure cap design, which will be produced near the end of the operational period.

IEC-8

Comment (New):

The PA should provide a technical basis for the long-term performance of the geotextile filter fabric and the upper and lower lateral drainage layers.

Basis

The geotextile filter fabric and the upper and lower lateral drainage layers significantly limit infiltrating water (e.g., the PORFLOW model files indicate that greater than 99% of the water infiltrating through the closure cap is shed via the lower lateral drainage layer at 8,000 years). Accordingly, the performance of the lateral drainage layers can have a significant effect on the dose as was noted in DOE's response to C-12 (RAI-2009-01).

The performance of these layers is subject to degradation of the filter fabric layer and the subsequent infilling of the porosity within the lateral drainage layer. As stated in WSRC-STI-2008-00244, "sufficient data is not currently available to estimate the service life of the filter fabric" but that "it will degrade due to oxidation and root penetration". Calculations were presented in Appendix I that account for the reduction in hydraulic conductivity of the lateral drainage layer due to the migration of colloidal clay into the lateral drainage layer. However, it is not clear why larger particles (which would decrease the effective lifetime of the lateral drainage layers) were excluded from these calculations, as there is very limited data regarding the service life of filter fabrics and degradation of the filter fabric is likely to result in the conveyance of larger particles. Infilling of the lateral drainage layers with particles larger than colloids may accelerate infilling and result in a more rapid decrease in the hydraulic conductivity of this layer. A decrease in hydraulic conductivity would limit the ability of the lateral drainage layer to shed water, leading to an infiltration rate that is greater than estimated in the PA.

In addition, Figure 4.2-15 in the PA illustrated the change in vertical hydraulic conductivity with respect to time for the lower lateral drainage layer. The PORFLOW model files and Appendix E of SRNL-STI-2009-00115 indicate that vertical hydraulic conductivity of this layer is one order of magnitude greater than stated in the PA.

Path Forward

Due to the risk significance of the lower lateral drainage layer, provide (i) data quantifying the percentage of infiltrating water being shed versus transmitted with respect to time via this layer, (ii) justification for excluding the migration of particles larger than colloids from the overlying backfill materials to the lateral drainage layer, and (iii) support for the long-term performance of this layer. In addition, discuss the apparent discrepancy in the vertical hydraulic conductivity of the lower lateral drainage layer in the PA and the PORFLOW model.

RESPONSE IEC-8:

As described in WSRC-STI-2008-00244 (Section 4.4), a 2-foot thick lower lateral drainage layer will be placed on top of a HDPE geomembrane and GCL over each FDC. The lower lateral drainage layer is on a minimum 2 % slope and terminates approximately 25 feet away from the individual disposal cell perimeter. The overlying lower backfill thickness varies from approximately 5 feet to 30 feet. This design will facilitate drainage off the disposal cell top to the backfill material between and outside disposal cell groups.

The performance of the lower lateral drainage layer is subject to degradation of the filter fabric layer and the subsequent infilling of the porosity within the lateral drainage layer. As shown in

Table IEC-8.1, after approximately 19,000 years the hydraulic conductivity and porosity of the lower drainage layer are estimated to be similar to those for the overlying lower backfill layer. SDF PA Figures 4.2-15 and 4.2-16 illustrate the decrease in the vertical hydraulic conductivity and porosity of the lower drainage layer as it degrades based on analyses described in WSRC-STI-2008-00244 (Section 8.0) and presented in SRNL-STI-2009-00115 (Table 22).

Table IEC-8.1: Hydraulic Parameters for Lower Lateral Drainage Layer

Time Period	Conductivity (cm/sec)	Porosity	Reference
Initially (Sand drainage layer)	5.0E-02 (vertical) 5.0E-02 (horizontal)	0.417	WSRC-STI-2008-00244
After 19,013 years (Backfill)	4.1E-05 (vertical) 7.6E-05 (horizontal)	0.35	SRNL-STI-2009-00115

Tables IEC-8.2 through IEC-8.4 for Vaults 1 and 4 and FDCs, respectively, provide a flow budget from the PORFLOW model for the portion of the lower lateral drainage layer that sits directly above the disposal unit. Table IEC-8.2 has the columns labeled "Percentage of Infiltration through Sand Drain" or the fraction of flow leaving the bottom of the lower lateral drainage layer (and entering the disposal unit) divided by the flow entering the lower lateral drainage layer from the top and "Percentage of Lateral Drainage" or the fraction of flow being drained off laterally divided by the flow entering the lower lateral drainage layer from the top. These two columns sum approximately to one. All results are for Base Case.

Tables IEC-8.2 through IEC-8.4 indicates that the lower lateral drainage layer and the geotextile filter fabric significantly limit infiltrating water. The PORFLOW model files indicate that greater than 99 % of the water infiltrating through the layers of the closure cap is shed via the lower lateral drainage layer beginning after year 300 for Vaults 1 and 4. Note that the flow volume entering the lower lateral drainage layer and drained off laterally above each disposal unit reaches a peak at year 7,500; however, the percentage of lateral drainage is still over 99 % at year 10,000.

Table IEC-8.2: Vault 1 Lower Drainage Layer Darcy Velocity and Flow Budget

Year	Flow Entering Sand Drain Layer (cm/yr/per cm per half-width)	Flow Leaving Bottom of Sand Drain Layer (cm/yr/per cm per half-width)	Flow Drained Off Laterally (cm/yr/per cm per half-width)	Percentage of Infiltration through Sand Drain (%)	Percentage of Lateral Drainage (%)
100	6.57E-03	4.01E-04	6.17E-03	6.10	93.90
200	1.05E-01	2.01E-03	1.03E-01	1.91	98.10
300	3.43E-01	3.22E-03	3.40E-01	0.94	99.07
400	1.14E+00	4.59E-03	1.14E+00	0.40	99.59
500	1.95E+00	5.18E-03	1.94E+00	0.27	99.73
1000	5.38E+00	6.92E-03	5.37E+00	0.13	99.88
2000	1.14E+01	8.66E-03	1.14E+01	0.08	99.94
3200	1.66E+01	1.02E-02	1.66E+01	0.06	99.96
5500	2.61E+01	1.32E-02	2.61E+01	0.05	99.95
7500	2.69E+01	1.55E-02	2.69E+01	0.06	99.95
10000	2.69E+01	1.67E-02	2.69E+01	0.06	99.93

Source Saltstone PORFLOW output files (IEC-8 Support)

Table IEC-8.3: Vault 4 Lower Drainage Layer Darcy Velocity and Flow Budget

Year	Flow Entering Sand Drain Layer (cm/yr/per cm per half-width)	Flow Leaving Bottom of Sand Drain Layer (cm/yr/per cm per half-width)	Flow Drained Off Laterally (cm/yr/per cm per half-width)	Percentage of Infiltration through Sand Drainage Layer (%)	Percentage of Lateral Drainage (%)
100	5.08E-03	4.61E-04	4.62E-03	9.08	90.94
200	8.35E-02	2.33E-03	8.11E-02	2.80	97.18
300	2.78E-01	3.40E-03	2.74E-01	1.23	98.77
400	9.64E-01	4.73E-03	9.59E-01	0.49	99.52
500	1.68E+00	5.79E-03	1.67E+00	0.35	99.64
1,000	4.81E+00	7.42E-03	4.80E+00	0.15	99.86
2,000	1.05E+01	9.53E-03	1.04E+01	0.09	99.90
3,200	1.53E+01	1.13E-02	1.52E+01	0.07	99.91
5,500	2.43E+01	1.50E-02	2.43E+01	0.06	99.95
7,500	2.50E+01	1.76E-02	2.50E+01	0.07	99.93
10,000	2.50E+01	2.51E-02	2.50E+01	0.10	99.89

Source Saltstone PORFLOW output files (IEC-8 Support)

Table IEC-8.4: FDC Lower Drainage Layer Darcy Velocity and Flow Budget

Year	Flow Entering Sand Drainage Layer (cm/yr/radian)	Flow Leaving Bottom of Sand Drainage Layer (cm/yr/radian)	Flow Drained Off Laterally (cm/yr/radian)	Percentage of Infiltration through Sand Drainage Layer (%)	Percentage of Lateral Drainage (%)
100	6.55E-03	1.74E-06	6.55E-03	0.03	100.00
200	1.05E-01	1.13E-04	1.05E-01	0.11	99.89
300	3.42E-01	4.60E-04	3.42E-01	0.13	99.86
400	1.14E+00	1.30E-03	1.14E+00	0.11	99.86
500	1.94E+00	2.06E-03	1.94E+00	0.11	99.90
1000	5.37E+00	4.10E-03	5.37E+00	0.08	99.93
2000	1.14E+01	5.29E-03	1.14E+01	0.05	99.93
3200	1.65E+01	5.96E-03	1.65E+01	0.04	99.95
5500	2.61E+01	6.75E-03	2.61E+01	0.03	99.97
7500	2.68E+01	7.02E-03	2.68E+01	0.03	99.97
10000	2.68E+01	7.34E-03	2.68E+01	0.03	99.97

Source Saltstone PORFLOW output files (IEC-8 Support)

As part of the SDF closure cap, an upper lateral drainage layer will be placed on a 4 % slope over a combined HDPE geomembrane and GCL. The middle backfill, which overlies a 0.1-inch minimum filter fabric, ranges in thickness from a minimum of 12 inches at the closure cap crest to a maximum of 20.6 feet thick at the closure cap side-slopes. The backfill provides significant water storage capacity and the upper lateral drainage layer will be designed to divert infiltrating water away from the underlying disposal cells and transport the water to the perimeter drainage system.

As described in the response to RAI IEC-7, the conservative assumptions utilized within the HELP modeling tend to restrict modeled evapotranspiration and drainage from the upper lateral drainage layer of the closure cap, and increase infiltration through the composite HDPE/GCL barrier layer. Therefore, the HELP model saturation should be greater than what would actually occur in the field. Note that the lower lateral drainage layer and the underlying disposal cell HDPE and GCL layers are not included in the HELP closure cap infiltration modeling. These layers do not extend across the closure cap, therefore, cannot be handled by the HELP model.

Silting-in of the lower lateral drainage layer is assumed to occur similar to that of the upper lateral drainage layer. Eluviation of colloid-sized clays from the overlying backfill and illuviation of the same clays within the underlying lateral drainage layer was assumed to occur, resulting in a decrease in saturated hydraulic conductivity and lateral drainage over time. [WSRC-STI-2008-00244 Section 6.5.1]

While clay migration is not the only mechanism for lateral drainage layer degradation, it is believed to be predominant due to the abundance of clay size particles and the potential to occlude more of the pore spaces within the lateral drainage layers. Migration of larger silt-and/or sand-size particles into the upper and lower lateral drainage layer, as an additional degradation process beyond that of colloidal clay, was not considered for the following reasons.

- The presence of the intact filter fabric is designed to minimize migration of silt- and sand-size particles. For modeling purposes, no credit was taken for the ability of the filter fabric to reduce the migration of colloidal clay to the lateral drainage layers.
- Heterogeneous pore size distribution, the number and shape of pore intersections, and the number of dead-end pores would strain larger silt- and sand-size grains within the backfill layers preventing migration into the lateral drainage layer.
- The conservative nature of the colloidal clay migration and deposition within the lateral drainage layer was assumed to encompass any degradation that might occur due to silt and sand migration.

Silting-in of the lateral drainage layers was assumed to occur due to a percolating water flux containing 63 mg/L colloidal clay. [WSRC-STI-2008-00244 Section 6.5.1] A colloidal clay content of 63 mg/L represents an upper end colloidal clay concentration. Colloid deposition may occur via colloid attachment and/or soil straining (VZJ 3:384-394). The attachment process comprises colloid collision with and attachment to the soil solid phase, resulting in colloid removal from infiltrating water. Straining is the trapping of particles in pore throats that are too small to allow particle passage. As a further conservative measure, it was assumed that the entire colloidal clay flux from the backfill was deposited within the lateral drainage layer, and no credit was taken for colloid mobilization and flushing from each of the drainage layers.

As outlined in WSRC-STI-2008-00244 (Section 5.4.1), the backfill above the lateral drainage layers will consist of onsite soil classified as clayey sands under the Unified Soil Classification System, or as sandy clay loam in the USDA soil textural classification (i.e., textural triangle). On average, typical SRS backfill consists of 3 % gravel, 61 % sand, 10 % silt, and 26 % clay. [WSRC-STI-2008-00244 Table 18]

SRS surficial soils (from which SRS backfill is typically obtained) are highly leached and consist predominately of quartz and kaolinite with a low organic and iron oxide content. [WSRC-STI-2008-00244 Table 19] Soil mineralogy is dominated by quartz at an average mass fraction of 0.93; the clay fraction is dominated by kaolinite at an average mass fraction of 0.84; and the organic content of the soil is very low at an average mass fraction of 0.0022. Iron oxide minerals present in many of the SRS soils give them their distinctive red coloration; however, the iron oxide levels were below the x-ray diffraction detection limits.

As outlined within WSRC-STI-2008-00244 (Section 6.4.1), most plant roots will be located within the top 24 inches of the ground surface (i.e., within the topsoil and upper backfill layers). Some of the deeper hardwood and pine roots may penetrate the filter fabric and the upper lateral drainage layer and reach the underlying HDPE geomembrane (i.e., 6 feet deep). Only the pines have roots that could potentially extend deeper than the geomembrane; however, in reality, deeper roots could only penetrate below the geomembrane in locations of existing geomembrane cracks or holes.

The rate of lower lateral drainage layer degradation is dependent upon the infiltration allowed by the upper lateral drainage layer/composite barrier system. Over time, colloidal clay will migrate with the water-flux from the lower backfill layer through the filter fabric to the underlying 2-foot thick lower lateral drainage layer. Because the lower backfill varies from approximately 5 feet to 30 feet in thickness, the layer will be regarded as providing a limitless volume of colloidal clay to the sand drainage layer while maintaining the same hydraulic conductivity, porosity, and other soil parameters.

The filter fabric layer, located between the overlying backfill and the lower lateral drainage layer, precludes silt- and sand-size particles from moving downward into the drainage layer, thus

prolonging the life of the sand drainage layer. This water-flux driven clay will accumulate in the lower drainage layer from the bottom up. The thickness of the clay filled portion increases with time, while the thickness of the unfilled portion decreases with time, which will result in an overall decrease in the porosity of the drainage layer. The hydraulic conductivity of the clay-filled portion of the drainage layer is reduced from $5.0\text{E-}02$ cm/s to that of the overlying backfill, $4.1\text{E-}05$ cm/s. [WSRC-STI-2008-00244 Section 6.5.1] The minimum depth to the lower lateral drainage layer is 13 feet and root penetration is assumed to not exceed 12 feet; therefore root penetration is not a factor for the filter fabric and lower lateral drainage layer overlying each disposal cell as it is for the upper lateral drainage layer (see WSRC-STI-2008-00244 Section 7.4 and Appendix I).

It is assumed that the filter fabric will disintegrate many years after placement. This could result in some amount of silt along the bottom of the backfill layer migrating into the lateral drainage layers for some distance before being 'strained' by small pore throats. It is not clear if or by how much larger particles would decrease the effective lifetime of the lateral drainage layers. It is believed that the conservative nature of estimating clay accumulation in the sand drainage layer (migration into the lateral drainage layer without any flushing out of the drainage layer) compensates for any potential silt migration. [WSRC-STI-2008-00244 Section 8.1, VZJ 3:384-394]

The risk significance of the geotextile filter fabric and the lateral drainage layers has been evaluated in the response to RAI PA-10 and found to be highly dependent on the hydraulic parameters of the disposal unit concrete and the saltstone grout. Please refer to the response to RAI PA-10 for further details.

The apparent discrepancy in the vertical hydraulic conductivity of the lower lateral drainage layer in the SDF PA and the PORFLOW model is explained in the response to RAI C-22. Figure C-22.1 in the response to RAI C-22 illustrates the vertical hydraulic conductivity based on the analytical solution and the PORFLOW input values.

In the current PA analysis the saturated hydraulic conductivity was determined using course time-stepping at later years (see SDF PA Figure 4.2-15). Without changing the drainage layer degradation process, as a modeling improvement, the Alternative Sensitivity Case K, described in detail in the response to RAI PA-8, applies more discrete time steps to better capture the significant changes to the drainage layer performance.

Further work described in the SDF PA Section 8.2 recognizes the importance of understanding and modeling of the lateral drainage layers and the long-term performance of the engineering cap as an infiltration barrier. Long-range program plans for evaluating the plugging rate of the lower lateral drainage layer and the long-term performance of the closure cap may be developed as part of the PA maintenance activities (SRR-CWDA-2011-00052 Table C.1-1) to identify additional field/lab testing and to identify test methods and equipment.

Saltstone Performance (SP)

SP-1

Comment:

Additional justification is required for the assumption that saltstone is hydraulically undegraded for 20,000 years.

DOE Response Discussion:

The DOE response focused on on-going research for overall assessment of degradation and in the case of sulfate attack, short-term experimental measurements that have been completed. The DOE response did not specifically address the NRC comments that had been replicated from a previous review on the expansive phase report.

The PA has to account for what is known and conservatively include the impact of uncertainties that are not yet fully understood. Considering the ongoing research, NRC staff believes it is optimistic to assume no hydraulic degradation over 20,000 years. The effects of degradation are evaluated in sensitivity cases, but the conservatism of those cases is unclear. Because the effects are included in a sensitivity case and not in the compliance case, it means the effects are not included in the case used to demonstrate compliance with the performance objectives.

The DOE response focused on sulfate attack whereas NRC was interested in a basis for neglecting degradation via all mechanisms. For example, the disposal facilities have embedded steel, some of which is exposed to the atmosphere now or will be exposed to the soil after facility closure. Much of that steel can be seen today to have already experienced corrosion. It is unrealistic to assume that the carbon steel will experience no corrosion. Corrosion of the steel would cause disruption of the surrounding concrete or saltstone.

Previous NRC comments on the expansive phase report to which DOE deferred a response include the following:

- 1) The conclusions of the expansive phase precipitation report are based on geochemical modeling results. It is unclear whether there are data and observations available for comparison to constrain the modeling calculations.
- 2) The expansive phase study does not consider the effects of organic additives or pozzolanic replacement on the dissolution and precipitation of cement-related compounds, which may have an effect on the generation of expansive phases. Future research could consider the effect that sulfide from the blast furnace slag might have on the phases and reactions present in this system.
- 3) Experiments that are designed to collect data on initial mineralogical conditions, fundamental thermodynamic data and reaction kinetics would provide much needed model support for this study.
- 4) Geochemist's Workbench is based on an equilibrium reaction model. However, reaction kinetics could result in metastable products that are often associated with an increase in volume. Subsequent studies might consider expansive phases produced by intermediate or metastable reaction products.
- 5) The conclusions reached in this study area could be integrated with other ongoing or recently completed studies. Dixon (SRNL-STI-2008-00421) recently completed a study on the physical properties of grout, which included bulk porosity measurements.

Updated measurements of the bulk porosity of saltstone grout may be useful in assessing whether expansive phase precipitation is likely to result in grout degradation.

Path Forward

Provide additional basis for assuming no hydraulic degradation of saltstone occurs in the base case or provide an updated base case analysis that reflects estimated saltstone hydraulic degradation (e.g., changes in hydraulic conductivity and effective diffusivity). Specifically, address the comments on the expansive phase report and additional degradation mechanisms. Provide model support for the long-term performance of saltstone and reinforced concrete.

RESPONSE SP-1:

As described in the original response to SP-1, additional research into saltstone material degradation is planned and on-going, as noted in item 2 of Table 8.2-1 in the SDF PA and Table C.1-1 of SRR-CWDA-2011-00052. The first phase of the long-range testing has been completed and is documented in SRNS-STI-2009-00477. The research is meant to take the next step, after the initial expansive phase work documented in WSRC-STI-2008-00236, in understanding the potential degradation mechanisms and degradation rates for saltstone. The results reported in SRNS-STI-2009-00477 were based on a simulant that did not conform with the saltstone grout composition being processed at the SPF. New testing is being performed with the SPF composition and the most recent results are reported in SRNL-STI-2010-00515. SRNL-STI-2010-00515 reports that the simulant material using the SPF composition has a higher compressive strength and about 100 times lower porosity, tortuosity, effective diffusion coefficient, and water permeability than the previous saltstone simulant tested and reported in SRNS-STI-2009-00477. Laboratory testing performed on saltstone wasteform simulates and a comparison to model predictions from the STADIUM computer code is described in SRNS-STI-2009-00477. The testing indicated that “the durability (stability) of the saltstone matrix upon immersion in water was found to be better than that of Portland cement paste with a similar water to cement ratio and a lower total porosity.” The testing also indicated that the code predictions for cement leach rates were similar to actual tested materials for the short duration of exposure in the report. While the leached zone did not show any obvious signs of degradation, additional work is planned and ongoing for longer exposure times and research into the physical signs of degradation and degradation properties for longer exposure times. Leach testing on the latest saltstone simulant is in progress by SIMCO personnel and the decalcification rate for this material is expected to be lower than that of the previous simulate tested because of the more tortuous and less porous microstructure of this latest simulant.

The physical testing is meant to provide assurance that any long-term code predictions of material conditions are reasonable resulting in “best estimation” or “most probable” values. The testing also provides physical data and laboratory observations that can be compared to field-scale physical properties (e.g., hydraulic conductivity, effective diffusivity) of as-emplaced saltstone to inform any future modeling, and provides a means to study the impacts of multiple potential degradation mechanisms such as those noted in the basis section of this comment.

In regards to Basis Items 1, 2, and 3, as described in SRNS-STI-2009-00477 and as noted in item 2 of Table 8.2-1 in the SDF PA and Table C.1-1 of the PA maintenance plan, additional data and observations into saltstone material degradation and the effects of the addition of pozzolans and organics to the cement is planned and on-going, which should support the expansive phase precipitation report.

As noted in Basis Item 4, *The Geochemist’s Workbench* is based on an equilibrium reaction model. The calculations were based on thermodynamic equilibrium, and kinetics were not

considered. Reaction kinetics could result in metastable products that for a short period of time are associated with an increase in volume. The equilibrium model creates some uncertainty, which can be constrained as follow-on studies to consider expansive phases produced by intermediate or metastable reaction products.

As noted in Basis Item 5 above, SRNL-STI-2008-00421 has been issued which evaluated the porosity of various saltstone samples. The 90-day cured porosities were 0.55, 0.59, and 0.59 for DDA, ARP/MCU, and SWPF stimulant mixes, respectively. The porosity of the simulant based on the SPF composition is reported in SRNL-STI-2010-00515 to be 0.603. These values all exceed the value of 0.46 utilized in WSRC-STI-2008-00236 and further support the conclusion that expansive phase degradation is unlikely.

Concrete degradation is dominated by internal sulfate attack from the saltstone; however, reinforced concrete structures are susceptible to other degradation mechanisms depending on environment. Other degradation mechanisms potentially observed in concrete structures include cracking from seismic events, settlement, and external static loading; carbonation or chloride ingress induced rebar corrosion; alkali-silica reactions; calcium leaching; and freeze thaw.

Degradation analyses on existing aging concrete structures at SRS, described in the response to RAI VP-2, have provided data for use in the evaluation of potential degradation mechanisms for the cement and embedded steel. The concrete degradation mechanisms considered are not expected to exceed the effect of sulfate attack from saltstone constituents within the vaults. Therefore, although they may contribute to the degradation of the concrete and embedded steel of the vaults and FDCs, they will not result in a large-scale difference in degradation rate from the current degradation model of the structure.

To supplement the original response to SP-1, and provide model support for the long-term performance of saltstone and reinforced concrete, Alternative Sensitivity Case K, a non-mechanistic modeling case, has been developed to further inform of the impact on dose due to deviations from the Base Case. Case K has been developed as a supplement to the Probabilistic Analyses (which also considers multiple assumptions and non-mechanistic modeling cases, but in addition assigns probabilities).

Alternative Sensitivity Case K should not be construed as representing an expected physical reality, but instead reflects a modeling tool for informing the impact when select barriers of concern were modified simultaneously and for investigating uncertainty. In Case K, complete degradation of all cementitious material occurs within the first 10,000 years following closure with degraded saltstone having a saturated hydraulic conductivity of $1.0\text{E-}06$ cm/sec and an effective diffusion coefficient of $5.0\text{E-}06$ cm²/sec using a semi-log relationship. For Case K, the cementitious materials are conservatively assumed to degrade such that the final hydraulic conductivity is on the same order of magnitude as the surrounding unsaturated soil.

The results of Case K indicate the peak dose to the MOP within the 10,000-year period of performance is 13.0 mrem/yr at year 8,720 in Sector I. This is less than the 25 mrem/yr performance objectives (10 CFR 61.41). Even given the very pessimistic, non-mechanistic assumption of premature cementitious degradation, the peak dose to the MOP does not exceed 25 mrem/yr within 10,000 years. See response to RAI PA-8 for further details and summaries of Alternative Sensitivity Case K modeling results.

SP-2

Comment:

A basis is required for the modeled extent of saltstone fracturing.

DOE Response Discussion:

The DOE response referenced Case C as including cracks. DOE indicated that the sensitivity studies provide information regarding the effect of crack variability.

NRC does not believe that the impact of cracking on the PA results is adequately captured by Case C, sensitivity analyses that address increased hydraulic conductivity, or alternate configurations such as Case E as currently represented. The references provided (T-CLC-Z-00006; SRNL-STI-2009-00115, Rev. 1) address cracking mechanisms for Vault 4 due to differential settlement and seismic events. Case C is intended to capture the impact of transverse structural cracks through saltstone caused by these mechanisms. However, a basis is not provided to extend the mechanisms responsible for Vault 4 cracking to saltstone and address fracture mechanisms that are unique to saltstone. Cracking of saltstone has been observed (SRNL-ESB-2008-00017) and the uncertainty and variability in (i) cracking (e.g., number of cracks, crack spacing, crack orientation, crack length, crack aperture, etc.) and (ii) crack evolution (e.g., acceleration of cracking) has not been evaluated. Therefore, it is expected that two longitudinal cracks do not adequately reflect the uncertainty associated with the extent or effects of potential cracking.

Sensitivity analyses with increased hydraulic conductivity do not evaluate the full matrix of the potential effects of cracks. For example, changes to the surface-area-to-volume ratio, which is dependent on crack representation, is not captured by varying the hydraulic conductivity. Removal of radionuclides and leaching of cementitious materials, which can lead to additional fracturing, is strongly correlated to the surface-area-to-volume ratio.

In addition, results from sensitivity analyses with increased hydraulic conductivity and Case E are inconclusive due to the moisture characteristic curves applied in the PA (see Comments SP-3 and SP-4).

Path Forward

Provide a basis for the extent of fracturing included in the base case representation. Demonstrate how the base case model appropriately represents current observations with respect to cracks. Address the mechanisms noted above as well as other mechanisms by which fractures could increase the rate of subsequent fracturing.

RESPONSE SP-2:

The observation of "saltstone cracking" reported in SRNL-ESB-2008-00017 does not imply that such cracking is indicative of cracking throughout the saltstone monolith. Recent observations, reported in SRR-CWDA-2011-00105, review video inspections of the saltstone monolith surface. This report describes surface cracking in the operational clean layer of multiple cells, but gives no indication that any of these cracks extend beyond the surface of the monolith. None of the surface cracks described was an aperture crack, and all observed cracks occurred in the clean grout layer used as an operational shielding measure. A similar report, SRR-CWDA-2011-00097, indicates that there was no evidence of concrete cracking around the anchor bolt penetrations in Vault 4 that are used to keep the drainwater collection piping anchored to the cell floor and no evidence of void spaces at the threads of the anchor bolts. Further observations of saltstone conditions will be provided as they become available.

An Alternative Sensitivity Case is presented in the response to RAI PA-8 which evaluates a non-mechanistic model approach to a degraded saltstone condition (i.e., the alternative sensitivity case imposes modeling assumptions without regard for the cause of such assumptions). The specifics of the degradation analysis of saltstone can be found in the response to RAI PA-8. In summary, the saltstone is assumed to degrade with a semi-logarithmic relationship with time so that within 10,000 years after closure the saltstone has a hydraulic conductivity (at all suction levels) of $1.0\text{E-}06$ cm/sec and a diffusivity of $5.0\text{E-}06$ cm²/sec, which are similar to soil conditions. In addition, fracture spacing within the saltstone monolith is assumed to occur in a semi-logarithmic relationship with time so that within 10,000 years after closure the saltstone monolith has a final fracture spacing of 10 centimeters at its fully degraded condition. This fracture spacing is utilized to simulate a shrinking core model for the release of technetium as the reducing capacity of the saltstone is depleted via oxidation. As indicated in the response to RAI PA-8, this degree of degradation to the saltstone grout is considered unlikely to occur within the 10,000-year performance period.

The results of the Alternative Sensitivity Case indicate the peak dose to the MOP within the 10,000-year period of performance is 13.0 mrem/yr at year 8,720 in Sector I. This is less than the 25 mrem/yr performance objectives (10 CFR 61.41). Even given the very pessimistic, non-mechanistic assumption of premature cementitious degradation, the peak dose to the MOP does not exceed 25 mrem/yr until 13,390 years after system closure. See response to RAI PA-8 for further details and summaries of Alternative Sensitivity Case K modeling results.

SP-3

Comment:

The moisture characteristic curve for intact saltstone implemented in the PORFLOW model does not sufficiently account for experimental uncertainties and is inconsistent with literature results for material similar to saltstone and other cementitious materials.

DOE Response Discussion:

The DOE agreed in their response that the moisture characteristic curve based on the INL dataset is somewhat inconsistent with literature (WSRC-STI-2007-00649). To evaluate the impact of using a modified moisture characteristic curve, the base case was rerun in PORFLOW with the relative permeability set to 1.0. The resulting contaminant release rate was approximately twice that of the base case for Vault 2 during the compliance period. For Vault 4, with the relative permeability equal to 1.0, the release rate of Tc-99 was almost doubled, while the I-129 and Ra-226 rates were each less than a 30% increase over the base case. DOE stated that these increases in release rates would not significantly impact the resulting dose to the MOP during the compliance period.

Increases in contaminant release rates of 30% and 100% for one-off sensitivity analyses may result in an insignificant increase in base case dose on an absolute basis (i.e. if the base case dose is small). However, when (i) many uncertainties exist, (ii) the margin between compliance and the base case dose is not very large, and (iii) it is not clear how all of these uncertainties are related, then the resultant dose from the inclusion of these outstanding uncertainties could be significant on a cumulative basis even if the increases for individual one-off analyses are insignificant on an absolute basis.

Path Forward

If adequate justification is not available for the moisture characteristic curves implemented in the PA model for intact saltstone, provide updated results for Case A, B, C, D, the synergistic case, and the sensitivity case in Section 5.6.6.7 that use a characteristic curve for intact saltstone that is more consistent with results in the literature.

RESPONSE SP-3:

As indicated in the initial response to this RAI, DOE acknowledged that the moisture characteristic curves used for intact saltstone were based on a limited moisture retention dataset provided in WSRC-STI-2006-00198. Subsequent testing, documented in SRNL-STI-2009-00419, has developed a new relative permeability curve for saltstone. This new relative permeability curve was also provided in the initial response to this RAI. However, to conservatively assess the hydraulic performance of saltstone, a relative permeability of one was used to evaluate the impact of assuming a constant saturated hydraulic conductivity for the Base Case at all suction levels. The results of this analysis were presented in the initial response to this RAI. The results indicated that the fluxes of the major dose contributing radionuclides from Vault 4 and from an FDC were not significantly impacted. A similar analysis was conducted in the initial response to RAI VP-2 and the results provided in the initial response to RAI VP-2 also indicated that the fluxes of the major dose contributing radionuclides from Vault 4 and from an FDC were not significantly impacted.

Rather than providing revised dose analyses for the cases analyzed in the SDF PA, a single, more comprehensive analysis enveloping other model parameters discussed within this RAI package has been developed. This more comprehensive analysis is described in the response to RAI PA-8 and is identified as Alternative Sensitivity Case K. Alternative Sensitivity Case K addresses concerns raised in other RAIs in this package related to saltstone performance, disposal unit concrete performance, inventory assessments, and updated K_d values. Dose results from Alternative Sensitivity Case K are based on the revised dose methodology and associated parameters presented in the responses to RAIs B-1, B-2, B-3, and B-4. Alternative Sensitivity Case K assumes all cementitious materials degrade to soil conditions within 10,000 years (3,500 years for the roof of Vaults 1 and 4) and moisture characteristic curves are not utilized. Rather, for all cementitious material, including saltstone, relative permeability, and saturation are set equal to one for all suction levels.

The resulting doses to the MOP, presented in the response to RAI PA-8, are less than the performance objectives for this very pessimistic Alternative Sensitivity Case K. This indicates that even with a relative permeability of one, which assumes fully saturated flow conditions at all suction levels the performance objectives are met.

SP-4

Comment:

Characteristic curves implemented in the PA are based on a continuum approach that does not reflect non-equilibrium flow.

DOE Response Discussion:

The DOE response discussed the effects of transient flow on contaminant leaching. However, NRC staff's concern is the inability of a continuum approach to represent unsaturated flow through porous or fractured media. Unsaturated flow is characterized by non-equilibrium, gravity-driven fingering that can lead to pulsating flow conditions, even in the presence of a steady state infiltration boundary condition (Pruess et al., 1999). Abstraction of unsaturated flow with moisture characteristic curves cannot replicate this flow behavior. Equilibrium flow through unsaturated media can significantly underestimate actual flow rates through a system.

Path Forward

Provide additional model support for unsaturated flow. Model support could include analogs, laboratory experiments, and/or field studies that verify consistency between numerical results and physical measurements. Alternatively, demonstrate that non-equilibrium flow through porous and fractured media does not significantly affect the performance of the system.

RESPONSE SP-4:

The DOE is aware of literature investigating the impacts of non-steady / episodic conditions on infiltration through fractured media, and alternative functional forms for characteristic curves such as the *An active fracture model for unsaturated flow and transport in fractured rocks* (DOI: 10.1029/98WR02040). While acknowledging the possibility of higher Darcy velocities with alternative water transport models, all else being equal, the DOE believes hydraulic degradation assumptions introduce more significant variability in overall system performance than the potential uncertainty associated with non-equilibrium flow. In the Alternative Sensitivity Case K, described in the response to RAI PA-8, the hydraulic performance of the saltstone and disposal unit concrete is severely degraded such that any impact on flow associated with non-equilibrium flow is expected to be inconsequential to the total flow associated with this degraded closure system. As described in the response to RAI PA-8, all cementitious materials are assumed to degrade to hydraulic conditions similar to soil with an assumed relative permeability of one at all suction levels. The resulting doses to the MOP, presented in the response to RAI PA-8, are less than the performance objectives even for this very pessimistic analysis.

SP-5

Comment:

Additional support is needed for the hydraulic conductivity of intact saltstone that is used in Case A, Case B, Case C, Case D and the synergistic case.

DOE Response Discussion:

The DOE response indicated that additional testing of hydraulic and physical properties has continued to be performed and provided a summary of additional test results. DOE indicated that the baseline test results yielded values of 1.3E-9 to 4.0E-9 cm/s which was consistent with the base case value of 2E-9 cm/s used in the PA. They also indicated that sensitivity analyses were performed to examine the impact of a much higher hydraulic conductivity, and the estimated doses were much less than 25 mrem/yr. The DOE response did not address the monitoring follow-up items provided in the original comment pertaining to the measurement of hydraulic properties. The original comment requested justification for logarithmic averaging of the hydraulic conductivity values for the limited data set with an unknown distribution, which was not provided.

Ongoing tests are helpful and fill some important data gaps, but the tests do not capture the full range of conditions that can be expected for actual emplaced saltstone. The test results provided in the comment response have values as large as 9E-9 cm/s for the impact of water to premix ratio and as high as 9E-7 cm/s for a baseline composition with organics, admixtures, and a 60°C cure temperature. Depending on the composition and curing temperature of saltstone, these values could arguably be representative of a reasonable starting point for a base case value. These measurements highlight the need to be conservative when selecting a base case deterministic value for a key parameter such as hydraulic conductivity. As DOE has collected additional measurements, the hydraulic property values have been consistently revised higher. In addition, these hydraulic tests are on laboratory prepared samples which do not account for (i) scale, (ii) emplacement (batching, pumping, curing), (iii) CO₂ contamination, and (iv) permeability evolution.

Path Forward

Provide adequate support for the hydraulic conductivity value that is implemented in the base case for the PA for intact saltstone. Additional support should include a description of how data from laboratory samples is scaled to represent full-scale, as-emplaced saltstone. Additional support should also address the specific analytical concerns raised in the original comment, including the potential impact of atmospheric CO₂ on the results. Provide justification for the logarithmic averaging of hydraulic conductivity for a limited data set or provide additional data to characterize the distribution.

RESPONSE SP-5:

In response to this RAI, saturated hydraulic conductivity data obtained from testing of saltstone simulants, conducted at the time of PA development and later, is provided below and followed by responses to specific questions presented in the RAI.

Simulant testing data for saturated hydraulic conductivity is obtained from the following:

- WSRC-STI-2007-00649, *Hydraulic and Physical Properties of MCU Saltstone*, issued March 2008, during SDF PA development
- SRNL-STI-2008-00421, *Hydraulic and Physical Properties of Saltstone Grouts and Vault Concretes*, issued November 2008, during SDF PA development
- SRNL-STI-2009-00419, *Hydraulic and Physical Properties of ARP/MCU Saltstone Grout*, issued May 2010, after SDF PA issuance

Table SP-5.1 provides the grout mix recipes for ARP/MCU, which simulated saltstone grout without additional admixtures or organics: MCU-1 from SRNL-STI-2008-00421, Batch 2 (60 % water to premix ratio), Batch 6 (55 % water to premix ratio) and Batch 7 (65 % water to premix ratio) from SRNL-STI-2009-00419. Table SP-5.2 provides the measured saturated hydraulic conductivity reported for these grout mixes. All results are reported for samples with a minimum curing time of 90 days. The arithmetic average of the data in Table SP-5.2 is 3.2E-9 cm/sec and the logarithmic average is 1.9E-9 cm/sec. Figure SP-5.1 illustrates graphically the measured hydraulic conductivity values reported in Table SP-5.2.

Table SP-5.1: Saltstone ARP/MCU Simulant Grout Mixes Tested Without CSSX Solvent and Admixtures

Ingredient	MCU-1 (Note a)	Batch 2 (Note b)	Batch 6 (Note b)	Batch 7 (Note b)
Premix (pm), (mass fraction)				
Type II Portland Cement	0.10	0.10	0.10	0.10
Grade 100 B F S	0.45	0.45	0.45	0.45
Class F Fly Ash	0.45	0.45	0.45	0.45
Salt Solution				
Sodium Hydroxide mol/L	1.594	1.594	1.594	1.594
Sodium Nitrate, mol/L	3.159	2.996	2.996	2.996
Sodium Nitrite, mol/L	0.368	0.368	0.368	0.368
Sodium Carbonate, mol/L	0.176	0.176	0.176	0.176
Sodium Sulfate, mol/L	0.059	0.059	0.059	0.059
Aluminum Nitrate, mol/L	0.054	0.054	0.054	0.054
Sodium Phosphate, mol/L	0.012	0.012	0.012	0.012
Water / premix ratio (mass fraction)	0.60	0.60	0.55	0.65
CSSX solvent, μ L/1600g	none	none	none	none
Admixtures, mass fraction	none	none	none	none

Note a: Tables 1 and 3 of SRNL-STI-2008-00421

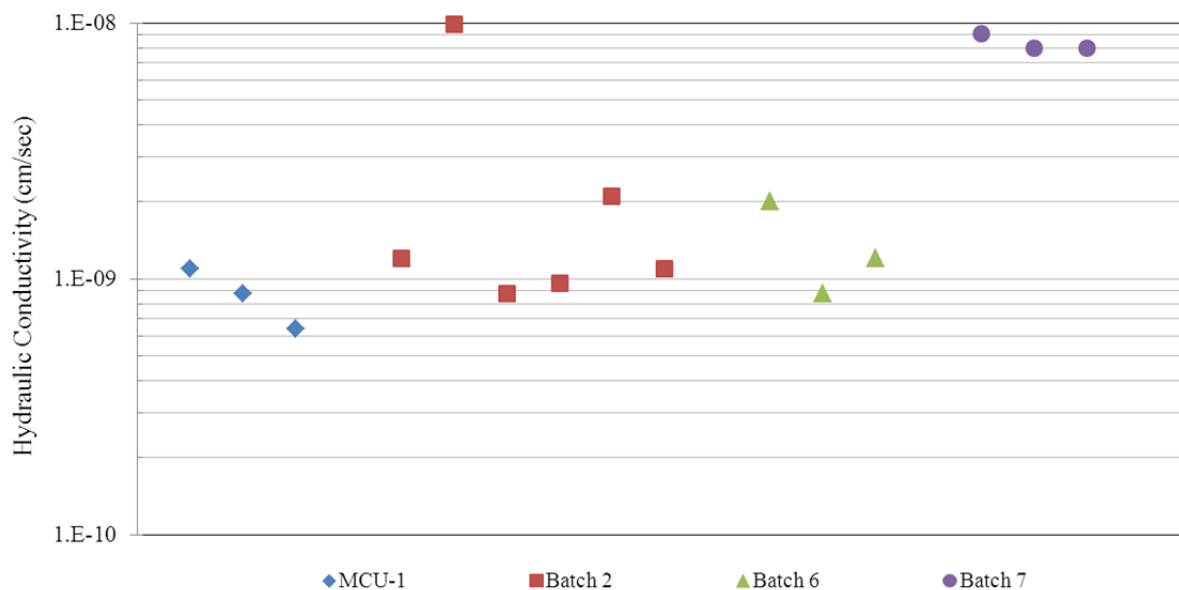
Note b: Tables 1, 2, and 4 of SRNL-STI-2009-00419

Table SP-5.2: Measured Saturated Hydraulic Conductivity for ARP/MCU Simulated Saltstone Grout with Varying Water to Premix Ratio

Grout Mix	Sample ID	Hydraulic Conductivity (cm/sec)	Notes
MCU-1	TR437-1	1.1 E-09	(1)
MCU-1	TR437-2	8.8 E-10	(1)
MCU-1	TR437-3	6.4 E-10	(1)
Batch 2	TR547-1	1.2E-09	(2)
Batch 2	TR547-2	9.9E-09	(2)
Batch 2	TR547-3	8.8E-10	(2)
Batch 2	TR548-1	9.6E-10	(2)
Batch 2	TR548-2	2.1E-09	(2)
Batch 2	TR548-3	1.1E-09	(2)
Batch 6	TR575-1	2.0E-09	(2)
Batch 6	TR575-2	8.8E-10	(2)
Batch 6	TR575-3	1.2E-09	(2)
Batch 7	TR577-1	9.1E-09	(2)
Batch 7	TR577-2	8.0E-09	(2)
Batch 7	TR577-3	8.0E-09	(2)

- (1) SRNL-STI-2008-00421, Table 20
(2) SRNL-STI-2009-00419, Table 9

Figure SP-5.1: Graphical Presentation of Data from Table SP-5.2



Grout recipes MCU-2 (from WSRC-STI-2007-00649) and Batch 4 (from SRNL-STI-2009-00419) simulate ARP/MCU grout associated with the CSSX process with no admixtures. Grout recipe Batch 5 (from SRNL-STI-2009-00419) simulates ARP/MCU grout associated with the CSSX process with admixtures. Grout recipe Batch 3 (from SRNL-STI-2009-00419) simulates ARP/MCU grout with only admixtures. Grout recipe Batch 11 (from SRNL-STI-2009-00419) is the same as Batch 5 except testing on Batch 11 occurred after the batch was cured inside an oven at an elevated external temperature of 60°C rather than at the nominal 22°C. Table SP-5.4 provides the measured saturated hydraulic conductivity reported for these grout mixes. Results reported from WSRC-STI-2007-00649 (grout mix MCU-2) are based on samples with a minimum curing time of 28 days; while a minimum curing time of 90 days is associated with the remaining results from SRNL-STI-2009-00419. The arithmetic average of the data in Table SP-5.4 (excluding MCU-2 and Batch 11) is 1.4E-9 cm/sec and the logarithmic average is also 1.4E-9 cm/sec. Figure SP-5.2 illustrates graphically the measured saturated hydraulic conductivity values reported in Table SP-5.4.

Table SP-5.3: Saltstone Simulant ARP/MCU Grout Mixes Tested With CSSX Solvent and Admixtures

Ingredient	MCU-2 (Note a)	Batch 3 (Note b)	Batch 4 (Note b)	Batch 5 (Note b)	Batch 11 (Notes b, c)
Premix (pm), (mass fraction					
Type II Portland Cement	0.10	0.10	0.10	0.10	0.10
Grade 100 B F S	0.45	0.45	0.45	0.45	0.45
Class F Fly Ash	0.45	0.45	0.45	0.45	0.45
Salt Solution					
Sodium Hydroxide mol/L	1.59	1.594	1.594	1.594	1.594
Sodium Nitrate, mol/L	3.16	2.996	2.996	2.996	2.996
Sodium Nitrite, mol/L	0.37	0.368	0.368	0.368	0.368
Sodium Carbonate, mol/L	0.18	0.176	0.176	0.176	0.176
Sodium Sulfate, mol/L	0.06	0.059	0.059	0.059	0.059
Aluminum Nitrate, mol/L	0.05	0.054	0.054	0.054	0.054
Sodium Phosphate, mol/L	0.01	0.012	0.012	0.012	0.012
Water/premix ratio (mass fraction	0.60	0.60	0.60	0.60	0.60
CSSX solvent, µL/1600g	100	none	100	100	100
Admixtures, mass fraction	none	0.01	none	0.01	0.01

Note a Section 3.1, Tables 1 and 2, and Appendix A of WSRC-STI-2007-00649

Note b Tables 1, 2, 3, and 4 of SRNL-STI-2009-00419

Note c Same recipe as Batch 5 but cured at 60°C rather than 22°C

Table SP-5.4: Measured Saturated Hydraulic Conductivity for ARP/MCU Simulant Saltstone Grout with Organics and Admixtures

Grout Mix	Sample ID	Hydraulic Conductivity (cm/sec)	Notes
MCU-2	SLT003	1.5 E-08	(1)
MCU-2	SLT004	5.3 E-09	(1)
Batch 3	TR549-1	2.1 E-09	(2)
Batch 3	TR549-2	1.5 E-09	(2)
Batch 3	TR549-3	1.1 E-09	(2)
Batch 4	TR557-1	1.2 E-09	(2)
Batch 4	TR557-2	1.8 E-09	(2)
Batch 4	TR557-3	1.3 E-09	(2)
Batch 5	TR565-1	8.4 E-10	(2)
Batch 5	TR565-2	1.4 E-09	(2)
Batch 5	TR565-3	1.6 E-09	(2)
Batch 11	TR604-1	8.0 E-07	(2), (3)
Batch 11	TR604-2	8.6 E-07	(2), (3)
Batch 11	TR604-3	7.5 E-07	(2), (3)

- (1) WSRC-STI-2007-00649, Table 4; SLT003 permeated with simulated groundwater equilibrated with vault concrete and SLT004 permeated with simulated saltstone pore water, both with a minimum curing time of 28 days.
(2) SRNL-STI-2009-00419, Table 9, with a minimum curing time of 90 days.
(3) Cured at an elevated oven temperature of 60°C.

Figure SP-5.2: Graphical Presentation of Data from Table SP-5.4

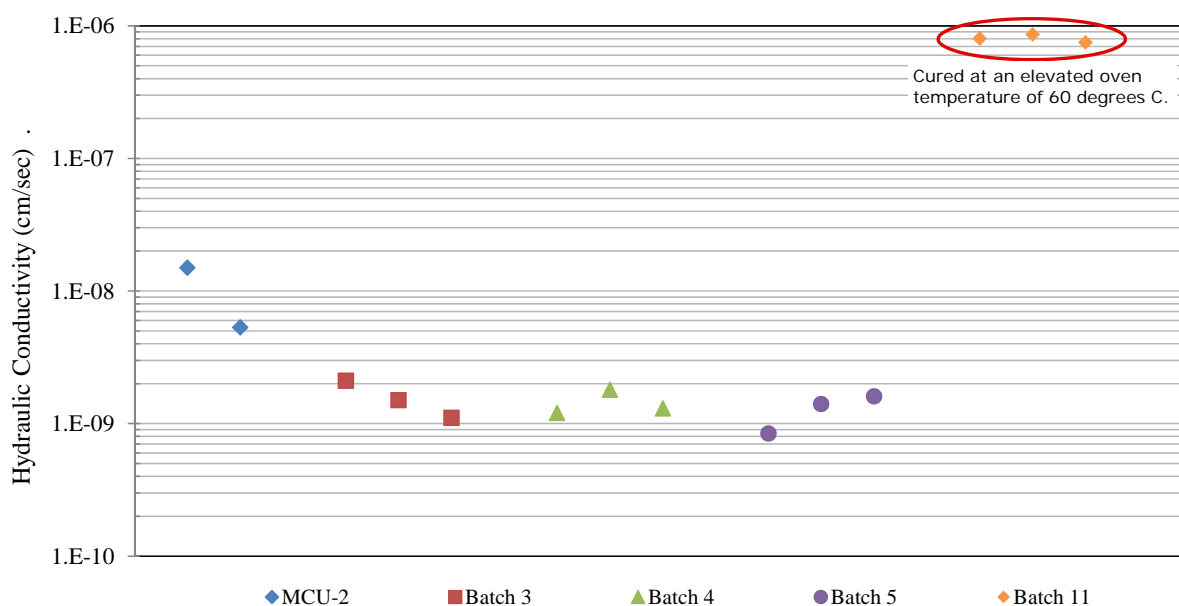


Table SP-5.5 provides ARP/MCU simulated saltstone grout mix recipes from SRNL-STI-2009-00419 which have an elevated aluminate concentration and a 55 % water to premix ratio (Batch 8), a 65 % water to premix ratio (Batch 9), and at the nominal 60 % water to premix ratio but with CSSX solvent and admixtures (Batch 10). Also included in Table SP-5.5 is the grout mix recipe for DDA and for SWPF simulated saltstone grout mixes from SRNL-STI-2008-00421. Table SP-5.6 provides the measured saturated hydraulic conductivity reported for these grout mixes. All results are reported for samples with a minimum curing time of 90 days. The arithmetic average of the data in Table SP-5.6 (excluding sample TR451-3) is 5.8E-10 cm/sec and the logarithmic average is 3.0E-10 cm/sec. Figure SP-5.3 illustrates graphically the measured saturated hydraulic conductivity values reported in Table SP-5.6.

Table SP-5.5: Additional Saltstone Simulant Grout Mixes Tested

Ingredient	Batch 8 (Note a)	Batch 9 (Note a)	Batch 10 (Note b)	DDA (Note c)	SWPF (Note d)
Premix (pm), mass fraction					
Type II Portland Cement	0.10	0.10	0.10	0.10	0.10
Grade 100 B F S	0.45	0.45	0.45	0.45	0.45
Class F Fly Ash	0.45	0.45	0.45	0.45	0.45
Salt Solution					
Sodium Hydroxide mol/L	2.497	2.497	2.497	0.769	2.866
Sodium Nitrate, mol/L	2.319	2.319	2.319	2.202	1.973
Sodium Nitrite, mol/L	0.368	0.368	0.368	0.110	0.485
Sodium Carbonate, mol/L	0.176	0.176	0.176	0.145	0.118
Sodium Sulfate, mol/L	0.059	0.059	0.059	0.044	0.055
Aluminum Nitrate, mol/L	0.280	0.280	0.280	0.071	0.114
Sodium Phosphate, mol/L	0.012	0.012	0.012	0.008	0.007
Water / premix ratio (mass fraction)	0.55	0.65	0.60	0.60	0.60
CSSX solvent, $\mu\text{L}/1,600\text{ g}$	none	none	100	none	none
Admixtures, mass fraction	none	none	0.01	none	none

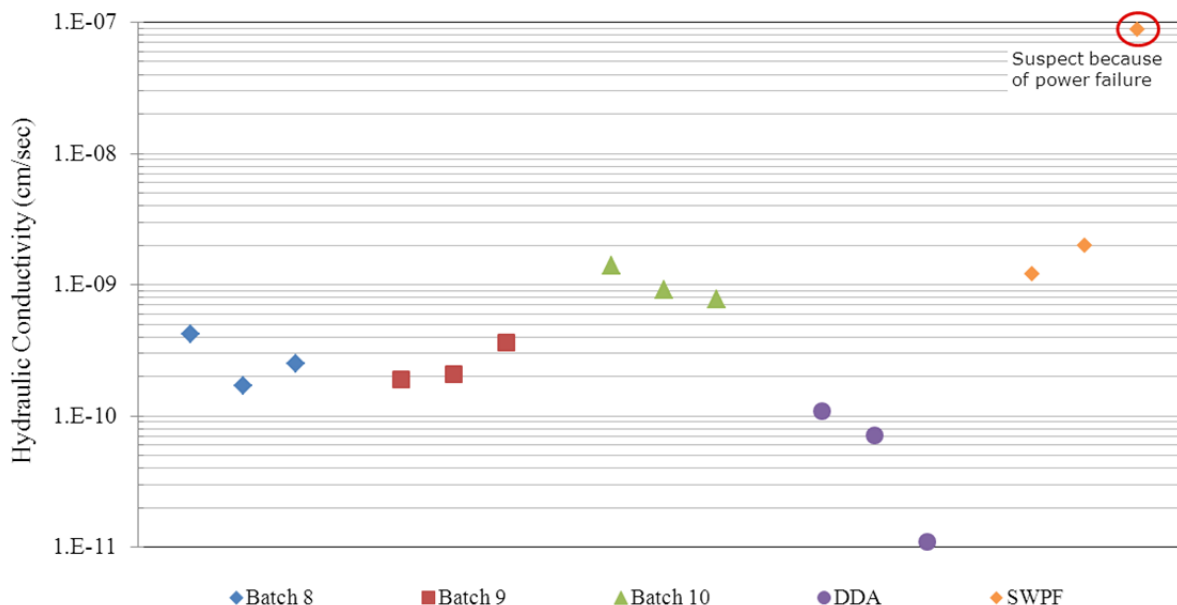
Note a Tables 1, 2, and 5 of SRNL-STI-2009-00419
 Note b Tables 1, 2, 3, and 5 of SRNL-STI-2009-00419
 Note c Tables 1 and 2 of SRNL-STI-2008-00421
 Note d Tables 1 and 4 of SRNL-STI-2008-00421

Table SP-5.6: Measured Hydraulic Conductivity for Additional Simulated ARP/MCU, DDA, and SWPF Saltstone Grout

Grout Mix	Sample ID	Hydraulic Conductivity (cm/sec)	Notes
Batch 8	TR582-1	4.2 E-10	(1)
Batch 8	TR582-2	1.7 E-10	(1)
Batch 8	TR582-3	2.5 E-10	(1)
Batch 9	TR588-1	1.9 E-10	(1)
Batch 9	TR588-2	2.1 E-10	(1)
Batch 9	TR588-3	3.6 E-10	(1)
Batch 10	TR602-1	1.4 E-09	(1)
Batch 10	TR602-2	9.2 E-10	(1)
Batch 10	TR602-3	7.8 E-10	(1)
DDA	TR431-1	1.1 E-10	(2)
DDA	TR431-2	7.2 E-11	(2)
DDA	TR431-3	1.1 E-11	(2)
SWPF	TR451-1	1.2 E-09	(3)
SWPF	TR451-2	2.0 E-09	(3)
SWPF	TR451-3	8.8 E-08	(3), (4)

- (1) SRNL-STI-2009-00419, Table 9
(2) SRNL-STI-2008-00421, Table 18
(3) SRNL-STI-2008-00421, Table 22
(4) Suspect result because of power failure

Figure SP-5.3: Graphical Presentation of Data from Table SP-5.6



From the data provided above (with sample TR451-3 from Table SP-5.6 excluded because of power failure) the maximum value for saturated hydraulic conductivity measured for samples cured for a minimum of 90 days and at a normal (not elevated) temperature is less than 1.0E-8

cm/sec (sample TR547-2 from Table SP-5.2). The arithmetic average for this data set of 38 measured values is $1.8\text{E-}9$ cm/sec and the logarithmic average is $9.0\text{E-}10$ cm/sec. These averages are less than the “best estimate” value provided in the SDF PA Table 4.2-16 ($2.0\text{E-}9$ cm/sec) for the saturated hydraulic conductivity of intact saltstone.

As noted above, samples from MCU-2 and Batch 11 were excluded from these averages, due to minimum curing times and curing temperatures that were inconsistent with the other samples considered. Batch 11 was intended to provide some initial insight on potential impacts of elevated curing temperature on the performance of the saltstone properties. However, the placement of the grout specimen inside an oven at an external temperature of 60°C would not mimic the expected curing conditions within the saltstone monolith. Saltstone remains essentially saturated while the grout specimen inside the oven would experience dry, arid conditions that would quickly drive off the water within the specimen.

Hydraulic Conductivity of Emplaced Saltstone

As stated in Section 6.1.2 of WSRC-STI-2006-00198, the permeability of concrete is influenced by the concrete mix properties as well as by its field placement, consolidation (the process of removing entrapped air from freshly placed concrete), and curing. Testing of emplaced saltstone is the most direct way to confirm test results of laboratory prepared samples and would address impacts of scale, emplacement, and permeability evolution (e.g., curing temperature profile). Core samples were taken from Cell E of Vault 4 in September 2008, as described in LWO-RIP-2008-00006. Three cores from three different locations within Cell E were obtained. However, in most cases aggressive techniques were required to remove the samples from the core drill bit, which caused cracking of the cores. SRNL-L3100-2009-00087 provides pictures of the samples as they were transferred from their original stainless steel containers to PVC containers in April 2009. Various core sample retrieval methods have been reviewed, as documented in SRNL-RSE-2008-00029, to identify a preferred method that would reduce the potential for core sample damage. One method being further investigated is the formed-core system, which entails the placement of one or more sampler tubes inside pipes strategically placed within the disposal unit prior to saltstone grout emplacement. [SRNL-STI-2010-00167]

CO₂ Contamination of Mixing Solution

Avoidance of CO₂ contamination in the preparation of simulated saltstone pore fluid and simulated groundwater equilibrated with vault concrete pore fluid is described in footnotes 1 and 3 of Table 3 of WSRC-STI-2007-00649. Further discussion on CO₂ contamination is provided in pages 31 and 32 in Appendix B of WSRC-STI-2007-00649. Appendix B of WSRC-STI-2007-00649 indicates that CO₂ contamination would lower the pH of the solution and, if there is carbonate in the solution, calcite would precipitate out of solution. The precipitation of calcite could adversely impact the estimated hydraulic properties of the samples tested. Earlier laboratory testing (WSRC-STI-2007-00649) was conducted in a CO₂ free environment so that the potential precipitation of calcite from CO₂ contamination would be avoided. However, because saltstone pore fluid would be contaminated with CO₂ in the field, subsequent testing (SRNL-STI-2008-00421 and SRNL-STI-2009-00419) with simulated saltstone pore fluid did not require a CO₂ free environment. The only testing results from WSRC-STI-2007-00649 presented in this response are for batch MCU-2 provided in Table SP-5.4. However, these results are not further considered because the cure time of these samples was limited to 28 days.

Use of Logarithmic Averaging in SRNL-STI-2008-00421

Section 4.4.3 of SRNL-STI-2008-00421 indicates that, because of the reported power failure that occurred during testing of the sample that yielded a hydraulic conductivity of 8.8E-8 cm/sec, this high permeable test result was likely an outlier. Including all three test's results (shown in Table 22 of SRNL-STI-2008-00421) the logarithmically averaged value is 6.0E-09 cm/sec as shown in Table 30 of SRNL-STI-2008-00421. Removing the highly permeable test result from the sample set yields a logarithmically averaged value of 1.5E-09 cm/sec for the remaining two samples. It is recognized that using an arithmetic, rather than logarithmic, average would increase the average as shown in Table 30. However, the arithmetic average (with the suspect sample removed from the data set) still yields a value of 1.6E-09 cm/sec.

Table SP-5.7 provides the linear and the logarithmic regression fits (R^2) for each sample set. This table demonstrates that the trend in the sampled data is roughly the same whether the data is fit to a linear curve or a logarithmic curve. The mean of the linear regression fit is 0.674 and the mean of the logarithmic regression fit is 0.682; therefore, the logarithmic approach provides a slightly better fit.

Table SP-5.7: Linear and Logarithmic Regression Fits for Each Sample Set

	Linear	Log
MCU-1	0.9994	0.9696
Batch 2	0.128	0.1143
Batch 3	0.9868	0.9968
Batch 4	0.0242	0.035
Batch 5	0.9304	0.9413
Batch 6	0.4808	0.503
Batch 7	0.75	0.7646
Batch 8	0.4433	0.5926
Batch 9	0.8369	0.7997
Batch 10	0.9089	0.9248
DDA	0.9823	0.9765
MEAN	0.6792	0.6926

Note: This table excludes sample data from MCU-2, SWPF, and Batch 11. MCU-2 was excluded because the sample only yielded two data points; therefore the $R^2 = 1$, regardless of linear or logarithmic approach. SWPF was excluded because omitting the suspect data point leaves only two samples, therefore the $R^2 = 1$, regardless of linear or logarithmic approach. Batch 11 was excluded as the sample was cured at an elevated temperature, which is inconsistent with the other data sets evaluated.

Regardless, the difference between using arithmetic or logarithmic averaging is minimal based on the difference between these arithmetic and logarithmic averages. For all samples cured for 90 days, only one saltstone simulant sample had a measured hydraulic conductivity that exceeded 2.0E-09 cm/sec and that is the sample test result that is suspect because of the power failure.

SP-6

Comment:

Additional basis is required for the values of the effective diffusivity of intact and degraded saltstone used in the base case and sensitivity cases.

DOE Response Discussion:

DOE indicated in their response that releases are primarily advection dominated, and calculated Péclet numbers for two separate cases: A and E. Because the Péclet number was large except for very early time periods in Case A, DOE concluded that uncertainty in the effective diffusion coefficient would not have a noticeable impact on calculated peak dose results.

The application of Péclet number as a criterion to neglect the importance of diffusion or advection is problematic (Huysmans and Dassargues, 2004). The importance of these transport mechanisms is more appropriately determined by extracting and comparing the model results. The PORFLOW model output files contain the diffusive and advective releases for each radionuclide at one-year time intervals for 20,000 years. NRC review of this data for key radionuclides (e.g., Ra-226, Tc-99, Pu-239) indicates that (i) diffusion strongly dominates radionuclide fluxes at early time periods (as much as four orders of magnitude) and (ii) continues to dominate throughout the 20,000-year period.

Path Forward

Provide a basis for using the effective diffusivity of intact saltstone in the two sensitivity cases that address degraded saltstone or update the sensitivity cases that address degraded saltstone with a value of effective diffusivity that reflects the physical degradation of the wastefrom. Provide adequate technical basis for the value of the effective diffusivity of intact saltstone. Similar to SP-5, the values assigned should reflect what has been measured and conservatively reflect the uncertainty associated with the results of experiments that are yet to be completed.

RESPONSE SP-6:

As reported in the initial response to this RAI, the effective diffusivity value (effective diffusion coefficient) for intact saltstone of $1.0\text{E-}07 \text{ cm}^2/\text{sec}$ is based on the recommended value for ordinary quality concrete taken from WSRC-STI-2006-00198, Table 6-47. Even though testing described in Section 6.2.2 of WSRC-STI-2006-00198 would indicate a more appropriate value of $5.0\text{E-}09 \text{ cm}^2/\text{sec}$ for the effective diffusivity of saltstone, the value of $1.0\text{E-}07 \text{ cm}^2/\text{sec}$ is conservatively used in PORFLOW. This conservative value of $1.0\text{E-}07 \text{ cm}^2/\text{sec}$ is used for all cases described in the SDF PA, including cases where saltstone is assumed degraded. In addition, this value of $1.0\text{E-}07 \text{ cm}^2/\text{sec}$ remains unchanged during the simulations of all the cases analyzed in the SDF PA. The value of $1.0\text{E-}07 \text{ cm}^2/\text{sec}$ for the effective diffusivity of saltstone was assumed constant in the SDF PA analyses because the change of advective flow (based on changes in hydraulic conductivity) was considered to be more critical in the flow analysis than diffusion.

Latest testing on simulated saltstone conducted by SIMCO Technologies, Inc., documented in SRNL-STI-2010-00515, indicates that the intrinsic diffusion coefficient (analogous to the effective diffusion coefficient used in PORFLOW) is less than $1.0\text{E-}08 \text{ cm}^2/\text{sec}$. This value is a factor of 10 lower than the conservative value assumed in the PORFLOW analysis.

To assess the impact of increased effective diffusivity in the SDF performance model, the conservative value of $1.0\text{E-}07 \text{ cm}^2/\text{sec}$ is assumed as the initial effective diffusivity of saltstone, in an Alternative Sensitivity Case K, that is described in the response to RAI PA-8. This effective diffusivity is assumed to increase as the saltstone degrades such that, within 10,000 years after closure, the effective diffusivity of saltstone increases to a value of $5.0\text{E-}06 \text{ cm}^2/\text{sec}$. This value of $5.0\text{E-}06 \text{ cm}^2/\text{sec}$ is similar to the effective diffusivity of the surrounding soil. All other cementitious materials in the model (grout and disposal unit concrete), for the Alternative Sensitivity Case K, are also assumed to degrade from their initial values; such that, at complete degradation these materials have an effective diffusivity of $5.0\text{E-}06 \text{ cm}^2/\text{sec}$.

The estimated doses to the MOP from Alternative Sensitivity Case K are less than the performance objectives, as shown in the response to RAI PA-8. The results of this analysis indicate that even with the increased effective diffusivity of the cementitious materials in the SDF model, the performance objectives are met.

SP-7

Comment:

Additional bases are needed for key assumptions used in the simulation of sulfate attack with the STADIUM code.

DOE Response Discussion:

The DOE response discussed the development of STADIUM by Simco Technologies. Data for blended cements have been developed but are part of a proprietary material database and are unpublished. Minor species are neglected because there is no self-diffusion data available. However, the model has been shown to reproduce experimental observations even though secondary phases are neglected.

The DOE response covered most of NRC's concerns. NRC is aware of the high quality of work performed by Simco. However, the use of proprietary unpublished information as a basis does not provide transparency for staff to verify the results. Staff is aware of similar research that has been performed at Vanderbilt University (it may also not yet be published). Research completed as part of the Cement Barriers Partnership showed the modeling results could be sensitive to initial mineralogy.

Path Forward

Given the constraints associated with proprietary information, evaluate whether the blended cement formulations that have been evaluated using STADIUM can be compared to the saltstone and concrete formulations used for saltstone disposal. Communicate the relative agreement between predicted and measured values. With respect to minor species, at a minimum an assumption regarding the neglect of minor species should be tracked and reevaluated as future pertinent research is completed. As research is published, provide a comparison of Simco and Vanderbilt assessment results.

RESPONSE SP-7:

The blended cement formulations that have been developed by SIMCO are comparable to the saltstone formulations used for saltstone disposal. Samples of the saltstone binder reagents, cement, slag, and fly ash, were shipped from SRS to SIMCO and were used to prepare simulated saltstone samples. Chemicals for preparing simulated non-radioactive salt solution were obtained from chemical suppliers. SIMCO personnel used the following proportions to prepare saltstone premix, slag with mass fraction 0.45, fly ash with mass fraction 0.45, and cement with mass fraction 0.10. They also prepared salt solution according to proportions provided.

The investigation of the simulated saltstone samples by SIMCO is ongoing and the final results have not been published. Preliminary experiments on the simulated saltstone samples obtained information required by the STADIUM code for simulation. Therefore, the relative agreement between the predicted and measured values is not available. Comparison to Vanderbilt University's assessment results is also not possible until the investigations are complete and the results published. The agreement between the predicted STADIUM code simulations and the experimental measured values will be investigated and evaluated against the analysis of the SDF PA as part of the PA maintenance.

With respect to the minor species exclusion because there is no self-diffusion data available, the assumption will be tracked and reevaluated as future pertinent research is completed as part of the PA maintenance.

SP-8

Comment:

The initial grout mineralogy used in evaluating expansive phase precipitation is inconsistent with the initial mineralogy used to determine Eh and pH transitions in pore fluids. Depending on which initial mineralogy is more appropriate, the conclusions of either report could change.

DOE Response Discussion:

The DOE response indicated why there were differences in the formulations (basically because of timing of the parallel development of products) and that research was ongoing. They also indicated that the uncertainty in Eh and pH transitions of +/- 50% was applied in the uncertainty and sensitivity analyses.

The explanation of why the differences were present is useful to provide understanding, but it does not address why the differences are acceptable or what the impact of the differences in composition may be on the conclusions of the reports. The uncertainty range for the Eh and pH transitions has not been demonstrated to capture the differences in the number of pore volumes that would result from the variability in the initial mineral compositions. The assigned uncertainty range is speculative, and the effects are limited to alternate cases and therefore are not reflected in the base case results.

Path Forward

Provide a basis for using different initial mineralogies in the calculations described in the basis of this comment, or provide information that demonstrates the calculation results are not significantly affected by the differences in initial mineralogy. Provide a basis for the uncertainty range assigned to the Eh and pH transitions.

RESPONSE SP-8:

The mineralogy used in WSRC-STI-2008-00236 and SRNL-TR-2008-00283 reflect the evolution of the saltstone formula. The initial grout mineralogy used in evaluating expansive phase precipitation assesses the potential for future precipitation of expansive phases that could cause fracturing in saltstone. [WSRC-STI-2008-00236] Using GWB reaction path model, the scenarios examined the effects of different infiltrating fluids, different saltstone formulations, and different amounts of minerals available for reaction. WSRC-STI-2008-00236 was initially prepared in 2006, though not issued until 2008. It used the saltstone formulation listed in the 1992 radiological performance assessment. [WSRC-RP-92-1360] It is anticipated that the relevance of this initial step in understanding expansive phase precipitation during saltstone evolution will be superseded by the results of ongoing laboratory and modeling studies of saltstone under various exposure scenarios.

Alternatively, SRNL-TR-2008-00283 used the saltstone formulation representative of SPF operations from WSRC-TR-2008-00037. Table SP-8.1 shows the minerals available in GWB for the calculations in SRNL-TR-2008-00283. The E_h transitions are directly related to the amount of pyrrhotite in the calculated mineralogy. The amount of pyrrhotite was calculated from the measured reducing capacity of the slag reported in SRNS-STI-2008-00045, the amount of slag used reported in WSRC-TR-2008-00037, and the measured bulk density and porosity of the saltstone reported in WSRC-STI-2006-00198.

Table SP-8.1: Minerals Allowed in GWB Simulations

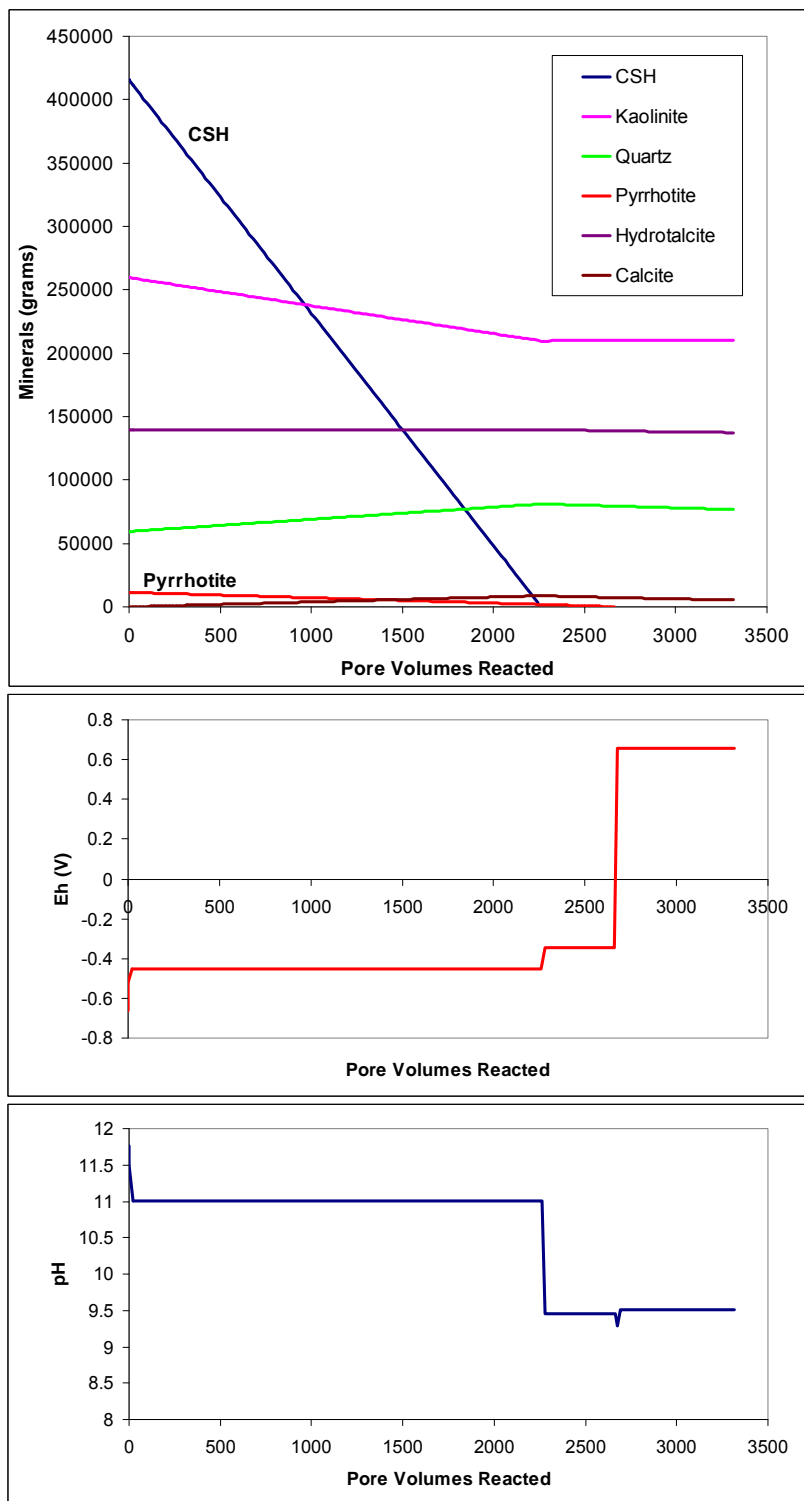
Brucite	Gypsum
C4AH13	Hydrotalcite
Calcite	Kaolinite
Ca-Carboaluminate	Monosulfate
Ettringite	Pyrite
Gehlenite	Pyrrhotite
Gibbsite	Quartz

In SRNL-TR-2008-00283, the E_n transitions calculated using GWB occurs when pyrrhotite is exhausted (Figure SP-8.1). The pH transitions calculated using GWB are directly related to the amount of CSH in the calculated mineralogy (Figure SP-8.1). The pH transition occurs when CSH is exhausted. The amount of CSH in the calculated mineralogy was directly proportional to the CaO mass fraction in the calculated chemical formula of the saltstone, which in turn, was calculated from the saltstone component formula (Portland cement, fly ash, slag, and water) reported in WSRC-TR-2008-00037. The chemical compositions of each component were obtained from WSRC-TR-2006-00067. Portland cement has the highest concentration of CaO and variations in the amount of Portland cement will have the greatest effect on the pH transition times. Variations in the amount of slag in the formula will also have an effect on pH transition times because the slag has a CaO mass fraction of approximately 0.37.

Hence, the differences in mineralogy used in WSRC-STI-2008-00236 and SRNL-TR-2008-00283 are understandable and consistent given the evolution of the saltstone formula. The differences in composition will have an impact on the conclusions of the reports. Experimental analysis on the potential for expansive phase formation in saltstone using updated saltstone mineralogies is ongoing and will be reported when the results become available.

The range of uncertainty for the E_n and pH transitions calculated in SRNL-TR-2008-00283 is directly dependent on the initial component formula used for saltstone. An estimate of how different formulas affect the transitions can be made by comparing the amount of slag and Portland cement used. The minor minerals or less reactive minerals can affect the E_n and pH transitions, although less significantly. For example, Figure SP-8.2 shows the difference when amorphous silica is substituted for quartz in the mineralogy and quartz is suppressed from precipitating. GWB always seeks an initial equilibrium mineral assemblage prior to proceeding with the reaction path calculation unless specific minerals are suppressed, forcing the system away from equilibrium, as in the case shown in Figure SP-8.2. Table SP-8.2 shows the mineralogy re-calculated by GWB, given the initial mineralogy in SRNL-TR-2008-00283. They are virtually identical. Another example is shown in Table SP-8.3 where a different mineralogy was calculated from the identical saltstone component formulation used in SRNL-TR-2008-00283 and input into GWB. The mineralogy re-calculated by GWB is shown in the third column and is very similar to the original used in SRNL-TR-2008-00283.

Figure SP-8.1: Mineralogical Controls on E_h and pH Transitions



[Modified from SRNL-TR-2008-00283]

Figure SP-8.2: Reaction Path Showing Difference in pH if Amorphous Silica is Substituted for Quartz and Quartz is not Allowed to Precipitate

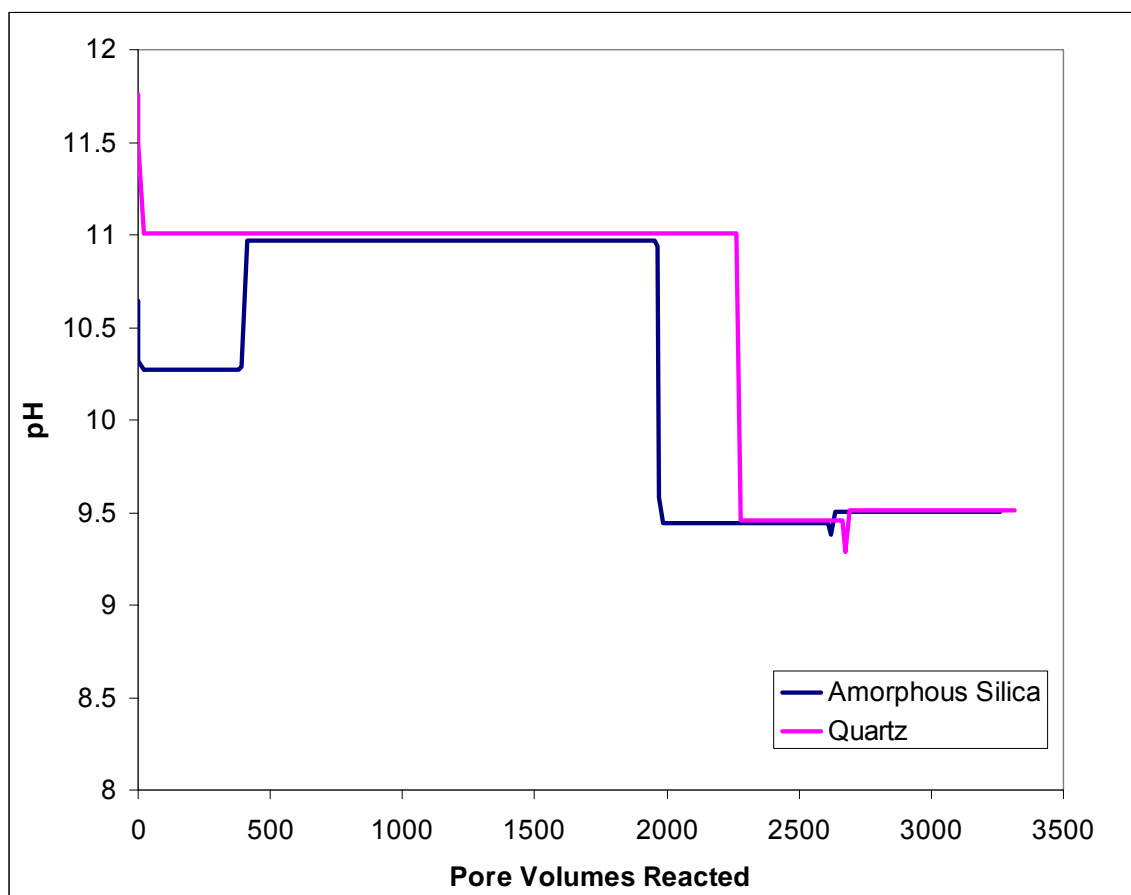


Table SP-8.2: Mineralogy Input into GWB and the Re-calculated Mineralogy

Mineral	Original g/m ³ Saltstone	Re-calculated g/m ³ Saltstone
CSH	4.15E+05	4.15E+05
Hydrotalcite	1.40E+05	1.40E+05
Kaolinite	2.59E+05	2.59E+05
Pyrrhotite	1.14E+04	1.13E+04
Quartz	5.94E+04	5.95E+04
Ca-Carboaluminate	-	3.4
Pyrite	-	52.0

Table SP-8.3: Alternative Mineralogy Calculated from the same Saltstone Formula

	Original	Re-calculated
Mineral	g/m ³ Saltstone	g/m ³ Saltstone
Gehlenite	3.78E+05	-
CSH	-	4.53E+05
Hydrotalcite	-	1.40E+05
Brucite	7.36E+04	-
Kaolinite	-	2.91E+05
Quartz	2.50E+05	2.78E+04
Pyrrhotite	1.14E+04	1.14E+04

The total amount of cementitious materials used per cubic yard also effects the transitions because it changes the bulk density. A formula with the same proportions of components but a higher bulk density will contain more CSH and pyrrhotite in the calculated mineralogy. Thus, the pH and E_n transitions will occur at higher numbers of pore volumes of infiltrating fluid reacted.

The bulk density in a mineralogically similar system also reflects the porosity. Lower bulk density equates to higher porosity. This has an added effect on the calculated E_n and pH transitions. At higher porosity, each pore volume of infiltrating fluid is larger and dissolves more of the key minerals. This effect is observed when comparing the bulk density and porosity used by SRNL-TR-2008-00283 to those used by the SDF PA. SRNL-TR-2008-00283 used a bulk density of 1.26 g/cm³ and a fractional porosity of 0.423. The SDF PA (Table 4.2-16) used a bulk density of 1.01 g/cm³ and a fractional porosity of 0.580. However, the relative proportion of components in the cementitious material was the same. This results in the differing mineralogies presented in Table SP-8.4.

An error in the mineralogy calculation in SRNL-TR-2008-00283 was noted in answering this RAI. With the exception of pyrrhotite, calculated mineral weights per cubic meter of saltstone were not normalized to the bulk density of 1.26 g/cm³. Pyrrhotite was normalized correctly because it was calculated separately. The saltstone mineralogy in Table 3 of SRNL-TR-2008-00283, pyrrhotite excluded, is actually very similar to that calculated for a bulk density of 1.01 g/cm³.

Table SP-8.4: Mineralogy of Similar Saltstone Formula with Different Bulk Densities

	Bulk Density=1.26 g/cm ³	Bulk Density=1.01 g/cm ³
Mineral	g/m ³ Saltstone	g/m ³ Saltstone
CSH	5.49E+05	4.39E+05
Pyrrhotite	1.14E+04	9.12E+03
Kaolinite	3.43E+05	2.75E+05
Hydrotalcite	1.85E+05	1.48E+05
Quartz	7.87E+04	6.29E+04
Assumed Inert	9.19E+04	7.35E+04
Sum	1.26E+06	1.01E+06

Figure SP-8.3 shows the different E_h and pH calculated reaction paths for saltstone, with a similar formula but different bulk densities and porosities, reacted with groundwater. The number of pore volumes reacted to reach the major E_h transition is 39 % different between the two mineralogies. The number of pore volumes reacted to reach the major pH transition is 42 % different.

Table SP-8.5 shows the E_h and pH transition values from SRNL-TR-2008-00283 compared to the corrected values for different bulk density and/or porosity values used in the SDF PA modeling. SRNL-TR-2008-00283 used a saltstone bulk density value of 1.26 g/cm³ and a fractional porosity value of 0.423 compared to values of 1.01 g/cm³ and 0.580 used in the PA modeling for density and porosity, respectively. For concrete, SRNL-TR-2008-00283 used a bulk density of 2.21 g/cm³ and a fractional porosity of 0.184. The PA modeling used the same bulk density, but a fractional porosity 0.120. There is no pH transition in the scenario of saltstone reacted with a fluid derived from equilibration of groundwater with CSH (GW+CSH), because the infiltrating fluid has a pH of 11.1. Hence, the values shown are actually the point of complete CSH depletion.

The uncertainty of ± 50 % for the E_h and pH transitions was intentionally large and was not arrived at in a quantitative way. It was meant to include uncertainty introduced by the factors of a similar formula but different bulk densities and porosities discussed in SRNL-TR-2008-00283, but it was also meant to accommodate the evolution of knowledge about saltstone as more data is collected.

Thus, the calculation results are affected by the differences in initial mineralogy, yet the different mineralogy from SRNL-TR-2008-00283 and the SDF PA are each appropriate given that they are calculated using similar chemical compositions of each component, but with differing bulk densities and porosities. The results illustrate the impact that the saltstone component formula, as well as different mineralogy and physical properties can have on E_h and pH reaction paths for saltstone. Given the uncertainty, the Base Case appropriately uses the calculated mean value from the uniform distribution of E_h and pH transitions in pore volumes taken from SRNL-TR-2008-00283. The calculated mean value and 50 % uncertainty captures the effect that the variability in E_h and pH transitions in pore volumes can have on the source term release given the current level of understanding of saltstone chemistry.

The response to RAI PA-8 includes a new analysis, Alternative Sensitivity Case K, which is a comprehensive assessment of various model parameters modified from the Base Case presented in the SDF PA. Included in the Alternative Sensitivity Case K assumptions are revised pore volumes necessary to initiate E_h and pH transitions. An E_h transition pore volume for saltstone was calculated to be 505 based on a saltstone porosity of 58 % with a revised reducing capacity that is one-fourth of the value determined in SRNS-STI-2008-00045 (0.206 meq e-/g rather than 0.822 meq e-/g). This value is more than a factor of three lower than the E_h transition volume of 1,653 reported in Table SP-8.5. The pH transition pore volume for saltstone was calculated to be 7,608 for Alternative Case K (based on a saltstone porosity of 58 %). This value is approximately two-thirds of the pH transition volume of 11,213 reported in Table SP-8.5. Thus, the saltstone values for E_h and pH transition volumes used in the Alternative Sensitivity Case K are significantly lower than the values reported in Table SP-8.5. Even with these lower transition volumes, the dose results to the MOP based on Alternative Sensitivity Case K are less than the performance objectives.

Figure SP-8.3: Reaction Paths of Saltstone with Similar Formula but Differing Bulk Densities and Porosities; Saltstone Assumed to React with Groundwater

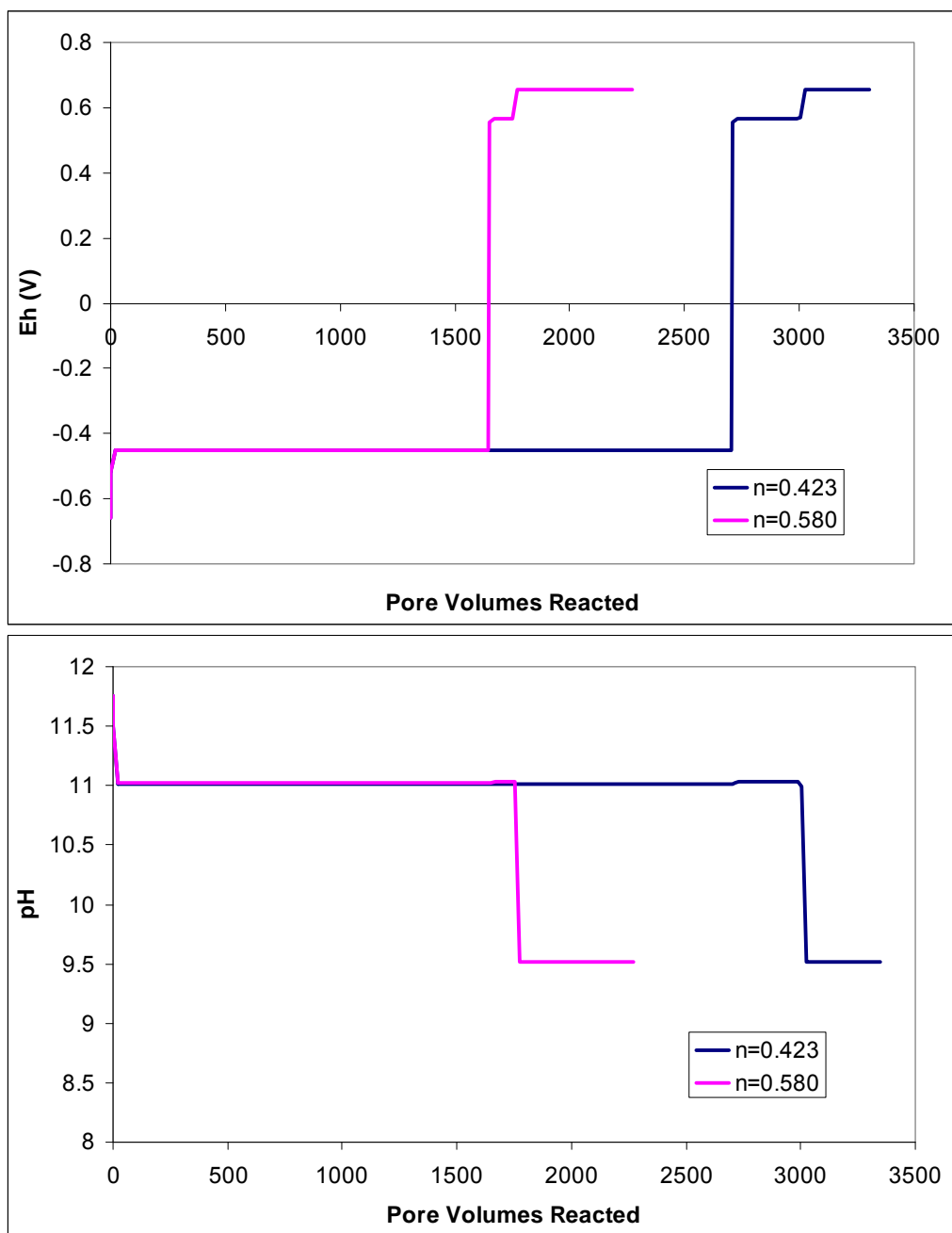


Table SP-8.5: E_h and pH Transitions in Pore Volumes for Different Bulk Densities and Porosities

Scenario	E_h Transition (PV)	pH Transition (PV)
Saltstone/fluid=GW		
SRNL-TR-2008-00283	2,734	2,274
Corrected for $\rho_{bulk}=1.26 \text{ g/cm}^3$	2,702	3,005
Corrected for $n=0.580$	1,642	1,752
Saltstone/fluid=GW+Calcite		
SRNL-TR-2008-00283	2,775	2,558
Corrected for $\rho_{bulk}=1.26 \text{ g/cm}^3$	2,804	3,442
Corrected for $n=0.580$	1,642	2,752
Saltstone/fluid=GW+CSH		
SRNL-TR-2008-00283	2,806	10,422 ^a
Corrected for $\rho_{bulk}=1.26 \text{ g/cm}^3$	2,818	14,024 ^a
Corrected for $n=0.580$	1,653	11,213 ^a
Concrete/fluid=GW		
SRNL-TR-2008-00283	3,230	4,206 ^b
Corrected for $n=0.120$	4,953	6,446 ^b

a) no real pH transition, this is estimated point of CSH depletion

b) extrapolated from CSH depletion trend

GW = Groundwater

PV = Pore Volumes

SP-9

Comment:

Uncertainty in groundwater composition was not considered in the Geochemist's Workbench simulations to estimate Eh and pH transitions in pore fluids.

NRC Response:

The DOE response is adequate.

SP-10

Comment:

There are indications that some measured plutonium and neptunium sorption coefficients in cementitious materials could reflect solubility rather than sorption, which could lead to a significant overestimate of plutonium and neptunium sorption.

DOE Response Discussion:

Recent DOE-sponsored research indicated that the dissolved concentrations of plutonium and neptunium were solubility limited rather than sorption controlled (SRNL-STI-2009-00636). DOE further stated that the models supporting the PA (i.e., PORFLOW and GoldSim) do not use solubility constraints but instead utilize apparent K_d values. However, it is not clear that solubility effects could be ruled out for the studies that form the basis for these plutonium and neptunium K_d values (WSRC-STI-2007-00640 and SRNS-STI-2008-00045). The use of K_d values based on sorption experiments in which solubility was actually the controlling process could lead to underestimation of the radionuclide release rates.

The K_d values measured in WSRC-STI-2007-00640 are extremely high; the solubility limit for plutonium may have been exceeded in these experiments. This report does not include information on the plutonium concentration used in these experiments and how it compares to the solubility limit. This report does state that no solids control samples were included to determine if precipitation was occurring, but the results of these samples were not included in the report. SRNS-STI-2008-00045 provides more information about the methodology used to account for the possibility of precipitation, but it is not clear how the information from the no solids control was used. On page 39, it is stated that the concentrations from samples 621-A, B, and C are used as the initial concentration in the calculation of the K_d . However, based on Table 13, it appears that this sample is not a 'no solids' control and that this sample contains simulated saltstone. Additionally, it seems that this sample is in a reducing environment rather than an oxidizing environment.

DOE also stated that the plutonium and neptunium K_d values used in the PA could be overestimated; however these values did not show up as sensitive parameters. In support of this finding, DOE conducted a sensitivity run that set the K_d value for plutonium and neptunium in cementitious material equal to zero in the GoldSim transport model. The results of these sensitivity runs indicated that the dose to the MOP during the compliance period increased by a factor of less than three for the base case; therefore, DOE concluded that any overestimation of plutonium or neptunium K_d values on cementitious materials would not impact the overall conclusions of the PA.

In addition to the limitations regarding one-off sensitivity analyses (see Comment PA-8), the relative increase in dose from reducing the K_d s to zero was significant. Table 5.5-2 in the PA indicates that for the base case, plutonium and neptunium each contribute less than 0.05 mrem/yr to the total peak dose of 1.4 mrem/yr in the 10,000-year performance period. In the sensitivity analysis with the K_d s for plutonium and neptunium set to zero, the result was that the total dose more than doubled from the original 1.4 mrem/yr. This large relative increase illustrates the sensitivity of the model to the cementitious material K_d for plutonium and neptunium. In light of the sensitivity of the model to these K_d values and the uncertainties in the PA, a one-off sensitivity analysis is not conclusive.

Path Forward

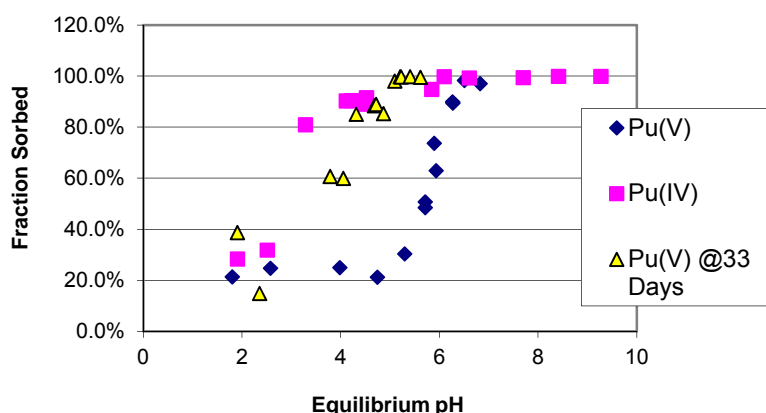
Provide an updated base case that includes technically defensible K_d values for plutonium and neptunium.

Provide information on the no solids control samples in WSRC-STI-2007-00640 and SRNS-STI-2008-00045, including the amount of precipitation observed in the no solids control samples (i.e., provide the initial and final concentrations in these samples). Provide information on the aqueous phase used in the no solids control samples and the pH of these samples. In addition, clarify which samples were used for the initial concentration in the K_d equation on p. 39 of SRNS-STI-2008-00045.

RESPONSE SP-10:

Under SRS vadose conditions, plutonium exists as Pu(IV). Plutonium, when it comes in contact with SRS vadose zone sediment under oxidizing conditions, exists in the reduced state. [WSRC-MS-2003-00889, DOI: 10.1021/es050073o, WSRC-TR-2003-00035] This assumption is based on actual measurements, not on thermodynamic calculations that do not take into consideration surface forces. As discussed in WSRC-TR-2003-00035, Pu(V) was added to SRS sandy subsurface sediment (benchtop experiment) at plutonium concentration below Pu(V) solubility, 1.0×10^{-7} kg/mol, and analyzed after both 24 hours and 33 days. After 33 days, the Pu(V) sorbed to the sandy subsurface sediment, under oxidizing conditions, in a manner similar to the plutonium geochemical behaving as Pu(IV) (Figure SP-10.1). It was explained as a surface enhanced reduction process. For example, at pH 5.2, Pu(V) K_d values were 9 and 3,700 ml/g at 1 and 33 days, respectively.

Figure SP-10.1: Pu(IV) and Pu(V) Sorption Edge at 25 hours and Pu(V) at 33 Days on an SRS Subsurface Sandy Sediment



[WSRC-TR-2003-00035]

In the presence of cementitious materials, where much greater surface areas exist and higher pH levels exist, the K_d values are expected to increase greatly compared to SRS subsurface sand. Because it is impossible to directly measure old age cement K_d values, DOE assigns K_d values that are between middle age cement K_d values and background native sediment K_d values. For this reason, old age cement materials were assigned values greater than those of native sediments.

WSRC-STI-2007-00640 concluded that there was precipitation in the neptunium and plutonium samples because the no-solids controls had neptunium and plutonium losses from the aqueous

phase. SRNL-STI-2009-00636 clearly identifies that precipitation of plutonium occurred during the experiments described above, even at one part per billion, $4.0\text{E-}09$ kg/mol. In document ISSN: 0956-053X_V12_I2-3, the only other known plutonium cement measurement, the plutonium solubility was measured to be in the range of $1.0\text{E-}08$ to $1.0\text{E-}09$ kg/mol. Therefore, adding plutonium at $4.0\text{E-}09$ kg/mol was reasonable, given that, as described in SRNL-STI-2009-00636, it was anticipated that plutonium sorption was going to occur and aqueous concentration would decrease immediately to well below solubility. The results in SRNL-STI-2009-00636 clearly demonstrated precipitation with the no-solid controls that were included with the sorption experiment as part of the QA/QC. [Figures 4.7 and 4.9 in SRNL-STI-2009-00636] In these controls, the very low concentrations of plutonium ($4.0\text{E-}09$ kg/mol) strongly sorbed to the glassware when the cement was not present. When the cement was present, the plutonium did not sorb to the glassware. It was demonstrated that plutonium likely precipitated because strong acid washes did not promote desorption.

It is important to note that unlike most research that in past relied on alpha counting, SRNL-STI-2009-00636 used an inductively coupled plasma mass spectrometer, which provided lower detection limits. The inductively coupled plasma mass spectrometer detection limit for Pu-242 is 0.000044 parts per billion or $1.0\text{E-}15$ kg/mol (Table 3.2 in SRNL-STI-2009-00636). A comparable alpha spectroscopy detection limit would be in the order of 4 parts per billion or $1.0\text{E-}10$ kg/mol (0.5 dpm/mL). Therefore, the revised K_d values reported in SRNL-STI-2009-00636 are the result, in part, of the improved detection limits.

DOE believes that plutonium sorption is primarily controlled by solubility at the high pH levels of cementitious environments. If below the solubility limit, K_d values are used in the SDF PA. Because solubility is so low at high pH levels there are no available K_d values in the literature where no-solid controls have not precipitated from solution. DOE also believes that due to the high surface area and the very low solubility of plutonium, the K_d values for plutonium are also very high. This belief stems from the experimental evidence described in SRNL-STI-2009-00636 and the extremely high tendency for plutonium to sorb even under very low plutonium concentrations to both SRS sediments and especially to cementitious materials.

A report has been issued subsequent to the issuance of Revision 0 of the SDF PA entitled *Geochemical Data Package for Performance Assessment Calculations Related to the Savannah River Site*. This report provided revised K_d s for cementitious materials, including plutonium and neptunium. [SRNL-STI-2009-00473 Table 14] For plutonium, the best estimate oxidized and reduced old age cementitious material K_d has changed from 1,000 to 2,000 mL/g and from 10,000 to 2,000 mL/g, respectively. For neptunium, the recommended oxidized middle age cementitious material K_d has changed from 1,600 to 10,000 mL/g, oxidized old age changed from 250 to 5,000 mL/g, reduced middle age changed from 3,000 to 10,000 mL/g, and the reduced old age changed from 3,000 to 5,000 mL/g. These revised K_d values were utilized in Alternative Sensitivity Case K, summarized in RAI PA-8.

SP-11

Comment:

In recent experiments used to help define K_d values for cementitious materials, the distinction between “middle” and “old” age conditions was based chiefly on water chemistry—not on the mineralogical assemblage. It is not clear whether the differences in solid phases for the different stages can be neglected.

DOE Response Discussion:

In the response, DOE states: “(d)ecreased sorption as a result of evolving mineral assemblage is not expected to be significant in the wasteform because the timing of re-crystallization of reducing old-age concrete is after the performance period, and because a decreasing trend between middle-age and old-age cement K_d s was implemented in the PA to account for this type of uncertainty.” NRC staff does not agree with this statement because the estimation of the timing of the re-crystallization is based on hydraulic assumptions that the NRC staff does not think are supported (see Comments PA-8 and PA-10).

In addition, the comment response states: “(a)s identified above, there is a potential for sorption of key radionuclides onto old-age concrete to decrease with increasing precipitation of quartz as CSH gel dissolves. Any potential impact this may have on underestimating releases from the wasteform are considered insignificant, because countering factors would tend to immobilize these same radionuclides under the old age conditions, either by incorporation into the re-crystallized structures, increased sorption to iron oxyhydroxides, or by increased precipitation of the radionuclide itself, effectively canceling out the effects.” NRC staff agrees that some of these factors may act to mitigate the decreased sorption in old-age concrete due to precipitation of quartz. However, NRC staff does not agree with the proposition that the two competing effects will necessarily cancel each other out. The net effect of competing effects is dependent on how strongly the different effects affect the system.

Finally, the comment response states: “(i)t is also proposed that the K_d s used in the PA are conservative in that they do reflect a decreasing trend in K_d s from middle-age to old-age cementitious material.” NRC staff also does not agree with this logic because whether or not something is conservative is dependent on the actual values chosen, not just the trend in the values.

Path Forward

Depending on the results of research on the predicted flow through the cementitious materials, this comment may be more significant in the future if the transitions are predicted to occur during the performance period. NRC staff will continue to track this topic under monitoring.

RESPONSE SP-11:

DOE agrees that under experimental conditions using only an aged aqueous phase and not a 1,000 to 10,000 year old aged solid phase is less than ideal. This is presently under review and to date no other surrogate aged cementitious solid phases have been identified in the literature. It is not clear whether the solids DOE uses, or that are used in the literature, sorb more or less than “true aged” solids. Because of the uncertainty that is introduced through the use of these unaged solids in the literature and SRS K_d values, DOE generally reduces actual “old” cement K_d values by up to one order of magnitude compared to “middle” K_d values.

As stated in Table C.1-1 of the PA maintenance plan (SRR-CWDA-2011-00052), and stated in SDF PA Section 8.2, a long-range program plan for on-going testing of degradation mechanisms associated with cementitious hydraulic properties is being developed to identify additional field/lab testing and identify test methods and equipment. Revised K_d values for cementitious materials will be incorporated in PA modeling as appropriate.

SP-12

Comment:

Model support is needed for the process models supporting PA predictions of Eh-pH evolution for cementitious materials.

DOE Response Discussion:

The comment response indicated that research is ongoing, and to account for the preliminary nature of the available information uncertainty and sensitivity analyses were performed.

NRC recognizes that additional work will be done to provide model support, and NRC is highly supportive of that work. However, using uncertainty analysis to account for lack of model support is generally insufficient unless it can be demonstrated:

- i) The justification is provided to show that the range of parameter values considered in the uncertainty analysis encompasses the uncertainty in the model,
- ii) The uncertainty and sensitivity analyses are reasonably conservative, and
- iii) The impact of the uncertainty is limited locally and globally in the analysis.

Since the model is not adequately supported, it is very difficult to define an appropriate representation for the uncertainty analysis. Uncertainty analysis is a useful tool for use in performance assessment, but should be used very cautiously if at all with respect to model support.

Path Forward

Provide model support for the Geochemist's Workbench results regarding pore fluid volumes necessary for transitions in Eh and pH of pore fluids in cementitious materials (SRNL-TR-2008-00283). For example, model support could include a comparison of model results with the results of pH and Eh measurements in accelerated physical testing using higher flow rates than anticipated in full-scale saltstone. Plans for developing model support may provide appropriate basis, because NRC could verify the implementation of those plans in its monitoring role. However, use of plans for model support could result in the development of information that does not support the decision.

RESPONSE SP-12:

As explained in the original response to SP-12, "the lack of experimental data is the primary reason the calculations in SRNL-TR-2008-00283 were done, so that there would be an analytical basis for incorporating chemical changes of pore fluid with aging into the PA modeling." Without experimental results, the GWB results represent the best estimate of pore fluid volumes necessary for the E_h and pH transitions. DOE does not have any specific plans for research activities in this area, but as explained in the original response to SP-12, it was "acknowledged in the SDF PA Section 8.2 ('Further Work'), the PA is considered a living document for the closure of the SDF and additional studies may be conducted to verify that it continues to bound the SDF model inputs. It is recognized that one area of future work is further support for the source term release model, potentially including physical testing on those areas currently addressed through GWB simulations."

The response to RAI PA-8 includes a new analysis, Alternative Sensitivity Case K, which is a comprehensive assessment of various model parameters modified from the Base Case presented in the SDF PA. For the Alternative Sensitivity Case K, the transition volumes necessary to initiate E_h and pH transitions in saltstone were revised from the Base Case values.

The E_h transition pore volume for saltstone was revised from 2,806 to 505, based primarily on a very pessimistic value for the reducing capacity of saltstone. The pH transition volume for saltstone was revised from 10,422 to 7,608. Details of the reductions to these pore volumes are provided in the response to PA-8. The results reported in the response to RAI PA-8 indicate that the compliance objectives are met even for this very pessimistic case.

In addition, as described in the response to RAI Comment SP-13, the radionuclide that is most influenced by the E_h transition, technetium, is evaluated using a shrinking core model. The shrinking core model, described in the response to RAI PA-8, is not a pore flush model. Thus, technetium is not dependent on the GWB results regarding pore fluid volumes necessary for E_h transitions in cementitious materials. The remaining radionuclides evaluated in the response to RAI SP-13 are less influenced by the E_h transition and therefore less influenced by the results of the GWB model evaluation. The response to RAI SP-13 also indicates that the E_h and pH transitions do not have a significant impact on the release and transport of those radionuclides that are important contributors to dose. Therefore, the GWB model evaluation results are not risk significant to the SDF PA model.

SP-13

Comment:

The effect of limiting the shrinking-core model to the effects of the Eh evolution of saltstone on Tc should be analyzed.

DOE Response Discussion:

DOE provided information to demonstrate that for key radionuclides the transitions from different Eh and pH conditions are not expected to have a significant influence on the results, and therefore switching to a shrinking core model for those radionuclides is not warranted. Tc-99 was the main radionuclide for which the transitions were expected to have a big impact, and so it was included in the shrinking core model.

NRC's comment also applied to radionuclides that did not contribute at least 0.05 mrem in the all-pathways base case dose. The approach to modeling the release for those radionuclides could cause them to be defined as important or not.

Path Forward

Demonstrate that the key radionuclide list is not impacted by the type of release model (i.e. shrinking core vs. step transitions) applied. For instance, compare the K_d values assigned at different Eh and pH states, the concentrations of those radionuclides in the waste, and their dose conversion factors for key pathways or provide shrinking core model results for those radionuclides.

RESPONSE SP-13:

In the original DOE Response to Comment SP-13, only those radionuclides with at least 0.05 mrem contributions to the all-pathways Base Case dose were considered when evaluating the potential impacts of the shrinking core model. [SRR-CWDA-2010-00033, Revision 1] To further support this response, all of the radionuclides corresponding to an element in SDF PA Table 4.2-18 are considered for evaluation with the shrinking core model. The results of this evaluation demonstrate that, for elements other than technetium, switching to a shrinking core model is not warranted.

Based on geochemical calculations (i.e., pore volume flushes per SDF PA Section 4.2.2), the E_h transition from reducing to oxidized conditions is predicted to occur before the pH transition from middle-aged to old-aged conditions. Therefore, the K_d transitions occur in the following order for SDF cementitious materials (i.e., saltstone and disposal unit concrete).

Reducing Middle Age → Oxidized Middle Age → Oxidized Old Age

The reducing middle age, oxidized middle age, and oxidized old age K_d values for all the elements, as presented in SDF PA Table 4.2-18 are reproduced in Table SP-13.1. The ratios of oxidizing middle age to reducing middle age and the ratios of oxidized old age to oxidized middle age are presented in Table SP-13.1.

For the purposes of this evaluation, a transition is considered "potentially significant" if the transition ratio is less than 0.05 indicating that there is a potentially significant difference between the K_d values before and after the transition. Elements with ratios that meet this criterion are shaded within these tables and discussed below.

Table SP-13.1: Selected K_d Value for All Elements Evaluated in the PA

Element	Reducing Middle Age (mL/g)	Oxidized Middle Age (mL/g)	Oxidized Old Age (mL/g)	Oxidized Middle Age / Reducing Middle Age Ratio	Oxidized Old Age / Oxidized Middle Age Ratio
Ac	5,000	6,000	600	1.2	0.1
Ag	1	1	0.1	1	0.1
Al	5,000	6,000	600	1.2	0.1
Am	5,000	6,000	600	1.2	0.1
Ar	0	0	0	N/A	N/A
As	1,000	1,000	100	1	0.1
At	10	15	4	1.5	0.27
Ba	3	100	70	33	0.7
Bk	5,000	6,000	600	1.2	0.1
C	10	10	0	1	N/A
Cd	5,000	4,000	1000	0.8	0.25
Ce	5,000	6,000	600	1.2	0.1
Cf	5,000	6,000	600	1.2	0.1
Cl	20	20	2	1	0.1
Cm	5,000	6,000	600	1.2	0.1
Co	5,000	4,000	1000	0.8	0.25
Cr	5,000	20	2	0.004	0.1
Cs	2	20	10	10	0.5
Cu	1	1	0.1	1	0.1
Eu	5,000	6,000	600	1.2	0.1
F	20	20	2	1	0.1
Fe	5,000	6,000	600	1.2	0.1
Fr	2	20	10	10	0.5
Gd	5,000	6,000	600	1.2	0.1
H	0	0	0	N/A	N/A
Hg	1,000	300	300	0.3	1
I	9	15	4	1.7	0.27
K	2	20	10	10	0.5
Mn	100	100	10	1	0.1
N	0	0	0	N/A	N/A
Na	1	1	0.5	1	0.5
Nb	1,000	1,000	500	1	0.5
Ni	5,000	4,000	1,000	0.8	0.25
Np	4,000	1,600	250	0.4	0.16
Pa	5,000	1,600	250	0.32	0.16
Pb	500	500	250	1	0.5
Pd	5,000	4,000	1,000	0.8	0.25
Pm	0	0	0	N/A	N/A
Po	500	500	250	1	0.5
Pr	0	0	0	N/A	N/A
Pt	0	0	0	N/A	N/A
Pu	10,000	10,000	1,000	1	0.1

Table SP-13.1: Selected K_d Value for All Elements Evaluated in the PA (Continued)

Element	Reducing Middle Age (mL/g)	Oxidized Middle Age (mL/g)	Oxidized Old Age (mL/g)	Oxidized Middle Age / Reducing Middle Age Ratio	Oxidized Old Age / Oxidized Middle Age Ratio
Ra	3	100	70	33	0.7
Rb	2	20	10	10	0.5
Re	5,000	1	0.5	0.00016	0.63
Rh	0	0	0	N/A	N/A
Rn	0	0	0	N/A	N/A
Ru	0	0	0	N/A	N/A
Sb	5,000	100	2	0.02	0.02
Se	300	300	150	1	0.5
Sm	5,000	6,000	600	1.2	0.1
Sn	5,000	4,000	2,000	0.8	0.5
Sr	3	30	15	10	0.5
Tc	5,000	1	0.5	0.00016	0.63
Te	300	300	150	1	0.5
Th	5,000	5,000	500	1	0.1
U	2,500	250	70	0.1	0.28
V	0	0	0	N/A	N/A
Y	5,000	5,000	500	1	0.1
Zn	5,000	4,000	1,000	0.8	0.25
Zr	5,000	5,000	500	1	0.1

N/A = Not Applicable

Table SP-13-2 provides the same evaluation using the updated K_d values, as presented in the description of the Alternative Sensitivity Case K sensitivity analysis in the response to PA-8.

Table SP-13.2: Selected K_d Value for All Elements Evaluated in Alternative Sensitivity Case K

Element	Reducing Middle Age (mL/g)	Oxidized Middle Age (mL/g)	Oxidized Old Age (mL/g)	Oxidized Middle Age / Reducing Middle Age Ratio	Oxidized Old Age / Oxidized Middle Age Ratio
Ac	7,000	6,000	600	0.86	0.1
Ag	5,000	4,000	400	0.8	0.1
Al	7,000	6,000	600	0.86	0.1
Am	7,000	6,000	600	0.86	0.1
Ar	0	0	0	N/A	N/A
As	200	320	100	1.6	0.31
At	9	15	4	1.67	0.27
Ba	100	100	70	1	0.7
Bk	7,000	6,000	600	0.86	0.1
C	3,000	3,000	300	1	0.1
Cd	5,000	4,000	400	0.8	0.1
Ce	7,000	6,000	600	0.86	0.1
Cf	7,000	6,000	600	0.86	0.1
Cl	10	10	1	1	0.1
Cm	7,000	6,000	600	0.86	0.1
Co	5,000	4,000	400	0.8	0.1
Cr	1,000	10	1	0.01	0.1
Cs	20	20	10	1	0.5
Cu	5,000	4,000	400	0.8	0.1
Eu	7,000	6,000	600	0.86	0.1
F	10	10	1	1	0.1
Fe	7,000	6,000	600	0.86	0.1
Fr	20	20	10	1	0.5
Gd	7,000	6,000	600	0.86	0.1
H	0	0	0	N/A	N/A
Hg	5,000	300	100	0.06	0.33
I	9	15	4	1.67	0.27
K	20	20	10	1	0.5
Mn	100	100	10	1	0.1
N	10	10	1	1	0.1
Na	1	1	0.5	1	0.5
Nb	1,000	1,000	500	1	0.5
Ni	4,000	4,000	400	1	0.1
Np	10,000	10,000	5,000	1	0.5
Pa	10,000	10,000	5,000	1	0.5
Pb	500	300	100	0.6	0.33
Pd	4,000	4,000	400	1	0.1
Pm	0	0	0	N/A	N/A
Po	5,000	300	100	0.06	0.33
Pr	0	0	0	N/A	N/A
Pt	5,000	4,000	400	0.8	0.1

Table SP-13.2: Selected K_d Value for All Elements Evaluated in Alternative Sensitivity Case K (Continued)

Element	Reducing Middle Age (mL/g)	Oxidized Middle Age (mL/g)	Oxidized Old Age (mL/g)	Oxidized Middle Age / Reducing Middle Age Ratio	Oxidized Old Age / Oxidized Middle Age Ratio
Pu	10,000	10,000	2,000	1	0.2
Ra	100	100	70	1	0.7
Rb	20	20	10	1	0.5
Re	5,000	1	0.5	0.00016	0.63
Rh	0	0	0	N/A	N/A
Rn	0	0	0	N/A	N/A
Ru	0	0	0	N/A	N/A
Sb	1,000	1,000	100	1	0.1
Se	300	300	150	1	0.5
Sm	7,000	6,000	600	0.86	0.1
Sn	5,000	4,000	2,000	0.8	0.5
Sr	15	15	5	1	0.33
Tc	1,000	1	0.5	0.0008	0.63
Te	300	300	150	1	0.5
Th	5,000	10,000	2,000	2	0.2
U	2,500	1,000	100	0.4	0.1
V	0	0	0	N/A	N/A
Y	7,000	6,000	600	0.86	0.1
Zn	5,000	4,000	400	0.8	0.1
Zr	5,000	10,000	2,000	2	0.2

N/A = Not Applicable

Using the Base Case PA K_d values, only four elements are identified as “potentially significant,” chromium, rhenium, antimony, and technetium (see Table SP-13.1). All four of these elements are “potentially significant” when evaluated based on the E_h transitions (from reducing to oxidizing conditions), whereas only antimony is “potentially significant” based on pH transitions (from middle aged to old aged).

Technetium has already been evaluated and included in the shrinking core model; therefore, no further discussion of technetium is warranted. Note that the description of the alternative modeling case (Alternative Sensitivity Case K) included in the response to RAI PA-8 discusses a shrinking core model approach used to evaluate technetium transport.

The following discussion provides justification for excluding chromium, rhenium, and antimony from the shrinking core model approach:

- *Chromium and Rhenium* - The total projected SDF disposal units' radionuclide inventory at closure is provided in SDF PA Table 3.3-7. As indicated by SDF PA Table 3.3-7, there are no radionuclides associated with chromium and rhenium in the SDF inventory at closure, thus these elements are not significant and may be excluded from the shrinking core model approach.
- *Antimony* - There is an inventory for antimony isotopes: Sb-125, Sb-126, and Sb-126m. These radionuclides are short-lived daughter products with half-lives of less than 3 years, much shorter than the time required for transport through the disposal cell or through the environment. Therefore, the transport of these radionuclides is not explicitly

modeled. The dose from these daughter products are accounted for by combining the dose conversion factor of the daughter product with the dose conversion factor of the parent radionuclide. The parent radionuclides of Sb-125, Sb-126, and Sb-126m are Sn-125 and Sn-126. The modeled transport of the antimony radionuclides is dependent on the transport of the parent radionuclides, making application of the shrinking core model inappropriate.

Finally, it should be noted that for Alternative Sensitivity Case K the transition evaluation yielded similar results, with all but one of the same elements identified as potentially significant (i.e., chromium, rhenium, and technetium). Antimony was not significant for either transition (see Table SP-13.2).

An analysis was performed using biosphere parameters that may influence the relative importance of the dose from a radionuclide, such as the dose conversion factors and the transfer factors. The dose model was used to determine dose contributions based on unit concentration inputs for all radionuclides (i.e., doses were based upon 100-meter well concentrations of 1 pCi/L per radionuclide). Each of the exposure pathways were totaled and individual radionuclide percentage of the greatest radionuclide dose was determined. Each radionuclide was ranked by overall importance in biosphere exposure as presented in Table SP-13.3.

The first 23 radionuclides listed (through Th-230) have a biospheric importance value that is within one order of magnitude of the highest (Pb-210). Therefore, these first 23 radionuclides shall each be evaluated. Of the 23 radionuclides, 19 can be screened from additional evaluation on the basis that they have relatively high K_d values. These 19 radionuclides have reducing middle-aged cementitious K_d values of at least 500 mL/g and oxidizing old aged cementitious K_d values of at least 250 mL/g. The four remaining radionuclides are Cs-137, Pa-231, Ra-226, and Ra-228.

The following discussion provides justification for excluding Cs-137, Pa-231, Ra-226, and Ra-228 from the shrinking core model approach:

- *Pa-231 and Ra-228* - The initial SDF PA inventory for Pa-231 and Ra-228, including contributions from their parent radionuclides, is small; therefore, these radionuclides are not expected to contribute greatly to the MOP dose.
- *Cs-137* – This radionuclide has a short half-life (just over 30 years) and would not have sufficient time to travel to the point of exposure before decay.
- *Ra-226* - As shown above in Tables SP-13.1 and SP-13.2, Ra-226 does not have a significant change in K_d between the reduced middle age to oxidized middle age to oxidized old age transition.

Therefore, the analysis of biosphere parameters did not identify any additional radionuclides that warranted application of the shrinking core model method.

As described by the results of both the K_d analysis and the biospheric importance analysis, technetium is the only radionuclide that is appropriate to model with the shrinking core approach.

Table SP-13.3: Radionuclide Ranking by Total Biosphere Influence

Radionuclide	Biospheric Importance (Percentage Relative to the Highest Ranked Radionuclide)
Pb-210	100 %
Ac-227	63 %
Cm-248	41 %
Pa-231	38 %
Ra-228	37 %
Th-229	28 %
Am-243	26 %
Am-242m	25 %
Am-241	25 %
U-232	21 %
Cf-251	19 %
Cf-249	18 %
Cs-137	14 %
Pu-239	13 %
Pu-240	13 %
Ra-226	13 %
Pu-244	13 %
Pu-242	13 %
Pu-238	12 %
Cm-245	11 %
Th-232	10 %
Cm-247	10 %
Th-230	10 %
I-129	8 %
Cm-243	8 %
K-40	7 %
Np-237	7 %
Cm-244	6 %
Se-79	6 %
Sn-126	6 %
U-233	2 %
Cm-246	2 %
U-234	2 %
Cs-135	2 %
U-238	2 %
U-235	2 %
U-236	2 %
Gd-152	2 %
Sr-90	1 %

Table SP-13.3: Radionuclide Ranking by Total Biosphere Influence (Continued)

Radionuclide	Biospheric Importance (Percentage Relative to the Highest Ranked Radionuclide)
Sm-147	1 %
Pu-241	0.3 %
Nb-94	0.3 %
Co-60	0.2 %
Eu-154	0.2 %
Al-26	0.2 %
Eu-152	0.1 %
Cl-36	0.1 %
Zr-93	0.1 %
Tc-99	0.05 %
C-14	0.03 %
Nb-93m	0.02 %
Ni-63	0.01 %
Sm-151	0.01 %
Ni-59	0.003 %
Pd-107	0.002 %
Pt-193	0.002 %
H-3	0.001 %

[Source: SP-13 Biosphere Results.xlsx; HTF_Model_SDF_SP_13.gsm]

SP-14

Comment:

Additional information is needed about the basis for the K_d values used for iodine and radium in cementitious materials.

DOE Response Discussion:

In the DOE response to this comment, it is stated that: "(r)esults for iodine partition coefficients onto old-age cements in an oxidizing environment from the same report were not recommended for update because the new results do not correspond to previously reported values (Table 2, WSRC-STI-2007-00640)."

NRC staff disagrees with this statement for two reasons:

- 1) It is not reasonable to ignore data simply because the results are unexpected, and
- 2) The reducing grout used in WSRC-STI-2007-00640 is based on a different formulation than saltstone (i.e., it contains sodium thiosulfate as a reducing agent).

The radium K_d information provided in the DOE comment response is adequate, but NRC staff would like to note that the K_d value for Ra is risk-significant, so it is important for future research to be done on the sorption of Ra on simulated saltstone instead of relying on literature values based on the sorption of strontium. NRC staff would also like to note that it is important for the performance assessment to adequately account for the uncertainty in this parameter value.

Path Forward

K_d values for I that are consistent with measurements made for simulated saltstone should be used in the PA. NRC suggests that future research include the sorption of Ra onto simulated saltstone, particularly under oxidizing conditions.

RESPONSE SP-14:

As mentioned in reason 2 in the Response Discussion above, the reducing grout used in WSRC-STI-2007-00640 is based on a different formulation than saltstone. Subsequent to the issuance of SDF PA, a new evaluation for iodine K_d values sorbed to saltstone was presented in SRNL-STI-2009-00636. Several samples were evaluated including two types of saltstone containing various amounts of slag. Sample TR547 (containing 45 % slag) is a baseline mixture more representative of the saltstone formulation and measured K_d values compare favorably with previously reported measurements. [SRNL-STI-2009-00636 Table 6.4] Based on the measured results documented in SRNL-STI-2009-00636, for the more representative saltstone formulation, the iodine K_d values that have been utilized in the SDF PA are consistent with K_d values from SRNL-STI-2009-00636, except for old age reducing cementitious materials. Therefore, only a change to the iodine K_d value for old age reducing cementitious materials has been made for the Alternative Sensitivity Case K, as shown in Table PA-8.6. Note, however, that this change has no impact on the analysis because the old age reducing condition for cementitious materials is not achieved in the SDF model. Cementitious materials transition from the middle age reducing condition to the middle age oxidizing condition in the SDF model.

An explanation of the uncertainty in these parameter values is provided in the response to SP-18 and is evaluated in Section 5.6 of the SDF PA. Distributions of K_d values for the uncertainty analysis may be truncated to prevent the occurrence of negative values in the modeling (K_d essentially zero), but the overall shape of the distributions are not affected by the change. Currently, there are no negative K_d values in the PA to require this adjustment.

As stated in Section 8.2 of the SDF PA, further study may be warranted for an enhanced estimate of the effective transport properties for saltstone contaminant release over time for Ra-226 release modeling, including the possibility of radium co-precipitation. The future work will be considered under the DOE Manual 435.1-1 required PA maintenance program.

SP-15

Comment:

The basis for the adopted technetium pseudo- K_d of 1,000 mL/g for reducing conditions is not clear.

DOE Comment Discussion:

The DOE response to this comment states that,

“(t)he technetium K_d value selected for the shrinking core model (1,000 mL/g) is a lower bound on the values recommended in SRNL-STI-2009-00636 for cementitious materials of varying age. The selected value also creates margin in comparison to the recommended value (5,000 mL/g) for young and medium age cementitious material. This margin can be used to account for uncertainty in the recommended value.”

NRC staff does not believe that the “recommended values” of 1000 mL/g or 5000 mL/g are applicable to the saltstone wasteform for the following reasons:

- 1) *The 5000 mL/g value was measured for a formulation that included a strong reducing agent and is very different than the saltstone formulation.*

According WSRC-TR-2006-00004 and WSRC-STI-2007-00640 the “recommended” value of 5000 mL/g K_d is originally based on a measurement value from Bradbury and Sarott (1995). The Bradbury and Sarott (1995) reference states “(i)n some recent work, using Tc(IV) at trace levels ($<10^{-11}$ M) and sodium dithionite as reducing agent, distributions of ~ 5 m³/kg (5,000 mL/g) have been reported (Bayliss et al., 1991).”

Because saltstone does not have the strong reducing agent sodium dithionite in it, this measured value is in no way applicable to the saltstone wasteform. In addition, the Bayliss et al., reference cited by Bradbury and Sarott is a symposium presentation that does not seem to be peer reviewed. It is inappropriate to use a non-peer reviewed source as the basis for a key assumption that strongly affects the calculated dose.

Similarly, staff from SRS have also told NRC staff that research described in Lukens et al., (2005) provided evidence that Tc would be reduced in saltstone (see meeting summary at ML101790054 [NRC, 2010b]). NRC staff disagrees with this statement because the reducing agent Na₂S was added to the waste simulant to reduce it in these experiments and this reducing agent is not added to the salt waste processed at the SPF.

- 2) *SRS staff measured much lower Tc K_d values for saltstone.*

In SRNL-STI-2009-00636, the measured K_d values for Sample Tr547, which has a composition similar to saltstone, ranged from 9.1 to 56 mL/g after 4 days (Table 10.30). It is not clear why this information is not being considered in the PA, and NRC staff believes that in the absence of any relevant experimental data (i.e., using a wasteform formulation that is comparable to saltstone and does not include a strong reducing agent), it is not reasonable to discount experimental results.

- 3) *If is unclear if the saltstone pore fluid has reducing conditions.*

The redox conditions of waste are important for the release of Tc from the wasteform because under reducing conditions Tc is expected to be retained much more strongly under reducing conditions than under oxidizing conditions. In SRNS-STI-2008-00045, Figure 5, the reported Eh value approaches 0 mV as water flows through the system. Additionally, it is not clear that the Eh measurements were measured correctly. On June 29, 2010, NRC staff and SRS staff held a

phone call to discuss the Eh measurements described in this report (see ML101790054 for summary of call). During this call, NRC staff asked what electrode was used and whether the reported values were corrected for the particular reference electrode used (i.e., referenced to a standard hydrogen electrode). SRS site staff stated that the electrode used in their experiments was an Ag/AgCl electrode and that the reported values were read directly from the instrument and were not corrected for the particular electrode used. It is the conclusion of the NRC staff that these redox potentials were incorrectly reported, and based on the half-cell potential of the Ag/AgCl electrode, the true Eh in this system would be 200 mV higher, or less reducing, than was reported.

NRC staff recognizes that the K_d tests for the sorption of Tc onto saltstone were intended to evaluate the transport of Tc through the saltstone once it has been released, rather than the release of Tc. However, because no relevant leaching data has been provided to the NRC, the K_d values measured by SRS for Tc represent the best available information on the release of Tc from the saltstone wasteform.

NRC staff is unable to conclude that the Tc will be retained by the saltstone wasteform to the extent that was assumed in the PA in the absence of appropriate data that clearly demonstrate that this assumption is valid. NRC staff, absent new information and bases on Tc leaching and K_d 's, will use the site-specific K_d values measured by SRS staff for the sorption of Tc onto saltstone in their independent modeling analyses and in their conclusions in the TER.

Path Forward

Use a K_d value that is consistent with the values measured by SRS staff for the saltstone wasteform in the PA.

RESPONSE SP-15:

The mobility of technetium is dependent on its form, with Tc(VII) being highly mobile and the reduced form Tc(IV) being highly immobile. Maintaining technetium in its reduced form (i.e., Tc(IV)) is an important feature of disposal cell and waste form design. Current modeling in the SDF PA assumes that technetium remains in its reduced state until oxidation converts the technetium into its more mobile species. Saltstone is a cementitious waste form containing blast furnace slag that imparts a reducing environment on the technetium. Previous testing had been ineffectual in demonstrating that the saltstone reduces the technetium to the extent assumed in the PA analysis due to the experimental conditions. However, report SRNL-STI-2010-00668 has been recently issued to summarize the results of a literature search regarding the sorption of technetium in cementitious materials containing blast furnace slag and the results of recent technetium sorption laboratory testing. The purpose of the literature review and the laboratory testing was to directly address the NRC's concerns noted in the discussion, specifically 1) the potential impact of a reducing agent on the transport properties of saltstone, 2) the selection of a technetium K_d value of 1,000 mL/g in cementitious materials under reducing conditions, and 3) if the existing saltstone formula results in reducing conditions.

Based on SRNL-STI-2010-00668, the following information is provided to directly address the NRC's concerns and to demonstrate that the mobility of technetium within the saltstone monolith can be modeled as a shrinking core with an initial reducing K_d value of 1,000 mL/g and an oxidizing K_d value of 10 mL/g. The shrinking core model describes the existence of an oxidized outer layer of cementitious material surrounding a shrinking core of reducing intact saltstone. For Alternative Sensitivity Case K, described in the response to RAI PA-8, saltstone degradation is modeled via fracture spacing within the saltstone monolith, which is assumed to occur in a semi-logarithmic relationship with time so that within 10,000 years after closure the saltstone

monolith has a final fracture spacing of 10 centimeters at its fully degraded condition. This fracture spacing is utilized to simulate a shrinking core model for the release of technetium as the reducing capacity of the saltstone is depleted via oxidation. This modeling approach is described in detail within the response to RAI PA-8.

The saltstone core sample utilized in SRNL-STI-2010-00668 was olive green color, indicating reducing conditions, with an external thin layer of light gray. It is not known if the thin layer of light gray is a dry surface or if this thin layer had been oxidized, but it represents a minimal portion of the total sample. The saltstone was originally poured in December 2007 and the sample was collected nine months later in September 2008. Leaching experiments on the saltstone sample were initiated in June 2010. [SRNL-STI-2010-00667] Future work on saltstone degradation will include focus on the timing of saltstone transitions from the reducing to the oxidizing state.

- SRS saltstone will reduce Tc(VII) to Tc(IV) in the absence of NaS or sodium dithionite (i.e., strong reducing agents) in a reducing atmosphere.
- Experiments conducted under reducing conditions (< 0.5 ppm $O_{2(g)}$, -585 mV, 2 % H_2 , pH 11.66) obtained K_d values of approximately 1,000 mL/g in saltstone formulated with 45 % slag (nominal saltstone concentration).
- The site-specific reduction capacity value of 820 $\mu\text{eq/g}$ for saltstone is in the realm of literature values that were either measured or theoretically estimated based on thermodynamic calculations of cementitious materials containing blast furnace slag.

The following information was also concluded in SRNL-STI-2010-00668, which addresses issues from previous research related to the impacts of oxygen on the experimental results.

- Only trace concentrations of atmospheric oxygen (30 to 60 ppm O_2 ; E_h 120 mV) at the high pH levels of cementitious systems is required to maintain technetium as Tc(VII).
- The wide variability of measured K_d values, such that they are either very low, approximately 1 mL/g, or they are very high approximately 1,000 mL/g, appears to be the result of experimental conditions, especially direct controls of oxygen contact with the sample.
- Based upon the information provided in SRNL-STI-2010-00668 (which is included as part of this transmittal package), the modeling parameters utilized in the SDF PA are appropriate and are supported by both existing literature from various sources and experimental results.

SP-16

Comment:

The basis for the range of reduction capacities over which the shrinking-core model transitions to oxidizing K_d values for technetium is not clear.

NRC Response:

The DOE response is adequate.

SP-17

Comment:

Neglecting gas-phase diffusion of oxygen appears to be inconsistent with the PORFLOW result that saltstone fractures are not completely saturated.

DOE Response Discussion:

The DOE response indicated that the transport of oxygen via the liquid phase is generally sufficient to keep the fracture faces near the oxygen solubility limit for Case C except at times less than 1,000 years, due to the very low flow through the cover system (and fractures) for those time periods. The impact of not addressing gas phase diffusion for Case E was considered minimal during the compliance period, since the FDC barrier is intact and effectively would maintain saturated conditions, thus supporting the assumption of saturated conditions being a barrier to gas-phase oxygen transport.

It is not clear to NRC staff that the transport of oxygen via the liquid phase for Case C is realistic or conservative as, (i) the flow of oxygen at early times may be underrepresented in the model due to very low flow through the fractures, (ii) the flow through the fractures in Case C remains low throughout the compliance period, and (iii) the difference between the transport of oxygen via the liquid phase and the gas phase may have an appreciable difference on the dose estimates. In regards to Case E, the impact of ignoring gas phase diffusion due to the performance of the FDCs resulting in saturated conditions is not appropriate as (i) the PORFLOW model appears to indicate saturation levels in the fractures for Case E at 40-50% and (ii) the performance of the FDCs as a hydraulic barrier should be reevaluated in light of recent hydrostatic tests (Comment VP-5).

Path Forward

Provide additional basis for neglecting gas-phase oxygen diffusion in cases representing fractured and degraded saltstone or provide updated dose estimates for cases representing fractured and degraded saltstone considering the potential effects of gas-phase oxygen diffusion.

RESPONSE SP-17:

The DOE has prepared Alternative Sensitivity Case K, which incorporates degraded saltstone and concrete that are assumed to fracture over time. Case K accounts for gas-phase oxygen transport through fractures and impacts on the chemical properties of reducing cementitious materials through time. The fracture spacing decreases through time and reaches 0.1 meter (10 centimeter or approximately 4 inches) at 10,000 years, corresponding to hundreds of fractures in each vault or FDC. Description of the progressive fracturing relationships and variation in oxidation through time are discussed in the response to RAI PA-8. Compared to Case C, Case K considers the effect of gas diffusion in far more fractures and assumes the dissolved oxygen concentration at fracture faces is always at the oxygen solubility limit.

Similar to Case E, Case K considers full hydraulic degradation of saltstone (although the specific properties and timing differ), but also assumes physical degradation of concrete. Thus, Alternative Sensitivity Case K provides information on the dose impact of gas-phase diffusion in fractures under even more pessimistic assumptions than either Case C or E. Even given the conservative assumptions of progressive fracturing and gas-phase diffusion of oxygen, the peak dose does not exceed 25 mrem/yr within the 10,000-year period of performance indicating that the concerns over: (i) low flow of oxygen at early times, (ii) the low flow throughout the compliance period, (iii) the difference between the transport of oxygen via the liquid phase and the gas phase, and (iv) the exclusion of gas phase diffusion when saturation levels may not be 100 % do not have an appreciable impact on the dose estimates.

The response to RAI VP-5 addresses the performance of the FDCs as a hydraulic barrier in light of recent successful hydrostatic tests following design modifications and concludes that the model is consistent with the expected final engineered condition and performance of the FDCs.

SP-18

Comment:

Additional justification is required for the uncertainty ranges used for K_d values in cementitious materials.

DOE Comment Discussion:

The DOE stated that the selection of the uncertainty distributions used for the K_d values were based on >730 K_d measurements of 8 radionuclides taken from 27 samples collected from the E-Area vadose and aquifer zones, as discussed in WSRC-STI-2008-00285. The provided reference indicated that the 27 depth-discrete samples were collected from a single borehole from E-Area. Variability in the distributions was attributed to general geochemical/geological differences in the site soils. The resulting data was used to estimate the statistical range and distribution of the K_d values for the studied radionuclides. Using these 8 radionuclides as analogues, the distribution coefficient variability was applied to >50 radionuclides. As site-specific cementitious K_d values were not available, the general rules for bounding the sandy sediment were applied to cement. This uncertainty range was considered conservative as SRS sediment is more heterogeneous than cementitious materials, which also contain fewer minerals than natural sediments.

NRC staff agrees that natural SRS sediment is likely more heterogeneous and has more minerals than cementitious materials; however, the heterogeneity and number of minerals does not dictate the potential range of K_d values. The relatively limited number of minerals in cementitious materials makes these materials less likely to have as large a range of K_d values as a natural soil; however, even two minerals with different surface chemistry can lead to significant variability. Research by Baur and Johnson (2003) demonstrated that the K_d for selenium can vary by more than two orders of magnitude depending on the cement phase.

The limited site-specific K_d data and an insufficient technical basis for adapting K_d values from sediment samples to cementitious materials results in significant uncertainty. An increase in the range of K_d values for cementitious materials over sediment samples is not a basis for uncertainty conservatism. Compensation for insufficient data by an increase in a parameter distribution range provides no additional confidence and it could (i) result an unnecessary degree of conservatism or (ii) result in risk dilution due to an artificial extension in the timing of arrival of a contaminant.

The lack of site-specific data demonstrates the importance of an appropriate base case such that a sensitivity and uncertainty analysis could inform research needs to evaluate the variability of data and reduce data uncertainty. Sorption of radionuclides to cementitious materials provides a significant barrier in the PA. Data support for these K_d values should be commensurate with the assumed risk reduction.

Path Forward

Depending on the extent to which DOE will rely on the GoldSim model, provide additional support for using the sandy-soil-based uncertainty distribution for cementitious materials K_d values and a basis for concluding that this approach does not underestimate uncertainty in radionuclide sorption to cementitious materials. For example, additional support could include laboratory analyses for risk-sensitive radionuclides. Plans for developing data support may provide appropriate basis, because NRC could verify the implementation of those plans in its monitoring role.

RESPONSE SP-18:

K_d measurements of nine radionuclides were obtained from 27 samples collected from the SRS E-Area vadose and aquifer zones. These nine radionuclides represent K_d values for eight elements in the SDF PA (K_d values for Co-57 and Co-60 were combined in WSRC-STI-2008-00285). [WSRC-STI-2008-00285, Figure 1 and Table 1] The variability, range, and distribution types (lognormal or normal) were assigned and statistical tests were conducted. The variability in the distributions is attributed to general geochemical and geological differences in site soils of the Upland Unit (SDF PA Section 3.1.4.2). Using these eight elements (nine radionuclides) as analogues, the distribution coefficient variability was applied to more than 50 elemental K_d values. Based on SRNL-STI-2009-00150, the uncertainty ranges used for K_d values in site soils are bounded as indicated in Table 5.6-5 of the SDF PA.

For sandy soils, it was assumed that the 95 % confidence level for the mean K_d was 1.5 times the mean, which is a combination of the range for the saturated zone and the Lower Vadose Zone. This would result in a calculation for the minimum ("Min") and maximum ("Max") values of the ranges as follows:

$$\text{"Min"} = K_d - (1.5 \cdot 0.5 \cdot K_d) = 0.25 \cdot K_d$$

$$\text{"Max"} = K_d + (1.5 \cdot 0.5 \cdot K_d) = 1.75 \cdot K_d$$

For clayey soils, it was assumed that the 95% confidence level for the mean K_d was 1.0 times the mean, which corresponds to the range for the Upper Vadose Zone. This would result in a calculation for the minimum and maximum values of the ranges as follows:

$$\text{"Min"} = K_d - (1.0 \cdot 0.5 \cdot K_d) = 0.5 \cdot K_d$$

$$\text{"Max"} = K_d + (1.0 \cdot 0.5 \cdot K_d) = 1.5 \cdot K_d$$

In general, isotopes in the interstratified clay and sandy saturated zone tend to exhibit the highest degree of variability followed by the silty/clay Upper Vadose Zone. Isotopes in the sandy Lower Vadose Zone, in contrast, have the tendency to exhibit the most consistency in K_d values. Isotopes in the sandy Lower Vadose Zone also have the tendency to display the lowest K_d values compared to those observed in the Upper Vadose and saturated zones. Finally, in general, the 95 % confidence window for the mean tends to be approximately one times the mean K_d in the silty/clay Upper Vadose Zone, 0.25 to 0.7 times the mean K_d in the sandy Lower Vadose Zone, and two times the mean K_d in the interstratified saturated zone for most isotopes. [WSRC-STI-2008-00285, Section 4.2]

DOE was not able to identify measurements in applicable literature that addressed the range of uncertainty associated with cement K_d values. While it is recognized that using data related to soil K_d values as a substitute for cement K_d values information is not optimal, the existing uncertainty approach used for soil K_d values was judged to be the best available approach given the lack of measured cement K_d uncertainty information. Given the relative similarity in mineral properties between soils and cementitious materials and the fact that the sandy soil ranges were the widest of the two soil ranges (i.e., wider than the clayey soil ranges), DOE believes the ranges of uncertainty of cement K_d values would be less than the ranges of K_d values in sandy soil and therefore, can be reasonably represented by the sandy soil ranges for the purpose of probabilistic modeling.

As part of SDF PA maintenance activities to address NRC TER factors (SDF PA Table 8.2-1), a long-range program plan for on-going testing of degradation mechanisms associated with cementitious hydraulic properties is being developed to identify additional field/lab testing and identify test methods and equipment. In particular, lysimeter studies will be conducted on saltstone and tank grout to determine reduction capacity, K_d values and solubility values for a suite of radionuclides/analogues including cesium, uranium, iodine, and technetium that are exposed to an outside environment. This effort, identified in Section 2.3.3.5 of *SRS Liquid Waste Facilities Performance Assessment Maintenance Program – FY2011 Implementation Plan*, SRR-CWDA-2011-00052, is anticipated to include 10 years of total exposure time with data available as soon as two years hence. Any future studies will be documented through the DOE M 435.1-1 required PA maintenance program.

SP-19

Comment (New):

Research related to the release of Tc-99 from saltstone appears to be inconsistent with the Tc-99 releases modeled in the PA.

Basis:

As discussed in WSRC-STI-2007-00056, experiments on Tc-99 leaching from saltstone simulated grout were conducted and the results incorporated into PORFLOW modeling. Figure 1 shows the modeled release of Tc-99 according to WSRC-STI-2007-00056 and the 2009 Saltstone PA. The modeled Tc-99 release for WSRC-STI-2007-00056 is approximately 60% over the 10,000-year compliance period for saltstone with a hydraulic conductivity of $1\text{E-}9$ cm/s, which is slightly less than the assumed hydraulic conductivity in the 2009 PA of $2\text{E-}9$ cm/s. According to the PORFLOW model files in the 2009 PA, the predicted release of Tc-99 from the saltstone material is 0.6% for the base case and 9.6% for the synergistic case.

The research presented in WSRC-STI-2007-00056 demonstrated the release of Tc-99 due to the presence of residual oxygen for an intact saltstone monolith. Residual oxygen would be consistent with field conditions at the SDF as would the transport of gas and liquid-phase oxygen to the fractured vaults and saltstone. In addition, the saltstone grout has been shown to be fractured which would increase the surface area-to-volume ratio, thereby increasing the oxidation of saltstone.

NRC staff recognizes that research is ongoing and that the results presented in Figure 1 below are based on a modeled system. However, this model is parameterized from experimental results conducted with a saltstone simulant whereas the shrinking core model utilized in the PA is less empirical. Additionally, some key parameters of the shrinking core model, such as the K_d are based on a formulation that is drastically different than saltstone (see SP-15).

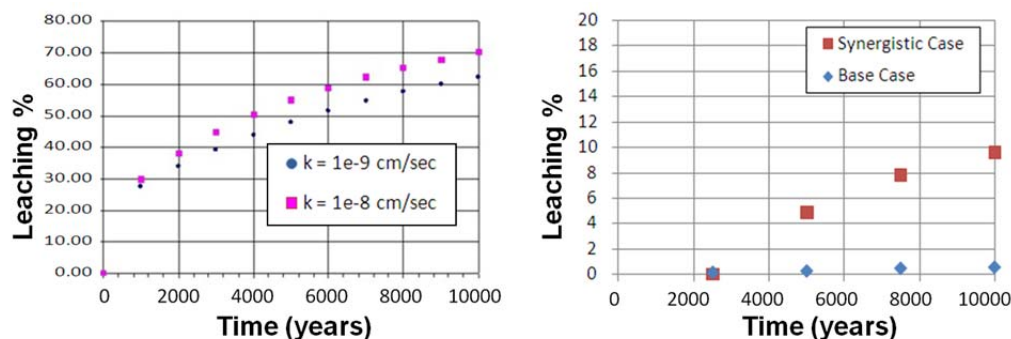


Figure 1: Tc-99 release over the 10,000-year compliance period based on results
(a) WSRC-STI-2007-00056 and (b) the 2009 PA model results

Path Forward

The PA should be consistent with relevant research or justification should be provided discussing why it was excluded. Provide any additional references on Tc-99 leaching from saltstone that have not already been provided to the NRC.

RESPONSE SP-19:

The research in WSRC-STI-2007-00056 contained sensitivity studies to provide insight into the increases in hydraulic conductivity and diffusivity of cementitious materials that must be achieved prior to significant release of Tc-99 from the waste form and from the disposal unit. The release of Tc-99 from saltstone and from the disposal cell is dependent not only on the hydraulic properties of the cementitious materials but also on the assumed infiltration rates. The estimated release of Tc-99 presented in Figure 1(a) of the Basis of this RAI demonstrates the release of Tc-99 based on a certain set of assumptions that are not indicative of the SDF closure system. The release of Tc-99 is highly dependent on the infiltration rate of water into the disposal unit and the value assumed in the analysis presented in WSRC-STI-2007-00056 is not indicated. However, based on Section 5.3 of WSRC-STI-2007-00056, PORFLOW modeling calculations were found to be equivalent to the calculations presented in WSRC-RP-2003-00362.

Review of WSRC-RP-2003-00362 indicates that the infiltration rate into the disposal unit was assumed to be a constant 40 cm/yr (15.7 in/yr) which is significantly larger than infiltration rate shown in SDF PA Table 3.2-7 that indicates the maximum infiltration rate through the closure cap is 10.6 in/yr, which does not occur until year 5,500. In addition, WSRC-STI-2007-00056 assumes a reduction capacity of 0.00925 milli electron equivalents per gram of solid (meq e-/g) for saltstone and disposal unit concrete. Electron equivalents are the units used to describe the concentration (more precisely, the activity) of free electrons that can participate in an oxidation-reduction, or redox, reaction. This reduction capacity is significantly less than the values used in the SDF PA analysis, 0.822 meq e-/g for saltstone and 0.240 meq e-/g for disposal unit concrete. The reduction capacities used in the SDF PA analysis are based on measured values of saltstone simulate and FDC concrete using representative mix recipes for these materials. [SRNS-STI-2008-00045] Thus, the Tc-99 release presented in the RAI Basis Figure 1(a) is not indicative of the current SDF closure system.

Additional insight into the release of technetium is provided via the Alternative Sensitivity Case K model, as described in the response to RAI PA-8. This modeling case evaluates a non-mechanistic model approach to a degraded saltstone condition to better understand system performance. In summary, the saltstone is assumed to degrade with a semi-logarithmic relationship with time so that within 10,000 years after closure the saltstone has a hydraulic conductivity (at all suction levels) of $1.0\text{E-}06$ cm/sec and a diffusivity of $5.0\text{E-}06$ cm²/sec, which are similar to soil conditions. In addition, fracture spacing within the saltstone monolith is assumed to occur in a semi-logarithmic relationship with time so that within 10,000 years after closure the saltstone monolith has a final fracture spacing of 10 centimeters at its fully degraded condition. This fracture spacing is utilized to simulate a shrinking core model for the release of technetium as the reducing capacity of the saltstone is depleted via oxidation. The initial reducing capacity of saltstone is assumed to be one-fourth of the SDF Base Case value or 0.206 meq e-/g, which is even less than the reducing capacity of the FDC concrete. This modeling approach is described in greater detail within the response to RAI PA-8.

For technetium in saltstone, the shrinking core model uses a maximum K_d value of 1,000 mL/g and a minimum K_d value of 10 mL/g to determine the time-dependent K_d values in the shrinking core model calculations (described in the response to RAI PA-8). The results of Case K indicate that Tc-99 is not a significant dose contributor within the first 10,000 years after closure. Two additional evaluations were performed to enhance understanding of the relative importance of the initial and final K_d values with respect to dose results. In these additional evaluations, all of the modeling parameters were held the same as in Case K, except for the bounding K_d values for technetium. The first evaluation (Case K1) used 500 mL/g and 0.8 mL/g for the initial

and final K_d values, respectively; whereas the second evaluation (Case K2) only modified the initial K_d value (using 500 mL/g instead 1,000 mL/g). Figures SP-19.1 and SP-19.2 provide the accumulated release of Tc-99 to the water table from Vault 4 and from an FDC, respectively for these three Tc-99 release cases.

Figure SP-19.1: Release of Technetium to the Water Table from Vault 4

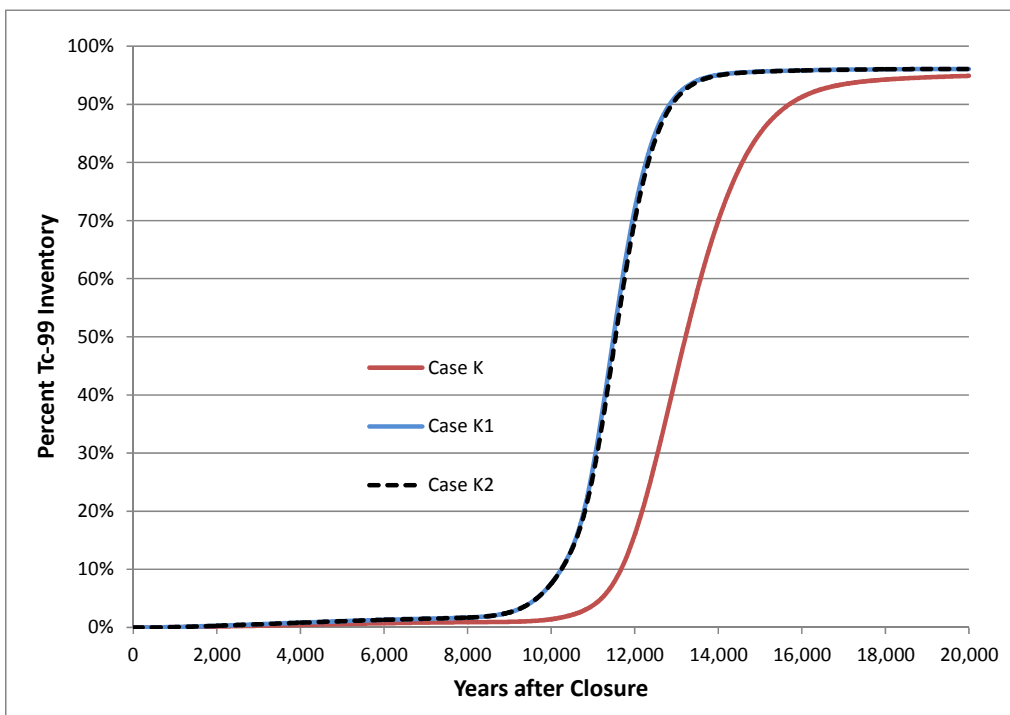
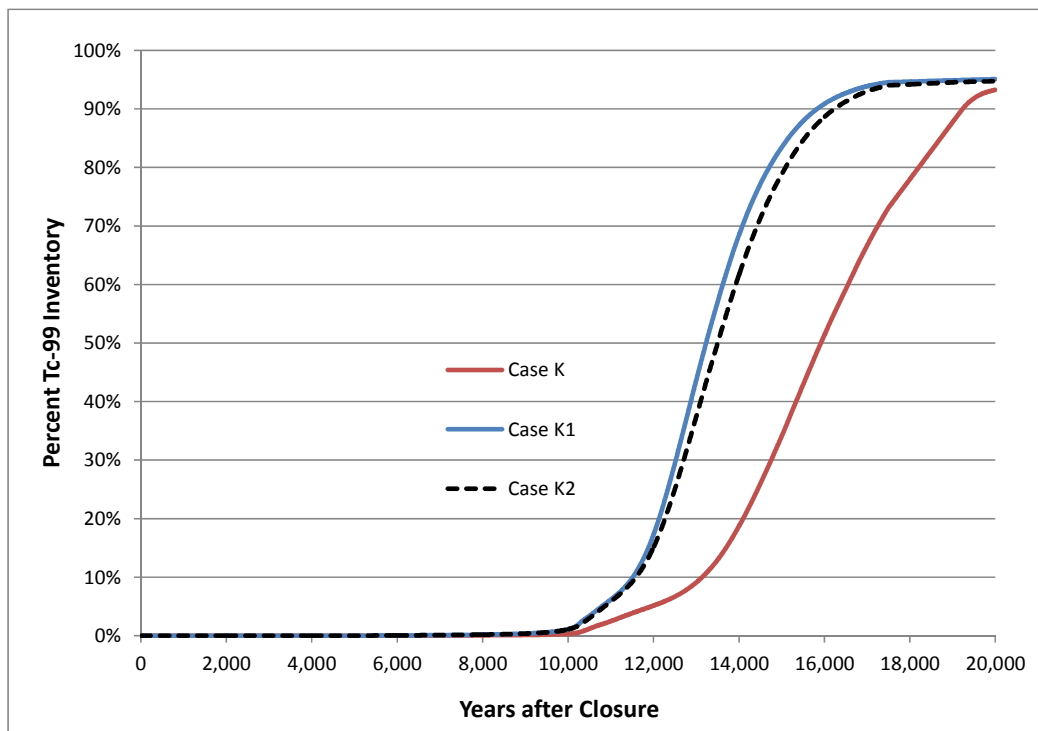


Figure SP-19.2: Release of Technetium to the Water Table from an FDC



Inspection of Figures SP-19.1 and SP-19.2 indicate that the Tc-99 release is more sensitive to the K_d value for reducing conditions than for oxidizing conditions. The difference between Alternative Sensitivity Case K (with an initial K_d value of 1,000 mL/g) and either Case K1 or Case K2 (both with an initial K_d value of 500 mL/g) is more pronounced than the difference between Case K1 (with a final K_d value of 0.8 mL/g) and Case K2 (with a final K_d value of 10 mL/g).

Figures SP-19.3 and SP-19.4 present final doses from the peak sector (Sector I) for the Alternative Sensitivity Case K and the two additional evaluations. Figure SP-19.3 shows the doses within 10,000 years of closure and Figure SP-19.4 shows the doses out to 20,000 years.

Figure SP-19.3: Sector I Dose Comparison for Alternative Sensitivity Case K and Additional K_d Sensitivity Evaluations, to 10,000 Years

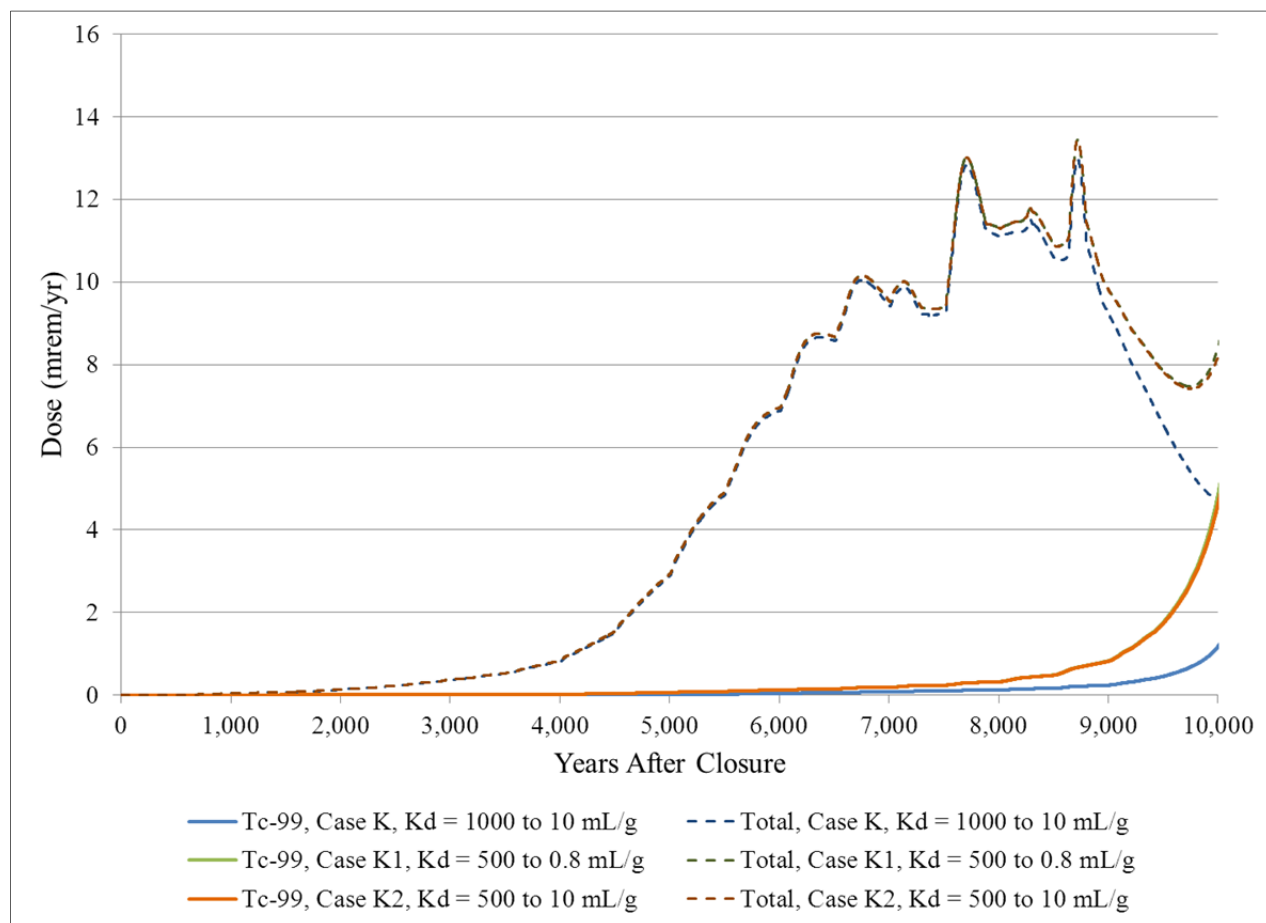
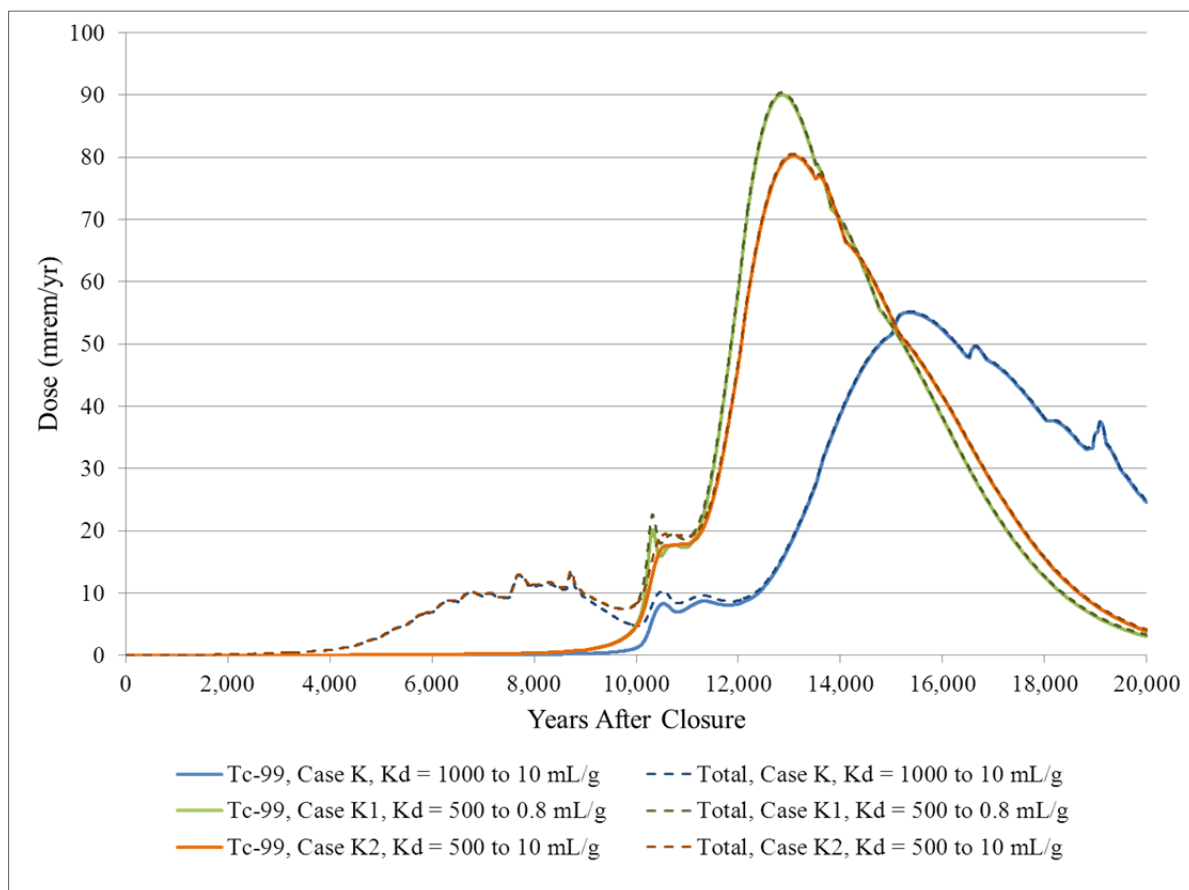


Figure SP-19.4: Sector I Dose Comparison for Alternative Sensitivity Case K and Additional K_d Sensitivity Evaluations, to 20,000 Years



Within the first 10,000 years after SDF closure, Tc-99 is not a significant contributor to the total dose for Case K or these additional evaluation runs. At the time of the peak dose (around 8,700 years), technetium contributes less than 2 % of the total dose for Case K and about 5 % of the total dose for the additional evaluations. At around 9,000 years after closure, this begins to change. Between 10,000 years and 20,000 years, Tc-99 is the most significant dose contributor, nearly 100 % of the total dose contribution for all three evaluations considered.

The most recent testing of technetium sorption is documented in SRNL-STI-2010-00668 and SRNL-STI-2010-00667. The testing results of saltstone simulant material are documented in SRNL-STI-2010-00668 and are summarized in the response to RAI SP-15. Testing conducted on samples of saltstone cored from Vault 4 is described in SRNL-STI-2010-00667 with results presented in SRNL-STI-2010-00667 as well as in SRNL-STI-2010-00668. The results from the testing of cored saltstone presented in SRNL-STI-2010-00667 indicate increased K_d values for technetium in young aged and middle aged oxidizing saltstone (from 0.8 mL/g to 10 mL/g) and decreased K_d values for technetium in young aged and middle aged reducing cementitious materials (from 5,000 mL/g to 1,000 mL/g). These, and other, updated K_d values are used in the Alternative Sensitivity Case K analysis presented in the response to RAI PA-8.

Additional testing is ongoing to provide further model support. In particular, various studies have been identified in the *SRS Liquid Waste Facilities Performance Maintenance Program – FY2011 Implementation Plan*, SRR-CWDA-2011-00052. These studies include:

1. The impact of saltstone formulations on reducing capacity (item 2.3.1.1)
2. Measurement of slag redoxidation stoichiometry (item 2.3.1.2)
3. Technetium solubility kinetics (item 2.3.1.3)
4. Technetium leach testing and K_d values and its distribution (item 2.3.1.4)

Vault Performance (VP)

VP-1

Comment:

Additional analysis is needed to assess the applicability of the degradation mechanisms responsible for the observed fracturing of Vaults 1 and 4 walls and the degradation mechanisms described in SRS-REG-2007-00041 to the FDCs and to other parts of Vaults 1 and 4.

NRC Response:

The DOE response is adequate at this time; the NRC staff is continuing to review several of the references that were provided by the DOE.

VP-2

Comment:

Additional basis is required for neglecting disposal unit degradation mechanisms other than sulfate attack.

DOE Response Discussion:

The DOE response contained two main elements: sensitivity analyses and ongoing research. A sensitivity case was provided with what DOE believes is pessimistic assumptions that demonstrated the doses would remain marginally below 25 mrem/yr. The DOE response did not address the NRC requests to address corrosion cracking or to provide analog information as technical basis (e.g. model support).

The response is mostly complete, but as previously indicated issues or uncertainties should be reflected in the base case and not in an alternative analysis case. For example, the analysis presented shows that the dose could approach 25 mrem/yr. Combined with any other issue that moderately increases the dose independently from this analysis, the performance objective could be exceeded. The original NRC comment provided many technical considerations that should result in modifications to the base case, based on DOE's currently available supporting information.

Path Forward

Update the base-case model to reflect the potential effects of applicable degradation mechanisms and their uncertainties based on currently available information.

Provide justification for neglecting other forms of degradation of disposal unit cementitious materials, including alkali silica reaction, corrosion cracking, and other relevant forms of degradation. The justification should address Vaults 1 and 4 floors and roofs as well as FDC walls, roofs, and floors.

If maintenance of an alkaline pH near steel components of the disposal units is relied upon to demonstrate steel passivity, the model generating predicted pH values should account for local effects near steel components (e.g., pH depression by carbonation in fractures near steel components) or address why such phenomena can be neglected.

A summary of observed reinforcement corrosion of concrete at SRS should be provided. Provide information to demonstrate that modeling of engineered systems in this application is consistent with observed performance of analogous systems at SRS.

RESPONSE VP-2:

Degradation of cementitious materials is dominated by internal sulfate attack emanating from the saltstone wasteform, as evaluated in the SDF PA (Section 4.2.3.2.4); however, as noted, reinforced concrete structures are susceptible to other degradation mechanisms depending on environment. Other degradation mechanisms observed in concrete structures include cracking from seismic events, settlement, and external static loading; carbonation or chloride ingress induced rebar corrosion; alkali-silica reactions; calcium leaching; freeze-thaw cycles; and microbial degradation. [NUREG-CR-5542]

Degradation analyses on existing aging concrete structures at SRS and other studies have provided data for use in the evaluation of potential degradation mechanisms for the saltstone disposal units during the timeframe of the SDF PA (i.e., 10,000 years). [T-CLC-P-00004; SRNL-L4420-2011-00008] The degradation mechanisms considered are not expected to exceed the

effect of sulfate attack from saltstone constituents within the disposal units as discussed below. Therefore, although they may contribute to the degradation of Vaults 1 and 4 and FDCs, they will not result in a large-scale difference in the degradation rate from the current degradation model; nor is it probable that the timing of these degradation mechanisms would result in the peak dose exceeding performance objectives within 10,000 years. The following supports that modeling of engineered saltstone systems is consistent with observed degradation and performance of analogous structures at SRS.

Cracking from Seismic Events, Settlement, and External Static Loading

The design of the FDCs includes significant amounts of carbon steel components (e.g., rebar, prestressing wires, diaphragms), and the roofs of Vault 4 and the FDCs have a significant number of carbon steel penetrations. Quality concrete has a very low hydraulic conductivity, typically about $1.0\text{E-}08$ to $1.0\text{E-}10$ cm/sec. The presence of just a few cracks, however, can increase the hydraulic conductivity by several orders of magnitude. Cracks in the concrete would allow water to penetrate beyond the exposed surface allowing degradation mechanisms to act on concrete and the steel components further inside.

The design of the FDCs includes a lateral seismic restraint system including wire pre-stressing for the concrete walls used to address potential movement during a seismic event. [T-CLC-Z-00022] As part of the overall vault and FDC design and construction process, an extensive soil investigation and backfilling study was performed and incorporated into the design calculations to address settlement and potential cracking. [WSRC-STI-2008-00244] In addition, the interior coating system of the FDCs is flexible enough to span and prevent macrocracks anticipated from overburden and the closure cap induced stress. [WSRC-TR-2008-00090]

The presence of macroscopic cracks in the exterior walls of Vaults 1 and 4 has been evaluated in SRNL-STI-2009-00115 and modeled in the Base Case by an increase in the hydraulic conductivity and the use of a developed characteristic curve for "fractured concrete." Therefore, cracking from seismic events, settlement, and external static load have been considered in the design and construction of the vaults and FDCs (T-CLC-Z-00022), and macroscopic cracks in the exterior vault walls are modeled in the SDF PA.

Carbonation

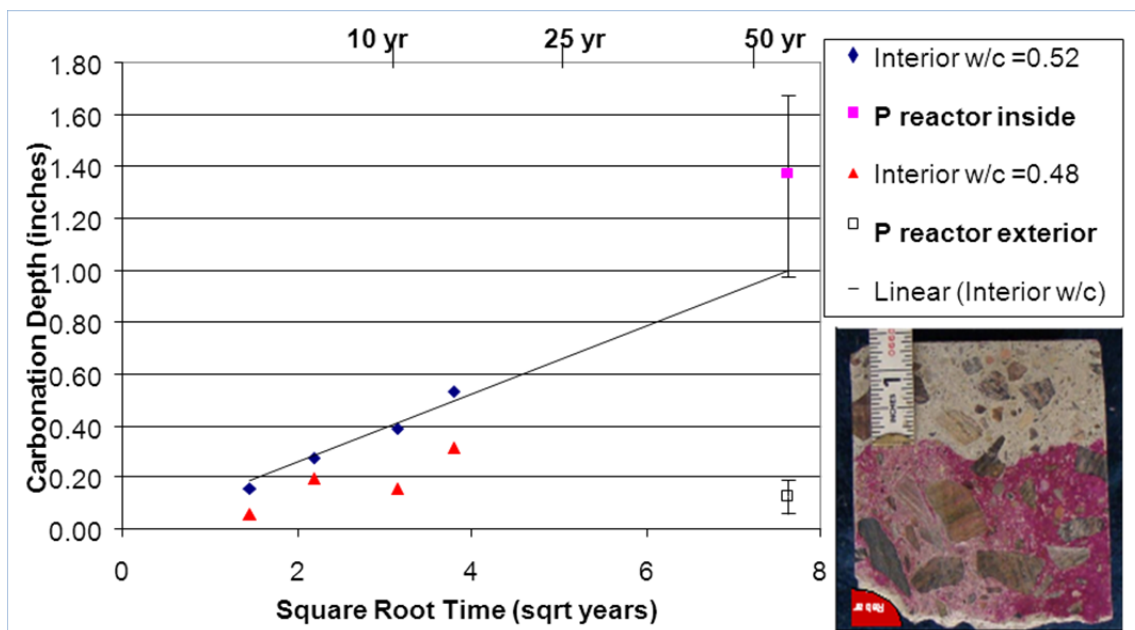
Carbonation is the reaction of carbon dioxide with portlandite ($\text{Ca}[\text{OH}]_2$ is one phase present in cement) to form calcium carbonate. In general, carbonation in itself does not cause degradation of the cementitious materials. In some cases, the formation of calcium carbonate may actually slow the migration of radionuclides through solid solution reactions. A negative side effect that occurs due to carbonation is a drop in pH towards neutral, from 12 to about 8. Typically, the reinforcing steel is protected by a thin passivating layer that forms in the alkaline (high pH) environment of the cementitious materials. This layer can break down if the pH significantly decreases due to carbonation, increasing the probability of rebar corrosion. [WSRC-STI-2007-00061]

Many factors can affect the rate of carbonation, including temperature, relative humidity, and composition of the cement paste. South Carolina has a hot, humid climate during the summer resulting in the cells having an extremely humid environment when curing. As relative humidity increases, the pores become saturated with moisture and the effective diffusivity of carbon dioxide is lowered. Carbonation rates for exterior exposure are generally lower due to the presence of more moisture (e.g., precipitation). In contrast, when concrete is kept dry at intermediate relative humidity, the pores can become less saturated, which allows carbon dioxide to diffuse more rapidly into the cementitious materials. Generally, the depth of

carbonation is roughly proportional to the square root of time the cementitious materials are kept continuously dry at ambient relative humidity. Hence, the carbonation rate is observed to maximize in conditions of low to moderate relative humidity typical of enclosed interior walls. [SRNL-L4420-2011-00008]

The 105-P building at SRS was constructed in the early 1950's. In 2008, an assessment was undertaken to evaluate the long-term integrity and condition of the 105-P reinforced concrete structure. [T-CLC-P-00004] Experimental results compared the carbonation depth of above grade P-Reactor concrete after approximately 60 years in conditions inside and outside of the same concrete wall (Figure VP-2.1). It was found that the carbonation rate for the interior sample far exceeds that of the exterior sample by an order of magnitude (1.4 inches versus 0.15 inches). The inset of Figure VP-2.1 shows the carbonation front of an interior P-Reactor sample. The carbonation front can be seen with the aid of a 1 % phenolphthalein solution applied to the concrete sample. When this solution is applied to normal concrete, it will turn bright pink. If the concrete has undergone carbonation, no color change is observed. An exterior surface exposed to the elements (like the current configuration of Vaults 1 and 4) should show minimal carbonation effect. [SRNL-L4420-2011-00008]

Figure VP-2.1: Plot of Average Carbonation Measurements for P-Reactor Interior and Exterior Specimens Relative to Carbonation Rates of Interior Concrete



[SRNL-L4420-2011-00008 Figure 1]

A buried concrete structure would be expected to have a much lower carbonation rate. This rate is due to the pores in the concrete remaining saturated and the carbonation rate is controlled by slower carbon dioxide diffusion in the liquid phase of the pore solution rather than vapor phase. Since the expectation is for Vaults 1 and 4 to be buried, the time required for the carbonation front to reach the rebar would be significantly longer than that of exposed concrete. A time interval for the concrete cover to be carbonated in the vaults can be extrapolated from the empirical rate measurement after 60 years for the P-Reactor. [SRNL-L4420-2011-00008 Figure 1] The estimate is in excess of 10,000 years. In addition, the outer layer of HDPE provides added protection for the sulfate resistant concrete roof of the FDCs. By comparison, the SDF PA predicted a similar length of time required to degrade the cover by sulfate attack.

Chloride Induced Corrosion

Chloride induced corrosion can cause localized de-stabilization of the passive film of iron oxide that would be present on reinforcement bars embedded in the concrete, and lead to pitting corrosion. If carbonation also reached the depth of the reinforcement bars, the oxide film on steel would have a tendency to dissolve, and gross steel corrosion would be expected, leading to eventual spallation. That is, chloride ingress alone would cause localized (e.g., pitting) attack, but with carbonation, gross steel corrosion could occur.

Chloride attack has been modeled as a two-step mechanism. The first step is the initiation time to the onset of corrosion due to chloride diffusion to the rebar. This initiation time can be given by an empirical equation. [NUREG-CR-5542, Equation 1]

$$t_c = \frac{129X_c^{1.22}}{(WCR)[Cl^-]^{0.42}}$$

t_c	=	time to onset (yr)
X_c	=	thickness of concrete cover (in)
WCR	=	water-to-cement ratio (mass)
Cl^-	=	Cl^- ion concentration at surface of concrete (ppm)

With an assumed concrete cover of 3 inches, a water-to-cement ratio of 0.36, and a chloride ion concentration of 3.3 parts per million (an estimate of ground water concentration), the initiation time of rebar pitting is approximately 790 years (530 years for water-to-cement ratio = 0.56). This does not consider various additives utilized to reduce permeability in the concrete to chlorides. [SRNL-L4420-2011-00008]

Vaults 1 and 4 are currently exposed but will be buried below grade during the timeframe of active corrosion. Once the structure is filled with saltstone and buried, the rebar no longer supports the load for which it was designed but is supported by the backfilled soil/saltstone on either side of it. The corrosion rate, in the case of a buried structure, is limited by oxygen diffusion and degradation will occur at a much lower rate than that of exposed concrete. An oxygen source and water are necessary for the active degradation of the reinforcement bar by general corrosion that can lead to loss of tensile strength and concrete spallation. Such an oxygen/water supply can occur through macrocracks in the concrete, which can result from mechanical stresses and/or the combined effects of CO_2 , Cl^- , and O_2 species.

A simplified model for rebar corrosion can be utilized to estimate the amount of rebar section that remains after a given exposure. [NUREG-CR-5542 Equation 7]

$$\% \text{ remaining} = 100 \left(1 - \frac{4 \left(9.4 \frac{cm^3}{mole} \right) s D_i C_{gw} (t - t_c)}{\pi d^2 x_c} \right)$$

where:

s	=	spacing between reinforcing bars
D_i	=	oxygen diffusion coefficient in concrete (cm ² /sec)
C_{gw}	=	oxygen concentration in groundwater
T	=	time (sec)
T_c	=	time to onset of oxid corrosion (sec)
D	=	diameter of rebar (cm)
X_c	=	thickness of concrete cover over rebar (cm)

Assuming an intermediate value for oxygen diffusion coefficient in concrete (5.0E-08 cm²/sec), 1-inch diameter (2.54 centimeters) rebar, at 1-foot spacing under a 3-inch (7.62 centimeters) concrete cover, and a time to onset of corrosion of 800 years, the length of time required to reduce even 5 % of the rebar section is over 6,000 years, and 10 % reduction is over 10,000 years. [SRNL-L4420-2011-00008] The effect of this potential physical degradation is cracks from the roof through the floor forming preferential or fast flow paths that allow contact with waste-bearing saltstone directly. Case scenarios have been conceptually identified and modeled in the SDF PA to better understand the variability of possible disposal unit behavior.

Samples of concrete used in the construction of FDCs were collected from Disposal Unit 2 for analysis to verify that the materials used in the field meet or exceed materials properties identified in the PA testing. [SRR-CWDA-2011-00052] Verification of FDC material properties and degradation mechanisms is anticipated as part of an overall performance verification process. This activity is expected to validate the hydraulic and physical properties assumed for the disposal units in the SDF PA and develop correlation between laboratory-cured samples and field-cured samples.

Controlling the composition of the cement paste can reduce oxygen diffusion and degradation. Silica fume, also known as microsilica, is a byproduct of the reduction of high-purity quartz with coke in electric arc furnaces. Silica fume is used as an additive in Portland cement concretes to improve compressive strength, bond strength, and abrasion resistance. Addition of silica fume also reduces slag oxidation by reducing the permeability of concrete, which has the effect of protecting concrete's reinforcing steel from corrosion cracking and the formation of fast flow paths.

In addition, the Class III sulfate resistant concrete of the FDCs (upper mud mat, floor, walls, and roof) do not come in direct contact with soils. As indicated in SDF PA Section 3.2.1.3.2, a minimum 4-inch thick lower concrete mud mat is laid directly on the soil and is overlaid by a geosynthetic clay liner and 100-mil HDPE liner. The upper mud mat and floor is poured on top of these components. The cell wall is surrounded by a steel shell, which is covered by shotcrete and followed by a 100-mil HDPE liner. The FDC cell roof will also be covered with a 100-mil HDPE liner. Thus, the soil backfill does not contact the Class III sulfate resistant concrete, which precludes chemical corrodents in the soil from attacking the exterior of the FDCs.

Alkali-Silica Reactions

Alkali-Silica reactions occur between reactive silica present in aggregates and alkali constituents (e.g., Na⁺, K⁺) in the cement phase(s). In similar fashion to sulfate attack, the alkali constituents form a gel at the aggregate/cement interface, which can cause expansion and cracking to occur over time. Water, reactive silica, and alkali constituents must be present in

cementitious materials for alkali-silica reaction to occur. Sand (a common fine aggregate) is composed of quartz, but is usually not reactive because it is what is left behind from mechanically and chemically degraded rock.

Alkali-silica reaction has not been documented in other SRS concrete structures on-site. In order to verify the occurrence of alkali-silica reaction, petrography must be performed on samples to identify the gel reaction zones. Petrographic testing was performed on the concrete samples taken from both the exterior and interior of the F- and H-Canyon structures. The testing indicated that the alkali-silica reaction was not present and only minor carbonation had occurred. Efflorescence was observed in local areas, but no rust stains were observed that would indicate corrosion of the reinforcing steel. [T-CLC-P-00004]

Although a detailed analysis has not been performed on concrete from Vaults 1 and 4, the likelihood of alkali-silica reaction resulting in degradation of the structure is believed to be low for the following reasons. First, the aggregate is igneous in nature (e.g., granite) with high nonreactive quartz content. In addition, because Vaults 1 and 4 have been exposed to elements since their construction, the degradation of these vaults by alkali-silica reaction should be evident (22 years later) considering the environmental exposure. The lack of physical evidence suggests that alkali-silica reaction is not a prevalent cause of degradation. The consequences of a synergistic degradation process, for example, simultaneous exposure to sulfate plus other chemicals, such as alkalis and hydroxide, may be obtained from continued exposure testing. [SRNS-STI-2008-00050] At this time however, exposure testing has resulted in negligible damage because of the high quality of the concrete.

Calcium Leaching

Cement components can be leached from cementitious materials only when water passes over the surface or through cracks. Specifically, calcium compounds in the concrete can be dissolved in unsaturated water and washed away. Since the most readily soluble calcium compound in concrete is calcium hydroxide (lime), water can leach lime from concrete. When calcium hydroxide is leached away, other cementitious constituents become exposed to chemical decomposition, eventually leaving behind silica and alumina gels with little or no strength. The extent of the leaching depends on the salt content and temperature of the water. In the present climatic environment, this mechanism is not expected to be a significant occurrence because of the temperature ranges of exposure. [NUREG-CR-5542]

Both sophisticated and simplistic models suggest that leaching beyond the very surface of the concrete requires thousands of years. For example, for the average Ca^{2+} concentration of 3.8 mg/L in the groundwater around 105-P, leaching would have only occurred in the outer 0.05 centimeters of the concrete. [T-CLC-P-00004] In addition, NUREG-CR-5542 determined leach penetration rates for groundwater with low calcium contents to be less than 0.1 of a centimeter at 1,000 years.

Modeling of cementitious material degradation is supported by ongoing field observations and laboratory testing performed by SIMCO Technologies personnel. SRNS-STI-2009-00477 describes laboratory testing performed on saltstone wasteform simulates, and comparison to STADIUM computer model predictions. The testing indicated "the durability (stability) of the saltstone matrix upon immersion in water was found to be better than that of Portland cement paste with a similar water to cement ratio and a lower total porosity." The testing also indicated that the code predictions for cement leach rates were similar to tested materials for the short duration of exposure, and sulfate in the extracted pore solution exhibited a higher concentration than that modeled in the SDF PA.

Based on these observations, leaching of calcium from contact with ground water is not anticipated to be significant in saltstone disposal units.

Physical Process such as Freeze-Thaw Cycles

Repeated cycles of freezing and thawing may change the mechanical properties and physical form of concrete. The durability of concrete to freeze/thaw mechanisms depends primarily on the porosity characteristics of aggregates, the presence of moisture to saturate the fine pores in aggregates, and the permeability of the hardened cement matrix to the passage of water. The source of moisture can be either internal (water already in the pores of concrete) or external (water entering the concrete from an external source, such as rainfall). For conventional mixtures, the durability has been accomplished by the use of a low water to cement ratio combined with adequate curing to ensure a minimum compressive strength before exposure to possible cycles of freezing and thawing. [NUREG-CR-5542]

The likelihood of damage from freeze/thaw cycles on saltstone disposal units is minimized by reducing the amount of freezable water in concrete. Vault and FDC concrete has the potential to be exposed to freezing conditions for short durations during the construction and operational life of the unit. The concrete itself has a low hydraulic conductivity so rainwater infiltration adds little to the internal water available to freeze during construction. After the operational life, the disposal units will be surrounded with backfill and a closure cap installed so that exposure to freezing conditions is not a concern for buried structures in the region. [WSRC-STI-2008-00244] The 100-mil HDPE precludes significant infiltration of rainwater for much of the 10,000-year compliance period. Furthermore, global climatic changes are not expected to impact the area to the extent that freeze/thaw degradation becomes a viable mechanism for breakdown of buried concrete structures. [SRNL-L4420-2011-00008]

Degradation by Microbial Organisms

Microbial organisms present in the environment could promote damage to cementitious materials and is an area of further review and research. A literature review of relevant literature currently published is planned to assess the relevant microbial species, key variables, conditions, growth factors, and kinetics on both saltstone and disposal unit materials, and develop recommendations for follow-up experiments. [SRR-CWDA-2011-00052]

Investigations on mechanisms of cementitious material degradation and mitigation of the effects of chemical reactions and corrosion cracking are ongoing. The Cementitious Barriers Partnership project a multi-disciplinary partnership of federal, academic, private, and international expertise are investigating cementitious degradation mechanisms. The partnership project's objective is to develop tools to improve understanding and prediction of structural, hydraulic, and chemical performance of cementitious barriers used in nuclear applications. Testing provides physical data and observations to inform future modeling and provides a means to study the impacts of multiple potential degradation mechanisms.

The deterministic Base Case of the SDF PA was developed using reasonably conservative, best-estimate assumptions (most probable modeling parameters) whenever possible. DOE maintains that uncertainty analyses and sensitivity analyses are appropriate approaches for assessing risks associated with various degradation mechanisms because of incomplete physical understanding of disposal unit structural response to differential settlement and corrosion of steel components due to uncertain future conditions. A true risk-informed PA will utilize this fact to determine where uncertainty is most significant and where additional degradation analysis and modeling emphasis should be placed. For example, an update to the SDF PA synergistic case (Case K, RAI PA-8) shows that when "fractured" concrete fully

degrades to soil properties within 10,000 years, with a saturated hydraulic conductivity of $1.0\text{E-}06$ cm/sec, and an effective diffusion coefficient of $5.0\text{E-}06$ cm²/sec, the performance objectives are still met.

Further work described in the SDF PA Section 8.2 recognizes the importance of understanding and modeling the potential for increased hydraulic degradation of the disposal unit floors, walls, and roofs in the Base Case. PA maintenance activities (SRR-CWDA-2011-00052) include the development of long-range program plans for on-going testing and research activities of 1) degradation mechanisms associated with cementitious hydraulic properties, 2) moisture flow through fractures, 3) modeling of waste oxidation, and 4) the extent and frequency of fractures in saltstone and disposal units. If new information regarding modeling assumptions show a different approach or value is more probable or appropriate, updates to the Base Case, as well as updated parameter distributions used in the uncertainty and sensitivity analyses, shall be considered and applied as appropriate.

VP-3

Comment:

The effect of modeling disposal unit floors as completely reducing for the entire performance period, and beyond 20,000 years, should be analyzed

DOE Response Discussion:

The DOE response stated that the exposed surfaces of the vault concrete floor begin oxidizing at time zero. The chemical transition times for the various cementitious materials were presented in Table 4.2-17 of the PA, as computed in PORFLOW except for the shrinking core simulations. The shrinking core model explicitly simulated the oxidation of saltstone and the vault concrete for Tc-99 simulations.

The shrinking core model represents a uniform oxidation front with an unreacted core. Rapid transport of redox-sensitive radioelements (e.g., Tc-99) through the oxidized region would occur followed by immobilization once the radionuclide reached the core. However, a fracture in the vault floors would quickly result in a non-reducing fast pathway. It is not clear that DOE has conducted adequate characterization of the floor to support the assumption that the floor is not fractured (initially or at any future time) in the base case. Based on the demonstrated floor performance of Vault 2 (due to cracking near anchor bolts) during recent hydrotesting, it is also not clear that the assumption of no fractures in the floors of Vaults 1 and 4 in the base case is realistic as Vaults 1 and 4 floors also contain anchor bolts. NRC staff understands that Vaults 1 and 4 floors are 24 inches thick versus 8 inches thick for the Vault 2 design which may affect the potential for fracturing at the anchor bolt sites.

Path Forward

Vault floor fractures should be included in the base case or provide a technical basis for not including this feature in the base case in light of limited vault floor characterization and the performance of the FDCs.

RESPONSE VP-3:

The deterministic Base Case of the SDF PA was developed using reasonably conservative, best-estimate assumptions (i.e., most probable modeling parameters) whenever possible. The Base Case reflects the expected condition where intact disposal unit concrete and saltstone lead to a diffusion-dominated release, prior to the cover system and the disposal units becoming significantly degraded. DOE does not believe that vault floor fractures should be included in the Base Case in light of current fracture analysis and recent vault floor observations. The probabilistic model and deterministic alternative modeling cases are provided as tools to inform on uncertainty associated with fracturing assumptions that were possible on an individual assumption basis (although less probable than the Base Case and often non-mechanistic when coupled with other assumptions) to assess the effects of deviations from the best-estimate Base Case assumptions.

DOE maintains that uncertainty and sensitivity analyses are appropriate approaches for assessing risks associated with vault floor fracturing because of uncertainty in both the materials physical properties, such as corrosion of steel components, and future conditions, such as differential settlement. A true risk-informed PA utilizes this fact to determine where uncertainty is most significant and where additional analysis and modeling emphasis should be placed. Investigations of potential vault fracturing and mitigation of the effects of fracturing are ongoing. If new information regarding modeling assumptions or parameters demonstrates a different approach or value is more updated than the Base Case then it will be considered and

applied, as appropriate. In the response to RAI PA-8 an additional sensitivity case, Alternative Sensitivity Case K, is described and analyzed that includes very pessimistic assumptions on the degradation rate of cementitious materials, saltstone and disposal unit concrete, within the SDF closure system.

The Base Case assumes that the floors of the disposal units are initially intact. Two recent evaluations of testing, design modifications, and observations of actual floor conditions, coincident with NRC onsite observations conducted under NDAA Section 3116, demonstrate that the disposal unit floor conditions remain within the parameters used in the Base Case. The first evaluation involves testing and design modifications to disposal units under construction, and the second evaluation involves assessment of existing conditions within the operational Vault 4.

The first evaluation is an example of testing and modification of disposal units that are under construction and not ready for use. NRC reviewed the results of preliminary water tightness testing conducted on Disposal Units 2A and 2B. During the preliminary testing, dyed water observed between the bottom of the floor and the top of the upper mud mat. This evidence indicated that there was a reasonable probability that the anchor bolt penetrations installed in the floor of the disposal unit to accommodate the drainwater collection piping were a potential pathway for liquid flow. Following this testing, the anchor bolt penetrations in Disposal Units 2A and 2B were cut flush with the floor, and an interior coating applied. In addition, an exterior Class III sulfate resistant curb was installed around the perimeter of the floor. Subsequent water tightness testing did not display evidence of dyed test water outside of the disposal units. To ensure that a continuous concrete barrier is present at the bottom of 2A and 2B an additional 14 inches of Class III sulfate resistant concrete was installed above the coating layer. This additional cell floor does not have any penetrations including anchor bolt penetrations. These corrective actions are to ensure that the construction and operation of the disposal units comply with the Base Case modeled in the SDF PA. [SRR-CWDA-2011-00043]

The second evaluation represents an evaluation of existing conditions within an operational disposal unit (Vault 4). During their July 2010 Salt Waste Monitoring Onsite Observation of Disposal Unit 2, NRC recommended that SRR assess the drainwater collection piping system anchor bolt penetrations in the Vault 4 floor to determine whether installation may have induced cracking or voids similar to those postulated in Disposal Unit 2. On March 29, 2011 SRR entered Vault 4, Cells B and H to inspect drainwater system anchor bolts for evidence of voids or cracking at the embed locations. The inspection revealed no cracking or voids in the visible areas of bolt embed. [SRR-CWDA-2011-00097]

Plans and procedures have been developed to perform regular visual disposal unit inspections to identify any structural deterioration (i.e., cracks, chips, fragments, leakage, moisture areas, etc.) or surrounding area wear (soil erosion, weeds, etc.) that may require evaluation. A review of Vault 4 cell entry pictures, floor slab design drawings, and groundwater monitoring data have not revealed any information to justify an alteration to the manner in which the vaults and FDCs were modeled in the SDF PA revision currently under NRC review. Consistent with the existing UDQE process and procedures, future observations of saltstone vault conditions will be evaluated as they become available.

Future disposal units will not be placed into service until the engineered barrier capabilities, consistent with the SDF PA, are valid. To mitigate deficiencies demonstrated during the hydrostatic tests on Disposal Unit 2, significant design modifications have been implemented to ensure that the disposal units comply with the Base Case assumptions. Furthermore, the lessons learned during construction of Disposal Unit 2 are being incorporated into the design and construction of future disposal units, including Disposal Units 3 and 5, which are currently under construction. For example, plans for future disposal units do not include anchor bolt penetrations in the floor of the FDCs.

VP-4

Comment:

The effects of the potential inventory in Vaults 1 and 4 floors on radionuclide release should be analyzed.

NRC Response:

The response is adequate. NRC staff agrees that the potential initial inventory in the floor is likely to be relatively small and not risk-significant.

VP-5

Comment (New):

The uncertainty in the performance of the vaults is not adequately represented in the PA and the PORFLOW model.

Basis

Recent hydrostatic tests for Vault 2, Cells 2A and 2B have demonstrated the complexities and uncertainties regarding the hydraulic integrity of engineered barriers. Discrete engineering features that can drive system performance are not captured within the PA. Features such as material interfaces, the vault liner coating, and anchor bolts led to unanticipated vault performance (SRR-CWDA-2010-00099). DOE has taken steps to eliminate the issues regarding these features; however, the unanticipated leak test results are indicative of optimistic performance assumptions regarding the hydraulic properties of the FDCs, as well as Vaults 1 and 4. The long-term performance of these engineered barriers has uncertainty that is not adequately represented in the PA.

The discrete features that have driven the performance of Cells 2A and 2B in the hydrotests are not currently incorporated into the PORFLOW analysis. Accordingly, the model would be inadequate with respect to the representation of these failures. The PORFLOW model does not include the potential for discrete failures beneath the anchor bolts, flawed liner coatings, or the discrete material interfaces.

Based on conversations with SRR staff, the recent FDC leaks are not considered significant to the performance of these vaults and they do not significantly impact the conclusions of the PA; the presence of engineered barriers such as the shotcrete and the HDPE-GCL around the FDCs provide a defense in depth. Due to the additional reliance on these engineered barriers and very limited performance data for the relatively unique applications of these barriers, additional model support would provide necessary confidence. Additionally, it is not clear that the HDPE/GCL was a completely redundant barrier i.e., the expected flow and transport through the HDPE/GCL may be correlated to the performance of FDCs.

Path Forward

Provide a technical basis demonstrating that recent events and discrete features will have a negligible impact on the dose results. This may include demonstration that barriers in addition to the FDC vaults will provide compensatory performance, such that the conclusions of the PA are not affected by (i) the observed performance of the FDCs to date and (ii) reasonably expected future performance.

Alternatively, reevaluate the expected performance of Vaults 1, 2, and 4 in light of evidence demonstrating the significance of discrete features. Reevaluation of vault performance may indicate that these discrete features should be incorporated into PA models.

RESPONSE VP-5:

The deterministic Base Case model represents the best estimate or most probable performance of the disposal units. Performance of alternative modeling cases including uncertainty, variability, and sensitivity analyses were evaluated probabilistically (GoldSim) and through alternative deterministic modeling cases. DOE uses results from this hybrid modeling approach to provide reasonable assurance that the performance objectives will be met.

Consistent with the Base Case configuration, new disposal units will not be placed into service until the engineered barrier capabilities consistent with the SDF PA are valid. In order to

mitigate the deficiencies demonstrated by the hydrostatic tests for Disposal Unit 2 (referenced in the NRC's comment), significant design changes have been implemented to compensate for the initial construction deficiencies prior to placing cells into service. This includes adding new construction interface materials (e.g., exterior curbing) and adding new interior "clean" grout pours prior to accepting the units for operations. [SRR-CWDA-2010-00137] Tank water tightness test reports have concluded that Cells 2A and 2B have successfully passed hydrostatic testing, demonstrating that the implementation of the design changes have mitigated these construction deficiencies. [WB00001K-058] The lessons learned during the construction of Disposal Unit 2 are being incorporated into the design and construction of the future disposal cells including Units 3 and 5, which are currently starting construction.

The items noted in the path forward were supplied as part of the response to RAI VP-1 in SRR-CWDA-2010-00033.

Note that Vaults 1 and 4 have been modeled in the SDF PA with cementitious material properties that reflect the known conditions (i.e., increased hydraulic conductivity to simulate the fractured concrete associated with the macroscopic cracks), as described in Sections 4.2.3.2.4 and 4.4 of SRR-CWDA-2009-00017.

VP-6

Comment (New):

The bypassing of flow through Vaults 1 and 4 walls may not have a physical basis.

Basis:

In Section 5.6.3.1, DOE discussed the result of water preferentially flowing through the vault walls and around the saltstone wasteform, which is due to the hydraulic model parameters for the Saltstone vaults and wasteform. The hydraulic conductivity of the walls for Vaults 1 and 4 for all cases in the PA is 4 orders of magnitude greater than that of the backfill or native soil. Although degrading the vault walls is locally conservative, globally the result is non-conservative. If there is not a physical basis for the walls to hydraulically degrade to the extent discussed in the PA, then the flow through the saltstone wasteform would be underestimated.

Path Forward

Provide additional support for the assumed hydraulic conductivity of the degraded Vaults 1 and 4 walls that result in the modeled bypassing of flow around the saltstone wasteform.

RESPONSE VP-6:

The SDF PA applies best estimate assumptions in the development of the Base Case model. These assumptions accounted for observed weeping conditions in the walls of Vault 1 and 4 by simulating fractured flow through these walls (see SDF PA Sections 4.2.3.2.4 and 4.4.1). The hydraulic conductivity of the vault walls is based on a fracture model presented in Section 3.7 of SRNL-STI-2009-00115, and uses the concrete degradation model presented in Section 3.5 of SRNL-STI-2009-00115. Figure VP-6.1 illustrates the hydraulic conductivity of backfill soil and the walls of Vaults 1 and 4 at various times after closure based on the fracture and concrete degradation models. According to SDF PA Section 4.4.4.1.2, GSA soil suction ranges between 50 centimeters and 200 centimeters.

To address, in part, the question pertaining to the bypassing of flow around the saltstone wasteform Alternative Sensitivity Case K was developed and is presented in the response to RAI PA-8. In Case K the walls of Vaults 1 and 4 are assumed to be initially degraded such that the hydraulic conductivity is set equal to $1.0\text{E-}06$ cm/sec, which is similar to the hydraulic conductivity of backfill soil. Figure VP-6.2 illustrates the hydraulic conductivity for the walls of Vaults 1 and 4 and backfill soil used in Case K. As shown in Figure VP-6.2, the use of a constant value of $1.0\text{E-}06$ cm/sec for the hydraulic conductivity of the walls of Vaults 1 and 4 is considerably more similar to the hydraulic conductivity associated with backfill soil at the expected suction levels.

In addition to the initially degraded walls, Alternative Sensitivity Case K also degrades the saltstone more quickly than in Base Case, such that the saltstone reaches complete hydraulic degradation by 10,000 years. Like the walls, the saltstone is simulated with an initial hydraulic conductivity that is greater than in Base Case and flow through the Case K saltstone has an initial velocity that is more than one order of magnitude faster than in Base Case. The degraded conditions of these material properties in the alternative sensitivity model have a significant effect on the PORFLOW-generated flow profiles.

Figures VP-6.3 and VP-6.4 present the flow profiles for Vaults 1 and 4, respectively, from both the Base Case and Case K (for the walls and the saltstone wasteform). These figures show that the difference in flow velocity between the wall and the saltstone is roughly two to three orders of magnitude throughout most of the simulated duration for the Base Case. Alternatively,

for Case K the difference begins at about two orders of magnitude then as the saltstone degrades the difference between the wall flow velocity and the saltstone flow velocity gradually diminishes until both have similar velocities. At this point, flow is no longer preferentially channeled through the vault walls (i.e., bypassing the saltstone wasteform). Thus, the pessimistic assumptions applied to Case K demonstrate the effects of flow through the wasteform.

The dose results from Case K, as presented within the response to RAI PA-8, show that even when applying overly pessimistic assumptions, with respect to generating the Case K flow profiles, the peak dose within the compliance period still meets the performance objective of 25 mrem/yr (i.e., the Case K peak dose within 10,000 years is 13.0 mrem/yr).

Figure VP-6.1: Hydraulic Conductivity of Walls for Vaults 1 and 4 and Backfill Soil (PA Analysis)

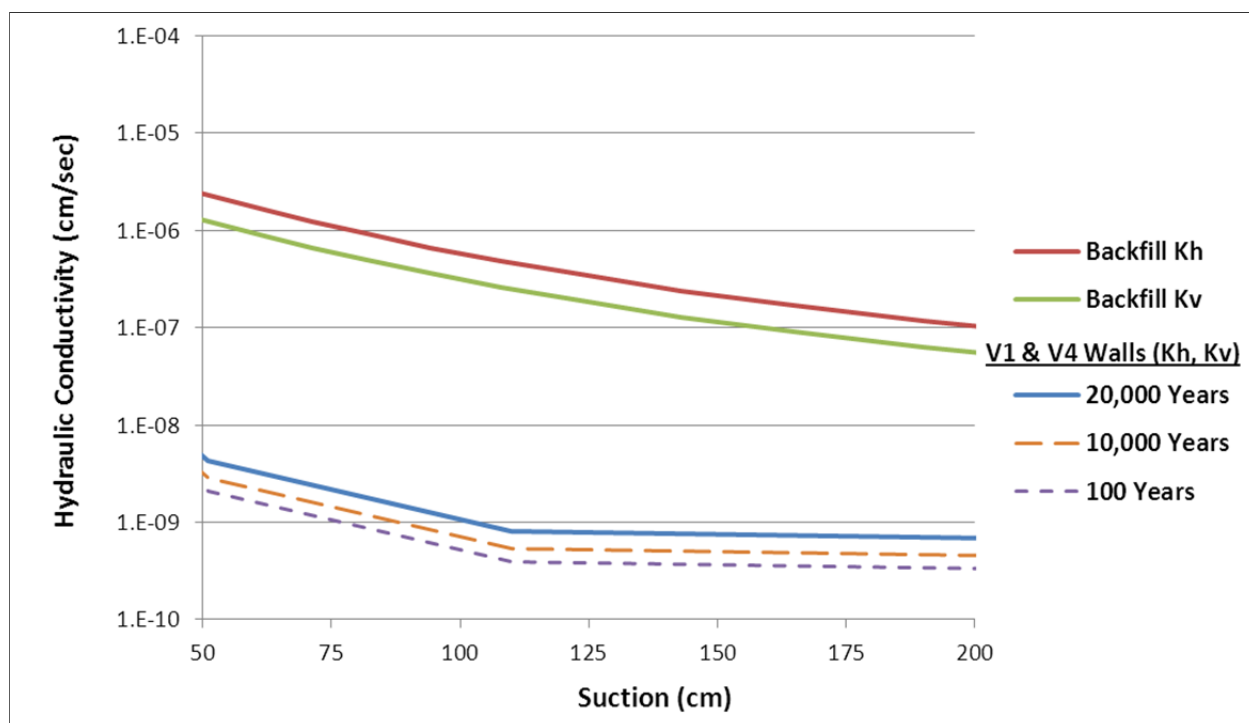


Figure VP-6.2: Hydraulic Conductivity of Walls for Vaults 1 and 4 and Backfill Soil (Case K)

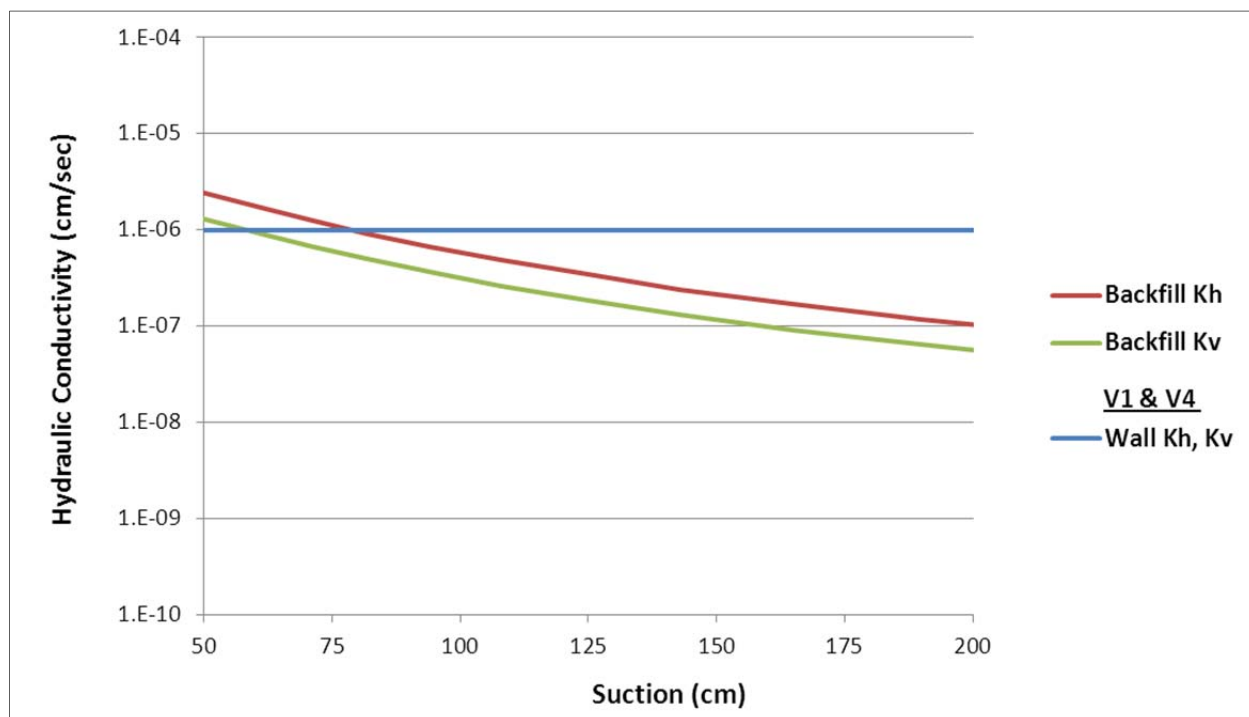
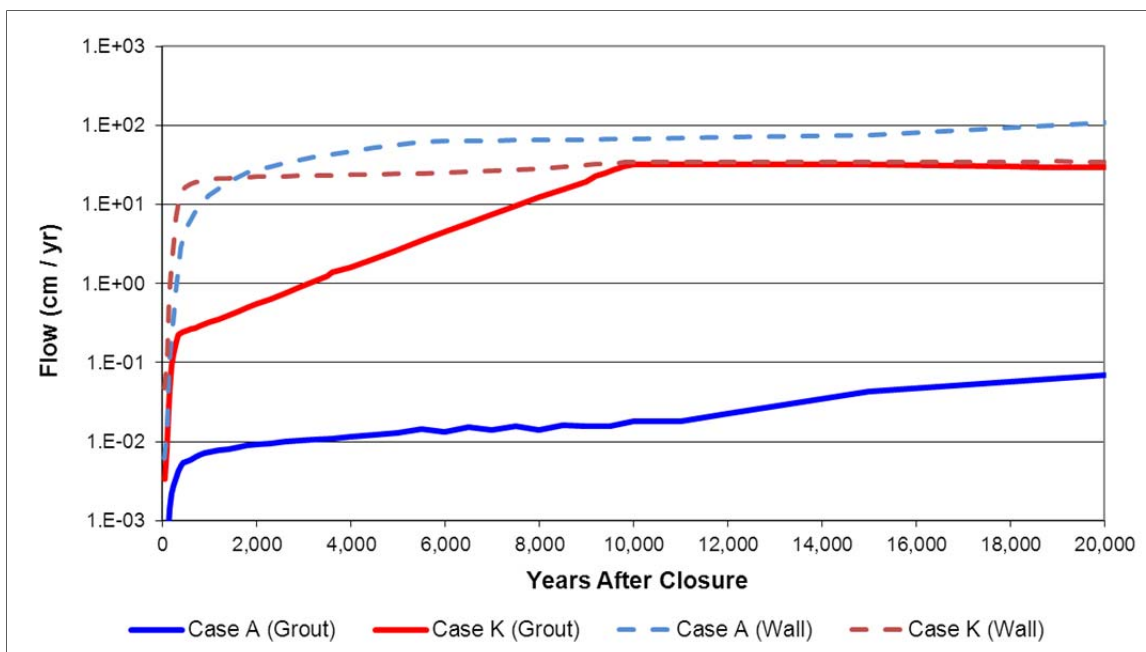
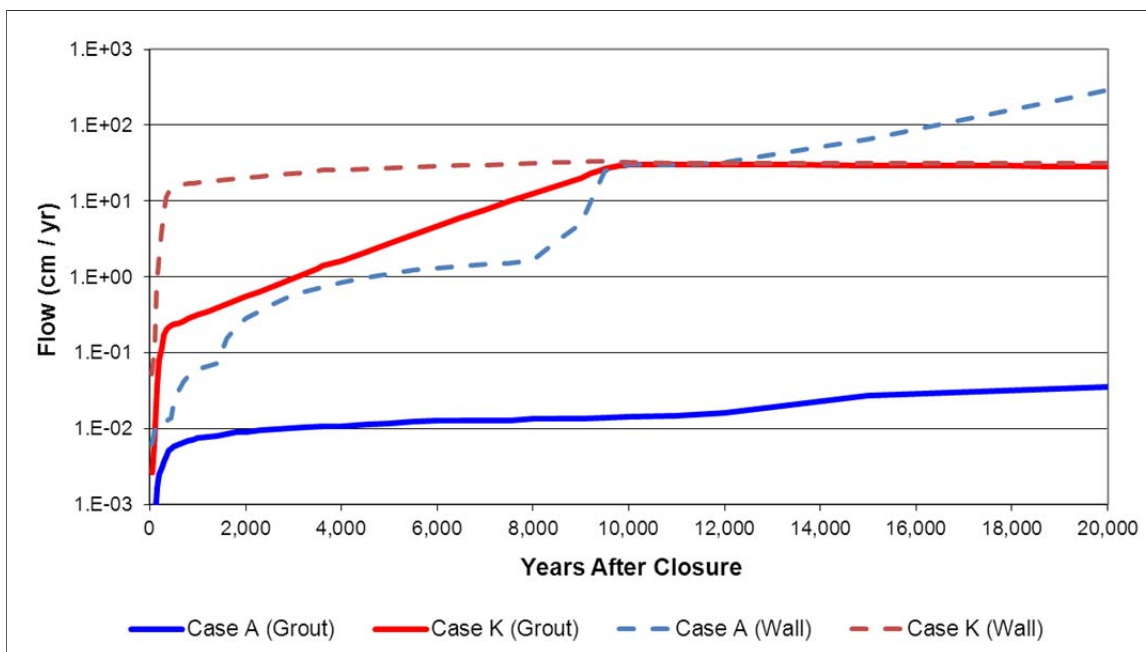


Figure VP-6.3: Vault 1 Flow Profile through Saltstone and Wall, Base Case and Case K



Case A = Base Case

Figure VP-6.4: Vault 4 Flow Profile through Saltstone and Wall, Base Case and Case K



Case A = Base Case

Far-Field Transport (FFT)

FFT-1

Comment

Additional justification is required for the uncertainty ranges used for K_d values in site soils.

DOE Response Discussion:

The DOE stated that the selection of the uncertainty distributions used for the K_d values were based on >730 K_d measurements of 8 radionuclides taken from 27 samples collected from the E-Area vadose and aquifer zones, as discussed in WSRC-STI-2008-00285. The provided reference indicated that the 27 depth-discrete samples were collected from a single borehole from E-Area. Variability in the distributions was attributed to general geochemical/geological differences in the site soils. The resulting data was used to estimate the statistical range and distribution of the K_d values for the studied radionuclides. Using these 8 radionuclides as analogues, the distribution coefficient variability was applied to >50 radionuclides.

WSRC-STI-2008-00285 evaluated the vertical variability of K_d values for 8 different radionuclides; however, lateral variability and radionuclide-specific chemistry may also affect K_d variability. Section 3.1.4.2 discusses the complexity and variability of the local geology and soils and it is not clear that a single borehole from E-Area would be representative of the soils at Z-Area. In addition, it is not clear that the variability in K_d values for 8 radionuclides would adequately capture the variability of all 50+ radionuclides.

Path Forward:

Depending on the extent to which DOE will rely on the GoldSim model, provide additional basis regarding the ability of K_d measurements on sediment samples from a borehole at E-Area for 8 radionuclides to bound the potential variability of >50 radionuclides at Z-Area.

RESPONSE FFT-1:

The geology of the GSA (which includes E Area and Z Area) has relatively uniform stratigraphy from the base of the Upland Unit in Z Area at about 260 feet MSL and the Barnwell Group/McBean contact at about 220 feet MSL. [Report 88-4221 Figures 6 and 7] The location of geologic cross sections 6 and 7 are shown in Report 88-4221 Figure 5. These cross sections are centered on borings in Z Area and show the uniform stratigraphy across the GSA.

As stated in Section 3.5.1.3 of SRR-CWDA-2009-00017, the base of Vaults 1 and 4, and Disposal Cells 2A and 2B are at 281.5, 269, and 269 feet above MSL, respectively. Therefore, the Upland Unit below the SDF comprises, at most, only a few feet of vadose zone thickness. Although the depositional environment of the Upland Unit can be complex, the composition of the formation predominantly consists of sandy, pebbly clay. The geologic formations below the Upland Unit, which comprise the majority of the modeled section, also have very consistent and predictable hydrogeologic characteristics of sands and clays. The aquifers and confining zones are well defined and can be projected across the GSA.

The discussion in SDF PA Section 3.1.4.2 focuses on the near-surface geology and surficial soils only. The discussion of a complex depositional environment relates specifically to the Upland unit, which as noted above, represents only a thin layer at the top of the model.

The soil samples utilized to determine K_d values in WSRC-STI-2008-00285 were collected from E-Area borehole BGO-3A. This boring was located approximately 7,000 feet southwest of Z Area. As stated above, the stratigraphy of Z Area is similar to the stratigraphy of the entire

GSA, which includes both Z Area and E Area. The base of the Upland Unit in BGO-3 is defined on Figure 1 of WSRC-STI-2008-00285 at 272 feet above MSL (base of the clayey sand with pebbles). Three of the samples analyzed in WSRC-STI-2008-00285 from the upper section of BGO-3A were above this horizon (Table 1 of WSRC-STI-2008-00285) and are representative of the Upland Unit. The remaining 24 samples are representative of the remaining formations.

The eight elements (nine radionuclides) selected for evaluation of K_d variability in WSRC-STI-2008-00285 were chosen to represent a broad range of elemental K_d values that would be expected for the suite of radionuclides in the SDF PA. The elements tested in WSRC-STI-2008-00285 in order of relative diminishing K_d magnitudes included americium, cerium, yttrium, cobalt, cadmium, mercury, cesium, and strontium and have a range of K_d values from approximately 1 mL/g to greater than 5,000 mL/g. As described in the response to SP-18, the distribution coefficient variability based on the 95 % confidence level for the mean for the eight elements (nine radionuclides) was applied to more than 50 elemental K_d values. The baseline K_d values by soil type reported in SDF PA Table 4.2-15 is the geometric mean for the truncated log-normal distributions utilized in SRNL-STI-2009-00150. Based on this information, it is reasonable to utilize the variability data from WSRC-STI-2008-00285 for the SDF PA probabilistic modeling.

FFT-2

Comment:

It is unclear whether any site-specific K_d value measurements have been performed for the sorption of radium to soil.

NRC Response:

The answer to this RAI is adequate, but NRC staff would appreciate receiving the document described in the response to this comment (SRR-CWDA-2010-00057) if it has been issued. If the measured K_d value is significantly different than the one assumed in the PA, the new value should be used in a revised base case.

Path Forward:

N/A

RESPONSE FFT-2:

Modeling for the SDF PA utilized radium and strontium K_d values presented in Table 4.2-15 of SRR-CWDA-2009-00017 of 5 and 17 mL/g for sandy and clayey soils, respectively. SRR-CWDA-2010-00057 was used to support the initial RAI responses and presented site-specific K_d values from preliminary testing for radium and strontium for sandy and clayey soils. SRR-CWDA-2010-00057 also indicated that the final results would be published in a later report.

The subsequent summary report, SRNL-STI-2010-00527, was issued in September 2010. SRNL-STI-2010-00527 Table 5-3 recommends the strontium K_d values utilized in the SDF PA remain at 5 and 17 mL/g for sandy and clayey soils, respectively. For radium, SRNL-STI-2010-00527 Table 5-3 recommends K_d values be increased to 25 and 185 mL/g for sandy and clayey soils, respectively. Because the K_d values for radium have increased, the modeling results for radium in the SDF PA are considered conservative. A copy SRR-CWDA-2010-00057 and SRNL-STI-2010-00527 are included with this response package.

FFT-3

Comment:

Additional justification is needed for the K_d of selenium in vadose and backfill soils.

DOE Response Discussion:

The DOE stated that a K_d for selenium of 1,000 mL/g is representative of a low pH soil and a low pH soil is considered appropriate as measurements ranged from 5.3 to 5.7 in the Z-Area background well, ZBG-1 (SRNS-TR-2009-00452). The impact of alkaline buffering on the selenium K_d values was evaluated in the probabilistic GoldSim model by using a minimum value of 250 mL/g, to account for the leaching of young-age cement. In addition, DOE ran a bounding sensitivity case using the Case A GoldSim model with both backfill and vadose zone soil K_d values for selenium set equal to zero. The effect on peak dose was less than 3% for Sector B within 20,000 years. DOE stated that the bounding sensitivity analysis provides confidence that lowering the selenium sorption onto soils has a negligible impact on dose results.

Although 3% represents a small absolute increase in dose, it represents a large relative increase in the dose derived from Se-79. According to SRNS-TR-2009-00452, the pH range of 5.3-5.7 appears to be too narrow for the Z-Area. Three wells within the Z-Area demonstrated pH values in excess of 5.7 and as high as 7. ZBG-1 represents the background well for the site; however part of NRC staff's concern is the variability across the site, including the potential impact of the cementitious materials in the SDF. In addition, the sensitivity case provided by DOE does not provide confidence as the conservatism of these sensitivity cases is unclear.

Path Forward

Depending on the extent to which DOE will rely on the GoldSim model, the selenium K_d values for soil should account for site variability in current conditions as well as reasonably expected future conditions.

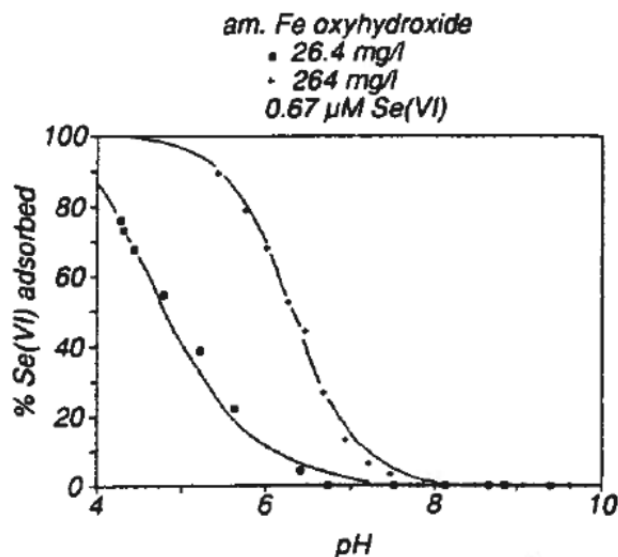
SRNS-TR-2009-00452, Z-Area Groundwater Monitoring Report for 2009, Savannah River Site, Aiken, SC, December 29, 2009.

Provide reference Kaplan, D. I., and S. M. Serkiz, 2006. *WSRC-RP-2006-00005, Influence of Dissolved Organic Carbon and pH on Anion Sorption to Sediment*, Washington Savannah River Company, Aiken, SC

RESPONSE FFT-3:

WSRC-TR-2006-00004 calculated selenium K_d values for both clayey (backfill) and sandy (vadose zone) soil. In evaluating the selenium K_d value for clayey soil, WSRC-TR-2006-00004, Table 10, indicates that selenate (SeO_4^{2-}) sorbs strongly to SRS sediments between the pH values of 3.9 and 6.7, which is within the range of pH values for Z Area listed in the comment above. The sorption curves for selenate are sigmoidal-shaped, with the sorption on the y-axis and pH on the x-axis (Figure FFT-3.1). These curves are presented for two different concentrations of amorphous iron oxyhydroxide, which is similar to the natural iron coatings contained on typical SRS sediments. It is estimated from the curve for iron oxyhydroxide at concentrations of that selenium K_d values will decrease sharply as the pH increases above pH 6; decreasing an order of magnitude as it approaches pH 7. [DOI: 10.10160016-7037(90)90369V]

Figure FFT-3.1: Adsorption of Selenate on Two Concentrations of Amorphous Iron Oxyhydroxide in 0.1 mol/L KCl as a Function of pH



Effects of various amounts of organic carbon in groundwater on the K_d values of selenium were evaluated in WSRC-TR-2006-00004. With 0 mg/L organic carbon (fulvic acid as a substitute for cellulose degradation products) added to SRS groundwater (which is the expected state of vadose zone and backfill soils), selenate K_d values for a clayey subsurface SRS sediment were 1041 ± 0.7 mL/g at pH 3.9; 1041 ± 0.4 mL/g at pH 5.3, and 1041 ± 0.3 mL/g at pH 6.7. As all these numbers are similar, there appears to be an upper sorption limit reached that yielded such similar K_d values as a function of pH; therefore, for clayey soil, variations in pH are not a factor in determining selenium K_d values. The “best estimate” selenium K_d value for clay (backfill) was set at 1,000 mL/g.

Under similar experimental conditions but using subsurface sandy sediment, selenate K_d values were 1041 ± 0 mL/g at pH 3.9, 1311 ± 384 mL/g at pH 5.3, and 601 ± 65 mL/g at pH 6.7. [WSRC-TR-2006-00004] Therefore, to aid in selecting the appropriate K_d values, Z-Area groundwater monitoring pH values were evaluated to establish a “best estimate” for groundwater pH.

Groundwater monitoring pH values for nine monitoring wells in Z Area were evaluated over a 5-year period (2006 through 2010). [WSRC-STI-2006-00360, WSRC-TR-2008-00001, SRNS-TR-2008-00310, SRNS-TR-2009-00452, SRNS-TR-2010-00374] The reported pH values are summarized in Tables FFT-3.1 (summarized by year) and FFT-3.2 (presenting individual well data).

Table FFT-3.1: Z-Area Well pH Data Averaged by Year

Well #	Average					5-year average
	2006	2007	2008	2009	2010	
ZBG-1	5.8	6.1	6.1	5.5	5.5	5.8
ZBG-2	6.3	5.4	6.7	N/S	6.1	6.1
ZBG-3	5.3	5.0	6.0	5.6	5.3	5.4
ZBG-4	5.6	6.3	6.2	6.2	5.4	5.9
ZBG-5	6.5	6.7	6.8	6.6	6.4	6.6
ZBG-6	N/S	5.4	5.9	5.2	4.5	5.2
ZBG-7	N/S	5.4	6.7	5.5	4.6	5.5
ZBG-8	N/S	6.6	6.3	6.2	4.7	5.9
Average	5.9	5.8	6.3	5.8	5.3	5.8

N/S = Not Sampled

Table FFT-3.2: Z-Area Well pH Data by Sampling Period

2010 Well Data		pH	Qualifier	Average
ZBG-1	4/26/2010	5.6	----	5.5
ZBG-1	7/20/2010	5.3	----	
ZBG-2	4/26/2010	5.8	----	6.1
ZBG-2	7/21/2010	6.4	----	
ZBG-3	4/26/2010	5.1	----	5.3
ZBG-3	7/21/2010	5.4	----	
ZBG-4	4/26/2010	4.7	----	5.4
ZBG-4	7/21/2010	6.0	----	
ZBG-5	4/26/2010	6.2	----	6.4
ZBG-5	7/20/2010	6.6	----	
ZBG-6	3/1/2010	4.4	----	4.5
ZBG-6	7/21/2010	4.5	----	
ZBG-7	3/1/2010	4.7	----	4.6
ZBG-7	7/21/2010	4.4	----	
ZBG-8	3/1/2010	5.3	----	4.7
ZBG-8	7/21/2010	4.0	----	
2010 Well Data		pH	Qualifier	Average
ZBG-1	2/23/2009	5.7	J	5.5
ZBG-1	2/23/2009	5.7	----	
ZBG-1	8/4/2009	5.3	----	
ZBG-2	N/S	N/S	N/S	N/S
ZBG-2	N/S	N/S	N/S	
ZBG-2	N/S	N/S	N/S	
ZBG-3	2/19/2009	5.2	J	5.6
ZBG-3	2/19/2009	5.5	----	
ZBG-3	8/4/2009	5.6	----	
ZBG-4	2/19/2009	6.0	J	6.2
ZBG-4	2/19/2009	6.0	----	
ZBG-4	8/4/2009	6.4	----	
ZBG-5	2/19/2009	7.5	J	6.6
ZBG-5	2/19/2009	7.0	----	

Table FFT-3.2: Z-Area Well pH Data by Sampling Period (Continued)

ZBG-5	8/4/2009	6.2	----	5.2
ZBG-6	2/23/2009	5.1	J	
ZBG-6	2/23/2009	5.1	----	
ZBG-6	8/4/2009	5.2	----	5.5
ZBG-7	2/23/2009	5.3	J	
ZBG-7	2/23/2009	5.7	----	
ZBG-7	8/4/2009	5.2	----	6.2
ZBG-8	2/23/2009	6.1	J	
ZBG-8	2/23/2009	6.7	----	
ZBG-8	8/4/2009	5.6	----	
2008 Well Data		pH	Qualifier	Average
ZBG-1	3/19/2008	5.8	----	6.1
ZBG-1	7/22/2008	6.4	----	
ZBG-2	3/28/2008	6.0	----	6.7
ZBG-2	7/23/2008	7.3	----	
ZBG-3	3/28/2008	5.9	----	6.0
ZBG-3	8/26/2008	6.1	----	
ZBG-4	3/28/2008	6.2	----	6.2
ZBG-4	8/26/2008	6.2	----	
ZBG-5	3/28/2008	7.4	----	6.8
ZBG-5	7/22/2008	6.1	----	
ZBG-6	3/18/2008	4.9	----	5.9
ZBG-6	7/22/2008	6.8	----	
ZBG-7	3/18/2008	5.5	----	6.7
ZBG-7	7/22/2008	7.8	----	
ZBG-8	3/18/2008	5.0	----	6.3
ZBG-8	7/22/2008	7.6	----	
2007 Well Data		pH	Qualifier	Average
ZBG-1	3/26/2007	4.8	J	6.1
ZBG-1	3/26/2007	6.3	----	
ZBG-1	9/11/2007	5.8	----	
ZBG-2	3/26/2007	3.2	J	6.4
ZBG-2	3/26/2007	5.5	----	
ZBG-2	9/5/2007	5.2	----	
ZBG-3	3/26/2007	4.7	J	5.0
ZBG-3	3/26/2007	5.0	----	
ZBG-3	9/5/2007	5.0	----	
ZBG-4	3/26/2007	5.3	J	6.3
ZBG-4	3/26/2007	5.8	----	
ZBG-4	9/24/2007	6.8	----	
ZBG-5	3/26/2007	6.0	J	6.7
ZBG-5	3/26/2007	6.2	J	
ZBG-5	3/26/2007	6.4	----	
ZBG-5	9/5/2007	7.0	----	
ZBG-6	3/27/2007	4.7	J	5.4

Table FFT-3.2: Z-Area Well pH Data by Sampling Period (Continued)

ZBG-6	3/27/2007	5.2	----	
ZBG-6	9/5/2007	5.6	----	
ZBG-7	3/27/2007	4.2	J	5.4
ZBG-7	3/27/2007	4.8	----	
ZBG-7	9/5/2007	5.9	----	
ZBG-8	3/27/2007	5.1	J	6.6
ZBG-8	3/27/2007	6.8	----	
ZBG-8	9/5/2007	6.3	----	
2006 Well Data		pH	Qualifier	Average
ZBG-1	2/28/2006	5.3	----	5.8
ZBG-1	7/12/2006	6.3	----	
ZBG-2	2/28/2006	5.7	----	6.3
ZBG-2	7/13/2006	6.8	----	
ZBG-3	3/22/2006	5.3	----	5.3
ZBG-3	7/10/2006	5.2	----	
ZBG-4	3/22/2006	5.3	----	5.6
ZBG-4	7/10/2006	5.8	----	
ZBG-5	3/22/2006	7.0	----	6.5
ZBG-5	7/12/2006	6.0	----	
ZBG-6	N/S	N/S	N/S	N/S
ZBG-6	N/S	N/S	N/S	
ZBG-7	N/S	N/S	N/S	N/S
ZBG-7	N/S	N/S	N/S	
ZBG-8	N/S	N/S	N/S	N/S
ZBG-8	N/S	N/S	N/S	
Summary of All Wells 2006 through 2010				pH
Average				5.82
Median				5.80
Standard Deviation				0.82
Maximum				7.80
Minimum				4.00

---- = Field measurement

J = Laboratory measurements not utilized in averaging

N/S = Not Sampled

The Z-Area groundwater monitoring well pH values collected during the 5-year period that were represented as “estimated” or “J” qualified were not used (16 out of 88 readings) in calculating the average because these values represented laboratory measurements of pH they may have been effected by a lack of sample preservation when the samples were brought from the field to the laboratory. The individual readings for the remaining 72 samples from the nine wells are field measurements of pH taken at the time of collection and ranged from 4.0 to 7.8. The pH values for the Z-Area monitoring wells varied slightly year to year and also with the time of year sampled. Wells with pH values reported above 7 were generally collected in the summer months, while samples from the same wells in the winter/spring reported pH values reported much lower (5-6 range). Out of the 72 pH values collected in the 5-year time period, only six readings were above a pH of 7.

The 5-year annual averages for the nine monitoring wells in Z Area ranged from 5.3 to 6.3 with an overall average of 5.8. As stated above, the K_d value presented in WSRC-TR-2006-00004 for both sand and clay were based on pH values that ranged from 3.9 to 6.7, which bounds the average annual pH values expected in Z-Area groundwater. The selenium K_d values for sand that correspond to this range of pH values are from approximately 600 to 1,300 mL/g and supports estimating the selenium K_d value for sand at 1,000 mL/g, which represents the variability in the current conditions as well as reasonably expected future conditions. In the probabilistic model, the distribution of the K_d value for selenium in sandy soil ranges from a minimum of 250 mL/g to a maximum of 1,750 mL/g.

As the selenium K_d values appear to decrease between a pH of 5.3 and 6.7, the lower selenium K_d value from the error range for pH 5.3 was selected as the “best estimate” for sandy soil. Therefore, the “best estimate” selenium K_d value for sand (vadose zone) was set at 1,000 mL/g.

The requested document, WSRC-RP-2006-00005, is an incorrect reference. The correct document is “WSRC-STI-2006-00037, *Influence of Dissolved Organic Carbon and pH on Iodide, Perrhenate, and Selenate Sorption to Sediment*.” WSRC-STI-2006-00037 is being provided with this response for completeness. WSRC-STI-2006-00037 also presents “best estimate” K_d values for selenium based on pH of groundwater as summarized in WSRC-TR-2006-00004. The “best estimate” selenium K_d values for both sand and clay are set at 1,000 mL/g. WSRC-STI-2006-00037 also evaluates the effect of cellulose degradation products on the selenium K_d values and provides recommended adjustments to the K_d values. Based on the lack of cellulose degradation products in the vadose zone and backfill soils at the SDF, no adjustment to the K_d values for selenium are recommended.

FFT-4

Comment (New):

The PA should discuss the implications of calcareous zones within the far field transport model.

Basis:

The presence of calcareous zones may require alternative flow conceptualization and modeling. Depending on the extent of these zones within the lower Upper Three Runs (UTR) aquifer, a dual porosity and dual permeability model may better represent flow through a porous matrix and open conduits. The presence of open conduits may (i) lead to preferential flow pathways through the subsurface, (ii) influence the location of the point of maximum exposure or compliance point, (iii) lead to decreased natural attenuation (sorption) to subsurface materials due to a decreased solids to pore water ratio, and (iv) lead to reduced K_d values for key radionuclides (e.g., Pu) due to elevated concentrations of carbonate, or non-equilibrium sorption due to the fast transport rates.

Path Forward

- 1) Provide a technical basis for neglecting potential open flow conduits within the calcareous zone of the lower UTR aquifer.
- 2) Provide support for the treatment of the calcareous zones as porous media in transport modeling in light of the fact that decreased solids and presence of high carbonate concentrations can lead to significantly higher mobility for key risk drivers such as Pu.
- 3) Provide the report, Mueser, Rutledge Consulting Engineers (1986) Saltstone disposal, Z-Area SRP, cited in WSRC-TR-99-4083, "Significance of Soft Zone Sediments at the SRS" that may contain additional information to evaluate the scope and magnitude of calcareous zones in the Z Area subsurface.

RESPONSE FFT-4:

Item 1

Although various early documents describe voids, drilling fluid losses, and grout takes associated with the Santee Formation (Calcareous Zone, Lower Aquifer Zone, etc.), there is in fact, no evidence of actual subsurface voids, karst, or caves that would act as open flow conduits in the lower UTR Aquifer within the GSA. Therefore, implementation of a dual porosity and dual permeability model is not appropriate for a risk-informed performance-based assessment. In historical and recent literature, no documentation was found of void spaces or other phenomena in Z Area or the GSA that would influence contaminant migration in a manner not already captured by the SDF flow model.

Even early SRS literature ascribes rod drops and loss of drilling fluid, observed in the GSA and elsewhere at SRS, to zones of soft, under consolidated sediment rather than actual voids:

"The 1951-52 boring and grouting work indicated that sudden dropping of drill rods results primarily from displacement of soft material, rather than from the drill rods entering a relatively unfilled cavity" (MPMR_04-23-1963).

"The void zones in the calcareous material at this location [F Tank Farm] are not open caverns but consist of zones of sponge-like nature, with openings filled with soft or semifluid material" (EWR 860438).

Years of subsequent research, including most recent efforts, reached similar conclusions:

"It appears that the "soft zones" are sediment filled, most likely with fine-grained, well-sorted sand" (WSRC-TR-94-0369).

"(T)he fact that low penetration resistance intervals exhibit P-wave velocities less than water may indicate that these zones consist of saturated, very loose sands" (WSRC-TR-96-0041).

"Most of these "soft zone" are sediment filled with a fine-grained sand" (WSRC-TR-96-0069).

"(M)uch of the time, recovery of soil in the sampler precludes the [soft] zone from being characterized as a void (K-TRT-F-00001).

Additionally, during the 20-year period spanned by investigations at more than 15 waste sites in the GSA, open flow conduits or other factors that would critically influence contaminant transport have not been discovered.

The soft zones and carbonates, located near the base of the UTR-LZ, are generally represented by very small and infrequent pockets in the UTR-LZ that do not continuously run the length of the flow path of the plume and appear to be filled in with fine sand from the surrounding formation. [WSRC-TR-94-0369] As such, to assume that the effects of the presence of soft zones on mobility should be spread across the entire aquifer and evaluated through a dual porosity and dual permeability model is not reasonable.

As discussed in Section 8.2 of the SDF PA, future work is planned in the area of model improvement through the DOE M 435.1-1 required PA maintenance process. Site studies are ongoing that may assist in gaining a better understanding of the factors effecting SDF radionuclide transport, including studies on site of soft zones within the Calcareous Zones. As future studies regarding hydrologic flow and transport are conducted and completed, new information will be evaluated for incorporation into the SDF conceptual models.

Item 2

As stated above, soft zones and carbonates are generally represented by very small and infrequent pockets in the UTR-LZ that do not continuously run the length of the flow path of the plume, are located near the base of the UTR-LZ, and appear to be filled in with fine sand from the surrounding formation. [WSRC-TR-94-0369] Should the decreased solids and presence of high carbonate concentrations lead to significantly higher mobility for specific radionuclides, the effect would be limited to a very short distance along the entire flow path. In addition, variabilities are captured in the uncertainty analyses provided in the PA. As such, to assume the effects of the presence of carbonate material and soft zones on mobility should be spread across the entire aquifer is not reasonable.

Item 3

The requested report, Mueser, Rutledge Consulting Engineers (87814-PT1) *Saltstone Disposal, Z-Area Savannah River Plant* is being provided as requested for completeness.

As part of the characterization effort described in 87814-PT1, 23 borings were installed over the entire SDF area, to a depth of up to 160 feet below ground surface. Of these 23 borings, only one encountered a zone that was considered a "void" or soft zone. This zone was in boring Z-217 at an elevation of 180 feet above MSL, or approximately 115 feet below ground level, and is located southwest of the corner of Vault 1. The "void" or soft zone is represented by a loss in drilling fluids and an associated, estimated 4-foot rod drop. Borings surrounding Z-217, within 200 feet, did not encounter any loss of drilling fluids or rods drops that would be indicative of

soft zones in the same geologic interval. This data would indicate that any soft zones associated with boring Z-217 are small and laterally discontinuous.

The boring log for Z-217 indicates that the formation surrounding the “void” interval consists of fine to medium calcareous sand with some shell fragments, consistent with the characterization of the soft zones horizons in other portions of the GSA. As stated above, soft zones in the GSA are represented by zones of soft, under consolidated sediment and most of these soft zones are in-filled with fine-grained sand.

One other boring, Z-210 (located approximately 800 feet northeast of boring Z-217), experienced a 6-inch rod drop at an elevation of 169 feet above MSL, but there was no loss of drill fluid or unusual grout take noted.

None of the other borings in the SDF area encountered zones that were considered “voids” or soft zones, indicating that the presence of any soft zones below the SDF would be small and laterally discontinuous. In addition, as summarized in 87814-PT1, there is no evidence of ground subsidence within the vicinity of SDF. 87814-PT1 also recommends that no type of grouting program for the “voids” or soft zones is necessary to stabilize the subsurface in the SDF to minimize potential for future subsidence.

Air Pathway (AP)

AP-1

Comment:

The dose from the radon pathway was not included in the dose assessment of the air pathway (Section 4.5 of the PA).

NRC Response:

The DOE response is adequate.

AP-2

Comment:

The calculations used for the air pathway dose may not have adequately evaluated the dose from this pathway. The materials were assumed to remain constant over the simulation period and degradation of the wasteform and vault does not seem to have been considered. Also, the sensitivity of the calculated land surface flux rates of radionuclides to the assumed moisture content in the cover was also not evaluated.

NRC Response:

The DOE response is adequate.

Inadvertent Intrusion (II)

II-1

Comment:

Key assumptions about the potential pathways of exposure of an inadvertent intruder appear to underestimate dose.

DOE Response Discussion:

In the analysis described in the PA, the intruder analysis was performed at a location of one (1) meter from the boundary of the SDF, which is one meter from some of the FDCs. In response to the NRC comment that the dose at one meter from Vault 4 may be higher, DOE provided a revised analysis that includes the dose at a distance of one meter from Vault 4. NRC staff finds that this portion of the response was acceptable (with the caveat that NRC staff does not agree with the use of Case A [see II-2]).

NRC staff also commented that the one-meter concentrations used in the intruder analysis were based on a 15.2 m (50 ft) grid that began at a distance of one meter from the disposal cells. NRC staff did not believe that it was appropriate to average the concentrations over this large a grid because the concentration of radionuclides that decay relatively quickly and are transported slowly may be very different over the 15.2 m (50 ft) cell. The new calculation for Vault 4 provided by DOE conservatively assumes that the concentration at one meter is equal to the concentration calculated under Vault 4. This response is acceptable to the NRC, but the NRC staff would like additional clarification on the Darcy Velocity assumed in this calculation.

The calculated dose at a distance of one meter from the FDCs was not evaluated in a similar manner and is still based on the concentration averaged over the 15.2 m (50 ft) grid. NRC staff needs an assessment of the dose at one meter from the FDCs to evaluate if the performance objectives can be met.

Additionally, as discussed in more detail in B-2, NRC staff does not agree with the exclusion of the poultry and egg pathway from the dose assessment and NRC staff believes that this should be included in the dose assessment for the intruder.

Path Forward

Provide an evaluation of the effect of the grid size assumption for the FDC. Consider the effect of including the poultry and egg pathway on the intruder (see B-2).

Provide a clarification on the Darcy Velocity assumed in the intruder calculation for Vault 4.

RESPONSE II-1:

The dose to the intruder in vicinity of an FDC will be computed using the same assumption as used for the intruder dose from Vault 4 that was provided in the initial response to RAI II-1. That is, the dose to the intruder in the vicinity of an FDC will be computed assuming that the well water source is located beneath the FDC and the stream concentrations (for fish ingestion, swimming and boating exposures) is from all SDF sources. Because ground water concentrations are calculated below an FDC (as was done for Vault 4), rather than downstream from the FDC, grid size dilution is not a factor and has no effect on this revised FDC analysis. The changes to the dose methodology discussed in the responses to RAIs B-2 (inclusion of the chicken and egg pathway and updated transfer factors), B-3 (25-year build-up of radionuclides in irrigated soil), and B-4 (inclusion of the leafy plant component in the soil-to-plant transfer factor) are used in this response.

The Darcy velocities associated with Vault 4 and an FDC are obtained directly from the PORFLOW output for the same grid zone where the contaminant mass flow (mole per year) enters the water table below the respective disposal unit. These Darcy velocities are spatial averages for each time period along the footprint of the respective disposal unit at the interface of the vadose zone and the water table. Table II-1.1 provides these Darcy velocities below Vault 4 and an FDC at the various time periods extending to 10,000 years after closure.

Table II-1.1: Darcy Velocity below a Disposal Unit at the Water Table

Time Period (years)	Darcy Velocity Below Vault 4 (cm/yr)	Darcy Velocity Below an FDC (cm/yr)	Time Period (years)	Darcy Velocity Below Vault 4 (cm/yr)	Darcy Velocity Below an FDC (cm/yr)
0 - 50	1.55E-03	1.93E-03	2,300 - 2,600	5.29E+00	7.31E+00
50 - 100	3.46E-03	4.37E-03	2,600 - 2,900	5.77E+00	7.96E+00
100 - 150	2.09E-02	2.73E-02	2,900 - 3,200	6.23E+00	8.61E+00
150 - 200	5.13E-02	6.87E-02	3,200 - 3,600	6.76E+00	9.33E+00
200 - 250	8.31E-02	1.12E-01	3,600 - 4,000	7.36E+00	1.02E+01
250 - 300	1.61E-01	2.18E-01	4,000 - 4,500	8.04E+00	1.11E+01
300 - 350	3.08E-01	4.19E-01	4,500 - 5,000	8.78E+00	1.21E+01
350 - 400	5.11E-01	6.98E-01	5,000 - 5,500	9.50E+00	1.31E+01
400 - 450	6.84E-01	9.33E-01	5,500 - 6,000	9.76E+00	1.35E+01
450 - 500	8.43E-01	1.16E+00	6,000 - 6,500	9.78E+00	1.35E+01
500 - 600	1.08E+00	1.48E+00	6,500 - 7,000	9.79E+00	1.35E+01
600 - 700	1.36E+00	1.87E+00	7,000 - 7,500	9.81E+00	1.35E+01
700 - 800	1.64E+00	2.26E+00	7,500 - 8,000	9.82E+00	1.35E+01
800 - 900	1.92E+00	2.65E+00	8,000 - 8,500	9.84E+00	1.36E+01
900 - 1,000	2.20E+00	3.02E+00	8,500 - 9,000	9.87E+00	1.36E+01
1,000 - 1,200	2.58E+00	3.54E+00	9,000 - 9,500	9.93E+00	1.36E+01
1,200 - 1,400	3.07E+00	4.22E+00	9,500 - 10,000	9.97E+00	1.36E+01
1,400 - 1,600	3.55E+00	4.89E+00	10,000 - 11,000	1.00E+01	1.36E+01
1,600 - 1,800	4.03E+00	5.57E+00	11,000 - 12,000	1.01E+01	1.37E+01
1,800 - 2,000	4.43E+00	6.11E+00	12,000 - 15,000	1.03E+01	1.38E+01
2,000 - 2,300	4.82E+00	6.66E+00	15,000 - 20,000	1.15E+01	1.48E+01

The Darcy velocities (centimeter per year) are multiplied by the area of the respective disposal unit footprint (square centimeter) to estimate a volumetric flow rate (cubic centimeter per year) for the entire disposal unit. The radionuclide concentrations (mole per cubic centimeter) at the water table below the respective disposal units are computed by dividing the contaminant mass flow (mole per year) by the volumetric flow rate (cubic centimeter per year) which is then converted into picocurie per cubic centimeter for use in the dose calculations.

The estimated peak dose to the chronic intruder within 10,000 years after closure, based on the Base Case, near Vault 4 is less than 49 mrem/yr and near an FDC is less than 1 mrem/yr. The major radionuclide and dose pathway contributors to the chronic intruder dose are presented in Tables II-1.2 and II-1.3 for the intruder in vicinity to Vault 4 and to an FDC, respectively. The peak dose to the chronic intruder provided in the SDF PA, Section 6.4 is 1.9 mrem/yr within the 10,000-year period after closure.

The significant difference in the estimated dose to the chronic intruder from Vault 4, as compared to the dose reported in the SDF PA at the one meter boundary, is attributed to the loss of retardation that would be provided by the distance from Vault 4 to the 1-meter boundary, which is approximately 500 feet.

Table II-1.2: Peak Dose Contributors to the Chronic Intruder for the Base Case Near Vault 4 within 10,000 Years

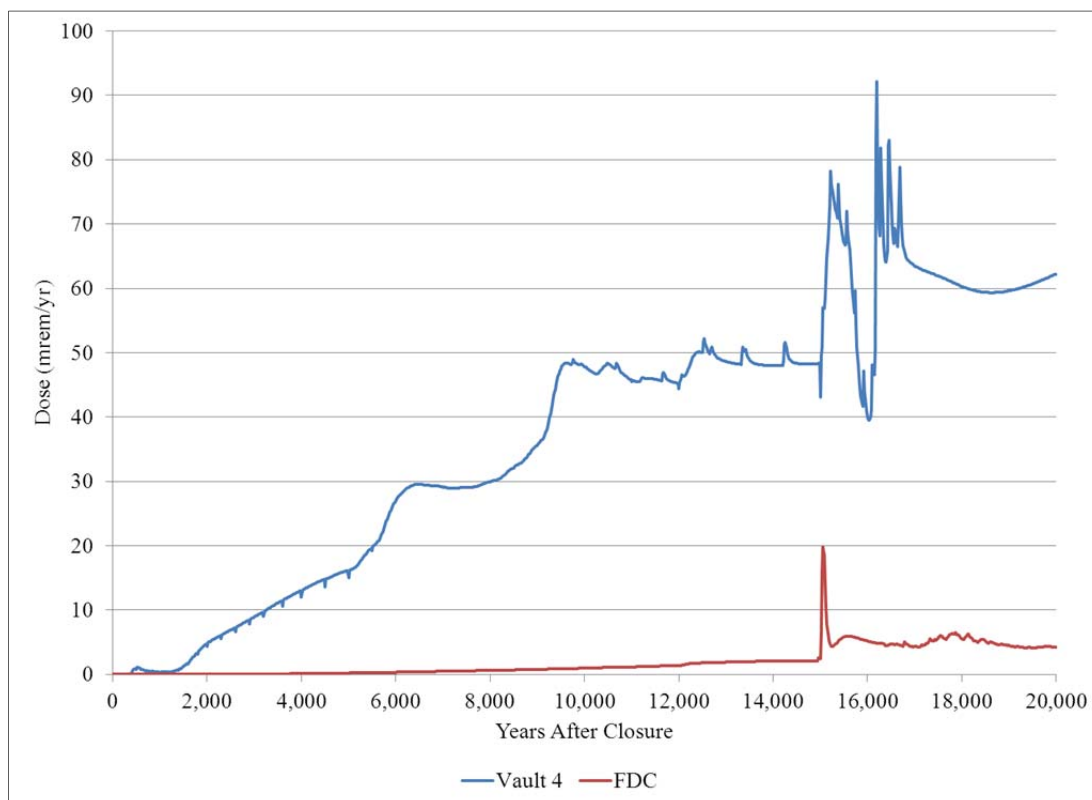
Radionuclide Contributors			Dose Pathway Contributors		
Isotope	Dose (mrem/yr)		Dose Pathway	Dose (mrem/yr)	
Ra-226	4.64E+01	95.0 %	Water Ingestion	3.56E+01	72.9 %
Tc-99	1.26E+00	2.6 %	Vegetable Consumption	9.93E+00	20.3 %
Pb-210	7.90E-01	1.6 %	Inhalation pathways	2.78E+00	5.7 %
I-129	2.12E-01	0.4 %	Beef Consumption	2.03E-01	0.4 %
Cs-135	8.37E-02	0.2 %	Milk Consumption	1.46E-01	0.3 %
C-14	3.47E-02	0.1 %	Egg Consumption	1.22E-01	0.2 %
Remainder	4.91E-02	0.1 %	Fish Consumption	3.27E-02	0.1 %
Total	4.89E+01	N/A	Chicken Consumption	1.86E-02	< 0.1 %
			Remainder	1.18E-02	< 0.1 %
			Total	4.89E+01	N/A

Table II-1.3: Peak Dose Contributors to the Chronic Intruder for the Base Case Near an FDC within 10,000 Years

Radionuclide Contributors			Dose Pathway Contributors		
Isotope	Dose (mrem/yr)		Dose Pathway	Dose (mrem/yr)	
I-129	5.99E-01	62.4 %	Water Ingestion	6.79E-01	70.8 %
Ra-226	3.48E-01	36.3 %	Vegetable Consumption	1.83E-01	19.1 %
Pb-210	5.80E-03	0.6 %	Fish Consumption	3.55E-02	3.7 %
C-14	4.64E-03	0.5 %	Milk Consumption	2.16E-02	2.2 %
Tc-99	1.47E-03	0.2 %	Inhalation Pathways	2.04E-02	2.1 %
Remainder	7.02E-05	< 0.1 %	Beef Consumption	9.88E-03	1.0 %
Total	9.59E-01	N/A	Egg Consumption	9.25E-03	1.0 %
			Chicken Consumption	1.56E-04	< 0.1 %
			Remainder	1.15E-04	< 0.1 %
			Total	9.59E-01	N/A

Figure II-1.1 shows the 20,000-year chronic intruder dose curves resulting from groundwater concentrations beneath Vault 4 and an FDC for the Base Case. This figure shows that Vault 4 dominates the chronic intruder dose for the Base Case.

Figure II-1.1: Base Case Chronic Intruder Dose at the Vicinity of Vault 4 and an FDC, within 20,000 Years



II-2

Comment:

The basis for the use of Case A to calculate the intruder dose is not provided. Additionally, the methodology used for determining the key radionuclides for the intruder uncertainty/sensitivity analysis may have resulted in radionuclides that are risk significant to the intruder being excluded from this analysis. As a consequence, the results of the uncertainty/sensitivity analysis may not capture the true uncertainty in the intruder dose.

DOE Response Discussion:

The response to the RAI provided by DOE states “(t)he deterministic intruder analysis results are based on Case A because Case A represents the reasonably expected degradation configuration for the SDF disposal units”. As stated in PA-8, the NRC staff believes that Case A is very optimistic and is not supported. NRC staff needs an intruder assessment that is based on a credible compliance case that includes all risk significant radionuclides to determine that compliance with the performance objectives of 10 CFR 61 can be met.

In the RAI response, DOE stated that the SDF PA Section 6.5 presents results that address the effects of uncertainty on the estimation of intruder dose and that the calculated mean dose to the intruder for all cases (Cases A through E) is less than 10 mrem/yr. NRC staff recognizes that the GoldSim uncertainty analysis considers the other, more realistic degradation cases. However, NRC staff has some concerns about the GoldSim modeling calculations (see PA-11), and it is not clear that the doses calculated using the GoldSim model are reasonable or meaningful.

Additionally, DOE stated in the RAI response that the potential dose to the intruder associated with the other cases can be inferred based on the dose results at 100 m presented in the SDF PA Section 5.6.6. NRC staff disagrees with this statement because radionuclides that are transported slowly and decay relatively quickly (e.g., Sr-90 and Cs-137) could cause a significant dose at a distance of one (1) meter, but it is unlikely that these radionuclides would travel quickly enough to reach 100 m before decaying. These radionuclides might not be modeled as being released quickly enough in Case A to be a problem at one (1) meter, but they could be released more quickly if more water enters the system than was predicted in that model.

Path Forward

Provide an assessment of the intruder dose based on a realistic and reasonable compliance case.

RESPONSE II-2:

The Base Case, as presented within the SDF PA, is a realistic and reasonable risk-informed compliance case. The response to RAI PA-8 provides additional justification for the use of the Base Case. The dose to the intruder for the Base Case is presented in the response to RAI II-1.

To address areas of concern described in RAI PA-8, an Alternative Sensitivity Case K has been developed and described in the response to RAI PA-8. This sensitivity case applies a non-mechanistic scenario for prematurely degrading the cementitious materials in the disposal units. For added confidence, the intruder dose from Alternative Sensitivity Case K has been estimated, using the changes to the dose methodology presented in the responses to RAIs B-2, B-3, and B-4). For Alternative Sensitivity Case K, the PORFLOW output directly provides the radionuclide concentrations below the disposal units as described in the response to RAI PA-8.

The dose results to the chronic intruder, associated with the Alternative Sensitivity Case K, are provided in the response to RAI PA-8. The peak dose to the chronic intruder within the vicinity of Vault 4 within 10,000 years is 49 mrem/yr for the Base Case (RAI II-1) and 8.1 mrem/yr for the Alternative Sensitivity Case K (RAI PA-8). The peak dose to the chronic intruder within the vicinity of an FDC within 10,000 years is less than one mrem/yr for the Base Case (RAI II-1) and 53 mrem/yr for the Alternative Sensitivity Case K (RAI PA-8).

These dose results demonstrate that, given both the reasonably conservative assumptions of the Base Case and the pessimistically conservative assumptions of Alternative Sensitivity Case K, the peak intruder dose still meets the performance objectives specified in 10 CFR 61, Subpart C.

Biosphere (B)

B-1

Comment:

The basis for excluding biotic transfer factors from the uncertainty analysis is unclear.

DOE Response Discussion:

The DOE response indicated that uncertainty in biotic transfer factors did not result in large changes to the total dose, therefore uncertainty in the transfer factors were not included in the probabilistic analysis. The absolute changes to dose as a result of biotic transfer factor uncertainty was small, however the relative changes were moderate to significant. The impact of biotic transfer factor uncertainty should be part of the base case assessment.

This comment has been expanded to include plant transfer factors and the conceptual approach for developing the values for the distributions and the expected values for the base case. Biotic transfer factors directly influence calculated doses and can have very broad ranges. In many instances, the DOE recommended values are equal to the minimum value of the distribution (for plant transfer factors, at almost a three to one ratio compared to values set to the maximum of the distribution). In effect, the distribution is defined such that the actual value will not be lower than the most likely value and the actual value is expected to be higher. These types of distributions are inconsistent with real world data and lack a conceptual basis.

Part of the reason for the distributions appears to be the derivation process documented in WSRC-STI-2007-00004. The process is not supported. DOE had derived transfer factors then updated them with a variety of sources, but primarily from PNNL-13421. For many transfer factors, the updating was performed by calculating a geometric mean of the old and PNNL-13421 values. This approach has no basis, and can result in a significant underestimation of biotic pathway doses. For example, the soil to plant transfer factor for Ra (a key radionuclide) was reduced by a factor of 100 from the previous value using this approach. A footnote infers that the PNNL-13421 values are site-specific, but NRC review of the reference indicates that the values are not site-specific but simply represent a different compilation of values.

Transfer factors operate on the concentrations derived at the end of the calculation, and can have very broad ranges. Many have very few observations. For the most part, the variance in observed values represents real world variability. Use of a geometric mean can result in a high likelihood of the actual value exceeding the assumed value and exceeding it by a large margin. Without actual site-specific measurements, transfer factors have to be selected conservatively.

Path Forward

Provide technical basis for the expected value and distributions of transfer factors used in the analysis. The results should not be aggregated with a geometric mean transfer factor.

RESPONSE B-1:

The distributions derived in WSRC-STI-2007-00004, Rev. 4 were intended to represent the range of values observed in the various literature sources, and were not developed to be used as the uncertainty range for the selected transfer factor. Although these distributions would be a good starting point to develop the uncertainty range since they are based on documented values, some of the data represented in the distributions have since been updated with newer sources of data, and others are not appropriate to represent site-specific conditions. In addition, a distribution type for the transfer factor data range was not determined in WSRC-STI-2007-

00004, Rev. 4. Should DOE decide to include the transfer factors in the uncertainty analysis, careful consideration of the transfer factor data would need to be taken to determine the appropriate uncertainty range and distribution type to be applied to the transfer factor data.

DOE did not develop uncertainty ranges for the transfer factors during initial PA development for several reasons. First, it was not expected that developing uncertainty ranges utilizing the maximum transfer factor values represented in the data range would result in large changes to the total dose. This expectation has been supported by sensitivity runs performed by DOE in "Response B-1" of the NRC RAIs on the SDF PA, SRR-CWDA-2010-00033. Second, a previous independent assessment provided in *Description of Methodology for Biosphere Dose Model BDOSE* concluded that applying a distribution to these transfer factors proved to be of no significant importance. [ML083190829 Page B-1] Third, DOE was concerned about risk dilution in the uncertainty analysis and desired not to introduce unnecessary and less important stochastic ranges into the analysis. For all these reasons, DOE made a risk-informed decision not to develop and include uncertainty ranges for the transfer factors.

WSRC-STI-2007-00004, Rev. 4 described the specific methodology used for selecting transfer factor values recommended for use in the SRS PAs. As indicated in the RAI, the methodology was to update values using information developed from PNNL-13421. Typically, the original values were replaced with the values from PNNL-13421. In some cases the geometric mean of the original values and the values from PNNL-13421 were determined to be more appropriate. The decision process is described on pages 7 and 8 of WSRC-STI-2007-00004, Rev. 4. Whenever the difference in the original value and the value from PNNL-13421 was more than two orders of magnitude, the geometric mean of the values was calculated and used.

The use of the geometric mean was not without precedence. The main references for the transfer factor data include ORNL-5786, PNNL-13421, and IAEA-364. PNNL-13421 uses the geometric mean to derive transfer factors for elements without transfer factors by calculating the geometric mean of the transfer factors of all the elements in the same chemical group. ORNL-5786 uses the geometric mean for the transfer factor when multiple data sets have different values, especially when the values span across several orders of magnitude. IAEA-364 uses the geometric mean in situations that require space or time averaging of observations. The use of the geometric mean in WSRC-STI-2007-00004, Rev. 4 was similar to the use of the geometric mean by ORNL-5786.

The concern over the application of the geometric mean described in the "Basis" section of this RAI appears to be that this approach could "result in significant underestimation of environmental pathway doses." An example was provided where the transfer factor for radium was reduced by a factor of 100 from the previous value using the geometric mean.

Using radium as an example, the original value was $4.0\text{E-}2$ and the PNNL-13421 value that was recommended was $3.9\text{E-}4$. Using the approach described in WSRC-STI-2007-00004, Rev. 4, the difference between these two values rounded to two orders of magnitude, so the geometric mean was used instead of simply replacing the previous value with the value from PNNL-13421, which would have resulted in a decrease by a factor of 100. The geometric mean of the original value ($4.0\text{E-}2$), the intruder analysis value ($6.42\text{E-}3$), and the recommended replacement value from PNNL-13421 ($3.9\text{E-}4$), is $4.6\text{E-}3$ (WSRC-STI-2007-00004 Table 5.3). Using this method resulted in selection of a value more conservative than simply selecting the more recently developed values from the PNNL study.

Furthermore, for 18 of the 23 instances where the geometric mean was used in WSRC-STI-2007-00004, Rev. 4, the value from PNNL-13421 was at least two orders of magnitude less than the currently used value, and the geometric mean approach resulted in a more

conservative value (relative to PNNL-13421). For the few cases where the geometric mean was non-conservative, the elements involved (i.e., rhenium, titanium, hafnium, and tungsten) were not associated with radionuclides of concern.

In 2010, the International Atomic Energy Agency published Technical Series Report 472, *Handbook of Parameter Values for the Prediction of Radionuclide Transfer in Terrestrial and Freshwater Environments*, which provides parameter values for radionuclide, bioaccumulation, and transfer in terrestrial and freshwater environments. [IAEA-472] This report supersedes IAEA-364 (*Handbook of Parameter Values for the Prediction of Radionuclide Transfer in Temperate Environments*) which was a key source of data in the PA. SRNL-STI-2010-00447, *Land and Water Use Characteristics and Human Health Input Parameters for use in Environmental Dosimetry and Risk Assessments at the Savannah River Site*, presents additional details on factors utilized in the past and discussion on factors developed for SRS use. This report does not include any data manipulations using a geometric mean. The bioaccumulation factors from this report are used in the response to RAI Comment B-2.

B-2

Comment:

The animal product pathways included in the dose assessment are the beef, milk, and finfish pathways. A basis for excluding the other animal product pathways (e.g., consumption of poultry and eggs) from the dose assessment is not provided.

DOE Response Discussion:

In the response to this comment, DOE states that the exposure pathway for poultry and eggs is not included in the SDF PA compliance model based on a survey of local practices within 50 miles of the SRS. WSRC-RP-91-17 cites a personal communication from T. Mathis who indicated that it is the local practice to source poultry feed from offsite. Based on this communication, DOE excluded poultry and eggs as an exposure pathway.

NRC staff believes that this study does not provide a sufficient technical basis to conclude that chicken feed is currently, or will in the future, be sourced from offsite. In addition, even if the poultry primarily consume commercial feed, the poultry may still consume other things (e.g. bugs and forage) which may contain site-derived radionuclides. Furthermore, the poultry would likely consume groundwater (extracted for domestic or agricultural purposes) from the site. For these reasons, the NRC staff does not believe it is appropriate to exclude the chicken and egg pathways from the PA.

Path Forward:

Provide an evaluation of the dose to the member of the public and intruder from chicken and egg pathways.

RESPONSE B-2:

An evaluation of the dose to the MOP from the chicken and egg ingestion pathways for the PA Base Case is provided in the response to this RAI. A similar evaluation is provided for the intruder in the response to RAI II-1. For the evaluation of this dose pathway, updated information on radionuclide transfer factors and dose conversion factors are used. These parameters are provided in the tables included in this response. Note that the results presented in this response also include a modified soil irrigation buildup factor described in the response to RAI B-3 and revised soil-to-plant bioaccumulation factors and a garden productivity yield discussed in the response to RAI B-4.

The chicken and egg ingestion pathway assumes chicken drink water from a 100-meter contaminated well and consume fodder irrigated from the same water source. The fodder is contaminated from direct deposition of contaminated irrigation water on plants and from deposition of contaminated irrigation water in soil followed by root uptake by plants. Following the chicken consumption of the contaminated water and fodder, the receptor consumes the contaminated chicken and eggs. Chicken and eggs are treated separately. The concentration in fodder and the dose is calculated using the following formulas.

$$C_f = C_{GW} \times I \times (LEAF + SOIL \times T_{SI}) \times F_I$$

Chicken:

$$D = T_p \times (FF_p \times C_f \times Q_{FP} + C_{GW} \times Q_{WP}) \times DCF \times U_p \times F_p$$

Eggs:

$$D = T_E \times (FF_P \times C_f \times Q_{FP} + C_{GW} \times Q_{WP}) \times DCF \times U_E \times F_E$$

where:

D	=	dose from 1-year consumption of contaminated chicken or eggs (rem/yr)
C_f	=	radionuclide concentration in fodder (pCi/kg)
C_{GW}	=	radionuclide concentration in groundwater from the 100-meter well (pCi/L)
I	=	irrigation rate (= 3.6 L/m ² -d), PA Table 4.6-6
$LEAF$	=	radionuclide deposition and retention rate on the vegetation's leaves defined in PA Section 5.4.1.1 (m ² d/kg)
$SOIL$	=	radionuclide deposition and buildup rate in the soil, (m ² d/kg), see the response to RAI B-3
T_{StV}	=	soil to vegetation ratio (unitless), Table B-2.1
F_I	=	fraction of the time vegetation is irrigated (= 0.2), PA Table 4.6-6
T_P	=	chicken transfer coefficient (d/kg), Table B-2.2
T_E	=	egg transfer coefficient (d/kg), Table B-2.2
FF_P	=	chicken or egg intake fraction from irrigated field/pasture (= 1.0)
Q_{FP}	=	consumption rate of fodder by chicken (= 0.1 kg/d), ML083190829, Table A-1
Q_{WP}	=	consumption rate of water by chicken (=0.3 L/d), ML083190829, Table A-1
DCF	=	ingestion DCF (rem/μCi), Table B-2.3
U_P	=	human consumption rate of chicken (= 25 kg/yr), ML083190829, Table A-1
U_E	=	human consumption rate of eggs (= 19 kg/yr), ML083190829, Table A-1
F_P	=	fraction of chicken produced locally (= 0.306), ML083190829, Table A-1
F_E	=	fraction of eggs produced locally (= 0.306), ML083190829, Table A-1

Table B-2.1 provides the bioaccumulation factors utilized for this response and the parameters used in the PA. The factors used in this response are based on SRNL-STI-2010-00447, *Land and Water Use Characteristics and Human Health Input Parameters for use in Environmental Dosimetry and Risk Assessments at the Savannah River Site*. This report presents additional details on factors utilized in the past and discussion on factors developed for SRS use. This report also established a standardized source for bioaccumulation factor parameters that represent current data including IAEA-472. Issued in 2010, IAEA-472, *Handbook of Parameter Values for the Prediction of Radionuclide Transfer in Terrestrial and Freshwater Environments*, provides parameter values for radionuclide, bioaccumulation, and transfer in terrestrial and freshwater environments. This report supersedes IAEA-364 (*Handbook of Parameter Values for the Prediction of Radionuclide Transfer in Temperate Environments*) which was a key source of data in PNNL-13421 and in the PA.

Table B-2.1: Bioaccumulation Factors for Vegetable, Milk, Beef, and Fish Pathways

Element	Soil to Plant (unitless)		Feed to Milk (d/L)		Feed to Beef (d/kg)		Water to Fish (L/kg)	
	RAI (a)	PA (b)	RAI (c)	PA (d)	RAI (e)	PA (f)	RAI (g)	PA (h)
Ac	6.11E-05	6.83E-05	2.00E-05	2.00E-05	4.00E-04	4.00E-04	25	25
Al	1.27E-04	1.27E-04	2.06E-04	2.06E-04	1.50E-03	1.50E-03	51	500
Am	7.33E-05	6.83E-05	4.20E-07	1.50E-06	5.00E-04	4.00E-05	240	30
C	1.37E-01	1.37E-01	1.20E-02	1.20E-02	3.10E-02	3.10E-02	3	3
Cf	6.11E-05	6.83E-05	1.50E-06	1.50E-06	4.00E-05	4.00E-05	25	25
Cl	3.49E+00	1.37E+01	1.70E-02	1.70E-02	1.70E-02	2.00E-02	47	50
Cm	1.27E-04	8.39E-05	2.00E-05	2.00E-05	4.00E-05	4.00E-05	30	30
Co	2.48E-02	1.31E-02	1.10E-04	3.00E-04	4.30E-04	1.00E-02	76	300
Cs	6.85E-03	9.00E-01	4.60E-03	7.90E-03	2.20E-02	5.00E-02	3,000	3,000
Eu	3.90E-03	3.90E-03	3.00E-05	3.00E-05	2.00E-05	2.00E-05	130	30
Gd	3.90E-03	3.90E-03	3.00E-05	3.00E-05	2.00E-05	2.00E-05	30	30
H	4.80E+00	4.80E+00	1.50E-02	1.50E-02	0.00E+00	1.20E-02	1	1
I	1.32E-02	7.80E-03	5.40E-03	9.00E-03	6.70E-03	4.00E-02	30	40
K	2.54E-01	1.07E-01	7.20E-03	7.20E-03	2.00E-02	2.00E-02	3,200	1,000
Nb	2.18E-03	4.88E-03	4.10E-07	3.20E-05	2.60E-07	2.90E-04	300	300
Ni	2.18E-02	1.17E-02	9.50E-04	1.60E-02	5.00E-03	5.00E-03	21	100
Np	3.91E-03	2.54E-03	5.00E-06	5.00E-06	1.00E-03	1.00E-03	21	21
Pa	6.11E-05	4.18E-04	5.00E-06	5.00E-06	4.47E-04	4.47E-04	10	10
Pb	5.18E-03	1.17E-03	1.90E-04	2.60E-04	7.00E-04	4.00E-04	25	300
Pd	1.28E-02	7.80E-03	1.00E-02	1.00E-02	4.00E-03	4.00E-03	10	10
Pt	4.88E-03	4.88E-03	5.15E-03	5.15E-03	4.00E-03	4.00E-03	35	35
Pu	1.97E-05	2.15E-04	1.00E-05	1.10E-06	1.10E-06	1.00E-05	30	30
Ra	1.19E-02	4.64E-03	3.80E-04	1.30E-03	1.70E-03	9.00E-04	4	50
Se	1.89E-02	5.14E-02	4.00E-03	4.00E-03	1.50E-02	1.50E-02	6,000	170
Sm	3.90E-03	3.90E-03	3.00E-05	3.00E-05	3.16E-04	3.16E-04	30	30
Sn	2.27E-03	1.17E-03	1.00E-03	1.00E-03	8.00E-02	8.00E-02	3,000	3,000
Sr	1.23E-01	9.75E-02	1.30E-03	2.80E-03	1.30E-03	8.00E-03	2.9	60
Tc	1.79E+01	4.68E-02	1.87E-03	1.87E-03	6.32E-03	6.32E-03	20	20
Th	3.14E-04	6.44E-05	5.00E-06	5.00E-06	2.30E-04	4.00E-05	6	100
U	6.69E-03	2.34E-03	1.80E-03	4.00E-04	3.90E-04	3.00E-04	1	10
Zr	7.80E-04	1.95E-04	3.60E-06	5.50E-07	1.20E-06	1.84E-04	22	300

- a) SRNL-STI-2010-00447, Table 2
- b) PA Table 4.6-1
- c) SRNL-STI-2010-00447, Table 3
- d) PA Table 4.6-2
- e) SRNL-STI-2010-00447, Table 4
- f) PA Table 4.6-3
- g) SRNL-STI-2010-00447, Table 5
- h) PA Table 4.6-4

SRNL-STI-2010-00447 did not include feed-to-chicken and feed-to-egg transfer factors. In order to account for local chicken and egg farmers that use free-range methods or home-grown fodder as feed, a methodology similar to that described above for SRNL-STI-2010-00447 was used to determine the feed-to-chicken and feed-to-egg transfer factors. The PNNL-13421 transfer factors were used and updated with the transfer factors from the IAEA-472. Elements in the model that feed-to-chicken or feed-to-egg transfer factors were not found were assigned a zero value. Table B-2.2 provides the bioaccumulation factors for the chicken and egg pathways used for this response.

Table B-2.2: Bioaccumulation Factors for Chicken and Egg Pathways

Element	Feed to Chicken (d/kg)	Feed to Egg (d/kg)
Ac	6.00E-03	4.00E-03
Al	0.00E+00	0.00E+00
Am	6.00E-03	3.00E-03
C	0.00E+00	0.00E+00
Cf	6.00E-03	4.00E-03
Cl	3.00E-02	2.70E+00
Cm	6.00E-03	4.00E-03
Co	9.70E-01	3.30E-02
Cs	2.70E+00	4.00E-01
Eu	2.00E-03	4.00E-05
Gd	2.00E-03	4.00E-05
H	0.00E+00	0.00E+00
I	8.70E-03	2.40E+00
K	4.00E-01	1.00E+00
Nb	3.00E-04	1.00E-03
Ni	1.00E-03	1.00E-01
Np	6.00E-03	4.00E-03
Pa	6.00E-03	4.00E-03
Pb	8.00E-01	1.00E+00
Pd	3.00E-04	4.00E-03
Pt	0.00E+00	0.00E+00
Pu	3.00E-03	1.20E-03
Ra	3.00E-02	3.10E-01
Se	9.70E+00	1.60E+00
Sm	2.00E-03	4.00E-05
Sn	8.00E-01	1.00E+00
Sr	2.00E-02	3.50E-01
Tc	3.00E-02	3.00E+00
Th	6.00E-03	4.00E-03
U	7.50E-01	1.10E+00
Zr	6.00E-05	2.00E-04

PA Table 4.7-1 presents the ingestion dose conversion factors used in the PA. Further review of these dose conversion factors revealed that the dose conversion factors for Pb-210 and U-232 did not include the contribution from all of the short-lived progenies for these radionuclides. Pt-193 was also updated. Table B-2.3 presents the ingestion dose conversion factors used in

this response and the dose conversion factors reported in PA Table 4.7-1. All data is obtained from the PA reference ICRP-72 as described in PA Section 4.7.1-1.

Table B-2.3: Ingestion Dose Conversion Factors

Ingestion Dose Conversion Factor Rem/ μ Ci					
Radionuclide	RAI Response	PA Table 4.7-1	Radionuclide	RAI Response	PA Table 4.7-1
Ac-227	4.47E+00	4.47E+00	Pa-231	2.63E+00	2.63E+00
Al-26	1.30E-02	1.30E-02	Pb-210	7.00E+00	2.55E+00
Am-241	7.40E-01	7.40E-01	Pd-107	1.37E-04	1.37E-04
Am-242m	7.41E-01	7.41E-01	Pt-193	1.15E-04	0.00E+00
Am-243	7.43E-01	7.43E-01	Pu-238	8.51E-01	8.51E-01
C-14	2.15E-03	2.15E-03	Pu-239	9.25E-01	9.25E-01
Cf-249	1.30E+00	1.30E+00	Pu-240	9.25E-01	9.25E-01
Cf-251	1.33E+00	1.33E+00	Pu-241	1.78E-02	1.78E-02
Cl-36	3.44E-03	3.44E-03	Pu-242	8.88E-01	8.88E-01
Cm-243	5.55E-01	5.55E-01	Pu-244	8.92E-01	8.92E-01
Cm-244	4.44E-01	4.44E-01	Ra-226	1.04E+00	1.04E+00
Cm-245	7.77E-01	7.77E-01	Ra-228	3.08E+00	3.08E+00
Cm-247	7.03E-01	7.03E-01	Se-79	1.07E-02	1.07E-02
Cm-248	2.85E+00	2.85E+00	Sm-151	3.63E-04	3.63E-04
Co-60	1.26E-02	1.26E-02	Sn-126	1.88E-02	1.88E-02
Cs-135	7.40E-03	7.40E-03	Sr-90	1.14E-01	1.14E-01
Cs-137	4.81E-02	4.81E-02	Tc-99	2.37E-03	2.37E-03
Eu-152	5.18E-03	5.18E-03	Th-229	2.27E+00	2.27E+00
Eu-154	7.40E-03	7.40E-03	Th-230	7.77E-01	7.77E-01
Gd-152	1.52E-01	1.52E-01	Th-232	8.51E-01	8.51E-01
H-3	6.66E-05	6.66E-05	U-232	1.75E+00	1.22E+00
I-129	4.07E-01	4.07E-01	U-233	1.89E-01	1.89E-01
K-40	2.29E-02	2.29E-02	U-234	1.81E-01	1.81E-01
Nb-93m	4.44E-04	4.44E-04	U-235	1.75E-01	1.75E-01
Nb-94	6.29E-03	6.29E-03	U-236	1.74E-01	1.74E-01
Ni-59	2.33E-04	2.33E-04	U-238	1.79E-01	1.80E-01
Ni-63	5.55E-04	5.55E-04	Zr-93	4.07E-03	4.07E-03
Np-237	4.10E-01	4.13E-01			

The dose to the MOP in Sector B (location of the peak dose within the first 10,000 years after closure) and in Sector I (location of the peak dose within 20,000 years after closure) from the ingestion of chicken and eggs are provided in Table B-2-4. The peak dose to the MOP within 10,000 years after closure is in Sector B and is 0.0025 mrem/yr in year 9,820 for the egg ingestion pathway and 0.00033 mrem/yr in year 9,980 for the chicken ingestion pathway. For the egg ingestion pathway, the peak dose to the MOP within 20,000 years is in Sector I at year 15,080 and is 0.025 mrem/yr. For the chicken ingestion pathway, the peak dose to the MOP within 20,000 years is in Sector B at year 16,240 and is 0.00062 mrem/yr. The contributions to the total peak dose to the MOP provided by the chicken and egg ingestion pathways are provided in Table B-2.5. As indicated in Table B-2.5 the chicken and egg ingestion pathways are not significant contributors to the total dose.

Table B-2.4: Peak Dose to the MOP in Sectors B and I from Egg and Chicken Ingestion for Base Case

Sector B in 10,000 Years Egg Ingestion (Year 10,000)			Sector B in 10,000 Years Chicken Ingestion (Year 9,980)		
Radionuclide	Dose (mrem/yr)	Contribution (%)	Radionuclide	Dose (mrem/yr)	Contribution (%)
Ra-226	1.6E-03	63.0	Ra-226	2.1E-04	62.0
Tc-99	4.5E-04	17.6	Pb-210	9.8E-05	29.7
I-129	3.9E-04	15.6	Cs-135	2.2E-05	6.6
Pb-210	9.1E-05	3.6	Tc-99	3.7E-06	1.1
Cs-135	2.4E-06	0.1	I-129	1.9E-06	0.6
Total	2.5E-03	--	Total	3.3E-04	--
Sector B in 20,000 Years Egg Ingestion (Year 16,240)			Sector B in 20,000 Years Chicken Ingestion (Year 16,240)		
Tc-99	1.9E-02	87.6	Tc-99	2.5E-04	40.8
Ra-226	1.7E-03	7.5	Ra-226	2.1E-04	33.8
I-129	9.8E-04	4.4	Pb-210	1.0E-04	16.6
Pb-210	9.8E-05	0.4	Cs-135	4.7E-05	7.5
Cs-135	5.3E-06	< 0.1	I-129	4.7E-06	0.7
Pa-231	9.7E-07	< 0.1	Pa-231	1.9E-06	0.3
Np-237	6.5E-07	< 0.1	Np-237	1.3E-06	0.2
Total	2.2E-02	--	Total	6.2E-04	--
Sector I in 10,000 Years Egg Ingestion (Year 10,000)			Sector I in 10,000 Years Chicken Ingestion (Year 10,000)		
I-129	7.5E-04	94.1	Ra-226	5.6E-06	47.2
Ra-226	4.4E-05	5.5	I-129	3.6E-06	30.2
Pb-210	2.5E-06	0.3	Pb-210	2.7E-06	22.4
Tc-99	1.6E-07	< 0.1	K-40	2.8E-08	0.2
K-40	5.3E-08	< 0.1	Tc-99	2.0E-09	< 0.1
Total	8.0E-04	--	Total	1.2E-05	--
Sector I in 20,000 Years Egg Ingestion (Year 15,080)			Sector I in 20,000 Years Chicken Ingestion (Year 15,080)		
I-129	2.5E-02	99.5	I-129	1.2E-04	83.7
Ra-226	1.2E-04	0.5	Ra-226	1.6E-05	11.0
Pb-210	7.1E-06	< 0.1	Pb-210	7.5E-06	5.3
Tc-99	6.1E-07	< 0.1	K-40	4.8E-08	< 0.1
Total	2.5E-02	--	Total	1.4E-04	--

Table B-2.5: Contribution to the Peak Dose in Sectors B and I from the Egg and Chicken Ingestion Pathways

Peak Dose in Sector B in 10,000 Years (Year 9,980)			Peak Dose in Sector B in 20,000 Years (Year 15,080)		
Pathway	Dose (mrem/yr)	Contribution (%)	Pathway	Dose (mrem/yr)	Contribution (%)
Water Ingestion	6.9E-01	77.1	Water Ingestion	1.3E+00	65.1
Vegetable Ingestion	1.1E-01	11.9	Fish Ingestion	3.7E-01	18.7
Inhalation	4.6E-02	5.1	Vegetable Ingestion	2.1E-01	10.4
Fish Ingestion	3.5E-02	3.9	Inhalation	5.2E-02	2.6
Beef Ingestion	3.9E-03	0.4	Milk Ingestion	2.4E-02	1.2
Milk Ingestion	2.8E-03	0.3	Beef Ingestion	1.5E-02	0.8
Egg Ingestion	2.4E-03	0.3	Egg ingestion	1.4E-02	0.7
Chicken Ingestion	3.3E-04	< 0.1	Chicken Ingestion	4.4E-04	< 0.1
All other pathways	8.0E-03	0.9	All other pathways	9.3E-03	0.5
Total	9.0E-01	- -	Total	2.0E+00	- -
Peak Dose in Sector I in 10,000 Years (Year 10,000)			Peak Dose in Sector I in 20,000 Years (Year 15,080)		
Water Ingestion	5.8E-02	53.9	Water Ingestion	1.4E+00	66.4
Fish Ingestion	3.5E-02	33.1	Fish Ingestion	3.7E-01	18.3
Vegetable Ingestion	8.8E-03	8.2	Vegetable Ingestion	2.1E-01	10.0
Inhalation	1.9E-03	1.8	Milk Ingestion	5.1E-02	2.5
Milk Ingestion	1.6E-03	1.5	Beef Ingestion	2.5E-02	1.2
Beef Ingestion	8.4E-04	0.8	Egg ingestion	2.5E-02	1.2
Egg ingestion	8.0E-04	0.7	Inhalation	7.2E-03	0.4
Chicken Ingestion	1.2E-05	< 0.1	Chicken Ingestion	1.4E-04	< 0.1
All other pathways	2.9E-05	< 0.1	All other pathways	6.5E-05	< 0.1
Total	1.1E-01	- -	Total	2.0E+00	- -

An additional evaluation was conducted to include soil consumption by the chickens to estimate the dose from chicken and egg consumption with this additional source of radionuclide uptake by the chickens. The additional chicken uptake from soil consumption assumes that the chicken consumes as much dirt as fodder (100 g/d) and the soil concentration is equal to the soil buildup calculation described in the response to RAI B-3 and identified as "SOIL" in that response. Table B-2.6 provides the MOP dose from the egg consumption and chicken consumption pathways with the inclusion of dirt consumption by chickens. As shown in this table, the increase of the respective doses may be significant on a relative basis (MOP dose from chicken consumption in Sector I) but on an absolute basis, the doses are insignificant. Based on these results, the inclusion of dirt consumption by chickens have not been included in the estimation of the egg consumption and chicken consumption dose pathways in other RAI responses.

Table B-2.6: Peak Dose to the MOP in Sectors B and I from Egg and Chicken Consumption Pathways with Dirt Consumption by Chickens

Peak Dose (mrem/yr)	With Dirt Consumption in Sector B	Peak Dose from Dirt Consumption by Chickens in Sector B	With Dirt Consumption in Sector I	Peak Dose from Dirt Consumption by Chickens in Sector I
Egg Consumption (within 10,000 yrs)	3.2E-03	6.5E-04	8.2E-04	2.4E-05
Egg Consumption (within 20,000 yrs)	2.3E-02	1.1E-03	2.5E-02	2.5E-04
Chicken Consumption (within 10,000 yrs)	7.9E-04	4.5E-04	2.3E-05	1.1E-05
Chicken Consumption (within 20,000 yrs)	1.4E-03	7.7E-04	2.7E-04	1.3E-04

B-3

Comment:

The effects of radionuclide build-up in irrigated soils may be underestimated.

DOE Response Discussion:

The DOE response indicated that use of a 30-year build-up time as compared to a 183-day build-up time for radionuclides in irrigated soils did not result in large changes to the total dose; therefore the effects did not need to be included in the base case.

Most releases from the SDF are expected to occur slowly over thousands of years. The 30-year buildup time may be exceeded for long-lived radionuclides, however NRC acknowledges that the assessment provided did not consider losses from erosion and leaching. Ambiguity could be reduced by including expected gain and loss processes to determine equilibrium build-up factors.

The absolute changes to dose as a result of increased build-up times were small; however the relative changes were significant. The impact of build-up time uncertainty should be part of the base case assessment.

Path Forward:

Include build-up of radionuclides during multiple years of irrigation in the base case PA model.

RESPONSE B-3:

In the initial response to RAI B-3 provided in SRR-CWDA-2010-00033, Rev. 1, the build-up of radionuclides in the soil from irrigation was conservatively assessed by using a 30-year build-up time with no credit taken for leaching. To assess more realistically the impact of soil build-up, credit is taken for leaching and the build-up time is considered to be 25 years based on SRNL-STI-2010-00447.

The expression for soil build-up [*SOIL*] is defined in the expressions provided below and is based on the formulation provided in *Description of Methodology for Biosphere Dose Model BDOSE*, ADAMS Accession Number ML083190829.

$$SOIL = \frac{1 - e^{-\lambda_B t_b}}{\rho_S \times \lambda_B}$$
$$\lambda_L = \frac{P_R + I_R - E_R}{S_D \times (S_M + \rho_{SS} \times K_d)}$$
$$\lambda_B = \lambda_i + \lambda_L$$

Where:

$SOIL$	=	radionuclide deposition and buildup rate in the soil (m^2d/kg)
ρ_S	=	areal surface density of soil (kg/m^2), SRR-CWDA-2009-00017, Table 4.6-6
λ_B	=	soil buildup rate (1/d)
λ_i	=	radiological decay constant (1/d)
λ_L	=	soil retention rate (1/d)
P_R	=	precipitation rate (= 49.14 in/yr), WSRC-STI-2008-00244, Table 47
I_R	=	irrigation rate (= 51.7 in/yr), based on 3.6 L/m ² -d, SRR-CWDA-2009-00017, Table 4.6-6
E_R	=	evapotranspiration rate (= 32.57 in/yr), WSRC-STI-2008-00244, Table 47
S_D	=	depth of garden (= 15 cm), SRR-CWDA-2009-00017, Table 4.6-6
S_M	=	soil moisture content (= 0.39), based on the porosity of the vadose zone soil provided in SRR-CWDA-2009-00017, Table 4.2-14 and assuming 100% saturation
ρ_{SS}	=	density of sandy soil (= 1.65 g/cm ³), SRR-CWDA-2009-00017, Table 4.2-14
K_d	=	distribution coefficient (mL/g), SRR-CWDA-2009-00017, Table 4.2-15 (Vadose Zone)
t_b	=	buildup time of radionuclides in soil (= 9,125 days), SRNL-STI-2010-00447, Table 1

To illustrate the impact of this parameter on the resulting soil concentrations, the term SOIL is provided in Table B-3.1 using three different parameters: 1) build-up time of 0.5 year with no leaching (used in the PA), 2) build-up time of 25 years with no leaching (to illustrate the impact from leaching), and 3) build-up of 25 years with leaching (case to be used in dose calculations provided in this RAI response package).

Table B-3.1: Soil Build-up Factors for Various Parameters

Radionuclide	Half-life (yrs)	SOIL-1 (a)	SOIL-2 (b)	Ratio SOIL-2 to SOIL-1	K _d (mL/g) (c)	SOIL-3 (d)	Ratio SOIL-3 to SOIL-1
Ac-227	2.18E+01	2.1E-03	7.2E-02	35	1,100	6.7E-02	32.40
Al-26	7.17E+05	2.1E-03	1.0E-01	50	1,300	9.7E-02	46.65
Am-241	4.32E+02	2.1E-03	1.0E-01	49	1,100	9.4E-02	45.23
Am-242m	1.83E-03	2.1E-03	9.8E-02	47	1,100	9.1E-02	43.50
Am-243	1.41E+02	2.1E-03	1.0E-01	50	1,100	9.6E-02	46.04
C-14	5.70E+03	2.1E-03	1.0E-01	50	0	1.4E-04	0.07
Cf-249	3.51E+02	2.1E-03	1.0E-01	49	1,100	9.4E-02	45.03
Cf-251	8.98E+02	2.1E-03	1.0E-01	49	1,100	9.5E-02	45.68
Cl-36	3.01E+05	2.1E-03	1.0E-01	50	0	1.4E-04	0.07
Cm-243	4.46E-01	2.1E-03	7.8E-02	38	1,100	7.3E-02	35.22
Cm-244	1.81E+01	2.1E-03	6.7E-02	32	1,100	6.3E-02	30.34
Cm-245	8.50E+03	2.1E-03	1.0E-01	50	1,100	9.6E-02	46.05
Cm-247	1.56E+07	2.1E-03	1.0E-01	50	1,100	9.6E-02	46.10
Cm-248	3.48E+05	2.1E-03	1.0E-01	50	1,100	9.6E-02	46.09
Co-60	5.27E+00	2.0E-03	3.1E-02	15	7	3.8E-03	1.87
Cs-135	2.30E+06	2.1E-03	1.0E-01	50	50	2.9E-02	13.86
Cs-137	3.00E+01	2.1E-03	7.9E-02	38	50	2.5E-02	12.13
Eu-152	1.35E+01	2.1E-03	5.9E-02	28	1,100	5.5E-02	26.75
Eu-154	8.59E+00	2.0E-03	4.5E-02	22	1,100	4.2E-02	20.74
Gd-152	1.08E+14	2.1E-03	1.0E-01	50	1,100	9.6E-02	46.03
H-3	1.23E+01	2.1E-03	5.6E-02	27	0	1.4E-04	0.07
I-129	1.57E+07	2.1E-03	1.0E-01	50	0	1.4E-04	0.07
K-40	1.25E+09	2.1E-03	1.0E-01	50	10	6.1E-03	2.91
Nb-93m	1.61E+01	2.1E-03	6.4E-02	31	0	1.4E-04	0.07
Nb-94	2.03E+04	2.1E-03	1.0E-01	50	0	1.4E-04	0.07
Ni-59	7.60E+04	2.1E-03	1.0E-01	50	7	4.3E-03	2.06
Ni-63	1.00E+02	2.1E-03	9.6E-02	46	7	4.3E-03	2.05
Np-237	2.14E+06	2.1E-03	1.0E-01	50	0.6	5.0E-04	0.24
Pa-231	3.28E+04	2.1E-03	1.0E-01	50	0.6	5.0E-04	0.24
Pb-210	2.22E+01	2.1E-03	7.2E-02	35	2,000	7.0E-02	33.60
Pd-107	6.50E+06	2.1E-03	1.0E-01	50	7	4.3E-03	2.06
Pt-193	5.00E+01	2.1E-03	8.8E-02	42	0	1.4E-04	0.07
Pu-238	8.77E+01	2.1E-03	9.4E-02	45	270	7.0E-02	33.72
Pu-239	2.41E+04	2.1E-03	1.0E-01	50	270	7.7E-02	36.68
Pu-240	6.56E+03	2.1E-03	1.0E-01	50	270	7.7E-02	36.65
Pu-241	1.43E+01	2.1E-03	6.0E-02	29	270	4.7E-02	22.92
Pu-242	3.75E+05	2.1E-03	1.0E-01	50	270	7.7E-02	36.69
Pu-244	5.65E-04	2.1E-03	1.0E-01	50	270	7.7E-02	36.69
Ra-226	1.60E+03	2.1E-03	1.0E-01	50	5	3.1E-03	1.49
Ra-228	5.75E+00	2.0E-03	3.3E-02	16	5	2.9E-03	1.41
Se-79	2.95E+05	2.1E-03	1.0E-01	50	1,000	9.5E-02	45.74

Table B-3.1: Soil Build-up Factors for Various Parameters (Continued)

Radionuclide	Half-life (yrs)	SOIL-1 (a)	SOIL-2 (b)	Ratio SOIL-2 to SOIL-1	K_d (mL/g) (c)	SOIL-3 (d)	Ratio SOIL-3 to SOIL-1
Sm-151	9.00E+01	2.1E-03	9.5E-02	45	1,100	8.8E-02	42.12
Sn-126	2.30E+05	2.1E-03	1.0E-01	50	2,000	1.0E-01	47.74
Sr-90	2.89E+01	2.1E-03	7.8E-02	38	5	3.1E-03	1.47
Tc-99	2.11E+05	2.1E-03	1.0E-01	50	0.6	5.0E-04	0.24
Th-229	7.34E+03	2.1E-03	1.0E-01	50	900	9.4E-02	45.26
Th-230	7.54E+04	2.1E-03	1.0E-01	50	900	9.5E-02	45.31
Th-232	2.91E+03	2.1E-03	1.0E-01	50	900	9.5E-02	45.31
U-232	6.89E+01	2.1E-03	9.2E-02	44	200	6.2E-02	29.99
U-233	1.59E+05	2.1E-03	1.0E-01	50	200	6.9E-02	33.22
U-234	2.46E+05	2.1E-03	1.0E-01	50	200	6.9E-02	33.22
U-235	7.04E+08	2.1E-03	1.0E-01	50	200	6.9E-02	33.22
U-236	2.34E+07	2.1E-03	1.0E-01	50	200	6.9E-02	33.22
U-238	4.47E+09	2.1E-03	1.0E-01	50	200	6.9E-02	33.22
Zr-93	1.53E+06	2.1E-03	1.0E-01	50	900	9.5E-02	45.31

- (a) SOIL-1 = soil build-up factor assuming 0.5 year build-up with no leaching
- (b) SOIL-2 = soil build-up factor assuming 25 years build-up with no leaching
- (c) Obtained from SRR-CWDA-2009-00017, Table 4.2-15 (Vadose Zone)
- (d) SOIL-3 = soil build-up factor assuming 25 years build-up with leaching

Note that the dose equations provided in the initial response to RAI B-3, and the "ROOT" component of the calculation for radionuclide concentration in vegetables and fodder provided in SRR-CWDA-2009-00017, Section 5.4.1.1, determine radionuclide build-up based on the *SOIL* expression and parameters shown above but with $\lambda_L = 0$.

Dose calculations performed to support responses in this RAI package include the use of this *SOIL* factor based on 25 years of irrigation with leaching. Peak dose results in Sectors B and I are provided in response to RAI Comment B-2, Table RAI B-2.4.

B-4

Comment (New):

The soil to plant transfer factors may be too low due to the elimination of the leafy plant component.

Basis:

WSRC-STI-2007-00004 uses soil to plant transfer factors for non-vegetative portions of food crops because local productivity of non-leafy vegetables is expected to be considerably greater than that of leafy vegetables (based on WSRC-RP-91-17). However, the transfer factors for leafy vegetables can be considerably larger than non-leafy vegetables for key radionuclides. For example, the reference most used as a source of transfer factors in the current analysis (PNNL-13421) has a factor of 210 for leafy vegetables and a value of 0.24 for non-leafy vegetables for Tc. At a 13% leafy vegetable fraction, the vegetable pathway dose from Tc would be over 100 times larger with the leafy and non-leafy components calculated separately and then combined compared to assigning all vegetables as non-leafy. In addition, the WSRC-RP-91-17 reference may have underrepresented garden production data due to limited survey response.

Path Forward:

Include the leafy vegetable pathway explicitly in the plant pathway dose calculation. Consider using EPA or NRC references for garden productivity data.

RESPONSE B-4:

DOE did not explicitly include the leafy plant transfer factor component in the SDF PA dose calculation because leafy vegetables represented only 5 % of the total vegetable production in the area surrounding the SRS, and were considered negligible to the total vegetable production. [WSRC-RP-91-17] However, DOE concurs that the transfer factors for leafy vegetables can be considerably larger than transfer factors for non-leafy vegetables for some radionuclides.

To support the response to this RAI, DOE performed a sensitivity analysis to ascertain the impact of revised transfer factors. The transfer factors for soil-to-plant, feed-to-milk, feed-to-beef, and water-to-fish provided in SRR-CWDA-2009-00017, Table 4.6-1 have been updated for use in responses to this RAI package. Table RAI B-2.1 in the response to RAI B-2 provides the updated transfer factors and the parameters used in the PA. The updated transfer factors are based on SRNL-STI-2010-00447. This report, issued after the issuance of Revision 0 of the PA, presents additional details on transfer factors utilized in the past and discussion on transfer factors developed for future use. This report also established a standardized source for transfer factors that represent current data including IAEA-472. Issued in 2010, IAEA-472 provides values for transfer factors in terrestrial and freshwater environments. This report supersedes IAEA-364, which was a key source of data in PNNL-13421, which was used as a primary data source for Revision 0 of the PA. The transfer factors presented in this report assumes that the leafy plant vegetables represent 20 % of the total plant production, non-leafy vegetables represent 55 % of the total plant production, tubers and root vegetables represent 10 % of total plant production, and leguminous vegetables represent 15 % of the total vegetable production. If a plant group was not represented in the source documents, it was not included in the weighted total, but an analog was used instead. Therefore, the leafy component ranges from 20 % to 100 % of the soil-to-plant transfer factor. For Tc-99, the leafy component represents 44 % of the soil-to-plant transfer factor, since a value for the non-leafy vegetables was not provided in the source documents.

With respect to Tc-99, the updated soil-to-plant transfer factor is a factor of 382 greater than the value used in the PA analysis. Dose calculations prepared for responses to this RAI package will use the updated transfer factors presented in Table RAI B-2.1. Peak dose results in Sectors B and I are provided in response to RAI Comment B-2, Table RAI B-2.4.

In addition, the vegetation production yield (referred to as “garden productivity” in the Path Forward) has been updated based on SRNL-STI-2010-00447. The vegetation production yield is used in the “LEAF” component of calculation for radionuclide concentration in vegetation (vegetables and fodder), as shown in SRR-CWDA-2009-00017, Section 5.4.1.1. For dose calculations prepared in support of responses in this RAI package, the vegetation production yield is updated from the PA value of 0.7 kg/m² (shown in SRR-CWDA-2009-00017, Table 4.6-5) to 2.2 kg/m².

The total peak doses to the MOP provided in Table RAI B-2.4 are less than the values reported in SRR-CWDA-2009-00017, Section 5.5.1.2 and are discussed in the response to RAI Comment B-2. These reductions in dose are attributed to a decrease in the dose from the fish ingestion pathway (caused by a decrease in the water-to-fish transfer factor for Ra-226 as discussed in the response to RAI Comment B-2) and a decrease in the vegetable ingestion pathway (caused by an increase in the vegetation production yield).

B-5

Comment (New):

The drinking water ingestion rate of 337 L/yr is inconsistent with an average member of the critical group definition.

Basis:

The drinking water ingestion rate is calculated by taking the mean per capita total water ingestion of 1233 mL/day and multiplying by the 75% value from community water. However, this is weighting the critical group member's consumption rate by the type of group the critical group member is in. Given the current site usage and definition of the receptor as a resident farmer, the drinking water consumption rate should be a minimum of 87% of the total water ingestion rate (subtract out the bottled water fraction). Consideration should also be given to adjusting the values for a receptor engaging in a more labor-intensive lifestyles than average in a climate that is warmer than average.

Path Forward:

Modify the drinking water consumption rates to be consistent with the defined receptor and scenario.

RESPONSE B-5:

As discussed in Section 5.6.3.7.1 of the SDF PA, a value of 337 L/yr is used as the nominal water ingestion rate for all members of the public and inadvertent intruder pathway analysis. An EPA drinking water survey (EPA-822-R-00-001) was used to develop the 337 L/yr value. The EPA drinking water survey reports the mean per capita total water ingestion is 1,233 mL/person/d (450 L/yr) when viewed across genders and all age categories with 75% from community water, 13% from bottled water, 10% from other sources (well, spring, and cistern, etc.), and 2% from non identified sources. This yields a mean of 924 mL/person/d (337 L/yr) from community water. In calculating the water ingestion doses, only the individual's primary water source (community water - 75%), was assumed to be contaminated water. The receptor's other water sources such as bottled water (13%), other sources (well, spring, and cistern, etc.; 10%), and non-identified sources (2%) were assumed to be uncontaminated. The fact that the receptor was assumed to drink from a contaminated well does not result in the water ingestion rate being increased by 10 % (the other sources, well, spring, and cistern, etc.) because it is expected that any increase would be offset by a decrease in the 75% value due to the receptor drinking "community water" that was not tied to the contaminated well.

In response to this RAI, DOE investigated using an ingestion rate derived from obtaining 87% of the water from a contaminated source (392 L/yr) versus the rate from obtaining 75% of the water from a contaminated source (337 L/yr). The difference between the two values represents an increase of 16% in contaminated water ingestion, and with a linear relationship between the water ingestion rate and the water ingestion dose, the resulting water ingestion dose component would also increase by the same 16%. Using the dose results presented in the response to RAI B-2 for comparison (Table RAI B-2.4), the water ingestion dose for the MOP at the 100-meter well from Sector B and Sector I range between 54% and 77% of the peak dose. If the water ingestion rates were based on obtaining 87% of the water from the well, the peak dose for the member of the public, at the 100-meter well, would increase by approximately 10% for both Sector B and Sector I. The results are provided in Tables B-5.1 and B-5.2.

The effect of variability in the receptor's water ingestion rate was addressed in the SDF PA through the probabilistic analyses. In the stochastic analyses of the water ingestion rate, the water ingestion rate range was assumed to be as high as 730 L/yr (2 L/d). As presented in SRR-CWDA-2009-00017, Table 5.6-12, the mean of the peaks for Base Case is 4.5 mrem/yr within 10,000 years in the probabilistic analysis, which includes all stochastic parameters including the water ingestion rate.

Table B-5.1: Peak Dose Comparison Based on 75 % and 87 % of the Water Ingested from the 100-Meter Well for the MOP in Sector B

	Contribution to Total Dose (mrem/yr) at Peak Year (9,980) in the first 10,000 years			
Exposure Pathway	337 L/yr water ingestion rate		392 L/yr water ingestion rate	
Water Ingestion	6.9E-01	77.1%	8.1E-01	79.6%
Vegetable Ingestion	1.1E-01	11.9%	1.1E-01	10.6%
Inhalation	4.6E-02	5.1%	4.6E-02	4.5%
Fish Ingestion	3.5E-02	3.9%	3.8E-02	3.5%
Beef Ingestion	3.9E-03	0.4%	3.9E-03	0.4%
Milk Ingestion	2.8E-03	0.3%	2.8E-03	0.3%
Egg Ingestion	2.4E-03	0.3%	2.4E-03	0.2%
Chicken Ingestion	3.3E-04	<0.1%	3.3E-04	<0.1%
All Other Pathways	8.0E-03	0.9%	8.0E-03	0.8%
<i>Total</i>	<i>9.0E-01</i>	<i>100%</i>	<i>1.0E+00</i>	<i>100%</i>
	Contribution to Total Dose (mrem/yr) at Peak Year (15,080) in the first 20,000 years			
Exposure Pathway	337 L/yr water ingestion rate		392 L/yr water ingestion rate	
Water Ingestion	1.3E+00	65.1%	1.5E+00	68.4%
Fish Ingestion	3.7E-01	18.7%	3.7E-01	17.0%
Vegetable Ingestion	2.1E-01	10.4%	2.1E-01	9.4%
Inhalation	5.2E-02	2.6%	5.2E-02	2.3%
Milk Ingestion	2.4E-02	1.2%	2.4E-02	1.1%
Beef Ingestion	1.5E-02	0.8%	1.5E-02	0.7%
Egg Ingestion	1.4E-02	0.7%	1.4E-02	0.6%
Chicken Ingestion	4.4E-04	<0.1%	4.4E-04	<0.1%
All Other Pathways	9.3E-03	0.5%	9.3E-03	0.4%
<i>Total</i>	<i>2.0E+00</i>	<i>100%</i>	<i>2.2E+00</i>	<i>100%</i>

Table B-5.2: Peak Dose Comparison Based on 75 % and 87 % of the Water Ingested from the 100-Meter Well for the MOP in Sector I

	Contribution to Total Dose (mrem/yr) at Peak Year (10,000) in the first 10,000 years			
Exposure Pathway	337 L/yr water ingestion rate		392 L/yr water ingestion rate	
Water Ingestion	5.8E-02	53.9%	6.7E-02	57.6%
Fish Ingestion	3.5E-02	33.1%	3.5E-02	30.5%
Vegetable Ingestion	8.8E-03	8.2%	8.8E-03	7.5%
Inhalation	1.9E-03	1.8%	1.9E-03	1.6%
Milk Ingestion	1.6E-03	1.5%	1.6E-03	1.4%
Beef Ingestion	8.4E-04	0.8%	8.4E-04	0.7%
Egg Ingestion	8.0E-04	0.7%	8.0E-04	0.7%
Chicken Ingestion	1.2E-05	<0.1%	1.2E-05	<0.1%
All Other Pathways	2.9E-05	<0.1%	2.9E-05	<0.1%
<i>Total</i>	<i>1.1E-01</i>	<i>100%</i>	<i>1.2E-01</i>	<i>100%</i>
	Contribution to Total Dose (mrem/yr) at Peak Year (15,080) in the first 20,000 years			
Exposure Pathway	337 L/yr water ingestion rate		392 L/yr water ingestion rate	
Water Ingestion	1.4E+00	66.4%	1.6E+00	69.6%
Fish Ingestion	3.7E-01	18.3%	3.7E-01	16.5%
Vegetable Ingestion	2.1E-01	10.0%	2.1E-01	9.1%
Milk Ingestion	5.1E-02	2.5%	5.1E-02	2.2%
Beef Ingestion	2.5E-02	1.2%	2.5E-02	1.1%
Egg Ingestion	2.5E-02	1.2%	2.5E-02	1.1%
Inhalation	7.2E-03	0.4%	7.2E-03	0.3%
Chicken Ingestion	1.4E-04	<0.1%	1.4E-04	<0.1%
All Other Pathways	6.5E-05	<0.1%	6.5E-05	<0.1%
<i>Total</i>	<i>2.0E+00</i>	<i>100%</i>	<i>2.3E+00</i>	<i>100%</i>

ALARA Analysis (A)

A-1

Comment:

Social, economic, and public policy considerations do not appear to have been considered in an analysis of maintaining doses “As Low As is Reasonably Achievable” (ALARA).

DOE Response Discussion:

The response to this RAI states that “the estimated dose pathways evaluated in the PA are well below the performance objectives; therefore, a qualitative assessment of disposal alternatives is justified.” NRC staff agrees with the concept that a less detailed ALARA is required when the predicted doses are low, but NRC staff would like to note that an assessment that includes the concerns raised in other RAIs (e.g., PA-11, PA-13, IN-1, etc.) may result in a higher calculated dose. In addition, the response to this RAI did not include a discussion on the processes that are being used to minimize the inventory that is disposed of at the SDF. A discussion on maintaining the worker dose at levels that are ALARA was also not included.

Path Forward

Provide additional information on the methodology used to minimize the inventory of radionuclides that are sent to the SDF. Also, provide more details on the controls that exist to minimize the dose to the workers.

RESPONSE A-1:

The SRS has an ALARA program and processes established in company level policies and procedures for the protection of workers that are well documented. [E7-1 Manual, Procedure DE-DP-384] Some of the existing controls to minimize the dose to workers include the remote handling of materials, shielding transfer lines as well as utilizing structural shielding, and sampling of feed material to ensure activity limits are met.

The goal of the ALARA process is the attainment of the lowest practical dose level after taking into account social, technical, economic, and public policy considerations. Depending on the situation, the ALARA analysis can range from simple qualitative statements evaluating different operation and disposal options for LLW to rigorous quantitative analyses that consider individual and collective doses to the MOP. The rigor of the ALARA analysis should be commensurate with the magnitude of the calculated dose and the decisions to be made regarding the disposal facility. Based on the results of the SDF PA, a qualitative assessment of ALARA alternative disposal analysis is justified. Additionally, an in-depth ALARA cost-benefit analysis is not appropriate at this time, because the cost of new technology and personnel exposures will not be available until following final waste removal and salt processing operations.

The ALARA process is applied to SDF in several ways, 1) making conservative assumptions when modeling SDF radionuclide inventory, releases, and dose to receptors, 2) by evaluating disposal cell design and alternatives, and 3) by evaluating and implementing alternative salt processing that could reduce the inventory disposed at SDF. Each is described below.

The following excerpts are from the two governing regulations that define performance objectives.

DOE M 435.1-1, Chapter IV, P.(2)(f) states:

Performance assessments shall include a demonstration that projected releases of radionuclides to the environment shall be maintained as low as reasonable achievable (ALARA).

DOE G 435.1-1 provides additional guidance on meeting this requirement. The guide states in part:

...that the goal of the ALARA process is not the attainment of a particular dose level (or, in this case, level of release), but rather the attainment of the lowest practical dose level after taking into account social, technical, economic, and public policy considerations. The PA should include assessments that focus on alternatives for LLW disposal. ALARA is meant to provide a documented answer to the question: "Have I done all that I can reasonably do to reduce radiation doses or releases to the environment?"

Code of Federal Regulations, 10 CFR 61, Section 61.41, *Protection of the General Population from Releases of Radioactivity*, states:

Reasonable effort should be made to maintain releases of radioactivity in effluents to the general environment as low as is reasonable achievable.

The DOE's approach to radiation protection is based on meeting the performance objectives identified in DOE M 435.1-1 and 10 CFR 61. These documents specify maximum doses for various pathways based upon the ALARA principle.

The SDF PA modeling effort provides evidence of the SRS efforts to reduce radioactive releases to the general environment to levels as low as reasonably achievable. Considerable conservatism is applied during the modeling effort and are summarized in Section 7.2. One of the appreciable conservatisms is the evaluation point for dose. In the SDF PA modeling, radionuclide dose to receptors is evaluated at a 1m and 100-meter buffer zone surrounding SDF and at the seepline. However, based on SRS land use plans, no MOP will have unrestricted access to the SDF, because current SRS boundaries will remain unchanged, and the land will remain under the ownership of the federal government, consistent with the site's designation as a NRMP. By demonstrating protection to the 1-meter and the 100-meter boundary, the PA is also demonstrating public protection at the site boundary (approximately 5 miles away). In fact, the dose due to radionuclides at the site boundary would only be greatly diminished in comparison to the 1-meter and 100-meter boundary dose, because as radionuclides travel a greater distance through the air and subsurface, the more dispersion and dilution occurs. Therefore, the PA demonstrates protection of the public at the site boundary to a much greater degree than at the 1-meter or 100-meter boundary.

The FDC's represent a significant improvement in design compared to the design of Vaults 1 and 4. Additional design features are being added to Disposal Cells 2A and 2B to ensure hydraulic performance consistent with the SDF PA. FDC's will be designed with all of the knowledge gained from Vaults 1 and 4 and Disposal Cells 2A and 2B.

The Small Column Ion Exchange technology is an alternative for salt processing that is being evaluated for implementation. This technology may achieve better salt processing by reducing the time required to complete the salt processing mission, representing a social and economic advantage. Other technologies for salt processing that could potentially reduce the inventory disposed at the SDF will be evaluated as the technologies emerge.

Social, technical, economic and public policy aspects were most recently considered in the alternative processing analysis included in the EIS for salt processing alternatives. [DOE/EIS-0082-S2] In June 2001, DOE issued the EIS on salt processing alternatives. DOE studied four alternatives:

1. Small Tank Precipitation
2. Ion Exchange
3. Solvent Extraction
4. Direct Disposal in Grout

DOE selected the "Solvent Extraction" as the preferred option with the best approach to minimize human health and safety risks associated with salt processing. [DOE/EIS-0082-S2] This represents the best available technology to minimize the inventory sent to SDF.

In summary, the analysis of alternative salt processing techniques; the evaluation of emerging technologies for salt processing and disposal cell design; and meeting the performance objectives of DOE M 435.1-1 and 10 CFR 61 are all evidence of the application of ALARA in limiting the release of radionuclides into the environment. Therefore, the principle of ALARA is satisfied.

In addition, the concerns expressed in other RAIs (e.g., PA-11, PA-13, IN-1, etc.) have been addressed in the comment responses to the respective RAIs. The estimated dose consequences to the MOP presented in the response to RAI PA-8 for the Alternative Sensitivity Case, Case K, are greater than some other cases evaluated in the PA. However, Case K was developed to consider more pessimistic performance parameters than expected during the performance period. Detailed descriptions of these pessimistic performance parameters are presented in the response to RAI PA-8.

Clarifying Questions (C)

As mentioned in the Structure of Comments section of this RAI, the staff found the remaining clarifying comment responses, not referred to in the section below, to be acceptable. In addition to referring to one Clarifying Comment from RAI-2009-01, the staff has added two new clarifying comments in RAI-2009-02.

Table C-0.1: Status of Clarifying Question Comments for RAI-2009-01

Clarifying Question	Status	Clarifying Question	Status
C-1	Acceptable / Omitted	C-13	Acceptable / Omitted
C-2	Acceptable / Omitted	C-14	Acceptable / Omitted
C-3	Acceptable / Omitted	C-15	Acceptable / Omitted
C-4	Clarify / Incomplete	C-16	Acceptable / Omitted
C-5	Acceptable / Omitted	C-17	Acceptable / Omitted
C-6	Acceptable / Omitted	C-18	Acceptable / Omitted
C-7	Acceptable / Omitted	C-19	Acceptable / Omitted
C-8	Clarify / Incomplete	C-20	Acceptable / Omitted
C-9	Acceptable / Omitted	C-21	Acceptable / Omitted
C-10	Acceptable / Omitted	C-22	New
C-11	Acceptable / Omitted	C-23	New
C-12	Acceptable / Omitted		

C-4

Comment:

Clarify the basis for the selenium K_d of 150 mL/g for old oxidizing conditions. It is not clear from the PA, or the supporting report WSRC-STI-2007-00640, how the value was selected. Clarify whether the evaluation considered the presence in solution of the selenium as selenate, which is potentially less sorptive than selenite.

DOE Response Discussion:

The DOE discussed site-specific batch experiments that showed selenium K_d values ranging from 29.7 to 78.5 mL/g. These experiments were discounted in favor of literature values due to the aqueous selenium concentrations being near the detection limits. The basis for the selenium K_d of 150 mL/g for old oxidizing conditions relied on the values reported in "Sorption of Selenite and Selenate to Cement Materials" (Baur and Johnson 2003). DOE stated that selenite is expected to convert to selenate under old oxidizing conditions and that the K_d values for selenate from the report by Baur and Johnson (2003) were between 180 and 380 mL/g. DOE further stated that as cementitious materials degrade, the selenium sorption constants ($K_d = 1041$ mL/g) approach that of the sediment. Selenium sorption was stated as being very high due to the ubiquitous presence of iron oxides and low pH of the sediment.

The K_d values of 180 and 380 mL/g reported in "Sorption of Selenite and Selenate to Cement Materials" were for selenite, not selenate. Baur and Johnson (2003) reported no significant uptake of selenate with calcium-silicate-hydrate (C-S-H) and only limited sorption with ettringite. Furthermore, it is not clear why the sorption coefficient for selenium would approach that of sediment as cementitious materials degrade. The chemistry of degraded cementitious material would not be expected to have the same chemical properties as sediment (high iron content and low pH), which is responsible for the high sorption coefficient for selenium.

Path Forward:

Provide support for the selenium K_d of 150 mL/g for old oxidizing conditions or revise the base case K_d value.

RESPONSE C-4:

The sorption coefficients used to simulate the release of contaminants from the saltstone are the K_d values developed by WSRC-STI-2007-00640 and shown in SDF PA Table 4.2-18. These K_d values are also used to determine the transport of the released contaminants through the disposal unit concrete. DOE expects that most of the selenium will exist as selenite, SeO_3^{2-} . Varying the cementitious formulations (i.e., water/solid, silica fume percent, and clay concentration) results in a range of selenite K_d values, as initially reported in ISSN: 0956-053X_V20_I7 where K_d values from an alkaline solution ranged from 250 to 930 mL/g. The K_d values of 180 to 380 mL/g reported in *Sorption of Selenite and Selenate to Cement Materials* (DOI: 10.1021/es020148d) were in fact for selenite, not for selenate, as DOE incorrectly stated in the initial response discussion. These values support the initial range of selenite K_d values.

Degradation of the disposal unit concrete (walls, roof, and floor) is believed to be dominated by external sulfate attack. As indicated in SDF PA Table 4.2-9, saltstone transitions from a reducing environment to an oxidizing environment (E_h turns positive) prior to transitioning from middle age (initial condition of saltstone) to old age (pH is less than 11) when groundwater is equilibrated with CSH. Sulfate, which is present in saltstone feedwater and remains at significant concentrations in pore water after grout curing, reacts with cement paste and creates ettringite, an expansive mineral phase.

Selenite, the reduced form of selenium, sorbs more strongly than selenate (SeO_4^{2-}) to sediments at all pH levels. If saltstone transitions to a more oxidizing environment, selenate could form and selenium K_d values should be lower. This is supported by DOI: 10.1021/es020148d, which reported no significant uptake of selenate with CSH, and only limited sorption with ettringite (K_d values of 30 mL/g); however, they did report significant removal of selenate by monosulfate (K_d values of 2,060 mL/g), which also forms in saltstone. Hydrated cement consists of about 0.40 to 0.60 mass fraction CSH phases and about 0.10 to 0.20 mass fraction ettringite and monosulfate; however, ettringite mass fraction increases as the ettringite front progresses with sulfate attack. [SRNS-STI-2008-00050]

In addition, as indicated in the SDF PA source document, SRNS-STI-2008-00045, site-specific batch experiments intended to replicate all three stages of an oxidizing cementitious environment measured selenium K_d values ranging from 29.7 to greater than 78.5 mL/g (standard deviation of 50.8). These measured selenium K_d values are, in general, lower than values reported in literature (e.g., ISSN: 0956-053X_V20_I7; DOI: 10.1021/es020148d).

Thus, the variability in K_d results from various cementitious formulations and batch experiments, and less sorption observed for selenate with ettringite and CSH under oxidizing conditions (per DOI: 10.1021/es020148d), suggest that a K_d value of 150 mL/g (between the results from the above studies) for old oxidizing conditions be used.

Although the original response to RAI C-4 stated that selenium sorption constants would approach that of sediment under old oxidizing conditions, the intent was that as the cementitious materials degrade they would begin to take on the properties of the surrounding materials. This occurs in part from a slow decline in pH and the formation of aluminum/iron-oxyhydroxide coatings and natural organic matter coatings forming over the surrounding surfaces, which would result in an increased K_d value. Selenate, as well as selenite, was found to sorb very strongly to the sediment; the K_d value was greater than 1,040 mL/g for the sand and clay sediments at most pH and organic concentrations. [WSRC-STI-2006-00037] With time, it is expected SRS soils will mix with the various cementation materials, along with iron oxide coating (i.e., goethite and hematite is commonly seen on buried cement foundations). That is true of the sediments of the region, which are coated with aluminum/iron/silicon oxides and organic matter. Thus, the K_d value of 150 mL/g for old-age oxidizing conditions would likely be conservative.

C-8

Comment:

For benchmarking cases B-E (Sections 5.6.2.3.5 through 5.6.2.3.8), the PA compares the doses predicted based on the PORFLOW model and post-benchmarking GoldSim model resulting from “all modeled radionuclides”. Clarify whether the term “all modeled radionuclides” in this context refers to the original list of radionuclides included in the PORFLOW model or a smaller list of radionuclides modeled during the benchmarking effort.

DOE Response Discussion:

The response to this clarifying comment only addressed the radionuclides included in the Case A PORFLOW and the GoldSim calculations. The radionuclides included in the PORFLOW calculations for Cases B-E were not discussed.

Path Forward:

Provide a list of the radionuclides provided in the PORFLOW calculations for Case B, Case C, Case D, and Case E.

RESPONSE C-8:

For Cases B, C, D, E, and the other cases analyzed in SRR-CWDA-2009-00017, Section 5.6.6, input to the PORFLOW analysis included the following radionuclides: I-129, Np-237, Pu-238, Tc-99, Th-230, U-234, and U-235. The principle dose contributing radionuclides, as identified in SRR-CWDA-2009-00017, Section 5.2.2, were captured in these analyses.

Based upon the modeling input identified above, concentrations for the following radionuclides were computed by PORFLOW:

- Ac-227 (from U-235 decay)
- I-129
- Np-237
- Pa-231 (from U-235 decay)
- Pb-210 (from decay of Th-230, Pu-238, and U-234)
- Pu-238
- Ra-226 (from decay of Th-230, Pu-238, and U-234)
- Tc-99
- Th-229 (from decay of Np-237)
- Th-230 (including decay of Pu-238 and U-234)
- U-233 (from decay of Np-237)
- U-234 (including decay of Pu-238)
- U-235

C-22

Comment (New):

Figure 4.2-15 in the PA shows the vertical hydraulic conductivity of the lower lateral drainage layer reducing in time to approximately $4\text{E-}5$ cm/s by 20,000 years. However, the PORFLOW model files indicate that the hydraulic conductivity is only reduced to $4.9\text{E-}3$ cm/s for all cases. The flux out of the vaults is directly dependent on the infiltration rates. As indicated in IEC-8, the conservatism of the calculations for the hydraulic conductivity of these lateral drainage layers is not clear and according to the PORFLOW model files, it is not clear if these calculations were implemented appropriately. Clarify why different hydraulic conductivity values were implemented in the PORFLOW model.

RESPONSE C-22:

SRR-CWDA-2009-00017 Figure 4.2-15 illustrates the change in the vertical hydraulic conductivity of the sand drainage layer based on the analytical solution presented in Table 22 of SRNL-STI-2009-00115, Revision 1. The values for the hydraulic conductivity used in the PORFLOW runs are provided in Appendix E to SRNL-STI-2009-00115. As shown in Appendix E, the vertical hydraulic conductivity of the sand drainage layer is $4.9\text{E-}3$ cm/sec during the time period starting at year 15,000 and ending at year 20,000. The difference between the analytical values and the PORFLOW input values is because the PORFLOW time period of 15,000 years to 20,000 years utilizes the average value spanning that time period ($4.9\text{E-}3$ cm/s) rather than an endpoint value ($4\text{E-}5$ cm/s).

C-23

Comment (New):

WSRC-STI-2008-00244 discussed the installation quality of the geomembrane as “Good”; however, the HELP model also requires the specification for the placement quality of the geomembrane. The Help model input data in Appendix J of WSRC-STI-2008-00244, listed the geomembrane placement quality as a “2”. According to the “HELP User’s Guide for Version 3” (Schroeder et al., 1994), an entry of 2, “assumes exceptional contact between geomembrane and adjacent soil that limits drainage rate (typically achievable only in the lab or small field lysimeters).” The basis for selecting the placement quality of the geomembrane should be provided.

RESPONSE C-23:

It appears that there is some confusion related to installation quality of the geomembrane versus placement quality of the geomembrane. Two HELP model geomembrane input parameters, both of which are associated with some aspect of the quality of geomembrane installation (EPA-600-R-94-168a; EPA-600-R-94-168b), are:

- Geomembrane Installation Defects (#/acre)
- Geomembrane Placement Quality

Geomembrane installation defects are defined as geomembrane damage resulting from seaming errors, abrasion, and punctures occurring during installation that result in the generation of holes. The number of installation defects is related to the level of geomembrane installation QA/QC program employed. The HELP model documentation (EPA-600-R-94-168a; EPA-600-R-94-168b) provides a recommended number of installation defects based upon categorization of the QA/QC program employed as excellent, good, fair, or poor.

For the current SDF closure cap design, a HDPE geomembrane quality assurance plan shall be developed and implemented that incorporates visual inspection during installation, wrinkle control, seam field testing, and defect repair, which will be performed in accordance with the approved drawings, plans, and specifications of the final design, which will be produced near the end of the operational period. These SDF closure cap QA/QC requirements represent “good” quality assurance according to EPA-600-R-94-168a and EPA-600-R-94-168b. Therefore, in conformance with HELP model guidance, four installation defects per acre were assumed.

Geomembrane placement quality is related to the degree of contact between the geomembrane and the underlying soil and the potential for lateral flow along the boundary between the two layers. Within the HELP model, there are six geomembrane placement quality designations (i.e., perfect, excellent, good, poor, worst case, geotextile separating geomembrane liner and drainage limiting soil). The cited reference to the HELP User’s Guide (EPA-600-R-94-168a) is further elaborated upon in the HELP Engineering Documentation (EPA-600-R-94-168b), which states the following regarding an “excellent” geomembrane placement quality:

“Excellent liner contact is achieved under three circumstances. Medium permeability soils and materials are typically cohesionless and therefore generally are able to conform to the geomembrane, providing excellent contact. The second circumstance is for very well prepared low permeability soil layer with exceptional geomembrane placement typically achievable in the laboratory, small lysimeters or small test plots. The third circumstance is by the use of a geosynthetic clay liner (GCL) adjacent to the geomembrane with a good foundation. The GCL, upon wetting, will swell to fill the gap between the geomembrane and the foundation, providing excellent contact.” [EPA-600-R-94-168b, p. 88]

Consistent with this HELP model guidance and the use of a HDPE geomembrane within the closure cap underlain by a GCL over a bentonite/soil blended upper foundation layer, an “excellent” (HELP model numerical designation 2) geomembrane placement quality designation was utilized for the recommended SDF closure cap. The information provided above associated with both geomembrane installation defects and geomembrane placement quality is also cited in WSRC-STI-2008-00244 Section 5.4.5.

In summary, consistent with HELP model guidance, the assigned number of SDF closure cap geomembrane installation defects was based upon having a good QA/QC program, whereas the selection of the geomembrane placement quality as excellent is based upon having the HDPE underlain by a GCL and specially prepared foundation layer. These two HELP model geomembrane input parameters, while both related to geomembrane installation quality, are distinctly different, and both are implemented within the SDF closure cap HELP modeling according to the appropriate HELP model guidance.

REFERENCES FOR COMMENT RESPONSES

Note 1: References identified as (Copyright) were used in the development, but are protected by copyright laws. No part of the publication may be reproduced in any form or by any means, including photocopying or electronic transmittal in any form by any means, without permission in writing from the copyright owner.

10 CFR 20, *Standards for Protection Against Radiation*, U.S. Nuclear Regulatory Commission, Washington DC, January 5, 2010, <http://www.nrc.gov/reading-rm/doc-collections/cfr/part020/>, Accessed January 20, 2011.

10 CFR 61, *Licensing Requirements for Land Disposal of Radioactive Waste*, U.S. Nuclear Regulatory Commission, Washington DC, January 5, 2010, <http://www.nrc.gov/reading-rm/doc-collections/cfr/part061/>, Accessed January 20, 2011.

10 CFR 835, *Occupational Radiation Protection*, U.S. Nuclear Regulatory Commission, Washington DC, May 13, 2011.

87814-PT1, *Saltstone Disposal Z-Area Savannah River Plant*, Mueser Rutledge Consulting Engineers, Savannah River Site, Aiken, SC, October 14, 1986.

CBU-PIT-2005-00040, Hutchens, G. J., *Estimate of Actinide Concentration by Radioactive Decay*, Savannah River Site, Aiken, SC, Rev. 0, March 15, 2005.

DHEC_09-30-2010, Litton, J., *Conceptual Approval of Disposal of Low-Level Containerized Waste A-Area SDF*, S.C. Department of Health and Environmental Control, Columbia, SC, September 30, 2010, <http://pbadupws.nrc.gov/docs/ML1033/ML103340171.pdf>, Accessed July 21, 2011.

DOE G 435.1-1, *Implementation Guide for use with DOE M 435.1-1*, U.S. Department of Energy, Washington DC, July 9, 1999, <https://www.directives.doe.gov/directives/current-directives/435.1-EGuide-1ch1/view?searchterm=doe+g+435>, Accessed January 20, 2011.

DOE M 435.1-1, *Radioactive Waste Management Manual*, U.S. Department of Energy, Washington DC, Chg. 1, January 9, 2007, <https://www.directives.doe.gov/directives/current-directives/435.1-DManual-1c1/view?searchterm=doe+m+435.1>, Accessed January 20, 2011.

DOE/EIS-0082-S2, *Record of Decision: Savannah River Site Salt Processing Alternatives*, Office of the Federal Register, National Archives and Records Administration, 66 FR 52752, Issue 201, October 9, 2001, <http://www.gpo.gov/fdsys/pkg/FR-2001-10-17/pdf/01-26082.pdf>, Accessed July 21, 2011.

DOI: 10.1021/es050073o (Copyright), Kaplan, D. I., et al., *Eleven-Year Field Study of Pu Migration from Pu III, IV, and VI Sources*, Environmental Science and Technology, 40(2), December 6, 2005.

DOI: 10.10160016-7037(90)90369V, (Copyright), Balistrieri, L.S., and Chao, T.T., *Adsorption of Selenium by Amorphous Iron Oxyhydroxide and Manganese Dioxide*, Geochimica et Cosmochimica Acta, Vol. 54, pp. 739-751, January 4, 1990.

DOI: 10.1021/es020148d, (Copyright), Baur, I., et al., *Sorption of Selenite and Selenate to Cement Materials*, Environmental Science and Technology, 2003, (37), pp. 3442-3447.

DOI: 10.1029/98WR02040, (Copyright) Liu, H. H., et al., *An Active Fracture Model for Unsaturated Flow and Transport in Fractured Rocks*, Water Resources Research Vol. 34, No. 10, Pages 2633-2646, 1998.

E7-1 Manual, Procedure DE-DP-384, *Design Engineering Conduct of Engineering and Technical Support, ALARA Design Considerations and Reviews*, Savannah River Site, Aiken SC, Rev. 1, November 20, 2008.

EPA-600-R-94-168a, Schroeder, P. R., et al., *The Hydrologic Evaluation of Landfill Performance (HELP) Model: User's Guide for Version 3*, U.S. Environmental Protection Agency, Cincinnati, OH, September 1994.

EPA-600-R-94-168b, Schroeder, P. R., et al., *The Hydrologic Evaluation of Landfill Performance (HELP) Model: Engineering Documentation for Version 3*, U.S. Environmental Protection Agency, Cincinnati, OH, September 1994.

EPA-822-R-00-001, *Estimated Per Capita Water Ingestion and Body Weight in the United States - An Update, Based on Data Collected by the United States Department of Agriculture's 1994 - 1996 and 1998 Continuing Survey of Food Intakes by Individuals*, U.S. Environmental Protection Agency, Washington DC, October 2004.

ERD-EN-2008-0056, *Z-Area Vault 4 Phase 1 Soil Sample Analytical Data Report*, Savannah River Site, Aiken, SC, Rev. 0, July 15, 2008.

ERD-EN-2008-0083, *Z-Area Vault 4 Phase 2 Soil Sample Analytical Data Report*, Savannah River Site, Aiken, SC, December 1, 2008.

ESH-WPG-2006-00132, *Z-Area Industrial Solid Waste Landfill Vault Cracking*, Savannah River Site, Aiken, SC, October 19, 2006.

EWR 860438, *EWR 860438 Foundation Investigation Building 241F Additional High Level Waste Storage Tanks Project 9S 1493 FY75 Tanks Nos. 25 Through 28 Project FY77 Tanks Nos. 44 Through 47 Savannah River Plant*, Mueser, Rutledge, Wentworth & Johnson Consulting Engineers, Savannah River Site, Aiken SC, May 19, 1975.

IAEA-364 (Copyright), *Handbook of Parameter Values for the Prediction of Radionuclide Transfer in Template Environments*, Produced in Collaboration with the International Union of Radioecologists, International Atomic Energy Agency, Technical Reports Series 364, International Atomic Energy Agency, Vienna, Rev. 10-23-56, Superseded, June 1994.

IAEA-472 (Copyright), *Handbook of Parameter Values for the Prediction of Radionuclide Transfer in Terrestrial and Freshwater Environments*, Technical Reports Series No. 472, International Atomic Energy Agency, Vienna, January 2010.

ISBN: 1-55899-189-1, (Copyright), Smith, R.W., et al., *The Role of Oxygen Diffusion in the Release of Technetium from Reducing Cementitious Waste Forms*, Material Resource Society Scientific Basis for Nuclear Waste Management XVI Symposium, April 1993.

ISSN: 0956-053X_V12_I2-3, (Copyright), Ewart, F. T., et al., *The Solubility of Actinides in a Cementitious Near-Field Environment*, Waste Management, Volume 12, Issues 2-3, 12, October 1991, <http://www.sciencedirect.com/science/article/pii/0956053X9290051J>.

ISSN: 0956-053X_V20_I7, (Copyright), Johnson, E. A., et al., *The Sorption of Selenite on Various Cement Formulations*, Waste Management, Vol. 20, Issue 7, November 2000.

K-ESR-G-00013, *SRS Soft Zone Initiative Historical Perspective*, Savannah River Site, Aiken, SC, Rev. 0, January 2008.

K-ESR-Z-00001, *Saltstone Vault No. 2 Geotechnical Investigation Report*, Savannah River Site, Aiken, SC, Rev. 0, April 2006.

K-ESR-Z-00002, *Saltstone Disposal Cells No. 3 and 5 Geotechnical Investigation Report*, Savannah River Site, Aiken, SC, Rev. 0, July 2009.

K-TRT-F-00001, Syms, F., *F-Area Northeast Expansion Report*, Savannah River Site, Aiken, SC, Part 1, Rev. 0, May 1999.

LWO-RIP-2008-00006, *Saltstone Sampling Summary for September 2008*, Savannah River Site, Aiken, SC, Rev. 0, November 4, 2008.

ML053010225, *Technical Evaluation Report for Draft Waste Determination for Salt Waste Disposal*, U.S. Nuclear Regulatory Commission, Washington DC, December 28, 2005.

ML081290367, *Nuclear Regulatory Commission Onsite Observation Report for the Savannah River Site Saltstone Production and Disposal*, U.S. Nuclear Regulatory Commission, Washington DC, June 5, 2008.

ML083190829 (Copyright), *Description of Methodology for Biosphere Dose Model BDOSE*, U.S. Nuclear Regulatory Commission, Washington DC, November 30, 2008.

ML103400571, *Second Request for Additional Information for the 2009 Performance Assessment for the Saltstone Disposal Facility at the Savannah River Site*, Docket Number PROJ0734, U.S. Nuclear Regulatory Commission, Washington DC, December 15, 2010, <http://pbadupws.nrc.gov/docs/ML1034/ML103400571.pdf>, Accessed March 30, 2011.

MPMR_04-23-1963, *Foundation Investigations and Treatment at Savannah River Plant*, Moran, Proctor, Mueser, & Rutledge Consulting Engineers, New York, NY, April 23, 1963.

NCRP-160, (Copyright), *Ionizing Radiation Exposure of the Population of the United States: Recommendations of the National Council on Radiation Protection and Measurements*, National Council on Radiation Protection and Measurements, Washington DC, March 2009.

NDAA_3116, *Public Law 108-375, Ronald W. Reagan National Defense Authorization Act for Fiscal Year 2005, Section 3116, Defense Site Acceleration Completion*, U.S. Department of Energy, Washington DC, October 28, 2004.

NRC_01-01-2011, *Biological Effects of Radiation*, U.S. Nuclear Regulatory Commission, Washington DC, January 2011.

NUREG-1623, Johnson, T. L., *Design of Erosion Protection for Long-Term Stabilization*, U.S. Nuclear Regulatory Commission, Washington DC, September 2002.

NUREG-1854, *NRC Staff Guidance for Activities Related to U.S. Department of Energy Waste Determinations, Draft Final Report for Interim Use*, U.S. Nuclear Regulatory Commission, Washington DC, August 2007.

NUREG-CR-5542, *Models for Estimation of Service Life of Concrete Barriers in Low-Level Radioactive Waste Disposal*, U.S. Nuclear Regulatory Commission, Washington DC, September 1990.

ORNL-5786, Baes, C. F., III, et al., *A Review and Analysis of Parameters for Assessing Transport of Environmentally Released Radionuclides through Agriculture*, Oak Ridge National Laboratory, Oak Ridge, TN, September 1984, Accessed February 1, 2011.

PNNL-13421, Staven, L. H., et al., *A Compendium of Transfer Factors for Agricultural and Animal Products*, Pacific Northwest National Laboratory, Richland, WA, June 2003 http://www.pnl.gov/main/publications/external/technical_reports/PNNL-13421.pdf, Accessed February 9, 2011.

Report 88-4221, *Reconnaissance Hydrogeologic Investigation of the Defense Waste Processing Facility and Vicinity, Savannah River Plant, South Carolina*, Water-Resources Investigation Report, U.S. Geological Survey, Columbia, SC, 1989.

SRNL-ESB-2008-00017, Dixon, K., *Video Survey of Saltstone Fault 4, Cell G, Savannah River Site*, Aiken, SC, April 25, 2008.

SRNL-L3100-2009-00087, *Pictures of Vault 4 Core Samples – Transfer of Samples at SRNL – April 6, 2009*, Savannah River Site, Aiken, SC, April 7, 2009.

SRNL-L4321-2011-00004, Flach, G., *Oxidation of Fractured Cementitious Materials in Performance Assessments*, Savannah River Site, Aiken, SC, Rev. 0, March 24, 2011.

SRNL-L4420-2011-00008, Duncan, A. J., *Response to NRC VP-2 Comment: Additional Basis Is Required for Neglecting Disposal Unit Degradation Mechanisms Other Than Sulfate Attack*, Savannah River Site, Aiken, SC, June 27, 2011.

SRNL-RSE-2008-00029, *Review of Grout Sampling Methods for Saltstone Facility Vaults*, Savannah River Site, Aiken, SC, May 28, 2008.

SRNL-STI-2008-00421, Dixon, K. L., et al., *Hydraulic and Physical Properties of Saltstone Grouts and Vault Concretes*, Savannah River Site, Aiken, SC, Rev. 0, November 2008.

SRNL-STI-2009-00115, Flach, G. P., et al., *Numerical Flow and Transport Simulations Supporting the Saltstone Disposal Facility Performance Assessment*, Savannah River Site, Aiken, SC, Rev. 1, June 2009, <http://pbadupws.nrc.gov/docs/ML1016/ML101600028.pdf>, Accessed March 29, 2011.

SRNL-STI-2009-00150, McDowell-Boyer, L., et al., *Distribution Coefficients (K_d s), K_d Distributions, and Cellulose Degradation Product Correction Factors for the Composite Analysis*, Savannah River Site, Aiken, SC, Rev. 1, April 2009.

SRNL-STI-2009-00419, Dixon, K. D., et al., *Hydraulic and Physical Properties of ARP/MCU Saltstone Grout*, Savannah River Site, Aiken, SC, Rev. 0, May 2010.

SRNL-STI-2009-00473, Kaplan, D. I., *Geochemical Data Package for Performance Assessment Calculations Related to the Savannah River Site*, Savannah River Site, Aiken, SC, Rev. 0, March 15, 2010.

SRNL-STI-2009-00636, Lilley, M. S., et al., *Iodine, Neptunium, Plutonium, and Technetium Sorption to Saltstone and Cement Formulations Under Oxidizing and Reducing Conditions*, Savannah River Site, Aiken, SC, Rev. 0, December 16, 2009.

SRNL-STI-2010-00167, Hera, K. R., *Design and Testing of the Formed-Core Sampling System for Saltstone Facility Vaults*, Savannah River Site, Aiken, SC, Rev. 0, March 15, 2010.

SRNL-STI-2010-00447, Jannik, G. T., et al., *Land and Water Use Characteristics and Human Health Input Parameters for Use in Environmental Dosimetry and Risk Assessments at the Savannah River Site*, Savannah River Site, Aiken, SC, Rev. 0, August 6, 2010.

SRNL-STI-2010-00493, Seaman, J. C., and Kaplan, D. I., *Chloride, Chromate, Silver, Thallium, and Uranium Sorption to SRS Soils, Sediments, and Cementitious Materials*, Savannah River Site, Aiken, SC, Rev. 0, September 29, 2010.

SRNL-STI-2010-00515, Langton, C. A., *Saltstone Characterization and Parameters for Performance Assessment Modeling*, Savannah River Site, Aiken, SC, August 27, 2010.

SRNL-STI-2010-00527, Kaplan, D., et al., *Iodine, Neptunium, Radium, and Strontium Sorption to Savannah River Site Sediments*, Savannah River Site, Aiken, SC, Rev. 0, September 20, 2010.

SRNL-STI-2010-00667, Almond, P. M., *Distribution Coefficients (Kd) Generated From A Core Sample Collected from the Saltstone Disposal Facility*, Savannah River Site, Aiken, SC, Rev. 0, April 25, 2011.

SRNL-STI-2010-00668, Kaplan, D. I., et al., *Long-term Technetium Interactions with Reducing Cementitious Materials*, Savannah River Site, Aiken, SC, Rev. 0, March 2011.

SRNL-STI-2011-00011, Kaplan, D. I., *Estimated Neptunium Sediment Sorption Values as a Function of pH and Measured Barium and Radium K_d Values*, Savannah River Site, Aiken, SC, Rev. 0, January 13, 2011.

SRNL-TR-2008-00283, Denham, M. E., *Estimations of Eh and pH Transitions in Pore Fluids During Aging of Saltstone and Disposal Unit Concrete*, Savannah River Site, Aiken, SC, December 2008.

SRNS-J2100-2008-00004, *Estimated Closure Inventory for the Saltstone Disposal Facility*, Savannah River Site, Aiken, SC, Rev. 2, June 22, 2009.

SRNS-STI-2008-00045, Kaplan, D. I., et al., *Saltstone and Concrete Interactions with Radionuclides: Sorption (Kd), Desorption, and Reduction Capacity Measurements*, Savannah River Site, Aiken, SC, October 30, 2008.

SRNS-STI-2008-00050, Langton, C. A., *Evaluation of Sulfate Attack on Saltstone Vault Concrete and Saltstone*, SIMCO Technologies, Inc., Part 1: Final Report, Savannah River Site, Aiken, SC, Rev. 1, August 28, 2009.

SRNS-STI-2009-00477, Langton, C. A., *Saltstone Matrix Characterization and Stadium Simulation Results*, SIMCO Technologies, Inc., Task 6 Report, Savannah River Site, Aiken, SC, July 30, 2009.

SRNS-TR-2008-00310, Wells, D., *Z-Area Groundwater Monitoring Report for 2008*, Savannah River Site, Aiken, SC, January 9, 2009.

SRNS-TR-2009-00452, Wells, D., *Z-Area Groundwater Monitoring Report for 2009*, Savannah River Site, Aiken, SC, December 29, 2009.

SRNS-TR-2010-00374, Wells, D., *Z-Area Groundwater Monitoring Report for 2010*, Savannah River Site, Aiken, SC, December 2010.

SRR-CWDA-2009-00017, *Performance Assessment for the Saltstone Disposal Facility at the Savannah River Site*, Savannah River Site, Aiken, SC, Rev. 0, October 29, 2009, <http://pbadupws.nrc.gov/docs/ML1015/ML101590008.pdf>, Accessed March 29, 2011.

SRR-CWDA-2009-00045, *F-Tank Farm Waste Tank Closure Inventory for Use in Performance Assessment Modeling*, Savannah River Site, Aiken, SC, Rev. 1, January 26, 2010, <http://pbadupws.nrc.gov/docs/ML1028/ML102850260.pdf>, Accessed March 29, 2011.

SRR-CWDA-2010-00033, *Comment Response Matrix for Nuclear Regulatory Commission (NRC) Requests for Additional Information (RAIs) on the Saltstone Disposal Facility Performance Assessment (SRR-CWDA-2009-00017, Revision 0, dated October 29, 2009)*, Savannah River Site, Aiken, SC, Rev. 1, July 23, 2010.

SRR-CWDA-2010-00057, Kaplan, D. I., *Preliminary Ra and SR Kd Values of Subsurface SRS Sediments*, Savannah River Site, Aiken, SC, May 2010.

SRR-CWDA-2010-00137, *July 28, 2010 U.S. NRC Onsite Observation for Salt Waste Disposal at the Savannah River Site Action Item Response*, Savannah River Site, Aiken, SC, September 15, 2010.

SRR-CWDA-2011-00043, *NRC Salt Waste Monitoring Open Item Status*, Savannah River Site, Aiken, SC, April 26, 2011.

SRR-CWDA-2011-00052, *Savannah River Site Liquid Waste Facilities Performance Assessment Maintenance Program FY2011 Implementation Plan*, Savannah River Site, Aiken, SC, Rev. 0, March 29, 2011.

SRR-CWDA-2011-00055, *FY2010 Annual Review Saltstone Disposal Facility (Z Area) Performance Assessment*, Savannah River Site, Aiken, SC, Rev. 1, April 20, 2011.

SRR-CWDA-2011-00097, *Saltstone Disposal Facility Vault 4 Cells B and H Drainwater Piping Anchor Bolt Inspection Summary*, Savannah River Site, Aiken, SC, Rev. 0, July 19, 2011.

SRR-CWDA-2011-00105, *Saltstone Disposal Facility Vault 4 Video Inspection Summary*, Savannah River Site, Aiken, SC, Rev. 0, July 2011.

SRR-CWDA-2011-00106, *Qualification and Management of K_d Data for Use in C&WDA Performance Assessments*, Savannah River Site, Aiken, SC, June 2, 2011.

SRR-CWDA-2011-00114, *Comparison of a Single-Porosity Shrinking Core Model with a Dual-Porosity Fractured Medium Model*, Savannah River Site, Aiken, SC, June 28, 2011.

SRR-CWDA-2011-00115, *Saltstone Disposal Facility Case K Inventory Determination*, Savannah River Site, Aiken, SC, August 2011.

SRR-LWP-2009-00001, *Liquid Waste System Plan*, Savannah River Site, Aiken, SC, Rev. 16, December 6, 2010, <http://pbadupws.nrc.gov/docs/ML1028/ML102850278.pdf>, Accessed March 29, 2011.

SRS-REG-2007-00002, *Performance Assessment for F-Tank Farm at the Savannah River Site*, Savannah River Site, Aiken, SC, Rev. 0, Superseded, June 27, 2008, <http://pbadupws.nrc.gov/docs/ML0826/ML082680170.pdf>, Accessed March 29, 2011.

SRS-REG-2007-00002, *Performance Assessment for F-Tank Farm at the Savannah River Site*, Savannah River Site, Aiken, SC, Rev. 1, March 31, 2010, <http://pbadupws.nrc.gov/docs/ML1028/ML102850339.pdf>, Accessed March 29, 2011.

SRS-REG-2007-00041, *Unreviewed Disposal Question Evaluation: Evaluation of Liquid Weeping from Saltstone Vault 4 Exterior Walls*, Savannah River Site, Aiken, SC, Rev. 1, April 3, 2008.

T-CLC-P-00004, Carey, S. A., *Long Term Assessment of 105-P Structure for In-Situ D&D Alternatives*, Savannah River Site, Aiken, SC, August 26, 2008.

T-CLC-Z-00022, Patel, R., *Evaluation of Selected Values from CROM's Calculation for the Z-Area Saltstone Storage Tanks (Vault 2)*, Savannah River Site, Aiken, SC, September 28, 2009.

VZJ 3:384-394, (Copyright) Bradford, S. A., et al., *Straining and Attachment of Colloids in Physically Heterogeneous Porous Media*, Vadose Zone Journal, Vol. 3:284-394, Soil Science Society of America, Madison, WI, 2004.

WB00001K-058, *Water Tank Tightness Test Reports*, Savannah River Site, Aiken, SC, Rev. A, February 16, 2011.

WDPD-11-65, *Second Request for Additional Information on the 2009 Performance Assessment for the Saltstone Disposal Facility at the Savannah River Site (SRS)*, U.S. Department of Energy, Savannah River Site, Aiken, SC, May 20, 2011.

WSRC-MS-2003-00889, Kaplan, D. I., et al., *Enhanced Plutonium Mobility During Long-Term Transport Through an Unsaturated Subsurface Environment*, Savannah River Site, Aiken, SC, January 23, 2004.

WSRC-RP-2003-00362, Kaplan, D. I., and Hang, T., *Estimated Duration of the Subsurface Reducing Environment Produced by the Z-Area Saltstone Disposal Facility*, Savannah River Site, Aiken, SC, Rev. 2, January 2003.

WSRC-RP-91-17, *Land and Water Use Characteristics in the Vicinity of the Savannah River Site*, Savannah River Site, Aiken, SC, March 1991.

WSRC-RP-92-1360, *Radiological Performance Assessment for the Z-Area Saltstone Disposal Facility*, Savannah River Site, Aiken, SC, Rev. 0, December 18, 1992.

WSRC-RP-94-54, Thayer, P., et al., *Petrographic Analysis of Mixed Carbonate-Clastic Hydrostratigraphic Units in the General Separations Area*, Savannah River Site, Aiken, SC, December 17, 1994.

WSRC-RP-97-311, *Composite Analysis E-Area Vaults and Saltstone Disposal Facilities*, Savannah River Site, Aiken, SC, September 1, 1997.

WSRC-STI-2006-00037, Kaplan, D., et al., *Influence of Dissolved Organic Carbon and pH on Iodide, Perrhenate, and Selenate Sorption to Sediment*, Savannah River Site, Aiken, SC, September 5, 2006.

WSRC-STI-2006-00198, Phifer, M. A., et al., *Hydraulic Property Data Package for the E-Area and Z-Area Soils, Cementitious Materials, and Waste Zones*, Savannah River Site, Aiken, SC, Rev. 0, September 2006.

WSRC-STI-2006-00360, Wells, D., *Z-Area Groundwater Monitoring Report for 2006*, Savannah River Site, Aiken, SC, December 19, 2006.

WSRC-STI-2007-00004, Lee, P. L., et al., *Baseline Parameter Update for Human Health Input and Transfer Factors for Radiological Performance Assessments at the Savannah River Site*, Savannah River Site, Aiken, SC, Rev. 4, June 13, 2008.

WSRC-STI-2007-00056, Harbour, J. R., et al., *International Program: Summary Report on the Properties of Cementitious Waste Forms*, Savannah River Site, Aiken, SC, Rev. 0, March 2007.

WSRC-STI-2007-00061, Subramanian, K. H., *Life Estimation of High Level Waste Tank Steel for F-Tank Farm Closure Performance Assessment*, Savannah River Site, Aiken, SC, Rev. 2, June 2008.

WSRC-STI-2007-00640, Kaplan, D. I., et al., *Partitioning of Dissolved Radionuclides to Concrete Under Scenarios Appropriate for Tank Closure Performance Assessments*, Savannah River Site, Aiken, SC, December 21, 2007.

WSRC-STI-2007-00649, Dixon, K., *Hydraulic and Physical Properties of MCU Saltstone*, Savannah River Site, Aiken, SC, Rev. 0, March 2008.

WSRC-STI-2008-00236, Denham, M. E., *Thermodynamic and Mass Balance Analysis of Expansive Phase Precipitation in Saltstone*, Savannah River Site, Aiken, SC, May 2008.

WSRC-STI-2008-00244, Jones, W. E., et al., *Saltstone Disposal Facility Closure Cap Concept and Infiltration Estimates*, Savannah River Site, Aiken, SC, Rev. 0, May 2008, <http://pbadupws.nrc.gov/docs/ML1016/ML101600430.pdf>, Accessed March 29, 2011.

WSRC-STI-2008-00285, Kaplan, D. I., et al., *Distribution of Sorption Coefficients (Kd Values) in the SRS Subsurface Environment*, Savannah River Site, Aiken, SC, June 30, 2008, <http://pbadupws.nrc.gov/docs/ML1021/ML102160599.pdf>, Accessed March 29, 2011.

WSRC-TR-2003-00035, Powell, B. A., et al., *Plutonium Oxidation State Geochemistry in the SRS Subsurface Environment*, Savannah River Site, Aiken, SC, December 27, 2002.

WSRC-TR-2005-00074, Cook, J. R., et al., *Special Analysis: Revision of Saltstone Vault 4 Disposal Limits*, Savannah River Site, Aiken, SC, Rev. 0, May 26, 2005, <http://pbadupws.nrc.gov/docs/ML0519/ML051930002.pdf>, Accessed March 29, 2011.

WSRC-TR-2006-00004, Kaplan, D. I., *Geochemical Data Package for Performance Assessment Calculations Related to Savannah River Site*, Savannah River Site, Aiken, SC, Rev. 0, February 2006.

WSRC-TR-2006-00067, Harbour, J. R., et al., 2006, *Characterization of Slag, Fly Ash and Portland Cement for Saltstone*, Savannah River Site, Aiken, SC, Rev. 0, February 2006.

WSRC-TR-2008-00001, *Z-Area Groundwater Monitoring Report for 2007*, Savannah River Site, Aiken, SC, January 9, 2008.

WSRC-TR-2008-00037, Dixon, K. L., et al., *Task Technical and QA Plan: Saltstone Grout and Vault Concrete Sample Preparation and Testing*, Savannah River Site, Aiken, SC, Rev. 0, February 29, 2008.

WSRC-TR-2008-00090, Skidmore, T. E., et al., *Saltstone Vault #2 Interior Lining Review*, Savannah River Site, Aiken, SC, Rev. 0, May 2008.

WSRC-TR-94-0369, Cumbest, R., *In-Tank Processing (ITP) Geotechnical Summary Report*, Savannah River Site, Aiken, SC, Rev.1, 1994.

WSRC-TR-96-0041, Cumbest, R., et al., *Evaluation of Cross-Hole Seismic Tomography for Imaging Low-Resistance Intervals and Associated Carbonate Sediments in Coastal Plain Sequences on the Savannah River Site*, Savannah River Site, Aiken, SC, April 1996.

WSRC-TR-96-0069, *F-Area Geotechnical Characterization Report*, Savannah River Site, Aiken, SC, Vol. 1, Rev. 0, September 1996.

WSRC-TR-99-4083, Aadland, R. K., et al., *Significance of Soft Zone Sediments at the Savannah River Site*, Savannah River Site, Aiken, SC, Rev. 0, September 1999.